

**Alkali Metal & Alkaline-Earth Metal Complexes of Various
Amidophosphines having P, N, Chalcogen and Borane as Donor
atoms/group – Syntheses, Structures and Ring-Opening
Polymerization of ϵ -Caprolactone**

-Ravi Kumar Kottalanka-

A Dissertation Submitted to
Indian Institute of Technology Hyderabad
In Partial Fulfillment of the Requirements for
The Degree of Doctor of Philosophy



भारतीय प्रौद्योगिकी संस्थान हैदराबाद
Indian Institute of Technology Hyderabad

Department of Chemistry

September, 2014

Declaration

I declare that this written submission represents my ideas in my own words, and where others' ideas or words have been included, I have adequately cited and referenced the original sources. I also declare that I have adhered to all principles of academic honesty and integrity and have not misrepresented or fabricated or falsified any idea/data/fact/source in my submission. I understand that any violation of the above will be a cause for disciplinary action by the Institute and can also evoke penal action from the sources that have thus not been properly cited, or from whom proper permission has not been taken when needed.

K. Ravi Kumar
(Signature)

Ravi Kumar Kottalanka
(- Student Name -)

CY10P010
(Roll No)

Approval Sheet

This thesis entitled “**Alkali Metal & Alkaline-Earth Metal Complexes of Various Amidophosphines having P, N, Chalcogen and Borane as Donor atoms/group–Syntheses, Structures and Ring-Opening Polymerization of ϵ -Caprolactone**” by *Ravi Kumar Kottalanka* is approved for the degree of Doctor of Philosophy from IIT Hyderabad.

-Name and affiliation-

Examiner

-Name and affiliation-

Examiner

Tarun Kanti Panda
TARUN K PANDA

-Name and affiliation-

Adviser

-Name and affiliation-

Co-Adviser

-Name and affiliation-

Chairman

Acknowledgements

First and foremost, I would like to express my heart-felt gratitude and appreciation to my supervisor *Dr. Tarun Kanti Panda* for his guidance and tremendous encouragement during my PhD study. He is a distinguished scientist and teacher and very good advisor. It was really a great honor for me to work under his guidance as a first PhD student.

I would like to thank my doctoral committee members *Dr. G. Prabusankar*, *Dr. Bhabani S. Mallik* and *Dr. Debaprasad Shee* for their valuable suggestions and guidance over the years. Especially, I am grateful to *Dr. Bhabani S Mallik* for his help for doing DFT calculations for some of my ligand systems.

I would like to thank *Prof. U. B. Desai*, Director, Indian Institute of Technology Hyderabad and *Prof. F. A. Khan*, Head of the Department, Department of Chemistry for providing infrastructure and facilities like Single-Crystal XRD, multinuclear NMR, HRMS, Glove Box, FT-IR, CHNS analyzer and other sophisticated instruments needed to complete my research work.

My heart-felt warm wishes and special thanks to my group members and colleagues, especially to *Kishor Naktode*, *Srinivas Anga*, *Harinath A*, *Jayeeta Bhattacharjee*, *Anirban Chakrabarty* and M.Sc project students *Mitali*, *Payel*, *Salil*, *Tigmanshu*, *Supriyo*, *Abhinanda* and *Sayak* who also stayed different times in our group. It was really great experiences with them to share the lab, share the thoughts during my PhD study. We had very good fruitful discussions with them in several times.

I also like to thank *Madam Arpita Panda* for nice dishes at several occasions when we all are invited at sir's residence and master *Jishnu Panda* for his nonstop activities with us.

I would like to take this opportunity to thank *Prof. Kazushi Mashima* and *Dr. Hayato Tsurugi* and group members of Mashima lab at Graduate School of Engineering Science, Osaka University, Japan where I worked for a very short duration but I made a very special bond with them, for their encouragement and helpful advices.

I am very much thankful to all of my friends in IIT Hyderabad, whose support in technical and personal issues must be acknowledged. I am in short of words to express my heart-felt gratitude and thanks to my beloved parents for their support and encouragement throughout my career.

I would like to thank U.G.C New Delhi for financial support provided for me during my PhD Study.

Dedicated to
My Beloved Parents

Table of Contents

Declaration.....	2
Approval Sheet.....	3
Acknowledgements	4
Abstract.....	14
Abbreviations	15
List of Schemes.....	17
List of Figures.....	19
List of Tables	22
Introduction.....	24
Table I. Similarities between the heavier alkaline-earth metals and divalent lanthanides.....	25
Chart I. A selection of ligand systems that are introduced into the alkaline-earth metal chemistry.	26
References.....	28
Chapter 1	31
Syntheses of aminophosphines and their corresponding chalcogenide derivatives and structural studies of sodium and potassium complexes.....	31
1.1 Introduction.....	31
1.1.1. Aminophosphines.....	31
1.1.2. Amidophosphine-chalcogenides.....	32
1.2 Results and Discussion.....	33
1.2.1. Synthesis of different aminophosphines.....	33
1.2.2. Synthesis of different amidophosphine-chalcogenides.....	35
1.2.3. Sodium and potassium complexes	38
1.3 Conclusion	48
1.4 Experimental Procedures.....	48
1.4.1. General	48
1.4.2. Synthesis of [Ph ₂ PNHCHPh ₂] (1).....	49
1.4.3. Synthesis of [Ph ₂ PNHCPh ₃] (2).....	49
1.4.4. Synthesis of [Ph ₂ P(O)NHCHPh ₂] (1a)	50
1.4.5. Synthesis of [Ph ₂ P(O)NHCPPh ₃] (2a)	50
1.4.6. Synthesis of [Ph ₂ P(S)NHCHPh ₂] (1b).....	51
1.4.7. Synthesis of [Ph ₂ P(S)NHCPPh ₃] (2b).....	51
1.4.8. Synthesis of [Ph ₂ P(Se)NHCHPh ₂] (1c)	51
1.4.9. Synthesis of [Ph ₂ P(Se)NHCPPh ₃] (2c)	52

1.4.10.	<i>Synthesis of</i> $[\{(THF)_2Na(Ph_2P(O)NCPH_3)}_2]$ (3)	52
1.4.11.	<i>Synthesis of</i> $[\{(THF)_2Na(Ph_2P(S)NCHPh_2)}_2]$ (4)	53
1.4.12.	<i>Synthesis of</i> $[\{K(THF)_2Ph_2P(S)N(CHPh_2)}_2]$ (5)	53
1.4.13.	<i>Synthesis of</i> $[\{(THF)_2Na(Ph_2P(S)NCPH_3)}\{(THF)Na(Ph_2P(S)NCPH_3)}]$ (6)	54
1.5	X-ray Crystallographic Studies	54
1.6	Tables	56
	Table 1.1. Crystallographic data of compounds 1 , 2 and 2b	56
	Table 1.2. Crystallographic data of compounds 1c , 2c and 3	57
	Table 1.3. Crystallographic data of compounds 4 , 5 and 6	58
	References:	59
Chapter 2		64
	Homoleptic complexes of alkaline-earth metals having bulky amidophosphine-chalcogenides in their coordination sphere: evidence for direct M-Se bond	64
2.1	Introduction-	64
2.2	Results and Discussion	66
2.2.1.	Alkali metal complexes	66
2.2.2.	Alkaline-earth metal complexes of phosphinoselenoic amide ligand	69
2.2.3.	Barium complex of diphenylphosphinothioic amido ligand	74
2.2.4.	Strontium, barium and lithium complexes of diselenoimidodiphosphinato ligand [HN(PPh₂Se)₂]	76
2.3	Conclusion	83
2.4	Experimental procedures	84
2.4.1.	<i>General</i>	84
2.4.2.	<i>Synthesis of</i> $[\{(THF)_2NaPh_2P(Se)N(CHPh_2)}_2]$ (7)	84
2.4.3.	<i>Synthesis of</i> $[\{(THF)_2KPh_2P(Se)N(CHPh_2)}_2]$ (8)	85
2.4.4.	<i>Synthesis of</i> $[M(THF)_2\{Ph_2P(Se)N(CHPh_2)}_2]$ (M = Ca (9), Sr (10) and Ba (11))	85
2.4.5.	<i>Synthesis of</i> $[Ba(THF)_2\{Ph_2P(S)N(CHPh_2)}_2]$ (12)	87
2.4.6.	<i>Synthesis of</i> $[\{\eta^2-N(PPh_2Se)_2\}_2Sr(THF)_2]$ (14)	88
2.4.7.	<i>Synthesis of</i> $[\{\eta^2-N(PPh_2Se)_2\}_2Ba(THF)_2]$ (15)	88
2.4.8.	<i>Synthesis of</i> $[\eta^2-N(PPh_2Se)Li(THF)_2]$ (16)	89
2.5	X-ray Crystallographic Studies	89
2.6	Tables	91
	Table 2.1. Crystallographic data of compounds 7 , 8 and 9	91
	Table 2.2. Crystallographic data of compounds 10 , 11 and 12	92

Table 2.3. Crystallographic data of compounds 14, 15 and 16	93
References:	94
Chapter 3	99
Novel amidophosphine-boranes into the alkali and heavier alkaline-earth metals coordination sphere: syntheses and structural studies	99
3.1 Introduction	99
3.2 Results and Discussion	102
3.2.1. Synthesis of amidophosphine-borane adducts	102
3.3 Synthesis and characterization of the alkali-metal complexes	104
3.4 Synthesis and characterization of the alkaline-earth-metal complexes	110
3.5 Conclusion	116
3.6 Experimental Procedures	117
3.6.1. General	117
3.6.2. Synthesis of [Ph₂P(BH₃)NH(CHPh₂)] (17)	117
3.6.3. Synthesis of [Ph₂P(BH₃)NHCPh₃] (18)	118
3.6.4. Synthesis of [(η²-Ph₂CHNP(BH₃)Ph₂)Li(THF)₂] (19)	118
3.6.5. Synthesis of [{(η³-Ph₂CHNP(BH₃)Ph₂)Na(THF)₂ }₂] (20)	119
3.6.6. Synthesis of [{(η³-Ph₂CHNP(BH₃)Ph₂)K(THF)₂ }₂] (21)	119
3.6.7. Synthesis of [M(THF)₂{Ph₂P(BH₃)N(CHPh₂) }₂] (M = Ca (22), Sr (23) and Ba (24))	120
3.7 X-ray Crystallographic Studies	122
3.8 Tables	123
Table 3.1. Crystallographic data of compounds 17, 18 and 19	123
Table 3.2. Crystallographic data of compounds 20, 21 and 22	124
Table 3.3. Crystallographic data of compounds 23 and 24	125
References:	126
Chapter 4	132
Bis(phosphinoselenoicamides) as versatile chelating ligands for alkaline earth metal (Mg, Ca, Sr and Ba) complexes: syntheses, structure and ε-caprolactone polymerization	132
4.1 Introduction	132
4.2 Results and Discussion	133
4.2.1. Bis(phosphinoselenoicamide) ligand	133
4.2.2. Alkaline-earth metal complexes	136
4.2.3. Bis(amidodiphenylphosphene borane) ligand	142
4.2.4. Bis(amidodiphenylphosphene-borane) barium complex	145

4.3	Ring-Opening Polymerization study	147
4.4	Conclusion	149
4.5.	Experimental Procedures	149
4.5.1.	<i>General</i>	149
4.5.2.	<i>Preparation of [(THF)₃Ca{Ph₂P(Se)NCH₂CH₂NPPH₂(Se)}] (26)</i>	150
4.5.3.	<i>Preparation of [(THF)₃Sr{Ph₂P(Se)NCH₂CH₂NPPH₂(Se)}] (27)</i>	150
4.5.4.	<i>Preparation of [(THF)₃Ba{Ph₂P(Se)NCH₂CH₂NPPH₂(Se)}] (28)</i>	151
4.5.5.	<i>Preparation of [(THF)₃Mg{Ph₂P(Se)NCH₂CH₂NPPH₂(Se)}] (29)</i>	151
4.5.6.	<i>Preparation of [Ph₂P(BH₃)NHCH₂CH₂NHPPH₂(BH₃)] (30)</i>	152
4.5.7.	<i>Preparation of [(THF)₂Ba{Ph₂P(BH₃)NCH₂CH₂NPPH₂(BH₃)}]₂ (31)</i>	152
4.5.8.	<i>Typical polymerisation experiment</i>	153
4.6	X-Ray crystallographic studies	153
4.7	Tables	155
	Table 4.2. Crystallographic data of compounds 25-cis , 25-trans and 26	155
	Table 4.3. Crystallographic data of compounds 27 , 28 and 29	156
	Table 4.4. Crystallographic data of compounds 30 and 31	157
	References:	158
Chapter 5		161
Novel alkaline-earth metal complexes having chiral phosphinoselenoic amides and boranes in the coordination sphere: chiral alkaline earth metal complexes having M-Se direct bond (M = Mg, Ca, Sr, Ba)		
		161
5.1	Introduction	161
5.2	Results and Discussion	162
5.2.1	Synthesis of chiral phosphinoselenoicamides	162
5.2.2.	Chiral phosphineamidosenoicamide potassium complexes	164
5.2.3.	Synthesis of alkaline-earth metal complexes	165
5.2.4.	Chiral amidophosphine-borane ligands	174
5.2.5.	Chiral-amidophosphine-borane barium complexes	177
5.3	Ring-opening polymerisation study	180
5.4	Conclusion	182
5.5	Experimental Procedures	182
5.5.1.	<i>General</i>	182
5.5.2.	<i>Synthesis of [Ph₂P(Se)HN(<i>R</i>-*CHMePh)] (32a):</i>	183
5.5.3.	<i>Synthesis of [Ph₂P(Se)HN(<i>S</i>-*CHMePh)] (32b): Same as above for 32a</i>	183

5.5.4.	Synthesis of $[K\{N(R-^*CHMePh)(Ph_2P(Se))\}(THF)_n]$ (33a).....	183
5.5.5.	Synthesis of $[(THF)_2Mg\{Ph_2P(Se)N(R-^*CHMePh)_2\}]$ (34a) :.....	184
5.5.6.	Synthesis of $[(THF)_2Ca\{Ph_2P(Se)N(R-^*CHMePh)_2\}]$ (35a) :.....	184
5.5.7.	Synthesis of $[(THF)_2Sr\{Ph_2P(Se)N(R-^*CHMePh)_2\}]$ (36a) :.....	185
5.5.8.	Synthesis of $[(THF)_2Ba\{Ph_2P(Se)N(R-^*CHMePh)_2\}]$ (37a) :.....	186
5.5.9.	Synthesis of $[Ph_2P(BH_3)HN(R-^*CHMePh)]$ (38a):.....	187
5.5.10.	Synthesis of $[Ph_2P(BH_3)HN(S-^*CHMePh)]$ (38b): Same as above for 38a	187
5.5.11.	Synthesis of $[(THF)_2Ba\{Ph_2P(BH_3)N(R-^*CHMePh)_2\}]$ (39a) :.....	188
5.6	X-Ray crystallographic studies	188
5.7	Tables	190
	Table 5.1. Crystallographic data of compounds 32a , 32b and 35a	190
	Table 5.2. Crystallographic data of compounds 35b , 36a and 36b	191
	Table 5.3. Crystallographic data of compounds 37a , 37b and 38a	192
	Table 5.4. Crystallographic data of compounds 38b , 39a and 39b	193
	References:	194
	Chapter 6	198
	Alkali and alkaline-earth metal complexes having rigid bulky-iminopyrrolyl ligand in the coordination sphere: syntheses, structures and ϵ-caprolactone polymerization	198
6.1	Introduction	198
6.2	Results and Discussion	199
6.2.1.	Ligand synthesis:	199
6.2.2.	Synthesis and characterization of alkali metal complexes:	201
6.2.3.	Synthesis and characterization of alkaline-earth metal complexes:	207
6.3	Ring-Opening Polymerization of ϵ-caprolactone study	216
6.4	Conclusion	220
6.5	Experimental Procedure:	220
6.5.1.	<i>General</i>	220
6.5.2.	Synthesis of $[2-(Ph_3CN=CH)-C_4H_3NH]$ (40)	221
6.5.3.	Synthesis of $[(2-(Ph_3CN=CH)-C_4H_3N)Li(THF)_2]$ (41)	221
6.5.4.	Synthesis of $[(2-(Ph_3CN=CH)-C_4H_3N)Na(THF)_2]$ (42)	222
6.5.5.	Synthesis of $[(2-(Ph_3CN=CH)-C_4H_3N)K(THF)_{0.5}]_4$ (43).....	222
6.5.6.	Synthesis of $[(2-(Ph_3CN=CH)-C_4H_3N)\{PhCH_2\}Mg(THF)_2]$ (44).....	223
6.5.7.	Synthesis of $[(2-(Ph_3CN=CH)-C_4H_3N)_2Mg(THF)_2]$ (45)	223

6.5.8.	<i>Synthesis of</i> [$\{2-(\text{Ph}_3\text{CN}=\text{CH})-\text{C}_4\text{H}_3\text{N}\}_2\text{M}(\text{THF})_n$] (M = Ca (46), Sr (47) and n = 2; M = Ba (48) and n = 3).....	224
6.6	X-ray crystallographic studies	225
6.7	Tables	227
	Table 6.2. Crystallographic data of compounds 40 , 41 and 42	227
	Table 6.3. Crystallographic data of compounds 43 , 44 and 45	228
	Table 6.4. Crystallographic data of compounds 46 , 47 and 48	229
	References:	230
	List of publications based on the research work:	233
	Curriculum vitae	235

Abstract

During the last decade, heavy alkaline-earth organometallic chemistry has emerged from obscurity to becoming a vibrant area of research, owing to a number of synthetic pathways that provide reliable access to these highly reactive target compounds. The complexes of heavy alkaline-earth metals were employed in various catalytic applications such as ring-opening polymerization of various cyclic esters, polymerization of styrene and dienes, and hydroamination and hydrophosphination reactions of alkenes and alkynes. Particularly, Group 2 metal complexes have been received considerable attention as initiators for the ROP of cyclic esters and some of them have demonstrated impressive results. Aliphatic polyesters are currently considered as alternatives to synthetic petrochemical-based polymers. Their biodegradable and biocompatible nature along with their mechanical and physical properties make them prospective thermoplastics with broad commercial applications such as single-use packaging materials, medical sutures and drug delivery systems. Ring-opening polymerization (ROP) of cyclic esters promoted by alkaline-earth & rare-earth metal initiators proved to be the most efficient way for preparing polyesters with controlled molecular weight and microstructure and narrow molecular-weight distribution. Therefore, the design and synthesis of new well-defined single-site catalysts that exhibits good activity, productivity and selectivity for cyclic ester polymerization is needed.

In my doctoral research work, we have mainly focused on the syntheses and structural characterization of various alkaline-earth metal complexes having various amidophosphine-chalcogenides and boranes in their coordination sphere as multi-dentate chelate ligands. We have studied the catalytic efficiency of alkaline-earth metal complexes as initiators for the Ring-opening polymerization of ϵ -caprolactone. We have developed a series of homoleptic alkaline earth metal complexes with amidophosphine chalcogenide ligands. To improve the catalytic activity, we have also synthesized homoleptic metal complexes with monoanionic amidophosphine boranes and heteroleptic complexes with dianionic bis(phosphino-selenoicamide) ligands. We have observed that metal complexes having larger ionic radii and less shielded by ligand moieties showed better activity and better control in catalytic ring opening polymerization of ϵ -caprolactone.

Abbreviations

%	-	Percentage
μ	-	Mu
Å	-	Angstrom
BTSA	-	Bis(trimethylsilyl)amide
Bu	-	Butyl
C ₆ D ₆	-	Benzene-d ₆
CDCl ₃	-	Chloroform-d
Cp	-	Cyclopentadienyl
d	-	Doublet
D _c	-	Density
Diox	-	Dioxane
Dipp	-	2,6-diisopropyl
DAD	-	1,4-diaza-1,3-butadiene
Et ₃ N	-	Triethylamine
FT-IR	-	Fourier transform Infrared spectroscopy
GOF	-	Goodness of Fit
h	-	Hour
Hz	-	Hertz
<i>i</i> -	-	Iso
Imp	-	Iminopyrrolyl
<i>J</i>	-	Coupling Constant
K	-	Kelvin
<i>m</i> -	-	Meta
m	-	Multiplet
Me	-	Methyl
Mes	-	Mesityl
MHz	-	Mega Hertz
ml	-	millileter
mmol	-	millimole
<i>n</i> -	-	Normal

NMR	-	Nuclear Magnetic Resonance
<i>o</i> -	-	Ortho
<i>p</i> -	-	Para
Ph	-	Phenyl
ppm	-	Parts per million
Pr	-	Propyl
r.t.	-	Room temperature
ROP	-	Ring-Opening Polymerization
s	-	Singlet
T	-	Temperature
t	-	Triplet
THF	-	Tetrahydrofuran
η	-	Eta
κ	-	Kappa
π	-	Pi
δ	-	Chemical shift
ε	-	Epsilon

List of Schemes

Chapter 1

- Scheme 1.1. Most common bonding modes of aminophosphine and amidophosphine ligands
- Scheme 1.2. Most possible bonding modes of amidophosphine-chalcogenides
- Scheme 1.3. Synthesis of different aminophosphine ligands
- Scheme 1.4. Synthesis of various amidophosphine-chalcogenides
- Scheme 1.5. Synthesis of dimeric sodium complex $[\{(THF)_2Na(Ph_2P(O)NCPPh_3)\}_2]$ (**3**)
- Scheme 1.6. Synthesis of Na and K complexes of diphenylphosphinothioicamide (**1b**)
- Scheme 1.7. Synthesis of dimeric sodium complex of triphenylphosphinothioicamide (**2b**)

Chapter 2

- Scheme 2.1. Synthesis of alkali and alkaline earth metal complexes with phosphine selenoicamide ligand (**1c**)
- Scheme 2.2. Synthesis of barium (**12**) complex of phosphinothioicamide ligand (**1b**).
- Scheme 2.3. Synthesis of strontium (**14**) and barium (**15**) complexes of $[HN(PPh_2Se)_2]$ ligand.
- Scheme 2.4. Synthesis of lithium complex **16**

Chapter 3

- Scheme 3.1. Synthesis of various aminophosphine-borane adducts **17** and **18**
- Scheme 3.2. Synthesis of alkali-metal complexes of ligand **17**
- Scheme 3.3. Synthesis of alkaline-earth metal complexes of ligand **17**

Chapter 4

- Scheme 4.1. *Cis* and *trans* forms of ligand **25**
- Scheme 4.2. Synthesis of alkaline earth metal phosphinoselenoic amide complexes **26-29**
- Scheme 4.3. Synthesis of the bis(amidodiphenylphosphene borane) ligand **30**
- Scheme 4.4. Synthesis of barium complex **31**

Scheme 4.5. Catalytic ROP of ϵ -CL by calcium, strontium and barium complexes **26–28**.

Chapter 5

Scheme 5.1. Synthesis of chiral-Phosphinoselenoicamine ligands **32a & 32b**

Scheme 5.2. Synthesis of potassium salts of chiral phosphinoselenoicamides **33a & 33b**

Scheme 5.3. Synthesis of alkaline-earth metal complexes of chiral phosphinoselenoic amides (**34a-37b & 34b-37b**)

Scheme 5.4. Synthesis of chiral amidophosphine-boranes **38a & 38b**

Scheme 5.5. Synthesis of Barium complex of chiral amidophosphine-boranes **39a & 39b**

Chapter 6

Scheme 6.1. Synthesis of bulky iminopyrrolyl ligand **40**

Scheme 6.2. Synthesis of alkali-metal complexes **41-43** of bulky iminopyrrolyl ligand

Scheme 6.3. Synthesis of magnesium complexes **44** and **45** of bulky iminopyrrolyl ligand

Scheme 6.4. Synthesis of heavier alkaline-earth metal complexes **46-48** of bulky iminopyrrolyl ligand

Scheme 6.5. Catalytic ROP of ϵ -CL by magnesium and calcium complexes **44** and **46**.

List of Figures

Chapter 1

- Figure 1.1. Solid state structures of compound **1** and **2**.
- Figure 1.2. Comparison of $^{31}\text{P}\{^1\text{H}\}$ NMR spectral data of various amidophosphine-chalcogenides recorded at 25°C in CDCl_3 .
- Figure 1.3. Solid state structures of compound **2b**, **1c** and **2c**
- Figure 1.4. Solid state structure of compound **3**. Hydrogen atoms are omitted for clarity
- Figure 1.5. Solid state structure of compound **4**. Hydrogen atoms are omitted for clarity
- Figure 1.6. Solid state structure of compound **5**. Hydrogen atoms are omitted for clarity
- Figure 1.7. Solid state structure of compound **6**. Hydrogen atoms are omitted for clarity

Chapter 2

- Figure 2.1. Solid state structure of compound **7**. Hydrogen atoms are omitted for clarity
- Figure 2.2. Solid state structure of compound **8**. Hydrogen atoms are omitted for clarity
- Figure 2.3. Solid state structure of compound **9**. Hydrogen atoms are omitted for clarity
- Figure 2.4. Solid state structure of compound **10**. Hydrogen atoms are omitted for clarity
- Figure 2.5. Solid state structure of compound **11**. Hydrogen atoms are omitted for clarity
- Figure 2.6. Solid state structure of compound **12**. Hydrogen atoms are omitted for clarity
- Figure 2.7. Solid state structure of compound **14**. Hydrogen atoms are omitted for clarity
- Figure 2.8. Solid state structure of compound **15**. Hydrogen atoms are omitted for clarity
- Figure 2.9. Solid state structure of compound **16**. Hydrogen atoms are omitted for clarity

Chapter 3

- Figure 3.1. Solid state structures of compounds **17** and **18**. Hydrogen atoms are omitted for clarity
- Figure 3.2. Solid state structure of compound **19**. Hydrogen atoms are omitted for clarity
- Figure 3.3. Solid state structure of compound **20**. Hydrogen atoms are omitted for clarity
- Figure 3.4. Solid state structure of compound **21**. Hydrogen atoms are omitted for clarity
- Figure 3.5. Solid state structure of compound **22**. Hydrogen atoms are omitted for clarity
- Figure 3.6. Solid state structure of compound **23**. Hydrogen atoms are omitted for clarity
- Figure 3.7. Solid state structure of compound **24**. Hydrogen atoms are omitted for clarity

Chapter 4

- Figure 4.1. Solid state structure of compound **25-cis**.
- Figure 4.2. Solid state structure of compound **25-trans**.
- Figure 4.3. Solid state structures of compounds **26** and **27**. Hydrogen atoms are omitted for clarity
- Figure 4.4. Solid state structure of compound **28**. Hydrogen atoms are omitted for clarity
- Figure 4.5. Solid state structure of compound **29**. Hydrogen atoms are omitted for clarity
- Figure 4.6. Solid state structure of compound **30**.
- Figure 4.7. Solid state structure of compound **31**. Hydrogen atoms are omitted for clarity

Chapter 5

- Figure 5.1. Solid state structures of compounds **32a** (*R*-isomer) and **32b** (*S*-isomer).
- Figure 5.2. Solid state structures of compounds **34a** (*R*-isomer) and **34b** (*S*-isomer). Hydrogen atoms are omitted for clarity.
- Figure 5.3. Solid state structures of compounds **35a** (*R*-isomer) and **35b** (*S*-isomer). Hydrogen atoms are omitted for clarity.
- Figure 5.4. Solid state structures of compounds **36a** (*R*-isomer) and **36b** (*S*-isomer). Hydrogen atoms are omitted for clarity.
- Figure 5.5. Solid state structures of compounds **37a** (*R*-isomer) and **37b** (*S*-isomer). Hydrogen atoms are omitted for clarity.
- Figure 5.6. Solid state structures of compounds **38a** (*R*-isomer) and **38b** (*S*-isomer).
- Figure 5.7. Solid state structures of compounds **39a** (*R*-isomer) and **39b** (*S*-isomer). Hydrogen atoms are omitted for clarity.

Chapter 6

- Figure 6.1. Solid state structure of bulky iminopyrrolyl ligand **40**.
- Figure 6.2. Solid state structure of lithium complex **41**. Hydrogen atoms are omitted for clarity.
- Figure 6.3. Solid state structure of sodium complex **42**. Hydrogen atoms are omitted except H13 for clarity.
- Figure 6.4. Solid state structure of potassium complex **43**. Hydrogen atoms are omitted except H24 for clarity.

- Figure 6.5. Solid state structure of magnesium complex **44**. Hydrogen atoms are omitted for clarity.
- Figure 6.6. Solid state structure of magnesium complex **45**. Hydrogen atoms are omitted for clarity.
- Figure 6.7. Solid state structure of calcium complex **46**. Hydrogen atoms are omitted for clarity.
- Figure 6.8. Solid state structure of strontium complex **47**. Hydrogen atoms are omitted for clarity.
- Figure 6.9. Solid state structure of barium complex **48**. Hydrogen atoms are omitted for clarity.

List of Tables

Chapter 1

Table 1.1. Crystallographic data for compounds **1**, **2** and **2b**.

Table 1.2. Crystallographic data for compounds **1c**, **2c** and **3**.

Table 1.3. Crystallographic data for compounds **4**, **5** and **6**.

Chapter 2

Table 2.1. Crystallographic data for compounds **7**, **8** and **9**.

Table 2.2. Crystallographic data for compounds **10**, **11** and **12**.

Table 2.3. Crystallographic data for compounds **14**, **15** and **16**.

Chapter 3

Table 3.1. Crystallographic data for compounds **17**, **18** and **19**.

Table 3.2. Crystallographic data for compounds **20**, **21** and **22**.

Table 3.3. Crystallographic data for compounds **23** and **24**.

Chapter 4

Table 4.1. Catalytic ROP of ϵ -caprolactone.

Table 4.2. Crystallographic data for compounds **25-cis**, **25-trans** and **26**.

Table 4.3. Crystallographic data for compounds **27**, **28** and **29**.

Table 4.4. Crystallographic data for compounds **30** and **31**.

Chapter 5

Table 5.1. Crystallographic data for compounds **32a**, **32b** and **35a**.

Table 5.2. Crystallographic data for compounds **35b**, **36a** and **36b**.

Table 5.3. Crystallographic data for compounds **37a**, **37b** and **38a**.

Table 5.4. Crystallographic data for compounds **38b**, **39a** and **39b**.

Chapter 6

Table 6.1. Catalytic ROP of ϵ -caprolactone.

Table 6.2. Crystallographic data for compounds **40**, **41** and **42**.

Table 6.3. Crystallographic data for compounds **43**, **44** and **45**.

Table 6.4. Crystallographic data for compounds **46**, **47** and **48**.

Introduction

Alkaline-earth metals are typically belong to Group 2 in the periodic table, for these metals stable oxidation state is +2. Among the alkaline-earth metals, the lighter metals beryllium and magnesium, with their small radii, display relatively high charge/size ratios, coinciding with the capacity for bond polarization and the induction of bond covalency. Therefore, Be–C and Mg–C bonds are much more polar indeed, and affording relatively stable species. Due to the toxicity of beryllium and its compounds,¹ little work has been done, but magnesium containing compounds have been most intensely studied as evidenced by the established use of Grignard and diorganomagnesium reagents in synthetic applications.² The wide utility and facile synthesis of RMgX compounds³ led to the assumption that the heavier alkaline-earth metal analogues would shortly follow. But due to larger radius, strongly negative redox potentials ($E^\circ = -2.87 \text{ V}(\text{Ca}^{2+})$; $E^\circ = -2.89 \text{ V}(\text{Sr}^{2+})$; $E^\circ = -2.90 \text{ V}(\text{Ba}^{2+})$),⁴ combined with high hydro- and oxophilicity, high electropositive character, and the lack of energetically accessible and empty d-orbitals, the organometallic compounds of heavier alkaline-earth metals are highly unstable or difficult to form. These metals react easily with oxygen or water under formation of oxides or hydroxides; the resulting compounds are highly sensitive to hydrolysis. Furthermore, the metal–ligand bond is typically quite weak, resulting in significant lability due to large differences in electronegativity; metal–ligand bonds are largely electrostatic, further contributing to the lability of the target compounds. Their large ionic radii (for CN = 6, $\text{Ca}^{2+} = 1.00$; $\text{Sr}^{2+} = 1.18$; $\text{Ba}^{2+} = 1.35 \text{ \AA}$)⁵ do not only promote metal ligand bonds but are also responsible for low solubility, as the metals' steric saturation is often achieved by aggregation requiring the use of polar co-solvents to break up the aggregates. However, *Beckmann et al.* in 1905⁶ and later *Eisch et al.* in 1981⁷ reported an arylcalcium derivatives, but their incomplete characterization and difficult access did not establish this group of compounds. It wasn't until the early 1980's that the first structurally characterized organometallic calcium species, polymeric calcocene, $[\text{Ca}(\text{C}_5\text{H}_5)_2]_n$, was reported by *Zerger et al.*⁸ This was soon followed by extensive synthetic work by the *Hanusa* group, reporting on monomeric metallocenes using sterically demanding cyclopentadienides, such as $[\text{M}(\text{C}_5\text{Me}_5)_2(\text{THF})_2]$ ($\text{M} = \text{Ca}, \text{Sr}, \text{Ba}$).⁹ Indeed, these were ground-breaking achievements towards the development of the heavier alkaline-earth metal chemistry which would not have been possible without applying key principles learnt from organolanthanoid chemistry. The similarity between

size and charge radii between the divalent lanthanide ions Eu^{2+} , Yb^{2+} and Sm^{2+} with Ca^{2+} and Sr^{2+} suggests a similar structural chemistry, and to a limited extent chemical principles.⁵ Concepts learned include the necessity for steric shielding of the rather large metal centers via the introduction of sterically hindered ligands, and the further decrease of nuclearity via coordination of neutral basic Lewis co-ligands.¹⁰

Table I. Similarities between the heavier alkaline-earth metals and divalent lanthanides

Atomic No.	Atomic Symbol	Name	Element, M Electronic Configuration	Ion, M^{2+} Electronic configuration	Ionic radius (Å) (CN≥6)	EN	$\text{E}^{\circ}(\text{V})$ $\text{M}^{2+}_{(\text{aq})} + 2\text{e}^{-} = \text{M}_{(\text{s})}$
20	Ca	Calcium	[Ar]4s ²	[Ar]	1.06	1.00	-2.87
38	Sr	Strontium	[Kr]5s ²	[Kr]	1.18	0.95	-2.89
56	Ba	Barium	[Xe]6s ²	[Xe]	1.35	0.89	-2.90
62	Sm	Samarium	[Xe]4f ⁶ 6s ²	[Xe]4f ⁶	1.36	1.17	-2.68
63	Eu	Europium	[Xe]4f ⁷ 6s ²	[Xe]4f ⁷	1.31	1.20	-2.81
70	Yb	Ytterbium	[Xe]4f ¹⁴ 6s ²	[Xe]4f ¹⁴	1.16	1.10	-2.76

With this in mind, *Lappert et al.* were able to prepare the first non-cyclopentadienyl derivative, $[\text{Ca}\{\text{CH}(\text{SiMe}_3)\}_2(\text{diox})_2]$ by the activation of the metal using co-condensation in toluene.¹¹ While structural data are available on the compound, *Lappert et al.* were unable to reproduce the synthesis. The isolation of *Eaborn's et al.* unique donor-free $[\text{Ca}\{\text{C}(\text{SiMe}_3)_3\}_2]$ compound impressively documented difficulties associated with the organometallic chemistry of the heavier alkaline-earth metals.¹² Since then, a significantly extended list of compounds have been prepared, including alkyl, alkynyl, benzyl derivatives.¹³ These compounds demonstrate the high reactivity and decomposes at temperatures above -35 °C.¹⁴ The further developments in the organometallic chemistry of heavier alkaline-earth metals is the introduction of the alkaline-earth metal bis(trimethylsilyl)amides.¹⁵ In the recent times, these are the versatile starting materials for the syntheses many critical organometallic compounds of heavier alkaline-earth metals.

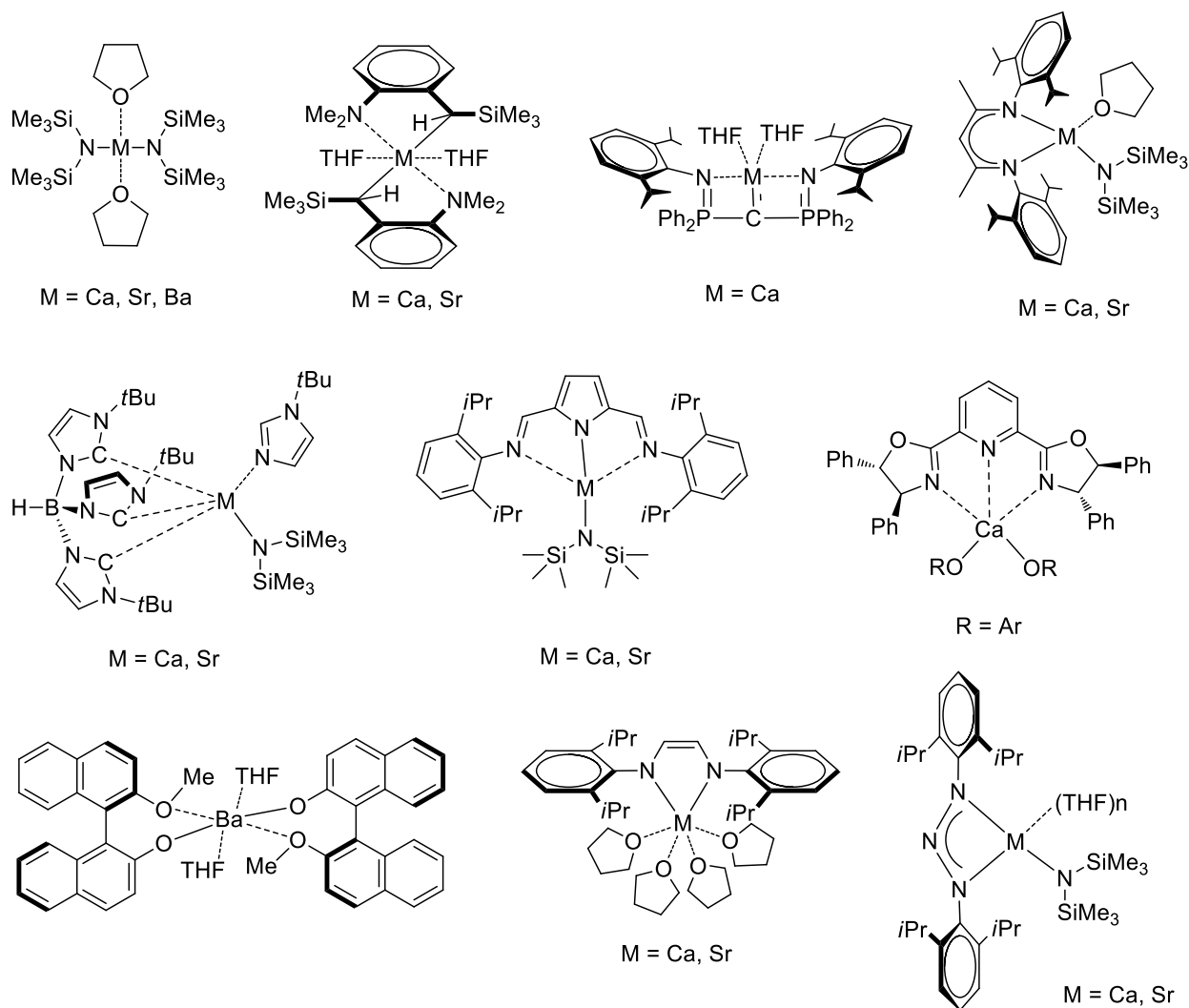


Chart I. A selection of ligand systems that are introduced into the alkaline-earth metal chemistry.

Because of these achievements in the heavier alkaline-earth metals and non-toxic nature of these metals compared to several late transition metals, large abundance of these metals have been attracted by the number research groups, and therefore, there are number nitrogen based ancillary ligands were successfully introduced into the heavier alkaline-earth metal coordination sphere to stabilize these highly oxophilic and electropositive metals. The various ligand systems that are introduced into the heavier alkaline-earth metals are represented in the Chart I. All these ligand system are useful to understand the basic reactivity, stability and coordination chemistry of the

alkaline-earth metals in various organic solvents which would not be possible before a decade. Interest in alkaline-earth metal compounds was further increased as the organometallic compounds of heavier alkaline-earth metals are gaining prominence, in the recent years, as efficient catalysts for the polymerization of cyclic esters¹⁶, polymerization of dienes and styrene,¹⁷ hydroamination and hydrosilylation of alkenes and alkynes,¹⁸ hydroamination reactions.¹⁹ Very recently, these alkaline-earth metal species were also successfully introduced into the field of asymmetric synthesis by introducing various sterically demanding chiral ligands into their coordination sphere. The use of alkaline-earth metal species in asymmetric synthesis as chiral catalyst, has been quite limited compared with that of transition metal catalysts.²⁰ Recently it was revealed that several catalytic asymmetric carbon-carbon bond-forming and related reactions proceeded smoothly in high enantioselectivities using the chiral Ca, Sr, and Ba catalysts.²¹ Their strong Brønsted basicity and mild Lewis acidity are promising and attractive characteristics and can influence their catalytic activity as well as their chiral modification capability in a positive manner. However, the vast potential of this field was still to be developed. Aside from these catalytic applications, interest in alkaline-earth metals was further increased as these metals are critical components in a multitude of materials with technical applications. Examples include BaTiO₃ (ferroelectric ceramics),²² Sr₂AlTaO₆ (dielectric materials),²³ CaGa₂S₄ (memory devices and optoelectronics)²⁴ and high temperature superconductors²⁵ among others. Further uses include the application as modulators of the semiconductor band gap.²⁶ However, suitable precursors for some of these materials are still lacking due to the limited volatility of the commonly used alkaline-earth metal sources. As an example, the industrial production of Pr_{1-x}Ca_xMnO₃ (x = 1/3 and 1/2) remains highly challenging, since the commonly utilized and available calcium source, calcium β-diketonate, is not sufficiently volatile.^{22,27} The lack of volatility is likely due to the oligomeric nature of the precursors, with strontium being trimeric,^{28a} and barium tetrameric.^{28b}

Among the various potential applications of alkaline-earth metal compounds, particularly in catalysis, these were best recognized as good initiators for ring-opening polymerization of cyclic esters affording biocompatible materials that are currently being used in medical research for biodegradable sutures or bone scaffolding.^{29,30}

References

- (1) Elschenbroich, C. *Organometallics* **2006**. Wiley-VCH Verlag GmH & Co. KGaA, Weinheim.
- (2) (a) Cahours, A. *Liebigs Ann. Chem.* **1860**, *114*, 227-255. (b) Grignard, V. *C R Hebd. Seances Acad. Sci.* **1900**, *130*, 1322. (c) Elschenbroich, C.; Salzer, A. *Organometallics: A Concise Introduction, 2nd ed.* VCH: Weinheim, **1992**. (d) Smith, J. D. *Adv. Organomet. Chem.* **1999**, *43*, 267-348. (e) Alexander, J. S.; Zuniga, M.F.; Guino-o, M. A.; Hahn, R.C.; Ruhlandt-Senge, K. *The organometallic chemistry of the alkaline earth metals* **2006**, Vol. 1, The Encyclopedia of inorganic chemistry. Wiley, New York, NY, p 116.
- (3) Richey, H. G. (eds), *Grignard Reagents New Developments* Wiley: Chichester, **2000**.
- (4) Miessler, G. L.; Tarr, D. A. *Inorganic chemistry* **2004**, Prentice Hall, N J.
- (5) Shannon, R. D. *Acta Crystallogr. Sect. A* **1976**, *A32*, 751-767.
- (6) Beckmann, E. *Ber. Dtsch. Chem. Ges.* **1905**, *38*, 904-906.
- (7) Eisch, J. J.; King, R. B. *Organometallic Synthesis* **1981**, Vol. 2, p.101. Academic Press: New York.
- (8) Zerger, R.; Stucky, G. *J. Organomet. Chem.* **1974**, *80*, 7-17.
- (9) (a) Sitzmann, H.; Dezember, M. R. *Angew. Chem. Int. Ed. Engl.* **1998**, *37*, 3113-3116. (b) Williams, R. A.; Hanusa, T. P.; Huffmann, J. C. *Organometallics* **1990**, *9*, 1128-1134. (c) Hanusa, T. P. *Coord. Chem. Rev.* **2000**, *210*, 329-367.
- (10) Hanusa, T. P. *Chem. Rev.* **1993**, *93*, 1023-1036.
- (11) Cloke, F. G. N.; Hitchcock, P. B.; Lappert, M. F.; Lawless, G. A.; Royo, B. *J. Chem. Soc. Chem. Commun.* **1991**, 724-726.
- (12) Eaborn, C.; Hawkes, S. A.; Hitchcock, P. B.; Smith, J. D. *Chem. Commun.* **1997**, 1961-1962.
- (13) See for example: (a) Hanusa, T. P. *Coord. Chem. Rev.* **2000**, *210*, 329-367. (b) Westerhausen, M. *Angew. Chem. Int. Ed.* **2001**, *40*, 2975-2977. (c) Alexander, J. S.; Ruhlandt-Senge, K. *Eur. J. Inorg. Chem.* **2002**, 2761-2774. (d) Burkey, D. J.; Hanusa, T. P. *Organometallics* **1996**, *15*, 4971-4976. (e) Green, D. C.; Englich, U.; Ruhlandt-Senge, K. *Angew. Chem., Int. Ed.* **1999**, *38*, 354-357. (f) Feil, F.; Harder, S. *Organometallics* **2000**, *19*, 5010-5015. (g) Harder, S.; Feil, F.; Weeber, A. *Organometallics* **2001**, *20*, 1044-1046. (h) Harder, S.; Feil, F. *Organometallics* **2002**, *21*, 2268-2274. (i) Feil, F. Müller, C.; Harder, S. *J. Organomet. Chem.* **2003**, *683*, 56-63. (j) Harder, S.; Müller, S.; Hübner, E.

- Organometallics* **2004**, *23*, 178-183. (k) Gärtner, M.; Fisher, R.; Langer, J.; Görls, H.; Walther, D.; Westerhausen, M. *Inorg. Chem.* **2007**, *46*, 5118-5124. (l) Mulvey, R.; Mongin, E. F.; Uchiyama, M.; Kondo, Y. *Angew. Chem. Int. Ed.* **2007**, *46*, 3802-3824. (m) Westerhausen, M. *Dalton Trans.* **2006**, 4755-4768. (n) Harder, S. *Chem. Rev.* **2010**, *110*, 3852-3876.
- (14) (a) Fisher, R.; Görls, H.; Westerhausen, M. *Inorg. Chem. Commun.* **2005**, *8*, 1159-1161. (b) Fischer, R.; Gärtner, M.; Görls, H.; Westerhausen, M. *Organometallics* **2006**, *25*, 3496-3500.
- (15) Westerhausen, M. *Coord. Chem. Rev.* **1998**, *176*, 157-210.
- (16) (a) Dechy-Cabaret, O.; Martin-Vaca, B.; Bourissou, D. *Chem. Rev.* **2004**, *104*, 6147-6176. (b) O'Keefe, B.; Hillmyer, J. M. A.; Tolman, W. B. *J. Chem. Soc. Dalton Trans.* **2001**, 2215-2224. (c) Wheaton, C. A.; Hayes, P. G.; Ireland, B. *Dalton Trans.* **2009**, 4832-4846. (d) Thomas, C. M. *Chem. Soc. Rev.* **2010**, *39*, 165-173.
- (17) Darensbourg, D. J.; Choi, W.; Karroonnirun, O.; Bhuvanesh, N. *Macromolecules* **2008**, *41*, 3493-3502. (m) Poirier, V.; Roisnel, T.; Carpentier, J.-F.; Sarazin, Y. *Dalton Trans.* **2009**, 9820-9827. (n) Xu, X.; Chen, Y.; Zou, G.; Ma, Z.; Li, G. *J. Organomet. Chem.* **2010**, *695*, 1155-1162. (o) Sarazin, Y.; Rosca, D.; Poirier, V.; Roisnel, T.; Silvestru, A.; Maron, L.; Carpentier, J.-F. *Organometallics* **2010**, *29*, 6569-6577. (p) Sarazin, Y.; Liu, B.; Roisnel, T.; Maron, L.; Carpentier, J.-F. *J. Am. Chem. Soc.* **2011**, *133*, 9069-9087.
- (18) (a) Harder, S.; Feil, F.; Knoll, K. *Angew. Chem., Int. Ed.* **2001**, *40*, 4261-4264. (b) Harder, S.; Feil, F. *Organometallics* **2002**, *21*, 2268-2274. (c) Jochmann, P.; Dols, T. S.; Spaniol, T. P.; Perrin, L.; Maron, L.; Okuda, J. *Angew. Chem., Int. Ed.* **2009**, *48*, 5715-5719.
- (19) (a) Barrett, A. G. M.; Crimmin, M. R.; Hill, M. S.; Procopiou, P. A. *Proc. R. Soc. London, Ser. A* **2010**, *466*, 927-963. (b) Harder, S. *Chem. Rev.* **2010**, *110*, 3852-3876.
- (20) (a) Kazmaier, U. *Angew. Chem. Int. Ed.* **2009**, *48*, 5790-5792. (b) Harder, S. *Chem. Rev.* **2010**, *110*, 3852-3876. (c) Kobayashi, S.; Yamashita, Y. *Acc. Chem. Res.* **2011**, *44*, 58-71. (d) Yanagisawa, A.; Yoshida, K. *Synlett.* **2011**, *20*, 2929-2938. (e) Yamashita, Y.; Tsubogo, T.; Kobayashi, S. *Chem. Sci.* **2012**, *3*, 967-975.
- (21) (a) Yamada, Y. M. A.; Ikegami, S. *Tetrahedron Lett.* **2000**, *41*, 2165-2169. (b) Suzuki, T.; Yamagiwa, N.; Matsuo, Y.; Sakamoto, S.; Yamaguchi, K.; Shibasaki, M.; Noyori, R. *Tetrahedron Lett.* **2001**, *42*, 4669-4671. (c) Berner, O. M.; Tedeschi, L.; Enders, D. *Eur. J. Org. Chem.* **2002**, *12*, 1877-1894. (d) Christoffers, J.; Baro, A. *Angew. Chem. Int. Ed.* **2003**,

- 42, 1688-1690. (e) Hayashi, T.; Yamasaki, K. *Chem. Rev.* **2003**, *103*, 2829-2844. (f) Saito, S.; Kobayashi, S. *J. Am. Chem. Soc.* **2006**, *128*, 8704-8705. (g) Almasi, D.; Alonso, D. A.; Na'jera, C. *Tetrahed. Asym.* **2007**, *18*, 299-365. (h) Tsogoeva, S. B. *Eur. J. Org. Chem.* **2007**, *11*, 1701-1716.
- (22) Chandler, C. D.; Roger, C.; Hampden-Smith, M. J. *Chem. Rev.* **1993**, *93*, 1205-1241.
- (23) Kautek, W. *Vacuum* **1992**, *43*, 403-411.
- (24) Braithwaite, N.; Weaver, G. *In Electronic Materials Butterworth: London*, **1990**.
- (25) See for example: Brook, R. J.; R. Cahn, W.; Bever, M. B. *Concise Encyclopedia of Advanced Ceramic Materials*, Pergamon Press: Oxford, England, **1991**.
- (26) Subba Ramaiah, K.; Su, Y. K.; Chang, S. J.; Juang, F. S.; Chen, C. H. *J. Crystal Growth* **2000**, *220*, 405-412.
- (27) (a) Llobet, A.; Garcia-Munoz, J. L.; Frontera, C.; Respaud, M.; Rakoto, H.; Lord, J. S. *Physica B: Condensed Matter (Amsterdam)* **2000**, *289 & 290*, 73-76. (b) Baum, T. H.; Paw, W.; *PCT Int. Appl.* **2000**, 26pp.
- (28) (a) Brooks, J. J.; Davies, H. O.; Leedham, T. J.; Jones, A. C.; Steiner, A. *Chem. Vap. Deposition* **2000**, *6*, 66-69. (b) Gleizes, A.; Sans-Lenain, S.; Medus, D. *Compt. Rend. Sci. Paris, Ser.II* **1991**, *313*, 761.
- (29) See for example: Westerhausen, M.; Schneiderbauer, S.; Kneifel, A. N.; Soetl, Y.; Mayer, P.; Noeth, H.; Zhong, Z.; P. Dijkstra, J.; Jeijen, J. *Eur. J. Inorg. Chem.* **2003**, 3432-3439.
- (30) Schiller, C.; Rasche, C.; Wehmöller, M.; Beckmann, F.; Eufinger, H.; Epple, M.; Weihe, S. *Biomaterials* **2004**, *25*, 1239-1247.

Chapter 1

Syntheses of aminophosphines and their corresponding chalcogenide derivatives and structural studies of sodium and potassium complexes

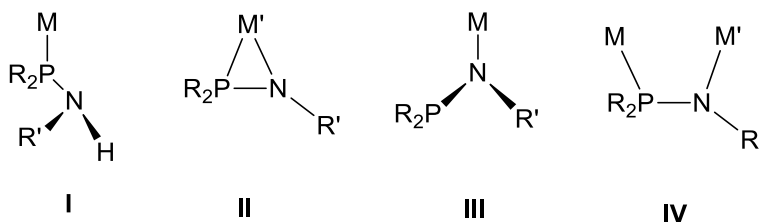
1.1 Introduction

Use of various P-N ligands is one of the alternatives of cyclopentadienyl ligands and using this approach, amide ligands are successfully used today for the design of new transition-metal compounds having well defined reaction centers.^{1,2} Recently, there has been a significant research effort in employing inorganic amines and imines. The P-N systems like monophosphanyl amides (R_2PNR'),³⁻⁶ diphosphanyl amides ($(Ph_2P)_2N$),^{4,7,8} phosphoraneiminato (R_3PN),⁹ phosphiniminomethanides [$((RNPR'_2)_2CH)$],¹⁰⁻¹⁴ phosphiniminomethandiides ($(RNPR'_2)_2C$),¹⁵⁻¹⁸ and diiminophosphinates ($R_2P(NR')^{19}$) are well known today as ligands and proved their potency into the transition and f-block metals. Roesky and co-workers introduced one chiral phosphinamine [$HN(CHMePh)(PPh_2)$] into the early transition-metal chemistry as well as in lanthanide chemistry.²⁰ It was shown that some of the early transition metal complexes having P-N ligands in the coordination sphere, may not only exhibit unusual co-ordination modes but also can be used for a number of catalytic transformations such as polymerization reactions.²¹ Very recently, Fryzuk and co-workers have reported a series of three member lanthanide phosphinamido complexes by using alkane elimination route.²² Other approach to introduce the ligand system into the metal chemistry is salt metathesis reaction.

1.1.1. Aminophosphines

Aminophosphines of the type PR_2NHR' containing a direct polar P(III)-N bonds have received considerable attention in recent years as versatile ligands for transition²³ as well as for rare earth metals.^{20b,24} They are accessible in large quantities through the use of relatively simple condensation processes from inexpensive starting materials, i.e., primary amines and PR_2Cl compounds which contain dialkyl or diaryl substituents. Thus, variation

of electronic, steric, and stereochemical parameters may be achieved in a very fascinating way. Due to the presence of soft/ hard donor atoms as well their acidic N-H hydrogen, these poly functional ligands exhibit numerous coordination modes as illustrated in Scheme 1.1.

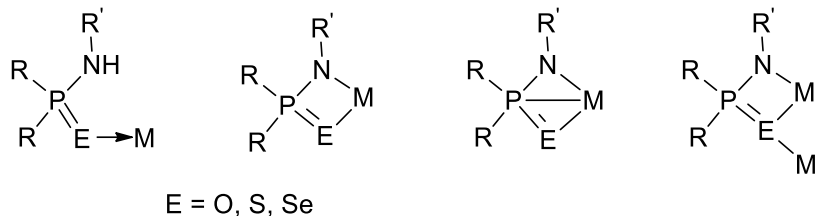


Scheme 1.1. Most common bonding modes of aminophosphine and amidophosphine ligands.

As middle and late transition metals M are concerned, $\text{PR}_2\text{NHR}'$ ligands are typically coordinated in $\kappa^1(\text{P})$ -fashion I,²⁵ while $\kappa^1(\text{N})$ -coordination is yet to know for these metals. Upon deprotonation of the $\text{PR}_2\text{NHR}'$ ligands, anionic amidophosphines $[\text{PR}_2\text{NR}']^-$ are readily obtained which exhibit a higher affinity toward electropositive metals due to their increased nucleophilicity at the N-site. Thus, in conjunction with early transition metals M' , amidophosphine ligands were shown to display $\kappa^2(\text{P,N})$ coordination II, and, albeit less common, also $\kappa^1(\text{N})$ -coordination III, while in the presence of both early and middle/late transition metals, amidophosphine ligands were shown to act as μ^2 bridging ligand thereby forming hetero-bimetallic complexes of the type IV.^{26,27}

1.1.2. Amidophosphine-chalcogenides

Amidophosphine-chalcogenides have attracted much attention in the recent times because of their structural novelty, reactivity and catalytic activity.²⁸⁻³⁹ Presence of three different types of donor sites N, P and E makes the chemistry of these ligands more fascinating as they can coordinate to the metal center in bidentate fashion or in tridentate way. The most possible coordinating modes are illustrated in Scheme 1.2.



Scheme 1.2. Most possible bonding modes of amidophosphine-chalcogenides

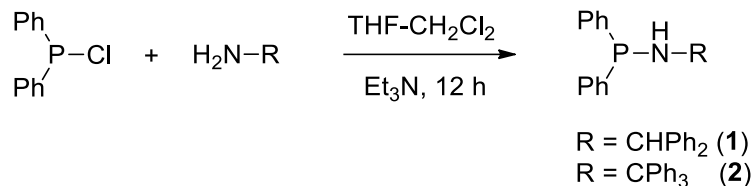
The stability and reactivity of the metal complexes bearing amidophosphine chalcogenide ligands heavily dependent on the nature substituents attached to nitrogen and phosphorus atoms. The weak M-E bond which is a result of hard acid and soft base interaction can be cleaved to create a vacant site which can pave the way to incoming substrates which is a prerequisite for oxidative addition reactions. Thus, such types of hemilabile ligands have great impact on oxidative addition reactions⁴⁰⁻⁴³ which is a key step in many catalytic transformations.

In this chapter, we have described the detailed synthetic procedures, characterizations by various spectroscopic and analytical methods. The molecular structures of the aminophosphines and their chalcogenides have been established by single crystal X-ray diffraction analysis. The bonding modes of various amidophosphine-chalcogenides with group 1 metals were explored by the preparation of alkali metal complexes using sodium and potassium bis(trimethylsilyl)amide and various amidophosphine-chalcogenides in 1:1 molar ratio in toluene/THF. The corresponding sodium and potassium complexes are also fully characterized and their solid state structures were established by single crystal X-ray diffraction technique.

1.2 Results and Discussion

1.2.1. Synthesis of different aminophosphines

The phosphineamines [Ph₂PNHCHPh₂] (**1**) and [Ph₂PNH(CPh₃)] (**2**) were prepared in good yield by the aminolysis reaction using the respective amines and chlorodiphenylphosphine in the presence of triethylamine as base in 1: 2 ratio of THF and CH₂Cl₂ solvent mixture at room temperature (Scheme 1.3).^{44,45}



Scheme 1.3. Synthesis of different aminophosphine ligands

Both the ligands were characterized by using standard spectroscopic and analytical techniques. In addition, crystal structures of compounds **1** and **2** were established by the single crystal X- ray diffraction analysis.

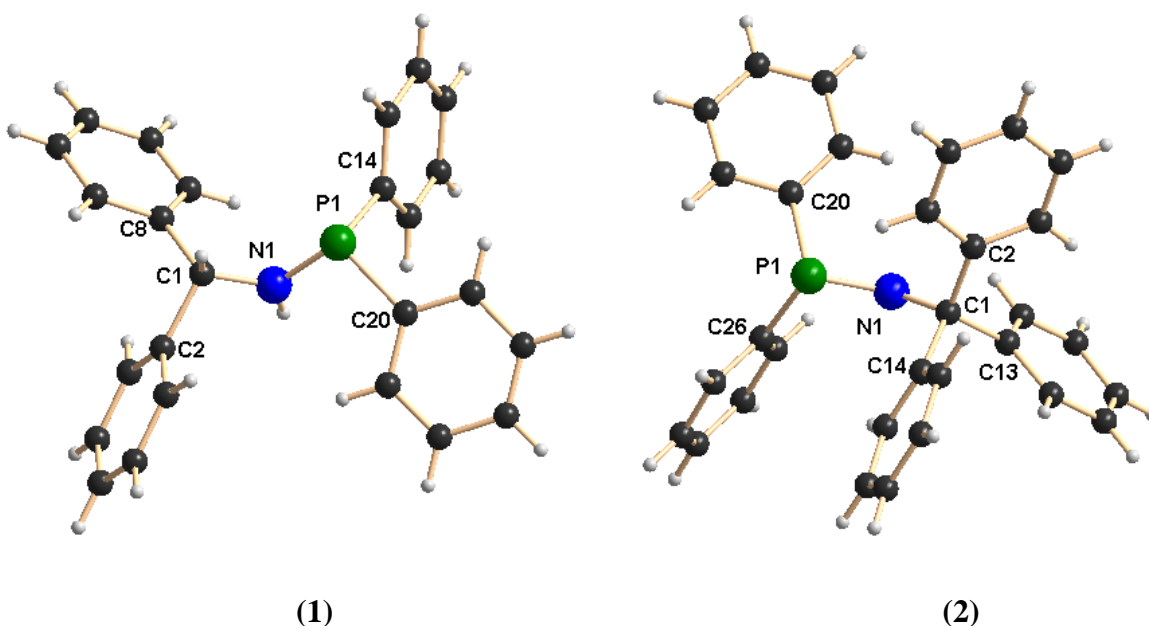


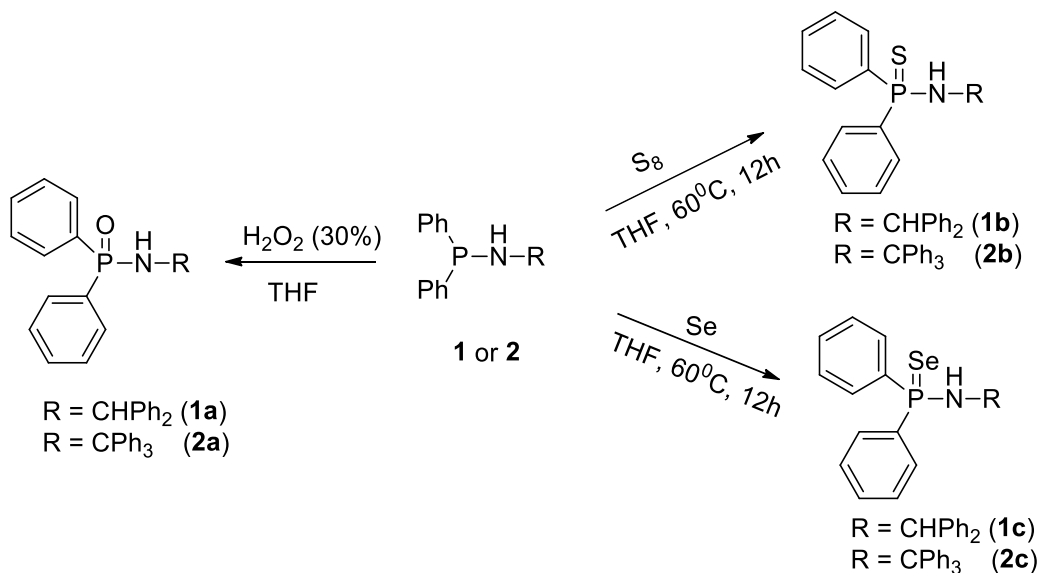
Figure 1.1. Solid State structure of compound **1** and **2**. Selected bond distances (Å) and bond angles (°): **1**: P1-N1 1.673(6), N1-C1 1.453(8), P1-C20 1.841(6), P1-C14 1.842(6), C1-N1-P1 118.2(4), N1-P1 C20 103.0(3), N1-P1-C14 104.2(3), C20-P1-C14 98.1(3); **2**: P1-N1 1.692(4), N1-C1 1.487(6), P1-C20 1.844(6), P1-C28 1.831(5), C1-N1-P1 125.2(3), N1-P1-C20 101.3(2), N1-P1-C26 101.5(2), C26-P1-C20 99.5(2).

$^{31}\text{P}\{^1\text{H}\}$ NMR spectrum of compound **1** shows a signal at 35.2 ppm which is slightly downfield shifted to the corresponding value of compound **2** (26.3 ppm). Compound **1** crystallizes in monoclinic space group *Cc* whereas compound **2** crystallizes in monoclinic space group *P2₁/c*. The Structural parameters are given in Table 1.1. Figure 1.1 shows the solid state structures of compound **1** and **2** respectively. In the solid state structures,

compound **1** and **2** shows similar P-N distances 1.673(6) Å for compound **1** and 1.692(4) Å for compound **2** are within the range of reported values.⁴⁶

1.2.2. Synthesis of different amidophosphine-chalcogenides

The phosphinicamides [Ph₂P(O)NHCHPh₂] (**1a**) and [Ph₂P(O)NH(CPh₃)] (**2a**) were prepared in good yield and high purity by the straight forward reactions involving compounds **1** or **2** with 30% hydrogen peroxide in 1:1 molar ratio at room temperature in THF (Scheme 1.4).⁴⁵ In FT-IR spectra of compound **1a** and **2a**, strong absorption bands at 1181 and 1184 cm⁻¹ were observed and can be assigned to P=O bond stretching frequency along with the absorbance for P-N (997 for **1** and 866 cm⁻¹ for **2**), and N-H (3196 for **1** and 3300 cm⁻¹ for **2**) bond stretching which are well in the expected ranges [47]. In the ³¹P{¹H} NMR spectra one signal is observed at 23.4 and 18.4 ppm for compound **1a** and **2a** respectively (Figure 1.2), representing slightly high field shift compared to their respective phosphineamine resonances.



Scheme 1.4. Synthesis of various amidophosphine-chalcogenides

The compounds **1b** and **2b** were prepared over 90% yield by the reactions involving either compound **1** or **2** and elemental sulfur in 1:1 molar ratio at ambient temperature in THF

(Scheme 1.4).⁴⁵ In FT-IR spectra of compounds **1b** and **2b**, the strong absorptions at 625 and 640 cm^{-1} respectively were observed which can be assigned to the P=S bond stretching frequency for each compound. In the $^{31}\text{P}\{^1\text{H}\}$ NMR spectra, one singlet resonance (60.3 ppm for **1b**, and 53.4 ppm for **2b**) was observed (Figure 1.2) with significant low field shift compared to that of respective phosphineamine compounds **1** and **2**.

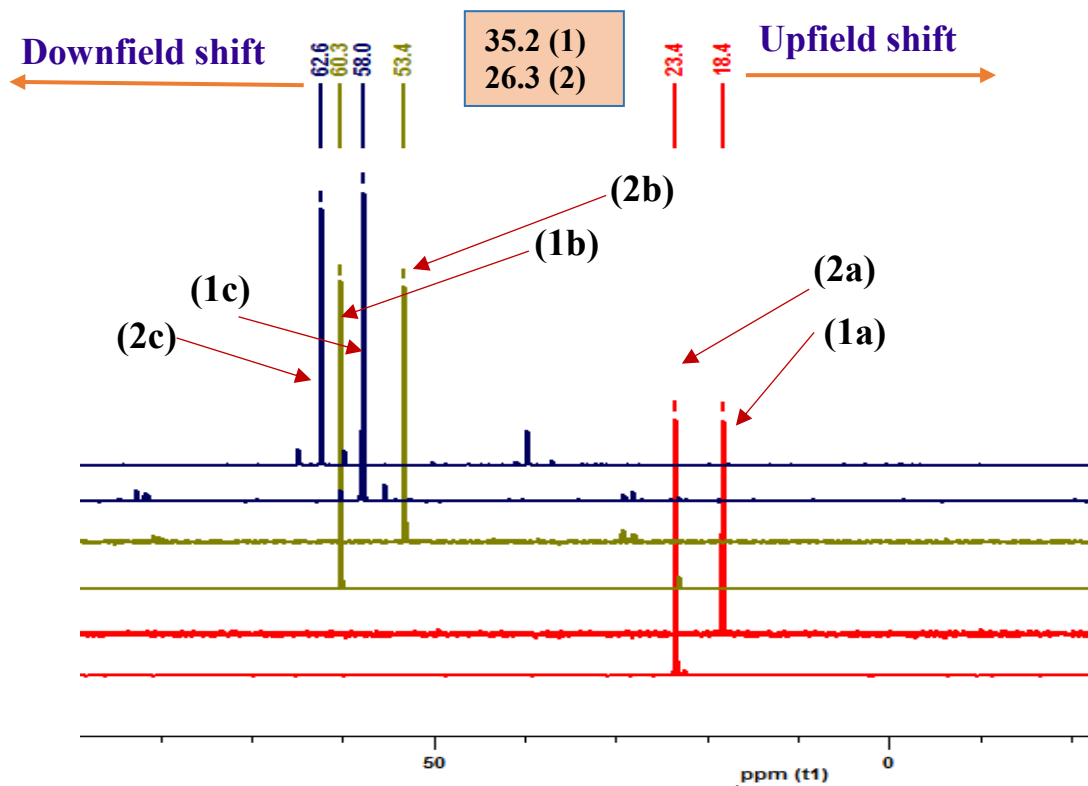


Figure 1.2. Comparison of $^{31}\text{P}\{^1\text{H}\}$ NMR signals of various amidophosphine-chalcogenides recorded at 25°C in CDCl_3 .

In the solid state, compound **2b** crystallizes in the monoclinic space group $P2_1/c$ having four molecules in the unit cell (See Table 1.1). The Solid state structure of compound **2b** was shown in Figure 1.3. The phosphorus atom is tetra-coordinated by two phenyl carbons, one nitrogen atom and one sulfur atom (See Figure. 1.3). The P-S distance 1.9472(8) Å is well agreement to consider the P-S bond as double bond and compatible with literature values (1.9421(7) Å).^{46,47}

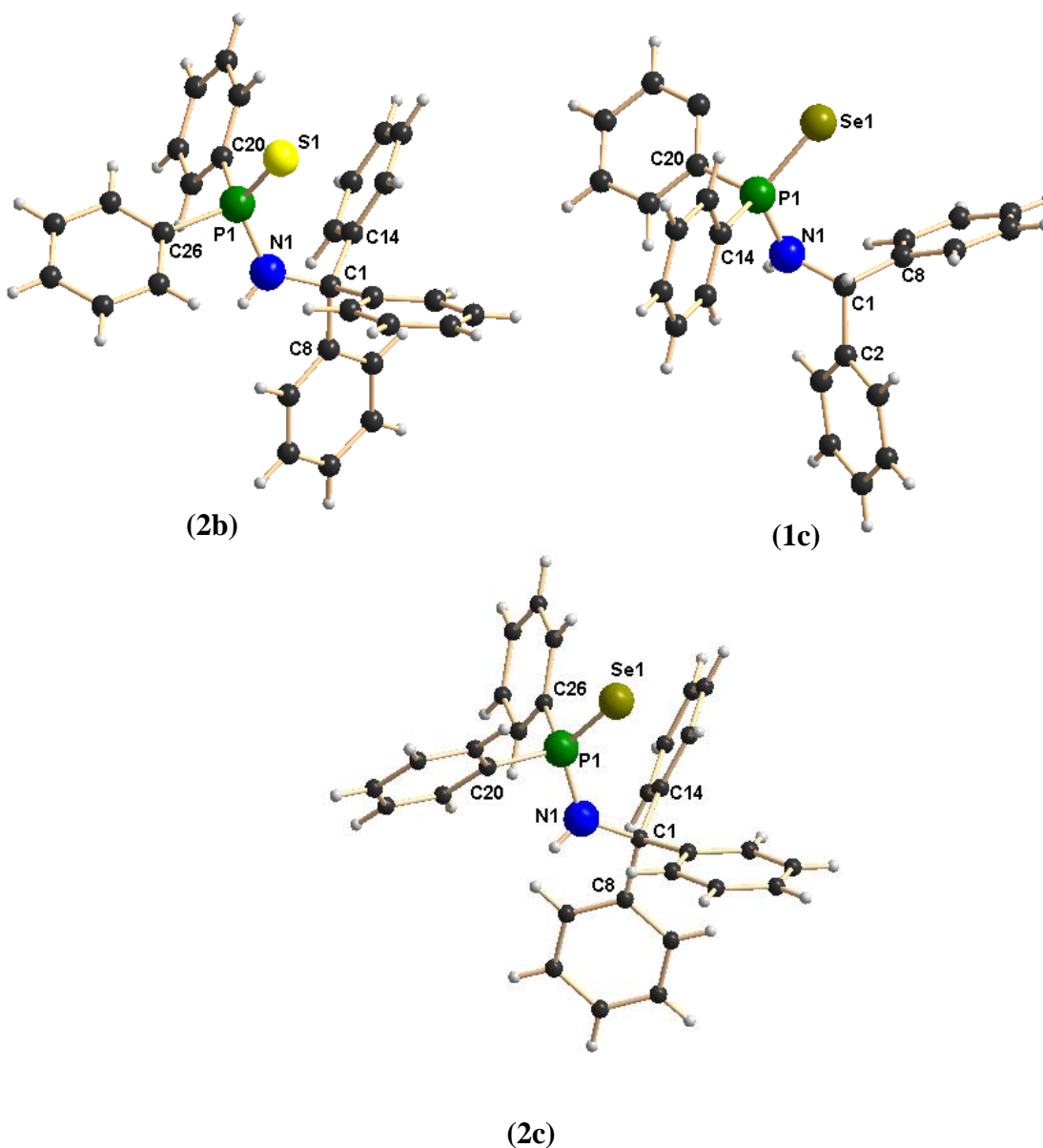
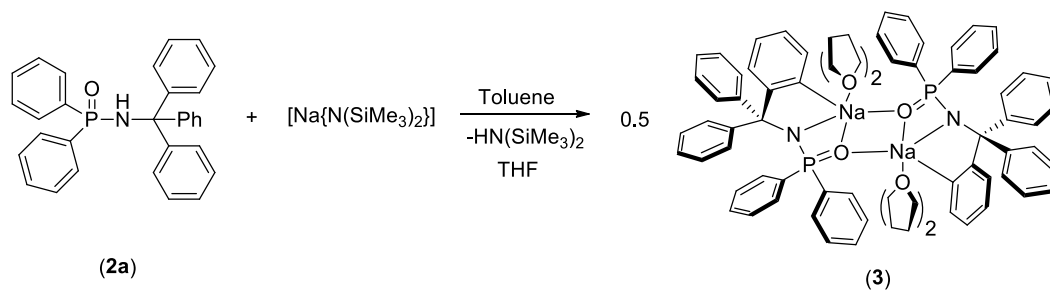


Figure 1.3. Solid State structures of compounds **2b**, **1c** and **2c**. Selected bond distances (Å) and bond angles (°): **2b**: P1-N1 1.6768(17), P1-S1 1.9472(7), P1-C20 1.816(2), P-C26 1.822(2), N1-C1 1.485(2), P1-N1AC1 129.55(13), N1-P1-S1 116.70(6), S1-P1-C20 112.56(7), S1-P1-C26 114.19(7). **1c**: P1-Se1 2.1086(12), P1-N1 1.642(4), P1-C14 1.804(4), P1-C20 1.812(4), N1-C1 1.459(6), C1-C2 1.543(5), C1-C8 1.541(6), Se1-P1-N1 113.75(14), P1-N1-C1 124.1(3), C14-P1-C20 104.16(19), C20-P1-Se1 111.19(14), C14-P1-Se1 114.48(14). **2c**: P1-N1 1.664(2), P1-Se1(1) 2.1166(8), P1-C20 1.826(3), P1-C26 1.825(3), N1-C1 1.496(4), C1-C2 1.541(4), C1-C14 1.540(4), C1-C8 1.547(4), P1-N1-C1 129.4(2), N1-P1-Se1 119.90(10), Se1-P1-C20 111.13(11), Se1-P1-C26 112.96(11).

The phosphinoselenoic amines [Ph₂P(Se)NH(CHPh₂)] (**1c**) and [Ph₂P(Se)NH(CPh₃)] (**2c**) were prepared in quantitative yield by the treatment of the respective phosphineamines, [Ph₂PNH(CHPh₂)] (**1**) and [Ph₂PNH(CPh₃)] (**2**) respectively, with little excess amount of elemental selenium in 1 : 1.2 molar ratio at ambient temperature in THF solvent (Scheme 1.4).⁴⁵ Both the compounds **1c** and **2c** have been characterized by standard analytical/spectroscopic techniques and the solid-state structures were established by single crystal X-ray diffraction analysis. In the FT-IR spectrum of compounds **1c** and **2c**, strong absorption bands at 568 cm⁻¹ and 599 cm⁻¹ respectively, were observed for characteristic P=Se bond stretching frequencies and are comparable with the reported value 555 cm⁻¹.⁴⁸ The characteristic signal of the methine proton (δ 5.62–5.68 ppm) in the ¹H NMR spectrum of compound **1c** is slightly downfield shifted compared to free phosphineamine **1** (δ = 5.26–5.37 ppm). ³¹P{¹H} NMR spectra is more informative as the compound **1c** shows a signal at 58.0 ppm and compound **2c** shows a signal at 62.6 ppm (Figure 1.2), which are slightly downfield shifted from those of compounds **1** (35.2 ppm) and **2** (26.3 ppm) upon addition of selenium atom to phosphorus atom. In the solid state structures, both compounds **1c** and **2c** crystallize in the monoclinic space group *P*2₁/*c*, having four independent molecules along with one THF molecule in the unit cell (Figure. 1.3). The details of the structural parameters are given in Table 1.2. The P–Se bond distances (2.1086(12) Å for **1c** and 2.1166(8) Å for **2c**) are almost the same and in good agreement with our previously observed values 2.1019(8) Å for [Ph₂P(Se)NH(2,6-Me₂C₆H₃)],⁴⁹ and can be considered as phosphorus–selenium double bond. P1–N1 bond distances (1.642(4) Å for **1c** and 1.664(2) Å for **2c**) and C1–N1 distances (1.459(6) for **1c** and 1.496(4) for **2c**) are also similar to those of phosphineamine compounds **1** (P1–N1 1.673(6) Å and C1–N1 1.453(8) Å) and **2** (P1–N1 1.692(4) Å and C1–N1 1.487(6) Å) respectively as shown in the Figure 1.1.

1.2.3. Sodium and potassium complexes

The dimeric sodium complex of molecular formula [{(THF)₂Na(Ph₂P(O)NCPH₃)₂ }] (**3**) was prepared by the reaction of compound **2a** with sodium bis(trimethyl)silylamide in toluene through the elimination of volatile bis(trimethyl)silylamine (Scheme 1.5).⁴⁵



Scheme 1.5. Synthesis of dimeric sodium complex [$\{(THF)_2Na(Ph_2P(O)NCPH_3)\}_2$] (**3**)

The complex **3** crystallizes in triclinic space group $P\bar{1}$ having one molecule in the unit cell (Table 1.2). The solid-state structure and selected bond length and bond angles are shown in Figure 1.4. The sodium complex **3** is centrosymmetric and dimeric in nature where each sodium atom is coordinated by two *P*, *P*-diphenyl-*N*-tritylphosphinicamido groups via one oxygen, one phosphorous and one amido nitrogen atom exhibiting a diamond shaped Na_2O_2 core with mean $O1-Na-O1^i$ of $82.70(10)^\circ$ and $Na1-O1-Na1^i$ of $97.30(10)^\circ$ angles. Both the oxygen atoms are bridging coordinated with two sodium atoms. In addition, each phosphorus atom is coordinated to each sodium atom to form highly strained three membered metallacycles having $P1-Na1$ $3.0348(17)$ Å. In complex **3**, two parallel planes containing $Na1, O1, P1, N1$ and $Na1^i, O1^i, P1^i, N1^i$ atoms are placed at a distance of 0.429 Å and two planes containing $Na1, O1, P1, N1$ and $Na1, O1, Na1^i, O1^i$ make a dihedral angle of 10.25° . A short contact $Na\dots H$ between sodium and one of the phenyl proton ($Na1\dots C19$ $3.086(4)$ Å and $Na1\dots H1a$ 2.598 Å) is observed which can be attributed as remote or secondary $M\dots C\dots H$ interaction.⁵⁰ However, in solution all phenyl protons are appeared equivalent as observed in 1H NMR study presumably due to dynamic behavior of the complex. Thus in the solid state, two additional five member metallacycles $Na1-N1-C1-C14-C19$ and $Na1^i-N1^i-C1^i-C14^i-C19^i$ are formed. An unusual structural motif is formed by fusion of four three member and two five member metallacycle rings.

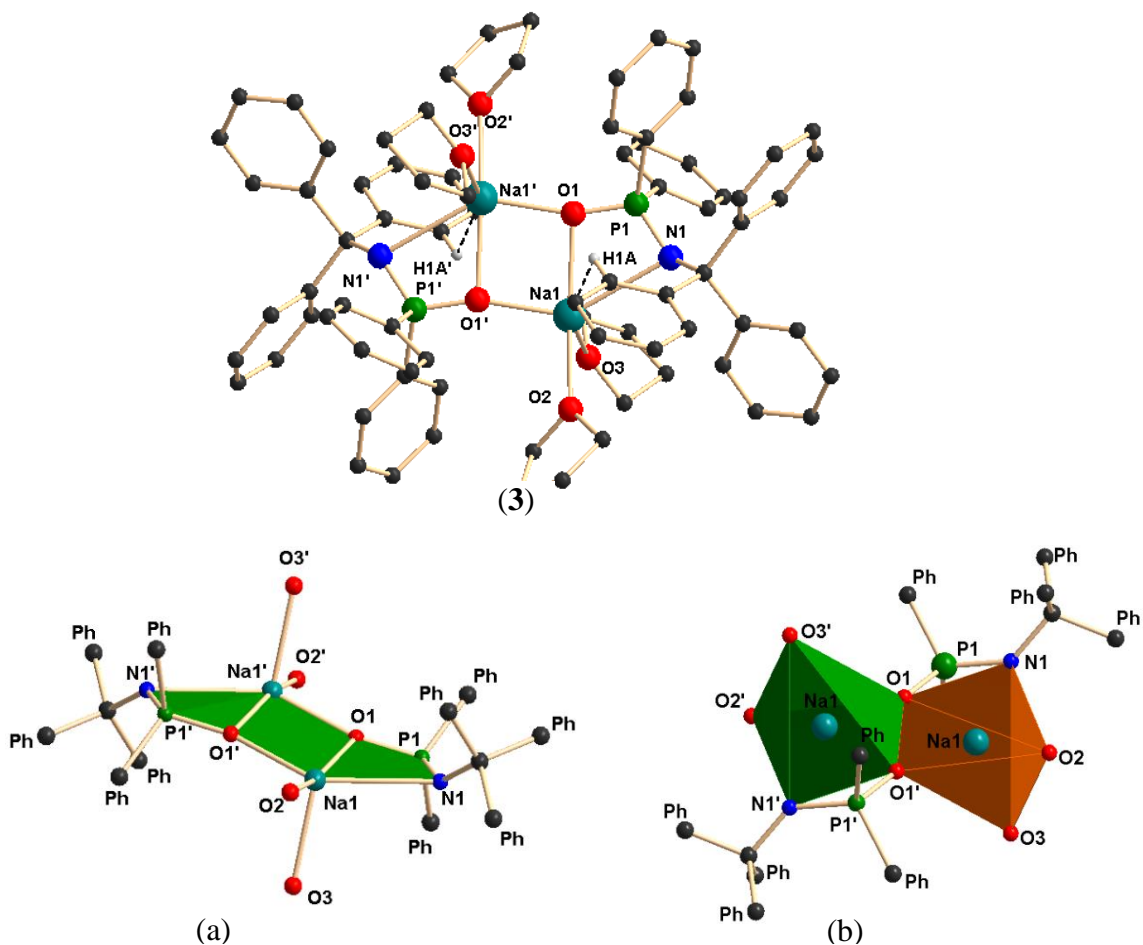
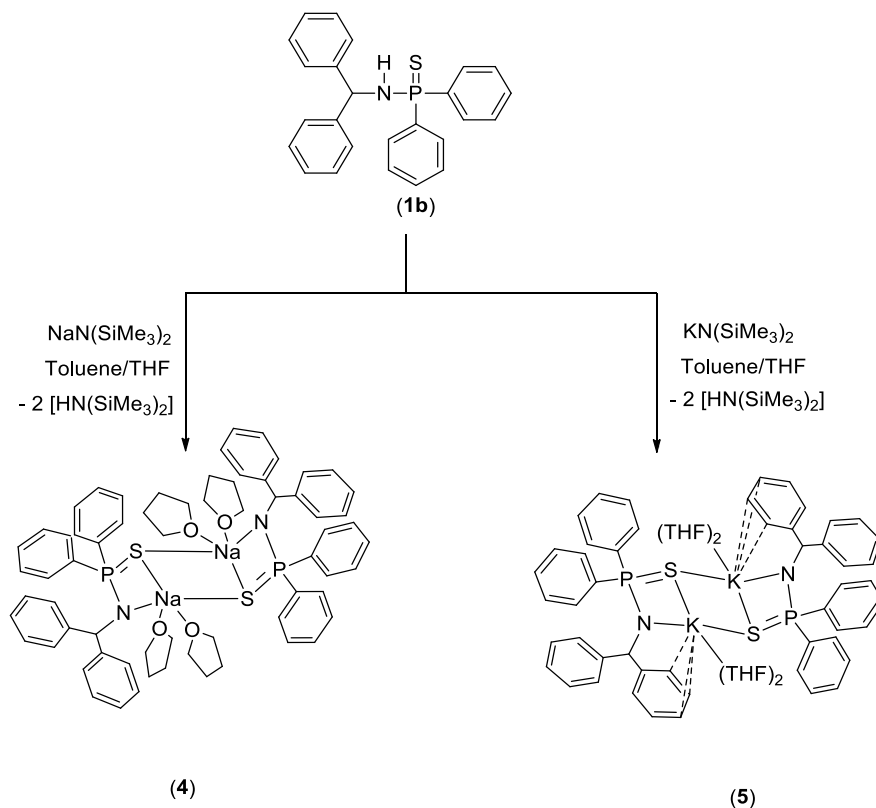


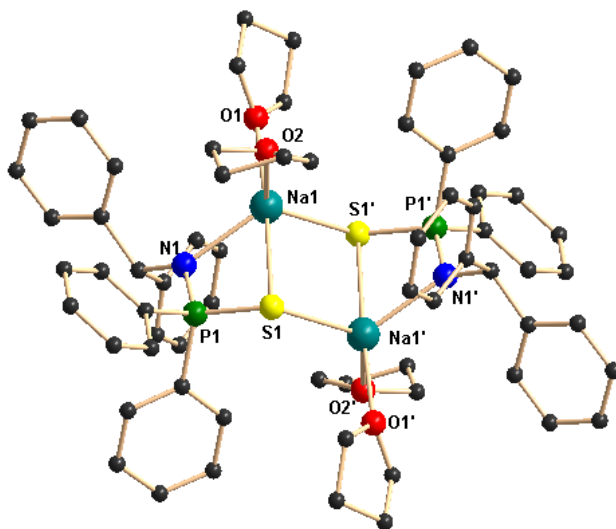
Figure 1.4. Solid state structure of compound **3**. Hydrogen atoms are omitted for clarity except H1A: (a) represents the 8-membered metallacyclic ring in **3**; (b) represents the geometry around each sodium ion in **3** (phenyl groups are omitted and represented as single carbon atom in (a) and (b) for clarity). Selected bond distances (Å) and bond angles (°): Na1-N1 2.792(3), Na1-P1 3.0348(17), Na1-O1 2.369(3), Na1-C19 3.086(4), Na1-O1ⁱ 2.218(3), Na1-O2 2.363(3), Na1-O3 2.338(3), Na1-N1-P1 83.20(12), P1-O1 1.520(2), P1-N1 1.564(3), Na1-P1-O1 50.16(10), Na1-O1-P1 100.31(13), N1-Na1-P1 30.79(6), P1-Na1-O1 29.52(6), Na1-N1-C1 118.3(2), C19-Na1-O1 78.12(10), C19-Na1-O2 82.93(11), C19-Na1-O3 149.33(11), C19-Na1-P1 68.72(8), C19-Na1-N1 57.91(9), N1-Na1-O1 59.85(9), O1-Na1-O1ⁱ 82.70(10), O3-Na1-O1 110.59(11), O2-Na1-O1 160.76(12), O1ⁱ-Na1-P1 112.19(9), O1ⁱ-Na1-C19 107.54(11), O1-P1-N1 114.94(15), Na1-O1-Na1ⁱ 97.30(10).

The sulfur analogue of complex 3 having molecular formula $[(\text{THF})_2\text{Na}(\text{Ph}_2\text{P}(\text{S})\text{NCHPh}_2)]_2$ (**4**) was prepared by the reaction of compound **1b** and sodium bis(trimethyl)silylamide in THF through the elimination of volatile bis(trimethyl)silylamine (Scheme 1.6).⁴⁵



Scheme 1.6. Synthesis of Na and K complexes of diphenylphosphinothioic amide (**1b**)

The sodium complex **4** crystallizes in triclinic space group $P-1$ having one molecule in the unit cell (Table 1.3). The solid-state structure of complex **4** and selected bond lengths and bond angles were shown in Figure 1.5. In the centrosymmetric molecule **4**, two phosphinothioic amide ligands are coordinating to two sodium atoms by one sulfur, one phosphorus and one amido nitrogen atom exhibiting a diamond shaped Na_2S_2 core with mean S1-Na-S1^i of $99.43(4)^\circ$ and Na1-S1-Na1^i of $80.57(4)^\circ$ angles. The Na1-S1 and Na1-S1^i bond distances are also almost similar $2.9521(15)$, and $2.8570(16)$ Å. Each of the sulfur atoms is μ -coordinated in between the two sodium atoms. Additionally, each phosphorus atom is coordinated to each sodium atom to form highly strained three



(4)

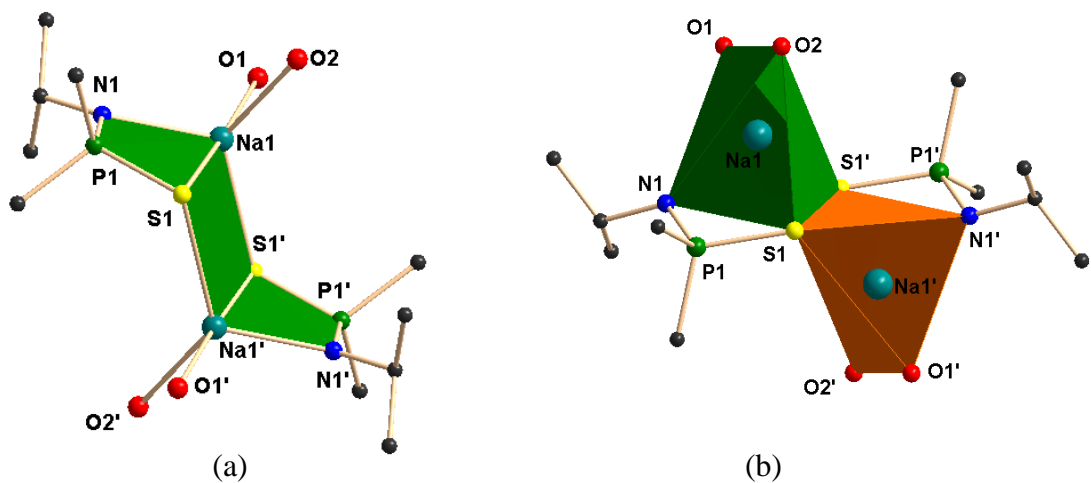
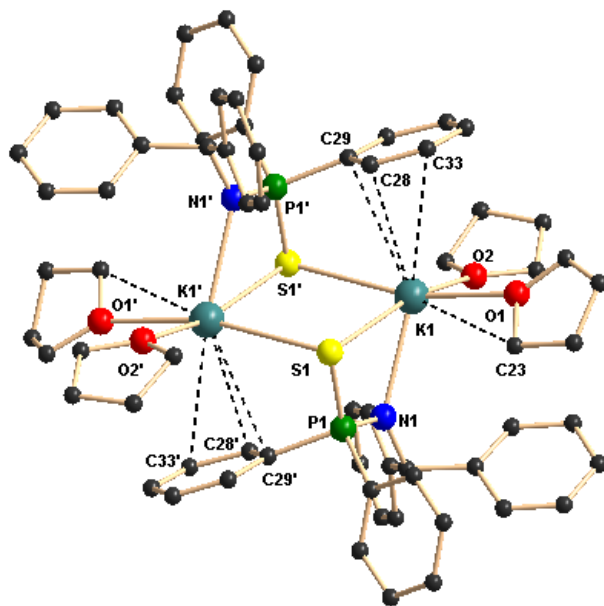


Figure 1.5. Solid state structure of compound **4**. Hydrogen atoms are omitted for clarity; a represents the 8-membered metallacyclic ring having chair conformation of **4**; (b) represents the geometry of the each sodium ion in **4** (phenyl groups are omitted and represented as single atom in (a) and (b) for clarity). Selected bond distances (Å) and bond angles (°): Na1-N1 2.381(3), Na1-P1 3.1733(14), Na1-S1 2.9521(15), Na1-S1ⁱ 2.8570(16), Na1-O1 2.378(3), N1-O2 2.418(3), N1-P1 1.593(3), P1-S1 1.9934(12), N1-Na1-P1 29.11(6), N1-Na1-S1 66.87(7), N1-Na1-S1ⁱ 118.37(8), P1-Na1-S1 37.77(3), P1-Na1-S1ⁱ 115.24(5), S1-Na1-S1ⁱ 99.43(4), N1-Na1-O1 112.89(11), N1-Na1-O2 109.53(10), Na1-P1-S1 77.15(4), Na1-S1-Na1ⁱ 80.57(4), P1-Na1-O1 141.01(9), P1-Na1-O2 98.46(7), S1-

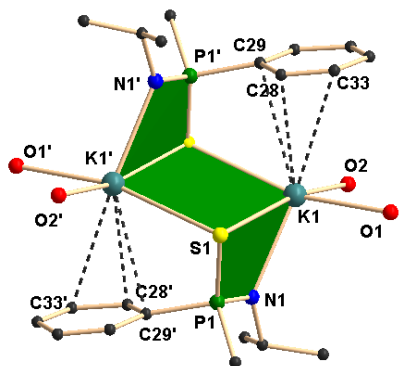
Na1-O1 171.28(8), S1-Na1-O2 84.45(7), Na1-S1ⁱ-P1ⁱ 115.85(5), O1-Na1-O2 87.59(10), O1-Na1-S1ⁱ 88.36(7), O2-Na1-S1ⁱ 129.39(8), N1-P1-C1 113.26(14).

membered metallacycles having P1-Na1 3.1733(14) Å. In complex **4**, two additional THF molecules are also coordinated to each sodium atom and the geometry of each sodium atom can be best described as distorted trigonal bipyramidal. The bond distances Na1-N1 2.381(3), Na1-O1 2.378 (3), and Na1-O2 2.418(3) Å are in the range of Na-O distances observed in complex **3** [2.338(3) to 2.363(3) Å]. The whole structure consists four three member rings fused together forming a penta-metallacyclo [4.2.0.0^{1,7}.0^{2,5}.0^{2,4}] octane structure. To the best of our knowledge, this is the first example of such kind of structural motif in sodium complexes.⁵¹

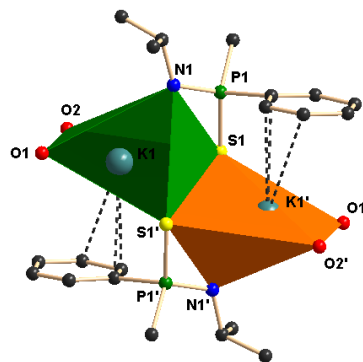
The dimeric potassium complex of molecular formula [$\{K(THF)_2Ph_2P(S)N(CHPh_2)\}_2$] (**5**) was prepared by the reaction of diphenylphosphinothioicamine [$Ph_2P(S)NH(CHPh_2)$] (**1b**) and potassium bis(trimethyl)silylamide in THF at ambient temperature through the elimination of volatile bis(trimethyl)silylamine (Scheme 1.6).⁴⁵ In FT-IR spectra of the compound **5** shows strong absorption at 632 cm⁻¹ can be assigned to P=S bond stretching frequency which is comparable with observed value 625 cm⁻¹ for the sodium complex **4**. In ¹H NMR spectra of the potassium complex **5** measured in C₆D₆, one set of signals were observed indicating the dynamic behavior of compound **5**. The characteristic doublet for the methine proton (δ 5.91 ppm) is slightly downfield shifted compare to free **1b** (δ 5.61 ppm). The coupling constant of 23.6 Hz (for **5**) was observed due to the coupling of α -proton and the phosphorus atom attached to nitrogen. The multiplet signals δ 3.58 and 1.40 ppm for compound **5** could be assigned to solvated THF molecules coordinated to the potassium ion. Additionally, one set of signals for the phenyl protons is also observed which is in the same range to that of ligand **1b**, indicating no significant effects of metal atoms on the phenyl groups due to complex formation. ³¹P{¹H} NMR spectra of compound **5** shows a signal at 73.2 ppm which is slightly downfield shifted to that of compound **1b** (60.3 ppm) upon addition of potassium atom onto the diphenylphosphinothioicamido moiety.



(5)



(a)



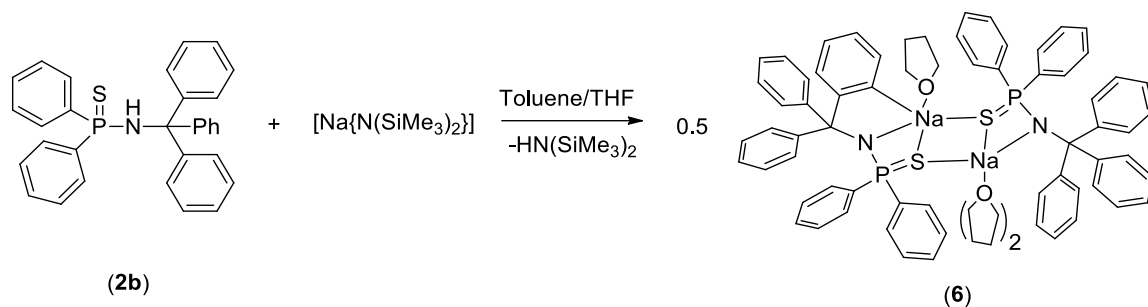
(b)

Figure 1.6. Solid state structure of compound **5**. Hydrogen atoms are omitted for clarity; (a) represents the 8-membered metallacyclic ring having chair conformation of complex **5**; (b) represents the geometry of the each potassium ion present in complex **5** (phenyl groups are omitted and represented as single carbon atom in (a) and (b) for clarity). Selected bond distances (Å) and bond angles (°): K1-N1 2.725(3), K1-S1 3.3702(13), K1-S1ⁱ 3.2394(13), K1-O1 2.711(3), K1-O2 2.668(3), K1-C33 3.514(4), K1-C28 3.194(4), K1-C29 3.326(4), K1-P1 3.5354(14), N1-P1 1.590(3), P1-S1ⁱ 1.9933(12), S1-K1-S1ⁱ 89.94(3), S1ⁱ-K1-N1 59.32(6), S1ⁱ-K1-P1 33.86(2), S1ⁱ-K1-O1 98.68(8), S1ⁱ-K1-O2 166.56(8), N1-K1-P1

25.46(6), N1-K1-O1 101.94(10), N1-K1-O2 107.39(10), N1-K1-S1 91.58(7), K1-S1-K1ⁱ 90.06(3), O1-K1-S1 166.33(8), O2-K1-S1 88.41(7).

Complex **5** crystallizes in triclinic space group *P*-1 having one molecule in the unit cell. The details of the structural parameters are given in Table 1.3. The solid state structure of the complex **5** is given in Figure 1.6. Each potassium ion in the dimeric complex **5** is coordinated by one {Ph₂P(S)N(CHPh₂)}⁻ ligand and two THF molecules. In complex **5**, a diamond shaped K₂S₂ core with mean S1-K1-S1ⁱ of 89.94(3)^o and K1-S1-K1ⁱ of 90.06(3)^o angles is observed. The K1-S1 bond distance (3.3702(13) Å), is slightly elongated compared to K1-S1ⁱ bond distance (3.2394(13) Å). Each of the sulfur atoms is μ-coordinated to each of the two potassium atoms. Additionally, each phosphorus atom is weakly coordinated to each potassium atom to form highly strained three membered metallacycles having P1-K1 distance of 3.5354(14) Å. Two additional THF molecules are also coordinated to each potassium atom to adopt as distorted trigonal bipyramidal geometry for each potassium metal atom. Short contacts between phenyl carbons and the potassium atom (K1...C28 (3.194(4) Å, K1...C29 (3.326(4) Å and K1...C33 3.514(4) Å) indicate a strong electron donation from the phenyl group to the positively charged potassium ion. However, in solution all phenyl carbon atoms appeared equivalent as observed in ¹³C{¹H} NMR study presumably due to dynamic behavior of the complex **5**. Considering all the interactions between potassium and other atoms, an unusual poly metallacyclic structural motif is formed. However, to the best of our knowledge, this is the first example of this kind of structural motif in potassium complexes having adjacent nitrogen, phosphorus and sulfur atoms in the coordination sphere.

The dimeric sodium salt [{(THF)₂Na(Ph₂P(S)NCPH₃)}{(THF)Na(Ph₂P(S)NCPH₃)}] (**6**) was prepared in a similar fashion involving the reaction of bulky phosphinthioic amide **2b** with sodium bis(trimethyl)silyl amide in toluene at room temperature via the elimination of volatile hexamethyldisilazane (Scheme 1.7).⁴⁵



Scheme 1.7. Synthesis of dimeric sodium complex of triphenylphosphinothioicamide (**2b**)

In the solid state, the sodium complex **6** is non-centrosymmetric and dimeric and two phosphinothioic amide ligands are coordinating to two sodium ions by sulfur, phosphorus and one amido nitrogen atom exhibiting a diamond shaped Na_2S_2 core with mean S1-Na1-S2 of $96.02(4)^\circ$ and S1-Na2-S2 $88.10(4)^\circ$ and Na1-S1-Na2 $84.96(4)^\circ$ and Na1-S2-Na2 $89.65(4)^\circ$ angles. Each of the sulfur atoms is μ -coordinated in between the two sodium atoms. In complex **6**, sodium atom Na2 is attached to two THF molecules and adopts distorted octahedral geometry whereas the second sodium atom Na1 is coordinated only with one THF molecule and one phenyl carbon (C10) making a distance of 3.017 \AA (Na1...H 2.649 \AA) can be attributed as short M-C-H interactions.⁵⁰ However, in solution all phenyl protons are equivalent as observed in ^1H NMR spectra. Thus, a five member metallacycle Na1-N1-C1-C9-C10 is formed and the geometry of Na1 is best described as distorted trigonal bipyramidal. In complex **6**, whole structure consists three four membered rings along with one five member ring fused together forming a hexametallacyclo-[5.4.0.0^{1,5}.0^{1,6}.0^{8,10}.0^{8,11}] undecane structure (Figure 1.7). To the best of our knowledge, this kind of structural motif is not previously described in the literature for sodium compounds.⁵¹ The three member metallacycles are highly strained as we can observe from the angles Na1-N1-P1 $29.73(5)^\circ$, N1-P1-S1 $60.15(4)^\circ$, P1-S1-N1 $80.56(4)^\circ$ and S1-Na1-N1 $68.52(6)^\circ$. Even though the complex **6** is non-centrosymmetric in the solid state, only one set of signals were recorded in the ^1H , $^{31}\text{P}\{^1\text{H}\}$ and $^{13}\text{C}\{^1\text{H}\}$ NMR spectra.

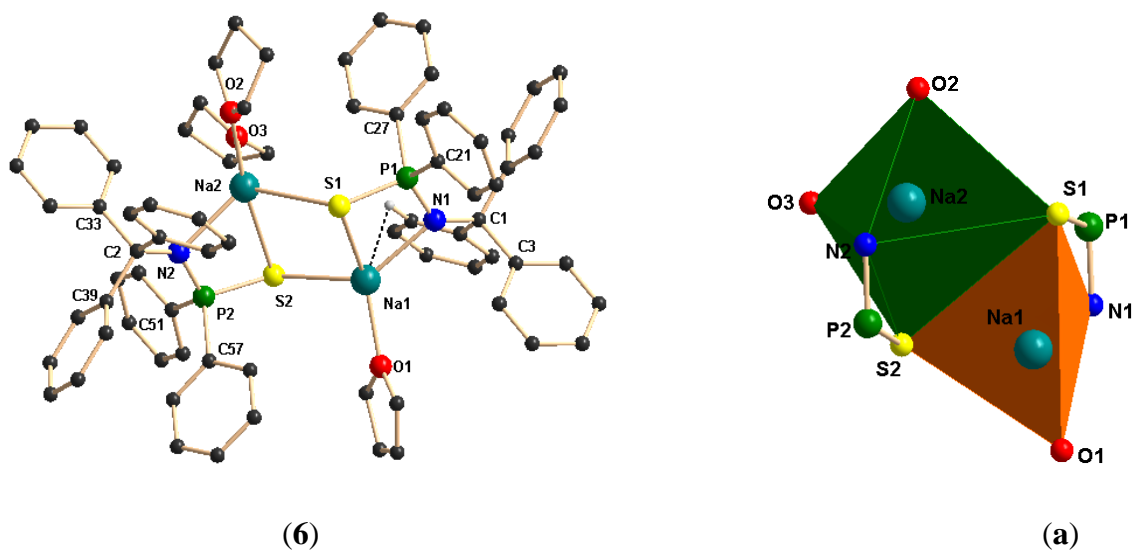


Figure 1.7. Solid state structure of compound **6**. Hydrogen atoms are omitted for clarity. (a) represents the geometry of the each sodium ion in **6** (phenyl groups are omitted in a for clarity). Selected bond distances (Å) and bond angles (°): Na1-O1 2.271(3), Na1-N1 2.430(2), Na1-S1 2.7580(15), Na1-S2 2.8498(15), Na1-P1 3.1367(13), Na2-O2 2.299(3), Na2-N2 2.419(2), Na2-O3 2.535(3), Na2-S2 2.8307(14), Na2-S1 3.1553(16), Na2-P2 3.1616(13), Na1-C10 3.017(3), O1-Na1-N1 120.41(10), O1-Na1-S1 141.00(10), N1-Na1-S1 68.52(6), O1-Na1-S2 98.54(8), N1-Na1-S2 134.94(8), S1-Na1-S2 96.02(4), O1-Na1-C10 111.15(11), N1-Na1-C10 60.86(8), S1-Na1-C10 105.86(7), S2-Na1-C10 85.67(7), O1-Na1-P1, 142.72(8), N1-Na1-P1 29.73(5), S1-Na1-P1 39.29(2), S2-Na1-P1 118.67(5), C10-Na1-P1 76.08(6), O1-Na1-Na(2) 136.71(8), N1-Na1-Na2 102.78(7), O2-Na2-N2 118.77(10), O2-Na2-O3 90.38(10), N2-Na2-O3 106.30(10), O2-Na2-S2 172.92(8), N2-Na2-S2 68.14(6), O3-Na2-S2 88.87(8), O2-Na2-S1 87.01(8), N2-Na2-S1 118.34(8), O3-Na2-S1 130.16(8), S2-Na2-S1 88.10(4), O2-Na2-P2 147.99(8), N2-Na2-P2 29.25(5), O3-Na2-P2 100.55(8), S2-Na2-P2 38.89(2), S1-Na2-P2 107.49(4), P1-S1-Na1 80.56(4), P1-S1-Na2 119.37(5), Na1-S1-Na2 84.96(4), P2-S2-Na2 79.45(4), P2-S2-Na1 128.52(5), Na2-S2-Na1 89.65(4), N1-P1-S1 108.69(9), S1-P1-Na1 60.15(4), N2-P2-S2 110.01(9), N2-P2-Na2 48.35(8), S2-P2-Na2 61.66(4).

1.3 Conclusion

We have reported two bulky phosphinamines and their respective chalcogenide derivatives which can able to stabilize the group 1 metal ions through coordination of amido nitrogen, phosphorous and chalcogenide atoms. Using the phsophinamine chalcogenides three different sodium and one potassium complexes were prepared where two different unusual structural motifs of pentametallacyclo-[4.2.0.0^{1,7}.0^{2,5}.0^{2,4}] octane and hexametalla-cyclo-[5.4.0.0^{1,5}.0^{1,6}.0^{8,10}.0^{8,11}] undecane are observed. The sodium or potassium complexes having various structural motifs can serve as the structural synthon for group 2, d-block and f-block metallacycles via salt metathesis reaction.

1.4 Experimental Procedures

1.4.1. General

All manipulations of air-sensitive materials were performed with the rigorous exclusion of oxygen and moisture in flame-dried Schlenk-type glassware either on a dual manifold Schlenk line, interfaced to a high vacuum (10^{-4} torr) line, or in an argon-filled M. Braun glove box. THF was pre-dried over Na wire and distilled under nitrogen from sodium and benzophenone ketyl prior to use. Hydrocarbon solvents (toluene and *n*-pentane) were distilled under nitrogen from LiAlH₄ and stored in the glove box. ¹H NMR (400 MHz), ¹³C{¹H} and ³¹P{¹H} NMR (161.9 MHz) spectra were recorded on a BRUKER AVANCE III-400 spectrometer. BRUKER ALPHA FT-IR was used for FT-IR measurement. Elemental analyses were performed on a BRUKER EURO EA at the Indian Institute of Technology Hyderabad. The starting materials chlorodiphenylphosphine, benzdihydrylamine, triphenylmethyl amine, adametylamine, sulfur-S₈, selenium metal powder and sodium/potassium bis(trimethyl)silylamides were purchased from Sigma Aldrich and used without further purification. The NMR solvents C₆D₆ and CDCl₃ were purchased from sigma Aldrich.

1.4.2. Synthesis of [Ph₂PNHCHPh₂] (1)

In a flame dried Schlenk flask 1.32 g (6.0 mmol) of chlorodiphenylphosphene was dissolved in 5 ml of dry THF. To this, benzhydrylamine (1.09 g, 6.0 mmol) and triethylamine (0.62 g, 6.0 mmol) in 10 ml of mixture of THF and CH₂Cl₂ solvents in 1:2 ratio was added dropwise at ice-cold temperature under constant stirring. Immediate white turbidity was observed. The solution mixture was stirred for another 3h at room temperature, and then white precipitate formed due to triethylammoniumchloride was filtered off by using G4 frit and filtrate was collected. Pale yellow powder was obtained upon evaporation of solvent and pure compound **1** was obtained after recrystallization from the hot toluene or THF/*n*-pentane mixture. Yield was 2.0 g (90%).

¹H NMR (400 MHz, CDCl₃): δ 7.00-7.34 (m, 20H, ArH), 5.26-5.37 (dd, 1H, *J* = 6.67 Hz, 2.37 Hz, CH), 2.52 (br t, 1H, *J* = 6.5 Hz, NH) ppm. ¹³C{¹H} NMR (100 MHz, CDCl₃): δ 144.8 (ArC), 144.7 (ArC), 141.9 (P-ArC), 141.8 (P-ArC), 131.4 (P attached *o*-ArC), 131.2 (P attached *o*-ArC), 128.5 (*m*-ArC), 128.4 (*o*-ArC), 128.2 (P attached *p*-ArC), 128.1 (P attached *p*-ArC), 127.4 (P attached *m*-ArC), 126.9 (*p*-ArC), 65.2, 65.0 (CH) ppm. ³¹P{¹H}NMR (161.9 MHz, CDCl₃): δ 35.2 ppm. FT-IR (selected frequencies): ν = 3262 (N-H), 1432 (P-C), 876 (P-N) cm⁻¹. Elemental analysis (C₂₅H₂₂NP): Calcd. C 81.72, H 6.04, N 3.81; Found C 80.96, H 5.82, N 3.43.

1.4.3. Synthesis of [Ph₂PNHCPh₃] (2)

Same as above for **1** Yield is 2.0 g (90%). ¹H NMR (400 MHz, CDCl₃): δ 7.29-7.31 (m, 6H, ArH), 7.06-7.16 (m, 19H, ArH), 3.06 (d, 1H, *J* = 9.8 Hz, NH) ppm. ¹³C{¹H} NMR (100 MHz, CDCl₃): δ 147.4 (ArC), 147.3 (ArC), 135.3 (P-ArC), 135.2 (P-ArC), 131.3 (P attached *o*-ArC), 131.2 (P attached *o*-ArC), 128.9 (*o*-ArC), 128.2 (P attached *p*-ArC), 128.1 (P attached *m*-ArC), 128.0 (P attached *m*-ArC), 127.8 (*m*-ArC), 126.5 (*p*-ArC), 71.32 (triphenylmethyl C) ppm. ³¹P{¹H}NMR (161.9 MHz, CDCl₃): δ 26.3 ppm. FT-IR (selected frequencies): ν = ≈ 3300 (very weak broad N-H), 1434 (P-C), 896 (P-N) cm⁻¹. Elemental analysis (C₃₁H₂₆NP): Calcd. C 83.95, H 5.91, N 3.16; Found C 83.26, H 5.72, N 2.91.

1.4.4. Synthesis of [Ph₂P(O)NHCHPh₂] (**1a**)

A 30% solution of H₂O₂ (0.15 ml) was added to a THF solution (10 ml) of N-benzhydryl-1,1-diphenylphosphinamine (500 mg, 1.46 mmol) with stirring and cooling. When the exothermal process was finished the mixture was evaporated in *vacuo*. A white powder was isolated, which was washed with *n*-pentane and then dried in *vacuo*. Yield was 0.525 g (100%).

¹H NMR (400 MHz, CDCl₃): δ 7.73-7.78 (m, 4H, ArH), 7.36-7.39 (m, 2H, ArH), 7.26-7.31 (m, 4H, ArH), 7.14-7.24 (m, 10H, ArH), 5.34-5.40 (t, 1H, *J* = 10.84 Hz, CH), 3.16-3.19 (t, 1H, *J* = 9.09 Hz, NH) ppm. ¹³C{¹H} NMR (100 MHz, CDCl₃): δ 143.4 (ArC), 143.3 (ArC), 132.9 (P-ArC), 132.3 (P attached *o*-ArC), 132.2 (P attached *o*-ArC), 131.9 (P attached *p*-ArC), 131.6 (P-ArC), 128.5 (*m*-ArC), 128.4 (P attached *m*-ArC), 128.3 (P attached *m*-ArC), 127.6 (*o*-ArC), 127.2 (*p*-ArC), 58.6 (CH) ppm. ³¹P{¹H}NMR (161.9 MHz, CDCl₃): δ 23.4 ppm. FT-IR (selected frequencies): ν = 3196 (N-H), 1435 (P-C), 997 (P-N), 1181 (P=O) cm⁻¹. Elemental analysis (C₂₅H₂₂NPO): Calcd. C 78.31, H 5.78, N 3.65; Found C 77.79, H 5.61, N 3.42.

1.4.5. Synthesis of [Ph₂P(O)NHCPH₃] (**2a**)

Same as above for compound **1a** Yield was 0.525 g (100%). ¹H NMR (400 MHz, CDCl₃): δ 7.61-7.66 (m, 4H, ArH), 7.15-7.28 (m, 13H, ArH), 7.08-7.09 (m, 8H, ArH), 4.20-4.19 (d, 1H, *J* = 5.12 Hz, NH) ppm. ¹³C{¹H} NMR (100 MHz, CDCl₃): δ 144.0 (ArC), 143.9 (ArC), 134.3 (P-ArC), 133.0 (P-ArC), 130.6 (P attached *o*-ArC), 130.5 (P attached *o*-ArC), 130.0 (P attached *p*-ArC), 128.5 (*m*-ArC), 127.2 (P attached *m*-ArC), 127.1 (P attached *m*-ArC), 126.6 (*o*-ArC), 126.2 (*p*-ArC), 70.2 (triphenylmethyl C) ppm. ³¹P{¹H}NMR (161.9 MHz, CDCl₃): δ 18.4 ppm. FT-IR (selected frequencies): ν ≈ 3300 (very weak broad N-H), 1439 (P-C), 866 (P-N), 1184 (P=O) cm⁻¹. Elemental analysis (C₃₁H₂₆NPO): Calcd. C 81.03, H 5.70, N 3.05; Found C 80.75, H 5.31, N 2.87.

1.4.6. Synthesis of [Ph₂P(S)NHCHPh₂] (**1b**)

N-benzhydryl-1,1-diphenylphosphinamine (300 mg, 0.82mmol) and elemental sulfur S₈ (26.3 mg, 0.82 mmol) were heated to 60 °C in toluene (5 ml) for 6 h. After removal of solvent in *vacuo* white solid was obtained. The title compound [Ph₂P(S)NHCHPh₂] was recrystallized from hot toluene. (Yield: 300 mg, (92%).

¹H NMR (400 MHz, CDCl₃): δ 7.74-7.79 (m, 4H, ArH), 7.32-7.36 (m, 2H, ArH), 7.12-7.28 (m, 12H, ArH), 5.58-5.64 (dd, 1H, *J* = 8.71 Hz, 5.72 Hz, CH), 3.16-3.19 (dd, 1H, *J* = 5.21 Hz, *J* = 2.58 Hz, NH) ppm. ¹³C{¹H} NMR (100 MHz, CDCl₃): δ 143.2 (ArC), 143.1 (ArC), 134.7 (P-ArC), 133.7 (P-ArC), 131.8 (P attached *o*-ArC), 131.7 (P attached *o*-ArC), 131.6 (P attached *p*-ArC), 131.5 (P attached *p*-ArC), 128.4 (*m*-ArC), 128.3 (P attached *m*-ArC), 128.2 (P attached *m*-ArC), 127.8 (*o*-ArC), 127.2 (*p*-ArC), 58.9 (CH) ppm. ³¹P{¹H} NMR (161.9 MHz, CDCl₃): δ 60.3 ppm. FT-IR (selected frequencies): ν = 3261 (N-H), 1432 (P-C), 902 (P-N), 625 (P=S) cm⁻¹. Elemental analysis (C₂₅H₂₂NPS): Calcd. C 75.16, H 5.55, N 3.51; Found C 74.87, H 5.44, N 3.37.

1.4.7. Synthesis of [Ph₂P(S)NHCPh₃] (**2b**)

Same as above for **1b** Yield: 500 mg, (92%). ¹H NMR (400 MHz, CDCl₃): δ 7.20-7.31 (m, 13H, ArH), 7.08-7.17 (m, 12H, ArH), 3.92 (d, 1H, *J* = 4.2 Hz, NH) ppm. ¹³C{¹H} NMR (100 MHz, CDCl₃): δ 143.8 (ArC), 143.7 (ArC), 135.8 (P-ArC), 134.8 (P-ArC), 130.4 (P attached *o*-ArC), 130.3 (P attached *o*-ArC), 129.9 (P attached *p*-ArC), 129.8 (P attached *p*-ArC), 128.8 (*m*-ArC), 127.2 (P attached *m*-ArC), 127.1 (P attached *m*-ArC), 126.5 (*o*-ArC), 126.2 (*p*-ArC), 70.9 (triphenylmethyl C) ppm. ³¹P{¹H}NMR (161.9 MHz, CDCl₃): δ 53.3 ppm. FT-IR (selected frequencies): ν = 3359 (N-H), 1437 (P-C), 860 (P-N), 640 (P=S) cm⁻¹. Elemental analysis (C₃₁H₂₆NPS): Calcd. C 78.29, H 5.51, N 2.95; Found C 77.86, H 5.32, N 2.71

1.4.8. Synthesis of [Ph₂P(Se)NHCHPh₂] (**1c**)

N-Benzhydryl-1,1-diphenylphosphinamine 1 (1.0 gm, 2.72 mol) and elemental selenium (250 mg, 3.16 mol) were heated to 60 °C in THF (10 ml) for 12 h. Unreacted selenium was

filtered off through a G4 frit and the filtrate was collected. After evaporation of filtrate in *vacuo*, a light yellow solid residue was obtained. The title compound was recrystallized from THF at room temperature. (Yield: 1.20 gm, 99%).

^1H NMR (400 MHz, CDCl_3): δ 7.72-7.77 (m, 4H, ArH), 7.12-7.33 (m, 16H, ArH), 5.62-5.68 (dd, 1H, $J = 14.8$ Hz, 6.4 Hz, CH), 3.17-3.14 (br t, 1H, $J = 5.2$ Hz, NH) ppm. $^{13}\text{C}\{^1\text{H}\}$ NMR (100 MHz, CDCl_3): δ 142.9 (ArC), 142.8 (ArC), 134.2 (P-ArC), 133.3 (P-ArC), 131.9 (P attached o-ArC), 131.8 (P attached o-ArC), 131.6 (P attached p-ArC), 128.4 (m-ArC), 128.3 (P attached m-ArC), 128.1 (P attached m-ArC), 127.8 (o-ArC), 127.2 (p-ArC), 59.8 (CH) ppm. $^{31}\text{P}\{^1\text{H}\}$ NMR (161.9 MHz, CDCl_3): δ 58.0 ppm. FT-IR (selected frequencies): $\nu = 3242$ (N-H), 1435 (P-C), 898 (P-N), 568 (P=Se) cm^{-1} . Elemental analysis ($\text{C}_{25}\text{H}_{22}\text{NPSe}$). Calcd. C 67.27, H 4.97, N 3.14; Found C 66.99 H 4.43, N 2.93.

1.4.9. Synthesis of $[\text{Ph}_2\text{P}(\text{Se})\text{NHCPh}_3]$ (**2c**)

Similar to compound **1c**. Yield 1.20 g (100%). ^1H NMR (400 MHz, C_6D_6): δ 7.74-7.79 (m, 4H, ArH), 7.19-7.22 (m, 6H, ArH), 6.59-6.99 (m, 15H, ArH), 3.71 (d, 1H, $J_{\text{H-H}} = 3.2$ Hz, CH), ppm. $^{13}\text{C}\{^1\text{H}\}$ NMR (100 MHz, C_6D_6): δ 143.9 (ArC), 143.8 (ArC), 136.1 (P-ArC), 135.1 (P-ArC), 130.8 (P attached o-ArC), 130.6 (P attached m-ArC), 129.5 (P attached p-ArC), 129.4 (P attached p-ArC), 129.1 (o-ArC), 126.7 (m-ArC), 126.1 (p-ArC), 71.3 (CH) ppm. $^{31}\text{P}\{^1\text{H}\}$ NMR (161.9 MHz, C_6D_6): δ 62.6 ppm. FT-IR (selected frequencies): $\nu = 3300$ (N-H, very weak), 1435 (P-C), 910 (P-N), 599 (P=Se) cm^{-1} . Elemental analysis ($\text{C}_{35}\text{H}_{34}\text{NOPSe}$) (**1c**·THF). Calcd. C 70.70, H 5.76, N 2.36; Found C 70.13 H 5.39, N 2.18.

1.4.10. Synthesis of $\{[(\text{THF})_2\text{Na}(\text{Ph}_2\text{P}(\text{O})\text{NCPH}_3)]_2\}$ (**3**)

In a 10 ml sample vial 1 equivalent (50 mg, 0.105 mmol) of ligand **2a** and 1 equivalent of sodium bis(trimethyl)silylamide (23 mg, 0.125 mmol) were mixed together with small amount of toluene (3 ml), after 6 h small amount of THF (1 ml) and *n*-pentane (2 ml) were added to it and kept in -40 $^\circ\text{C}$ freezer, after 24 h, crystals of complex **3** were obtained. ^1H NMR (400 MHz, C_6D_6): δ 7.73-7.68 (m, 3H, ArH), 7.39-7.38 (m, 4H, ArH), 7.06-6.82 (m, 18H, ArH) ppm. $^{13}\text{C}\{^1\text{H}\}$ NMR (100 MHz, C_6D_6): δ 143.8 (ArC), 143.7 (ArC), 135.8 (P-ArC), 134.8 (P-ArC), 130.4 (P attached o-ArC), 130.3 (P attached o-ArC), 129.9 (P

attached p-ArC), 129.8 (P attached p-ArC), 128.8 (m-ArC), 127.2 (P attached m-ArC), 127.1 (P attached m-ArC), 126.5 (o-ArC), 126.2 (p-ArC), 70.9 (triphenylmethyl C) ppm. $^{31}\text{P}\{^1\text{H}\}$ NMR (161.9 MHz, C_6D_6): δ 73.1 ppm. Elemental analysis ($\text{C}_{74}\text{H}_{74}\text{N}_2\text{Na}_2\text{O}_3\text{P}_2\text{S}_2$): Calcd. C 73.37, H 6.16, N 2.31; Found C 73.05, H 5.96, N 1.99.

1.4.11. Synthesis of $[(\text{THF})_2\text{Na}(\text{Ph}_2\text{P}(\text{S})\text{NCHPh}_2)]_2$ (**4**)

In a 10 ml sample vial 1 equivalent (50 mg, 0.125 mmol) of ligand **1b** and 1 equivalent of sodium bis(trimethyl)silylamide (23 mg, 0.125 mmol) were mixed together with small amount of toluene (3 ml). After 6 hs, small amount of THF (1 ml) and *n*-pentane (2 ml) were added to it and kept in $-40\text{ }^\circ\text{C}$ freezer and after 24 h crystals of complex **4** were obtained. ^1H NMR (400 MHz, C_6D_6): δ 7.82-7.87 (m, 4H, ArH), 7.07 (m, 4H, ArH), 6.82-7.06 (m, 12H, ArH), 5.78-5.84 (dd, 1H, $J = 8.88\text{ Hz}$, 5.88 Hz CH) ppm, 3.45-3.48 (m, THF), 1.29-1.33 (m, THF) ppm. $^{13}\text{C}\{^1\text{H}\}$ NMR (100 MHz, C_6D_6): δ 143.8 (ArC), 143.7 (ArC), 135.9 (P-ArC), 134.9 (P-ArC), 132.2 (P attached o-ArC), 132.1 (P attached o-ArC), 131.2 (P attached p-ArC), 131.1 (P attached p-ArC), 128.4 (P attached m-ArC), 128.2 (m-ArC), 127.9 (o-ArC), 127.1 (p-ArC), 58.9 (CH) ppm. $^{31}\text{P}\{^1\text{H}\}$ NMR (161.9 MHz, C_6D_6): δ 73.3 ppm. Elemental analysis ($\text{C}_{66}\text{H}_{74}\text{N}_2\text{Na}_2\text{O}_4\text{P}_2\text{S}_2$): Calcd. C 70.07, H 6.59, N 2.48; Found C 69.88, H 6.25, N 2.33.

1.4.12. Synthesis of $[\text{K}(\text{THF})_2\text{Ph}_2\text{P}(\text{S})\text{N}(\text{CHPh}_2)]_2$ (**5**)

In a 10 ml sample vial one equivalent (100 mg, 0.25 mmol) of ligand **1b** and one equivalent of potassium bis(trimethylsilyl)amide (50.0 mg, 0.25 mmol) were mixed together with THF (2 ml). After 6 h of stirring at ambient temperature, *n*-pentane (2 ml) was added and placed in $-40\text{ }^\circ\text{C}$ freezer; after 24 h colorless crystals of the title compound **5** were obtained. Yield 140.0 mg (95%). ^1H NMR (400 MHz, C_6D_6): δ 7.92-7.98 (m, 4H, ArH), 7.16-7.18 (m, 4H, ArH), 6.90-7.06 (m, 12H, ArH), 5.91 (d, 1H, $J_{\text{H-P}} = 23.6\text{ Hz}$, CH) ppm, 3.58 (m, THF), 1.40 (m, THF) ppm. $^{13}\text{C}\{^1\text{H}\}$ NMR (100 MHz, C_6D_6): δ 143.9 (ArC), 143.8 (ArC), 135.9 (P-ArC), 134.9 (P-ArC), 132.3 (P attached o-ArC), 132.1 (P attached o-ArC), 131.4 (P attached p-ArC), 131.3 (P attached p-ArC), 128.5 (P attached m-ArC), 128.3 (m-ArC), 128.2 (o-ArC), 127.2 (p-ArC), 67.9 (THF), 58.9 (CH), 25.7 (THF) ppm. $^{31}\text{P}\{^1\text{H}\}$ NMR (161.9 MHz, C_6D_6): δ 73.2 ppm. FT-IR (selected frequencies): $\nu = 1436$ (P-C), 925 (P-N),

632 (P=S) cm^{-1} . Elemental analysis: $\text{C}_{66}\text{H}_{72}\text{K}_2\text{N}_2\text{O}_4\text{P}_2\text{S}_2$ (1161.54): Calcd. C 68.24 H 6.25 N 2.41; Found C 67.89 H 5.91 N 2.22.

1.4.13. Synthesis of $\{[(\text{THF})_2\text{Na}(\text{Ph}_2\text{P}(\text{S})\text{NCPH}_3)]\{(\text{THF})\text{Na}(\text{Ph}_2\text{P}(\text{S})\text{NCPH}_3)\}\}$ (**6**)

In a 10 ml sample vial 1 equivalent (50 mg, 0.105 mmol) of ligand **2b** and 1 equivalent of sodium bis(trimethyl)silylamide (23 mg, 0.125 mmol) were mixed together with small amount of toluene (3 ml), after 6 h small amount of THF (1 ml) and *n*-pentane (2 ml) were added and kept in -40°C freezer; after 24 h, crystals of complex **6** were obtained. ^1H NMR (400 MHz, C_6D_6): δ 7.73-7.68 (m, 3H, ArH), 7.39-7.38 (m, 4H, ArH), 7.06-6.82 (m, 18H, ArH) ppm. $^{13}\text{C}\{^1\text{H}\}$ NMR (100 MHz, C_6D_6): δ 143.8 (ArC), 143.7 (ArC), 135.8 (P-ArC), 134.8 (P-ArC), 130.4 (P attached o-ArC), 130.3 (P attached o-ArC), 129.9 (P attached p-ArC), 129.8 (P attached p-ArC), 128.8 (m-ArC), 127.2 (P attached m-ArC), 127.1 (P attached m-ArC), 126.5 (o-ArC), 126.2 (p-ArC), 70.9 (triphenylmethyl C) ppm. $^{31}\text{P}\{^1\text{H}\}$ NMR (161.9 MHz, C_6D_6): δ 73.1 ppm. Elemental analysis ($\text{C}_{74}\text{H}_{74}\text{N}_2\text{Na}_2\text{O}_3\text{P}_2\text{S}_2$): Calcd. C 73.37, H 6.16, N 2.31; Found C 73.05, H 5.96, N 1.99.

1.5 X-ray Crystallographic Studies

In each case a crystal of suitable dimensions was mounted on a CryoLoop (Hampton Research Corp.) with a layer of light mineral oil and placed in a nitrogen stream at 150(2) K. All measurements were made on an Agilent Supernova X-calibur Eos CCD detector with graphite monochromatic $\text{CuK}\alpha$ (1.54184 Å) radiation. Crystal data and structure refinement parameters are summarized in Table 1.1-1.3. The structures were solved by direct methods (SIR92)⁵² and refined on F^2 by full-matrix least-squares methods; using SHELXL-97.⁵³ Non-hydrogen atoms were anisotropically refined. H-atoms were included in the refinement on calculated positions riding on their carrier atoms. The function minimized was $[\sum w(F_o^2 - F_c^2)^2]$ ($w = 1 / [\sigma^2(F_o^2) + (aP)^2 + bP]$), where $P = (\text{Max}(F_o^2, 0) + 2F_c^2) / 3$ with $\sigma^2(F_o^2)$ from counting statistics. The function R_1 and wR_2 were $(\sum ||F_o| - |F_c||) / \sum |F_o|$ and $[\sum w(F_o^2 - F_c^2)^2 / \sum (wF_o^4)]^{1/2}$, respectively. The Diamond-3 program was used to draw the molecule. Crystallographic data (excluding structure factors) for the structures

reported in this chapter have been deposited with the Cambridge Crystallographic Data Centre as a supplementary publication no. CCDC 889246-889251.

1.6 Tables

Table 1.1. Crystallographic data of compounds **1**, **2** and **2b**

Crystal	1	2	2b
CCDC No.	889249	889247	889251
Empirical formula	C ₂₅ H ₂₂ N ₁ P ₁	C ₃₁ H ₂₆ N ₁ P ₁	C ₃₁ H ₂₆ N ₁ P ₁ S ₁
Formula weight	367.41	443.50	475.56
<i>T</i> (K)	150(2)	150(2)	150(2)
λ (Å)	1.54184	1.54184	1.54184
Crystal system	Monoclinic,	Monoclinic	Monoclinic
Space group	<i>Cc</i>	<i>P2₁/c</i>	<i>P2₁/c</i>
<i>a</i> (Å)	22.237(4)	8.9955(8)	14.5362(5)
<i>b</i> (Å)	10.648(2)	18.6976(16)	10.9798(4)
<i>c</i> (Å)	9.551(2)	15.5059(19)	15.6321(4)
α (°)	90	90	90
β (°)	112.38(3)	108.089(9)	90.970(3)
γ (°)	90	90	90
<i>V</i> (Å ³)	2091.1(7)	2479.1(4)	2494.60(14)
<i>Z</i>	4	4	4
<i>D</i> _{calc} g cm ⁻³	1.167	1.188	1.266
μ (mm ⁻¹)	1.208	1.106	1.896
<i>F</i> (000)	776	936	1000
Theta range for data collection	4.30 to 71.76 ^o	3.82 to 70.76 ^o	3.04 to 70.81 ^o
Limiting indices	-27 ≤ <i>h</i> ≤ 18, -11 ≤ <i>k</i> ≤ 12, -10 ≤ <i>l</i> ≤ 11	-10 ≤ <i>h</i> ≤ 9, -16 ≤ <i>k</i> ≤ 22, -15 ≤ <i>l</i> ≤ 18	-16 ≤ <i>h</i> ≤ 17, -13 ≤ <i>k</i> ≤ 11, -19 ≤ <i>l</i> ≤ 18
Reflections collected / unique	3859 / 2385 [<i>R</i> (int) = 0.0432]	10162 / 4624 [<i>R</i> (int) = 0.0776]	10314 / 4704 [<i>R</i> (int) = 0.0287]
Completeness to theta = 71.25	97.1 %	97.0 %	97.8 %
Absorption correction	Multi-scan	Multi-scan	Multi-scan
Max. and min. transmission	0.880 and 0.790	0.876 and 0.81	0.738 and 0.616
Refinement method	Full-matrix least-squares on <i>F</i> ²	Full-matrix least-squares on <i>F</i> ²	Full-matrix least-squares on <i>F</i> ²
Data / restraints / parameters	2385 / 2 / 245	4624 / 0 / 299	4704 / 0 / 307
Goodness-of-fit on <i>F</i> ²	0.962	0.960	1.028
Final <i>R</i> indices	<i>R</i> 1 = 0.0774, <i>wR</i> 2 = 0.1949	<i>R</i> 1 = 0.0807, <i>wR</i> 2 = 0.1766	<i>R</i> 1 = 0.0446, <i>wR</i> 2 = 0.1143
<i>R</i> indices (all data)	<i>R</i> 1 = 0.0889, <i>wR</i> 2 = 0.2104	<i>R</i> 1 = 0.1970, <i>wR</i> 2 = 0.2671	<i>R</i> 1 = 0.0541, <i>wR</i> 2 = 0.1232
Absolute structure parameter	0.12(7)	0.0029(4)	
Largest diff. peak and hole	0.303 and -0.262 e.Å ⁻³	0.326 and -0.365 e.Å ⁻³	0.580 and -0.345 e.Å ⁻³

Table 1.2. Crystallographic data of compounds **1c**, **2c** and **3**

Crystal	1c.THF	2c.THF	3
CCDC No.	903851	903856	889248
Empirical formula	C ₂₉ H ₃₀ NOPSe	C ₃₅ H ₃₄ NOPSe	C ₇₈ H ₈₂ N ₂ Na ₂ O ₆ P ₂
Formula weight	518.47	594.56	1251.38
<i>T</i> (K)	150(2)	150(2)	150(2)
λ (Å)	1.54184	1.54184	1.54184
Crystal system	Monoclinic,	Monoclinic	Triclinic,
Space group	<i>P</i> 2 ₁ / <i>c</i>	<i>P</i> 2 ₁ / <i>c</i>	<i>P</i> – 1
<i>a</i> (Å)	9.4326(8)	12.2406(3)	11.0777(13)
<i>b</i> (Å)	14.8835(14)	13.6069(4)	13.3008(18)
<i>c</i> (Å)	20.239(2)	20.4841(6)	14.0442(19)
α (°)	90	90	100.720(11)
β (°)	116.921	121.334(2)	112.259(12)
γ (°)	90	90	111.066(12)
<i>V</i> (Å ³)	2533.4(4)	2914.16(14)	1658.1(4)
<i>Z</i>	4	4	1
<i>D</i> _{calc} g cm ⁻³	1.359	1.355	1.253
μ (mm ⁻¹)	2.760	2.474	1.163
<i>F</i> (000)	1072	1232	664
Theta range for data collection	3.85 to 70.86 ⁰	4.12 to 70.78 ⁰	3.67 to 71.07 ⁰
Limiting indices	-10 ≤ <i>h</i> ≤ 11, -18 ≤ <i>k</i> ≤ 17, -19 ≤ <i>l</i> ≤ 24	-14 ≤ <i>h</i> ≤ 11, -16 ≤ <i>k</i> ≤ 16, -21 ≤ <i>l</i> ≤ 24	-12 ≤ <i>h</i> ≤ 13, -15 ≤ <i>k</i> ≤ 16, -17 ≤ <i>l</i> ≤ 11
Reflections collected / unique	10946 / 4807 [<i>R</i> (int) = 0.0516]	12004/5495 [<i>R</i> (int) = 0.0354]	11,652/6230 [<i>R</i> (int) = 0.0643]
Completeness to theta = 71.25	98.2 %	98.1%	97.1 %
Absorption correction	Multi-Scan	Multi-Scan	Multi-Scan
Max. and min. transmission	0.79 and 0.578	0.660 and 0.560	0.890 and 0.810
Refinement method	Full-matrix least-squares on <i>F</i> ²	Full-matrix least-squares on <i>F</i> ²	Full-matrix least-squares on <i>F</i> ²
Data / restraints / parameters	4807 / 0 / 298	5495/0/352	6230/0/406
Goodness-of-fit on <i>F</i> ²	1.028	0.757	1.054
Final <i>R</i> indices [I > 2σ(<i>I</i>)]	<i>R</i> 1 = 0.0595, <i>wR</i> 2 = 0.1534	<i>R</i> 1 = 0.0426, <i>wR</i> 2 = 0.1209	<i>R</i> 1 = 0.0679 , <i>wR</i> 2 = 0.1603
<i>R</i> indices (all data)	<i>R</i> 1 = 0.0761, <i>wR</i> 2 = 0.1675	<i>R</i> 1 = 0.0562, <i>wR</i> 2 = 0.1386	<i>R</i> 1 = 0.1215 , <i>wR</i> 2 = 0.1965
Largest diff. peak and hole	1.569 and -0.746 e.Å ⁻³	1.741 and -0.734 e.Å ⁻³	0.274 and -0.434 e.Å ⁻³

Table 1.3. Crystallographic data of compounds **4**, **5** and **6**

Crystal	4	5	6
CCDC No.	889246	928617	889250
Empirical formula	C ₆₆ H ₇₄ N ₂ Na ₂ O ₄ P ₂ S ₂	C ₆₆ H ₇₂ K ₂ N ₂ O ₄ P ₂ S ₂	C ₇₄ H ₇₄ N ₂ Na ₂ O ₃ P ₂ S ₂
Formula weight	1131.33	1161.54	1211.42
<i>T</i> (K)	150(2)	150(2)	150(2)
λ (Å)	1.54184	1.54184	1.54184
Crystal system	Triclinic,	Triclinic,	Triclinic,
Space group	<i>P</i> - <i>I</i>	<i>P</i> - <i>I</i>	<i>P</i> - <i>I</i>
<i>a</i> (Å)	10.5054(11)	10.6191(11)	10.7308(6)
<i>b</i> (Å)	12.9521(12)	12.9110(13)	11.6146(8)
<i>c</i> (Å)	13.3762(13)	13.4716(15)	26.1362(17)
α (°)	108.731(9)	108.184(9)	79.662(6)
β (°)	108.054(9)	96.182(9)	85.030(5)
γ (°)	104.940(9)	113.202(9)	78.126(5)
<i>V</i> (Å ³)	1504.2(3)	1555.6(3)	3131.8(3)
<i>Z</i>	1	1	2
<i>D</i> _{calc} g cm ⁻³	1.249	1.240	1.285
μ (mm ⁻¹)	1.830	2.831	1.784
<i>F</i> (000)	600	614	1280
Theta range for data collection	3.86 to 70.69°	3.58 to 70.76°	3.44 to 71.04°
Limiting indices	-12 ≤ <i>h</i> ≤ 12, -15 ≤ <i>k</i> ≤ 15, -16 ≤ <i>l</i> ≤ 16	-12 ≤ <i>h</i> ≤ 12, -15 ≤ <i>k</i> ≤ 15, -16 ≤ <i>l</i> ≤ 10	-12 ≤ <i>h</i> ≤ 11, -14 ≤ <i>k</i> ≤ 14, -31 ≤ <i>l</i> ≤ 22
Reflections collected / unique	10,292/5570 [<i>R</i> (int) = 0.0514]	11200/5836 [<i>R</i> (int) = 0.0401]	20,573/11,831 [<i>R</i> (int) = 0.0346]
Completeness to theta = 71.25	96.2 %	97.8 %	97.6 %
Absorption correction	Multi-Scan	Multi-Scan	Multi-Scan
Max. and min. transmission	0.71 and 0.60	1.000 and 0.605	0.740 and 0.630
Refinement method	Full-matrix least-squares on <i>F</i> ²	Full-matrix least-squares on <i>F</i> ²	Full-matrix least-squares on <i>F</i> ²
Data / restraints / parameters	5570/0/352	5836/0/356	11,831/1/782
Goodness-of-fit on <i>F</i> ²	1.036	1.171	1.027
Final <i>R</i> indices [I > 2σ(I)]	<i>R</i> 1 = 0.0582, <i>wR</i> 2 = 0.1528	<i>R</i> 1 = 0.0521, <i>wR</i> 2 = 0.1553	<i>R</i> 1 = 0.0600, <i>wR</i> 2 = 0.1639
<i>R</i> indices (all data)	<i>R</i> 1 = 0.0862, <i>wR</i> 2 = 0.1721	<i>R</i> 1 = 0.0746, <i>wR</i> 2 = 0.1694	<i>R</i> 1 = 0.0857, <i>wR</i> 2 = 0.1883
Largest diff. peak and hole	0.551 and -0.376 e.Å ⁻³	0.509 and -0.341 e.Å ⁻³	0.681 and -0.500 e.Å ⁻³

References:

- (1) Britovsek, G. J. P.; Gibson, V. C. D.; Wass, F. *Angew. Int. Ed.* **1999**, *38*, 428–447.
- (2) Kempe, R. *Angew. Int. Ed.* **2000**, *39*, 468–493.
- (3) Fenske, D.; Maczek, B.; Maczek, K. *Z. Anorg. Allg. Chem.* **1997**, *623*, 1113–1120.
- (4) Kuehl, O.; Koch, T.; Somoza, F.B.; Junk, P.C.; Hey-Hawkins, E.; Plat, D.; Eisen, M. S. *J. Organomet. Chem.* **2000**, *604*, 116–125.
- (5) Kuehl, O.; Junk, P. C.; Hey-Hawkins, E. *Z. Anorg. Allg. Chem.* **2000**, *626*, 1591–1594.
- (6) (a) Wetzels, T.G.; Dehnen, S.; Roesky, P.W. *Angew. Chem.* **1999**, *111*, 1155–1158. (b) Wetzels, T. G.; Dehnen, S.; Roesky, P. W. *Angew. Chem. Int. Ed.* **1999**, *38*, 1086–1088. (c) Wingerter, S.; Pfeiffer, M.; Baier, F.; Stey, T.; Stalke, D. *Z. Anorg. Allg. Chem.* **2000**, *626*, 1121–1130.
- (7) Roesky, P.W.; Gamer, M.T.; Puchner, M.; Greiner, A. *Chem. Eur. J.* **2002**, *8*, 5265–5271.
- (8) (a) Braunstein, P.; Durand, J.; Kickelbick, G.; Knorr, M.; Morise, X.; Pugin, R.; Tiripicchio, A.; Ugozzoli, F. *J. Chem. Soc., Dalton Trans.* **1999**, *23*, 4175–4186. (b) Knoerr, M.; Strohmman, C. *Organometallics* **1999**, *18*, 248–257. (c) Braunstein, P.; Cossy, J.; Knorr, M.; Strohmman, C.; Vogel, P. *New J. Chem.* **1999**, *23*, 1215–1222.
- (9) (a) Dehnicke, K.; Weller, F. *Coord. Chem. Rev.* **1997**, *158*, 103–169. (b) Dehnicke, K.; Krieger, M.; Massa, W. *Coord. Chem. Rev.* **1999**, *182*, 19–65.
- (10) (a) Panda, T. K.; Roesky, P. W. *Chem. Soc. Rev.* **2009**, *38*, 2782–2804. (b) Imhoff, P.; Guelpen, J. H.; Vrieze, K.; Smeets, W. J. J.; Spek, A. L.; Elsevier, C. J. *Inorg. Chim. Acta* **1995**, *235*, 77–88.
- (11) (a) Avis, M. W.; Boom, M. E. V.; Elsevier, C. J.; Smeets, W. J. J.; Spek, A. L. *J. Organomet. Chem.* **1997**, *527*, 263–276. (b) Avis, M. W.; Elsevier, C. J.; Ernsting, J. M.; Vrieze, K.; Veldman, N.; Spek, A. L.; Katti, K. V.; Barnes, C. L. *Organometallics* **1996**, *15*, 2376–2392. (c) Avis, M. W.; Vrieze, K.; Kooijman, H.; Veldman, N.; Spek, A. L.; Elsevier, C. J. *Inorg. Chem.* **1995**, *34*, 4092–4105. (d) Imhoff, P.; Van Asselt, R.; Ernsting, J. M.; Vrieze, K.; Elsevier, C. J.; Smeets, W. J. J.; Spek, A. L.; Kentgens, A. P. M. *Organometallics* **1993**, *12*, 1523–1536.
- (12) Ong, C. M.; McKarns, P.; Stephan, D. W. *Organometallics* **1999**, *18*, 4197–4208.
- (13) Gamer, M. T.; Dehnen, S.; Roesky, P. W. *Organometallics* **2001**, *20*, 4230–4236.

- (14) Aharonian, G.; Feghali, K.; Gambarotta, S.; Yap, G. P. A. *Organometallics* **2001**, *20*, 2616–2622.
- (15) Review Cavell, R. G.; Kamalesh Babu, R. P.; Aparna, K. *J. Organomet. Chem.* **2001**, *617–618*, 158–169.
- (16) Kamalesh Babu, R. P.; McDonald, R.; Cavell, R.G. *Chem. Commun.* **2000**, 481–482.
- (17) (a) Aparna, K.; Kamalesh Babu, R. P.; McDonald, R.; Cavell, R. G. *Angew. Chem.* **2001**, *113*, 4535–4537. (b) Aparna, K.; Kamalesh Babu, R. P.; McDonald, R.; Cavell, R. G. *Angew. Chem., Int. Ed.* **2001**, *40*, 4400–4402.
- (18) (a) Kasani, A.; Kamalesh Babu, R. P.; McDonald, R.; Cavell, R. G. *Organometallics* **1999**, *18*, 3775–3777. (b) Aparna, K.; McDonald, R.; Ferguson, M.; Cavell, R. G. *Organometallics* **1999**, *18*, 4241–4243.
- (19) (a) Edelmann, F. T. *Top. Curr. Chem.* **1996**, *179*, 113–148. (b) Reissmann, U.; Poremba, P.; Noltemeyer, M.; Schmidt, H.-G.; Edelmann, F. T. *Inorg. Chim. Acta* **2000**, *303*, 156–162. (c) Recknagel, A.; Steiner, A.; Noltemeyer, M.; Brooker, S.; Stalke, D.; Edelmann, F. T. *J. Organomet. Chem.* **1991**, *414*, 327–335. (d) Recknagel, A.; Witt, M.; Edelmann, F. T. *J. Organomet. Chem.* **1989**, *371*, C40–C44.
- (20) (a) Wiecko, M.; Gimt, D.; Rastatter, M.; Panda, T. K.; Roesky, P. W. *Dalton Trans.* **2005**, *36*, 2147–2150. (b) Panda, T. K.; Gamer, M. T.; Roesky, P. W. *Inorg. Chem.* **2006**, *45*, 910–916.
- (21) (a) Agarwal, S.; Mast, C.; Dehnicke, K.; Greiner, A. *Macromol. Rapid Commun.* **2000**, *21*, 195–212. (b) Ravi, P.; Groeb, T.; Dehnicke, K.; Greiner, A. *Macromolecules* **2001**, *34*, 8649–8653.
- (22) Halcovitch, N. R.; Fryzuk, M. D. *Dalton Trans.* **2012**, *41*, 1524–1528.
- (23) (a) Gopalakrishnan, J. *Appl. Organomet. Chem.* **2009**, *23*, 291–318. (b) Ansell, J.; Wills, M. *Chem. Soc. Rev.* **2002**, *31*, 259–268. (c) Fei, Z.; Dyson, P. J. *Coord. Chem. Rev.* **2005**, *249*, 2056–2074. (d) Appleby, T.; Woollins, J. D. *Coord. Chem. Rev.* **2002**, *235*, 121–140. (e) Balakrishna, M. S.; Sreenivasa Reddy, V.; Krishnamurthy, S. S.; Nixon, J. F.; Burckett, J. C. T. R.; Laurent, St. *Coord. Chem. Rev.* **1994**, *129*, 1–90.
- (24) (a) Roesky, P. W.; Gamer, M. T.; Puchner, M.; Greiner, A. *Chem. Eur. J.* **2002**, *8*, 5265–5271. (b) Roesky, P. W.; Gamer, M. T.; Marinos, N. *Chem. Eur. J.* **2004**, *10*, 3537–3542. (c) Gamer, M. T.; Roesky, P. W. *Inorg. Chem.* **2004**, *43*, 4903–4906.

- (25) (a) Priya, S.; Balakrishna, M. S.; Mague, J. T. *J. Organomet. Chem.* **2003**, *679*, 116-124. (b) Priya, S.; Balakrishna, M. S.; Mobin, S. M.; McDonald, R. *J. Organomet. Chem.* **2003**, *688*, 227-235. (c) Gaw, K. G.; Slawin, A. M. Z.; Smith, M. B. *Organometallics* **1999**, *18*, 3255-3257. (d) Fenske, D.; Maczek, B.; Maczek, K. *Z. Anorg. Allg. Chem.* **1997**, *623*, 1113-1120. (e) Kühl, O.; Junk, P.C.; Hey-Hawkins, E. *Z. Anorg. Allg. Chem.* **2000**, *626*, 1591-1594. (f) Kühl, O.; Blaurock, S.; Sieler, J.; Hey-Hawkins, E. *Polyhedron* **2001**, *20*, 111-117. (g) Kühl, O.; Koch, T.; Somoza Jr., F. B.; Junk, P. C.; Hey-Hawkins, E.; Plat, D.; Eisen, M. S. *J. Organomet. Chem.* **2000**, *604*, 116-125. (h) Suss-Fink, G.; Pellingelli, M. A.; Tiripicchio, A. *J. Organomet. Chem.* **1987**, *320*, 101-113. (i) Ainscough, E. W.; Brodie, A. M.; Wong, S. T. *J. Chem. Soc. Dalton Trans.* **1977**, 915-920.
- (26) For recent examples see: (a) Kuppaswamy, S.; Bezpalko, M. W.; Powers, T. M.; Turnbull, M. M.; Foxman, B. M.; Thomas, C. M. *Inorg. Chem.* **2012**, *51*, 8225-8240. (b) Evers, D. A.; Bluestein, A. H.; Foxman, B. M.; Thomas, C. M. *Dalton Trans.* **2012**, *41*, 8111-8115. (c) Cooper, B. G.; Fafard, C. M.; Foxman, B. M.; Thomas, C. M. *Organometallics* **2010**, *29*, 5179-5186.
- (27) (a) Nagashima, H.; Sue, T.; Oda, T.; Kanemitsu, A.; Matsumoto, T.; Motoyama, Y.; Sunada, Y. *Organometallics* **2006**, *25*, 1987-1994. (b) Sunada, Y.; Sue, T.; Matsumoto, T.; Nagashima, H. *J. Organomet. Chem.* **2006**, *691*, 3176-3182.
- (28) Braunstein, P.; Matt, D.; Dusausoy, Y.; Fischer, J.; Mitschler, A.; Ricard, L. *J. Am. Chem. Soc.* **1981**, *103*, 5115-5125.
- (29) Surana, G. P.; Mastroilli, P.; Nobile, C. F.; Keim, W. *Inorg. Chim. Acta* **2000**, *305*, 151-156.
- (30) Sekabunga, E. J.; Smith, M. L.; Webb, T. R.; Hill, W. E. *Inorg. Chem.* **2002**, *41*, 1205-1214.
- (31) Colton, R.; Panagiotidou, P. *Aust. J. Chem.* **1987**, *40*, 13-25.
- (32) Schmidbaur, H.; V. Eschenbach, J. E.; Kumberger, O.; Muller, G. *Chem. Ber.* **1990**, *123*, 2261-2265.
- (33) Bhattacharya, P.; Slawin, A. M. Z.; Williams, D. J.; Woollins, J. D. *J. Chem. Soc., Dalton Trans.* **1995**, 3189-3194.
- (34) Balakrishna, M. S.; Panda, R.; Smith, D. C.; Klaman, A.; Nolan, S. P. *J. Organomet. Chem.* **2000**, *599*, 159-165.
- (35) Slawin, A. M. Z.; Smith, M. B.; Woollins, J. D. *J. Chem. Soc., Dalton Trans.* **1996**, 1283-1293.
- (36) Dean, P. A. W. *Can. J. Chem.* **1979**, *57*, 754-761.

- (37) (a) Bhattacharya, P.; Woollins, J. D. *Polyhedron* **1995**, *14*, 3367-3388. (b) Witt, M.; Roesky, H. W. *Chem. Rev.* **1994**, *94*, 1163-1181.
- (38) Dutta, D. K.; Woollins, J. D.; Slawin, A. M. Z.; Konwar, D.; Das, P.; Sharma, M.; Bhattacharya, P.; Aucott, S.M. *Dalton Trans.* **2003**, 2674-2679.
- (39) Miller, E. M.; Shaw, B. L. *J. Chem. Soc., Dalton Trans.* **1974**, 477-480.
- (40) (a) Dilworth, J. R.; Miller, J. R.; Wheatly, N.; Baker, M. J.; Sunley, J. G. *J. Chem. Soc., Chem. Commun.* **1995**, 1579-1581. (b) Maitlis, P. M.; Haynes, A.; Sunley, G. J.; Howard, M. J. *J. Chem. Soc., Dalton Trans.* **1996**, 2187-2196.
- (41) (a) Baker, M. J.; Giles, M. F.; Orpen, A. G.; Taylor, M. J.; Watt, R. J. *J. Chem. Soc., Chem. Commun.* **1995**, 197-198. (b) Howard, M. J.; Jones, M. D.; Roberts, M. S.; Taylor, S.A. *Catal. Today* **1993**, *18*, 325-354.
- (42) (a) Wegman, R. W.; Abatjoglou, A. G.; Harrison, A. M. *J. Chem. Soc., Chem. Commun.* **1987**, 1891-1892. (b) Slawin, A. M. Z.; Smith, M. B.; Woollins, J. D. *J. Chem. Soc., Dalton Trans.* **1996**, 4575-4581. (c) Das, P.; Sharma, M.; Kumari, N.; Konwar, D.; Dutta, D. K. *Appl. Organomet. Chem.* **2002**, *16*, 302-306.
- (43) US Patent 5488153, **1996**.
- (44) Contreras, R.; Grevy, J. M.; G-Hernandez, Z.; G-Rodriguez M.; Wrackmeyer, B. *Heteroat. Chem.* **2001**, *12*(6), 542-550.
- (45) Bonding situation in the drawings of the ligand system is simplified for clarity.
- (46) Poellnitz, A.; Irisli, S.; Silvestru, C.; Silvestru, A. *Sulfur, Silicon, Relat. Elem.* **2010**, *185*, 910-919.
- (47) Gusev, O. V.; Ustynyuk, N. A.; Peganova, T. A.; Gonchar, A.V.; Petrovskii, P.V.; Lyssenko, K. A. *Sulfur, Silicon, Relat. Elem.* **2009**, *184*(2), 322-331.
- (48) Aydemira, M.; Baysala, A.; Guerbuezb, N.; Oezdemirb, I.; Guemguema, B.; Oezkarc, S.; Caylak, N.; Yildirimd, L. T. *Appl. Organomet. Chem.* **2010**, *24*, 17-24.
- (49) Englich U.; Ruhland-Senge, K. *Z. Anorg. Allg. Chem.* **2001**, *627*, 851-856.
- (50) (a) Klooster, W. T.; Brammer, L.; Schaverien, C. J.; Budzelaar, P. H. M. *J. Am. Chem. Soc.* **1999**, *121*, 1381-1382. (b) Scherer, W.; McGrady, G. S. *Angew. Chem., Int. Ed.* **2004**, *43*, 1782-1806.

- (51) For sodium macrocycles see (a) Chekhlov, A. N. *Zhurnal Neorganicheskoi Khimii* **2005**, *50*(3), 472–476. (b) Chekhlov, A. N. *J. Struct. Chem.* **2002**, *43*(3), 530–534. (c) Bravo, P.R.; Cardoso, M. L.; Garcia, P. C.; Pineda, G.V.; Oliveres, R. C. *Inorg. Chem. Commun.* **2012**, *18*, 97–100.
- (52) M. Sheldrick, SHELXS-97, *Program of Crystal Structure Solution, University of Göttingen, Germany, 1997.*
- (53) G. M. Sheldrick, SHELXL-97, *Program of Crystal Structure Refinement, University of Göttingen, Germany, 1997.*

Chapter 2

Homoleptic complexes of alkaline-earth metals having bulky amidophosphine-chalcogenides in their coordination sphere: evidence for direct M-Se bond

2.1 Introduction-

Homoleptic and heteroleptic alkaline-earth metal complexes are attractive to organometallic chemists because of their oxophilic and electropositive nature compare to those of early d-transition metals.¹The alkaline earth metal compounds have recently been employed in various catalytic applications for ring-opening polymerization of various cyclic esters,²⁻³ polymerization of styrene and dienes,⁴ and hydroamination and hydrophosphination reactions of alkenes and alkynes.⁵ Determining the structure and reactivity of alkaline-earth metal species is an important step toward the design and development of efficient catalysts; however, full realization of the catalytic potential of these elements still requires substantial advances in understanding their basic coordination and organometallic chemistry. To stabilize these extremely oxophilic and electropositive metals, a wide variety of nitrogen-based ancillary ligands, such as tris(pyrazolyl)borates,⁶ aminotroponimines,⁷ β -diketiminates,⁸ iminopyrroles,⁹ and 1,4-diaza-1,3-butadiene¹⁰ have been introduced to prepare well defined alkaline-earth metal complexes revealing that the catalytic activity and selectivity of the alkaline-earth metal complexes can be controlled via the well-defined nitrogen-based ligand architecture. Another important application of alkaline-earth metal chalcogenolates is in high temperature superconductors and ferroelectrics. In particular, alkaline-earth metal oxide compounds used as suitable precursors.¹¹ Much less attention has been paid to the alkaline-earth-metal thiolates and selenates, although many heavier chalcogenates are known as potential dopants for chalcogen-based semiconductors.¹² The chelating ligands having selenium as the donor atom to stabilize the heavier alkaline-earth metal complexes are rare. Over the last few years very few alkaline-earth selenium-based complexes have been reported and

structurally characterized, among these are $[\text{Mg}(\text{SeMes}^*)_2(\text{THF})_2]$ ($\text{Mes}^* = 2,4,6\text{-}t\text{Bu}_3\text{C}_6\text{H}_2$),¹³ $[\text{M}(\text{SeMes})_2(\text{THF})_4]$ ($\text{M} = \text{Ca}, \text{Sr}, \text{Ba}$),¹⁴⁻¹⁶ $[\text{Ca}\{\text{CH}(\text{Py})(\text{Se})\text{PPh}_2\}_2(\text{THF})_2]$ ($\text{Py} = \text{pyridine}$),¹⁷ $[(\text{TMEDA})_2\text{Ca}(\text{SeSi}(\text{SiMe}_3)_3)]$,¹⁸ Full structural characterization of strontium selenides is even scarce.^{14,19} The complex having barium selenium bond is limited as the structurally authenticated examples are mostly restricted for the various sulfur derivatives $[\{(\text{H}_2\text{O})_2\text{Ba}(\text{tmtH}_2)_2\}_n]$ ($\text{tmt} = 2,4,6\text{-trimercaptotriazine}, \text{S}_3\text{C}_3\text{N}_3$),²⁰ $[[18]\text{crown-6}]\text{Ba}(\text{hmpa})\text{SMes}^*[\text{SMes}^*](\text{Mes}^* = 2,4,6\text{-}t\text{Bu}_3\text{C}_6\text{H}_2)$,²¹ $[\text{Ba}(\text{hmpa})_3\{\text{Na-PhNNNC}(\text{S})\}_2]$,²² $[\text{Ba}(\text{hmpa})_3(\text{C}=\text{S})\text{NOPh}_2]$,²³ and few more examples including $[\text{Ba}(\text{SCMe}_3)_2]$,²⁴ $[\text{Ba}(\text{tmeda})_2(\text{SeSi}(\text{SiMe}_3)_3)_2]$ ²⁵ are reported. Ruhlandt-Senge and coworkers reported barium selenoates like $[\text{Ba}(\text{THF})_4(\text{SeMes}^*)_2]$, $[[18]\text{crown-6}]\text{Ba}(\text{hmpa})_2(\text{SMes}^*)_2]$, $[\text{Ba}(\text{Py})_3(\text{THF})(\text{SeTrip})_2]$ ($\text{Trip} = 2,4,6\text{-}i\text{Pr}_3\text{C}_6\text{H}_2$), and $[\text{Ba}([18]\text{crown-6})(\text{SeTrip})_2]$,²⁶ however vast potential of this field of chemistry is still to be developed. In chapter 1, we have described a number of alkali metal poly-cyclic compounds using various phosphineamine chalcogenide ligands. In addition to those phosphineamine chalcogenides we have also introduced new bulky seleno-phosphineamines $[\text{Ph}_2\text{P}(\text{Se})\text{NH}(\text{CHPh}_2)]$ (**1c**) and $[\text{Ph}_2\text{P}(\text{Se})\text{NH}(\text{CPh}_3)]$ (**2c**) derived from the bulky phosphineamines $[\text{Ph}_2\text{PNH}(\text{CHPh}_2)]$ (**1**) and $[\text{Ph}_2\text{PNH}(\text{CPh}_3)]$ (**2**) respectively with elemental selenium, having (Se, P, N)-chelating coordination sites, into alkaline-earth metal chemistry. This unique ligand is potentially capable of coordinating through hard nitrogen and phosphorus donor atoms along with the soft selenium donor atom. Thus, by deprotonation reactions of the amine group present in these ligands, the neutral ligands can be converted to monoanionic ligands which can potentially form complexes with heavier alkaline-earth metals via coordination of three donor atoms (N, P and Se). The work will enable us to better understand the alkaline-earth metal–selenium bond strengths and characteristics, and provide important information on the association and aggregation behaviour depending on selenium atoms, ligands and donors.

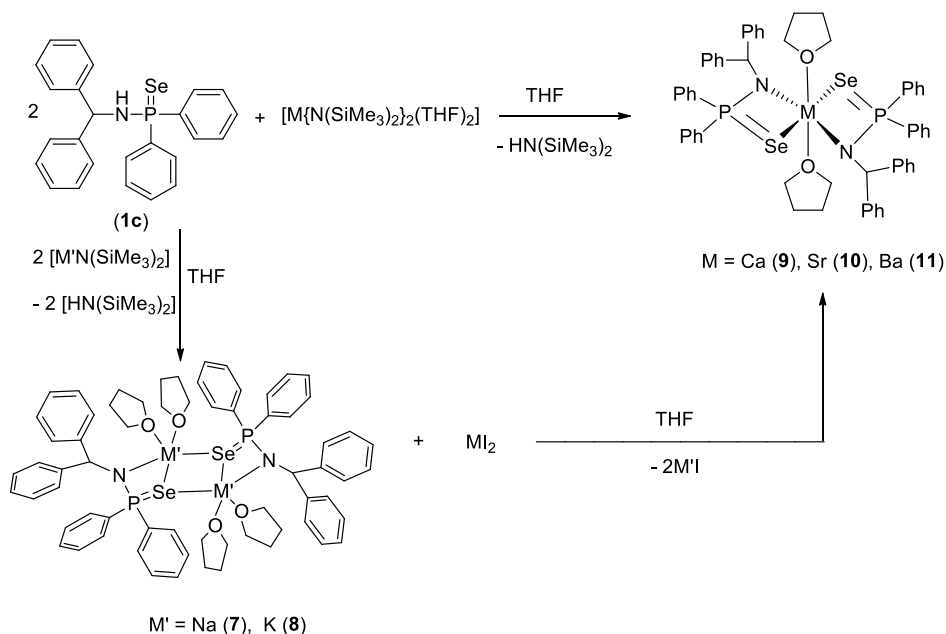
In this chapter, the selenium-containing alkali metal complexes of composition $[\{(\text{THF})_2\text{MPh}_2\text{P}(\text{Se})\text{N}(\text{CHPh}_2)\}_2](\text{M}' = \text{Na}$ (**7**) and K (**8**)) were prepared by the reaction of compound **1c** and sodium bis(trimethyl)silylamide (or potassium bis(trimethylsilyl)amide in case of **8**) in THF through the elimination of volatile bis(trimethylsilyl)amine and heavier alkaline-earth metal complexes $[\text{M}(\text{THF})_2\{\text{Ph}_2\text{P}(\text{Se})\text{N}(\text{CHPh}_2)\}_2]$ ($\text{M} = \text{Ca}$ (**9**), Sr

(**10**), Ba (**11**)) are described, which can be prepared in good yield and high purity by two synthetic routes. We have also synthesized the homoleptic complex $[\text{Ba}(\text{THF})_2\{\text{Ph}_2\text{P}(\text{S})\text{NCHPh}_2\}_2]$ (**12**) by two synthetic routes. Thus, the heavier alkaline earth metal complexes described in this chapter, $[\text{M}(\text{THF})_2\{\text{Ph}_2\text{P}(\text{X})\text{N}(\text{CHPh}_2)\}_2]$ ($\text{M} = \text{Ca}$ (**9**), Sr (**10**), Ba (**11**) and $\text{X} = \text{Se}$; $\text{M} = \text{Ba}$ (**12**) and $\text{X} = \text{S}$), are examples of a rare class of complexes with a direct chalcogenide–alkaline-earth metal contact. This chapter covers the full accounts of two synthetic routes and the solid state structures of all the complexes.

2.2 Results and Discussion

2.2.1. Alkali metal complexes

The dimeric sodium and potassium complexes of molecular formula $[\{(\text{THF})_2\text{M}'\text{Ph}_2\text{P}(\text{Se})\text{N}(\text{CHPh}_2)\}_2]$ ($\text{M}' = \text{Na}$ (**7**) and K (**8**)) were prepared by the reaction of compound **1c** and sodium bis(trimethyl)silylamide (or potassium bis(trimethylsilyl)amide in case of **8**) in THF through the elimination of volatile bis(trimethylsilyl)amine (Scheme 2.1).²⁷



Scheme 2.1. Synthesis of alkali metal and alkaline earth metal phosphinoselenoic amide complexes.

Complex **7** crystallizes in triclinic space group $P\bar{1}$ having one molecule in the unit cell. The solid state structure of complex **7** is given in Figure 2.1. The details of the structural parameters are given in Table 2.1. In the centrosymmetric molecule **7**, two phosphinoselenoic amide ligands are coordinated to each of two sodium atoms by one selenium, one phosphorus and one amido nitrogen atom exhibiting a diamond shaped Na_2Se_2 core with mean angles Se1-Na-Se1i of $99.14(3)^\circ$ and Na1-Se1-Na1i of $80.86(3)^\circ$.

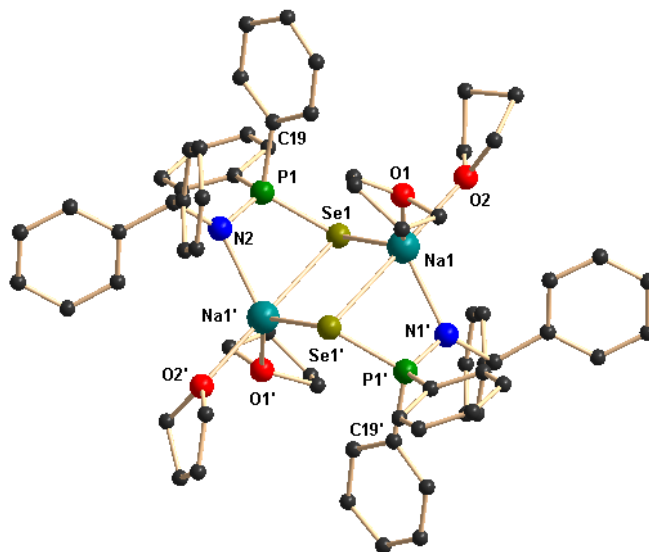


Figure 2.1. Solid state structure of compounds **7**. Hydrogen atoms are omitted for clarity. Selected bond distances (\AA) and bond angles ($^\circ$): Na1-N1^i 2.380(2), Na1-Se1 2.9956(12), Na1-Se1^i 3.0694(11), Na1-O1 2.426(2), Na1-O2 2.399(2), Na1-P1^i 3.2214(13), N1-P1 1.594(2), P1-Se1 2.1519(8), Se1-Na1-Se1^i $99.14(3)$, Se1-Na1-N1^i $115.92(6)$, $\text{Se1}^i\text{-Na1-P1}^i$ $39.915(19)$, Se1-Na1-P1^i $114.01(4)$, $\text{Se1}^i\text{-Na1-O1}$ $83.95(6)$, $\text{Se1}^i\text{-Na1-O2}$ $171.24(6)$, $\text{N1}^i\text{-Na1-P1}^i$ $28.30(5)$, $\text{N1}^i\text{-Na1-O1}$ $108.79(8)$, $\text{N1}^i\text{-Na1-O2}$ $112.65(8)$, $\text{N1}^i\text{-Na1-Se1}^i$ $68.15(5)$, Na1-Se1-Na1^i $80.86(3)$, O1-Na1-Se1^i $83.95(6)$, O2-Na1-Se1^i $171.24(6)$.

The Na1-Se1 and Na1-Se1^i bond distances of $2.9956(12)$ \AA and $3.0694(11)$ \AA are similar, each of the selenium atoms is μ -coordinated between the two sodium atoms. Additionally, each phosphorus atom is weakly coordinated to each sodium atom to form highly strained three membered metallacycles having P1-Na1 -distance $3.2214(14)$ \AA . In complex **7**, two additional THF molecules are also coordinated to each sodium atom and the geometry of each sodium atom can be best described as distorted trigonal bipyramid. The bond distances Na1-N1 $2.380(2)$, Na1-O1 $2.426(2)$, and Na1-O2 $2.399(2)$ \AA are in the range of

the previously observed sodium phosphinthioic amide complexes described in the Chapter 1. The whole structure consists of four three-member rings fused together forming a pentametalloacyclo[4.2.0.0^{1,7}.0^{2,5}.0^{2,4}]octane structure.

The potassium phosphinoselenoic amido complex **8** crystallizes in the triclinic space group *P*-1 having one molecule in the unit cell and is isostructural with the sodium complex **7** due to the similar ionic radii of sodium and potassium. The details of the structural parameters are given in Table 2.1. The solid state structure of complex **8** is given in Figure 2.2. Each potassium atom in the dimeric complex **8** is coordinated by one {Ph₂P(Se)N(CHPh₂)}⁻ ligand and two THF molecules. Similar to complex **7**, a diamond-shaped K₂Se₂ core with mean angles Se2A–K–Se2Aⁱ of 91.12(2)° and K–Se2A–Kⁱ of 88.88(2)° is observed. The K–Se2A and K–Se2Aⁱ bond distances are also similar at 3.3090(10) and 3.5150(10) Å, respectively. Each of the selenium atoms is μ-coordinated between each of the two potassium atoms. Additionally, each phosphorus atom is weakly coordinated to each potassium atom to form highly strained three-membered metallacycles having P–K-distance 3.5579(13) Å. Two additional THF molecules are also coordinated to each potassium atom to adopt a distorted trigonal bipyramidal geometry for each potassium metal atom. The bond distances K–N 2.725(3), K–O1 2.659(3), and K–O7 2.695(3) Å are slightly elongated compare to that of sodium complex **7**, but are in the range of the previously observed potassium complexes reported in literature. Unlike the analogous sodium complex, a short contact between potassium and one of the phenyl carbons (K⋯C1C (3.194(3) Å)) is observed, which can be interpreted as a remote or secondary M–C interaction. However, in solution all phenyl carbons appeared equivalent in the ¹³C{¹H} NMR study, presumably due to dynamic behavior of the complex. Thus in the solid state, two additional five member metallacycles K1–C1C–C20–P1–Se1 and K1ⁱ–C1Cⁱ–C20ⁱ–P1ⁱ–Se1ⁱ are formed. An unusual structural motif is formed by fusion of four threemember and two five-member metallacycle rings. To the best of our knowledge, this is the first example of such kind of structural motif in potassium complexes. Even the complexes **7** and **8** are dimeric in the solid state, only one set of signals were recorded in the ¹H, ³¹P{¹H} and ¹³C{¹H} NMR spectra in each case due to the dynamic nature of the complexes in solution.

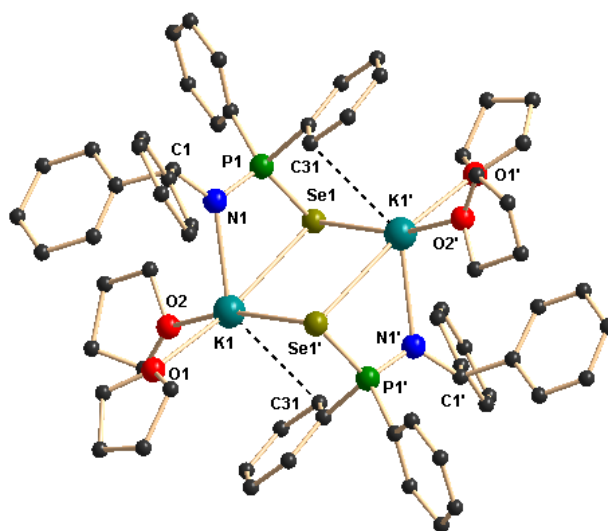


Figure 2.2. Solid state structure of compounds **8**. Hydrogen atoms are omitted for clarity. Selected bond distances (Å) and bond angles (°): K-N 2.725(3), K-Se2a 3.3090(10), K-Se2aⁱ 3.5150(9), K-O1 2.659(3), K-O7 2.695(3), K-C1cⁱ 3.194(3), K-P 3.5579(12), N-P 1.589(3), P-Se2a 2.1476(9), Se2a-K-Se2aⁱ 91.12(2), Se2a-K-N 61.31(6), Se2a-K-P 36.22(17), Se2a-K-O1 171.26(8), Se2a-K-O7 94.77(10), N-K-P 25.09(6), N-K-O1 109.95(10), N-K-O7 102.29(10), N-K-Se2aⁱ 90.75(6), K-Se2a-Kⁱ 88.88(2), O1-K-Se2aⁱ 88.87(8), O7-K-Se2aⁱ 166.95(9).

2.2.2. Alkaline-earth metal complexes of phosphinoselenoic amide ligand

Reaction of **1c** with alkaline-earth metal bis(trimethylsilyl)amides [M{N(SiMe₃)₂]₂(THF)_n] (M = Ca, Sr, Ba) in a 2 : 1 molar ratio in THF followed by crystallization from THF/*n*-pentane, homoleptic phosphinoselenoic amido alkaline-earth metal complexes of composition [M(THF)₂{Ph₂P(Se)N(CHPh₂)₂}]₂ (M = Ca (**9**), Sr (**10**), Ba (**11**)) were obtained in good yield via the elimination of hexamethyldisilazane (Scheme 2.1).²⁷ The same alkaline-earth metal complexes **9–11** can also be prepared by another route, salt metathesis reaction involving the alkali metal phosphinoselenoic amides with alkaline-earth metal diiodides in THF. The silylamide route was followed for all the three complexes **9–11**, whereas both the routes were used for calcium complex **9** only. The new complexes have been characterized by standard analytical/spectroscopic techniques, and the solid-state structures were established by single-crystal X-ray diffraction analysis. A strong

absorption at 570 cm^{-1} (for **9**), 569 cm^{-1} (for **10**) and 569 cm^{-1} (for **11**) in FT-IR spectra indicates the evidence of P=Se bond into the each complex. The resonance of the methine proton (δ 5.93–5.87 ppm for **9**, 5.40–5.33 ppm for **10** and 5.46–5.39 ppm for **11**) in the ^1H NMR spectrum of the diamagnetic complexes **9–11** are unaffected due to complex formation. In $^{31}\text{P}\{^1\text{H}\}$ NMR spectra, complexes **9–11** show only one signal at 71.9 ppm, 71.8 ppm and 71.9 ppm, respectively, and these values are significantly downfield shifted compared to that of compound **1c** (58.0 ppm) upon coordination of calcium, strontium or barium atom onto the selenium atom of the phosphinoselenoic amido ligand. The two phosphorus atoms present in the two $\{\text{Ph}_2\text{P}(\text{Se})\text{N}(\text{CHPh}_2)\}^-$ moieties are chemically equivalent.

The calcium and strontium complexes **9** and **10** crystallize in the triclinic space group $P-1$, having one molecule of either **9** or **10** and two THF molecules as solvate in the unit cell. The details of the structural parameters are given in Table 2.1 & Table 2.2. The solid-state structures of the complexes **9** and **10** are shown in Figure 2.3 and 2.4 respectively.

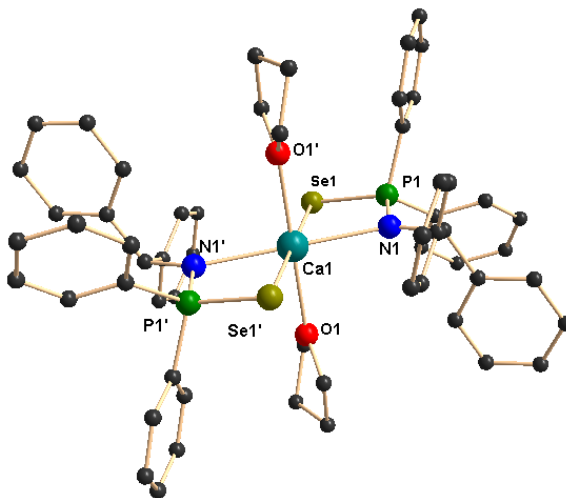


Figure 2.3. Solid state structure of compounds **9**. Hydrogen atoms are omitted for clarity. Selected bond distances (\AA) and bond angles ($^\circ$): Ca1–N1 2.479(5), Ca1–P1 3.2737(16), Ca1–Se1 2.9889(8), Ca1–O1 2.427(5), N1–Ca1–O1 89.23(17), N1–Ca1–P1 28.95(13), P1–Se1–Ca1 77.31(5), P1–Ca1–Se1 39.73(3), Se1–Ca1 N1 68.20(13), O1–Ca1–Oⁱ 180.00(1), Se1–Ca–Se1ⁱ 180.0.

Both the complexes **9** and **10** are isostructural to each other due to similar ionic radii (1.00 and 1.18 Å for coordination number 6).²⁸ In the centrosymmetric molecule **9**, the coordination polyhedron is formed by two monoanionic {Ph₂P(Se)N(CHPh₂)}⁻ ligands, and two THF molecules which are *trans* to each other. Each {Ph₂P(Se)N(CHPh₂)}⁻ ligand coordinates to the calcium atom via chelation of one amido nitrogen atom and one selenium atom and a very weak P–Ca interaction (3.274 Å) of the {Ph₂P(Se)N(CHPh₂)}⁻ moiety is observed. Thus the {Ph₂P(Se)N(CHPh₂)}⁻ group can be considered as a pseudo-bidentate ligand. The central atom calcium adopts a distorted octahedral geometry due to coordination from two {Ph₂P(Se)N(CHPh₂)}⁻ moieties and two THF molecules. The Ca–N distance (2.479(5) Å) is slightly elongated compare with the calcium–nitrogen covalent bond (2.361(2) and 2.335(2)) reported for [Ca(Dipp₂DAD)(THF)₄] (Dipp₂DAD = N,N'-bis(2,6-diisopropylphenyl)-1,4-diaza-1,3-butadiene in the literature.²⁹ The most interesting thing is that the Ca–Se bond 2.989(8) Å is within the same range of Ca–Se bond (2.945(1) Å) reported for [(THF)₂Ca{(PyCH)(Se)PPh₂)}₂] and (2.93 to 3.00 Å) reported for [(THF)₄Ca(SeMes')₂] and (2.958(2) to 3.001(2) Å) reported for [(THF)₂Ca(Se₂PPh₂)₂] in the literature.^{13,15} Thus the compound **9** is one example of the few complexes known having a direct calcium–selenium bond.¹¹⁻¹³ The P–Se distance (2.1449(2) Å) in complex **9** is slightly elongated (2.111(2) Å) but within the same range as that of free ligand **1c** indicating no impact on P–Se bond upon coordination of the calcium atom to the selenium atom.

In compound **10**, the strontium atom is hexa-coordinated by two selenium atoms, two amido nitrogen atoms of two {Ph₂P(Se)N(CHPh₂)}⁻ ligands and two THF molecules. The solvate THF molecules are *trans* to each other and the strontium atom adopts a distorted octahedral geometry (Figure 2.4). Like compound **9**, a weak interaction (P–Sr 3.426(2) Å) between phosphorus and metal atom is noticed. The strontium nitrogen bond distance (2.609(3) Å) fits well (2.6512(2) and 2.669(2) Å) with our previously observed strontium complex [(ImpDipp)₂Sr(THF)₃] (ImpDipp = 2,6-ⁱPr₂C₆H₃N=CH)-C₄H₃N).³⁰ The Sr–Se bond distance (3.136(9) Å) is slightly elongated compare to that of Ca–Se bond distance (2.989(8) Å) observed in complex **9** due to the larger ionic radius of strontium than calcium ion. The observed Sr–Se distance in our compound **10** is within the range of Sr–Se distances (3.138(7) to 3.196(9) Å) of structurally characterized complex [(THF)₃Sr(Se₂PPh₂)₂] published very recently by Westerhausen and coworkers^{16b} and that

(3.066(1) Å) for the complex $[\text{Sr}\{\text{Se}(2,4,6\text{-}t\text{Bu}_3\text{C}_6\text{H}_2)\}_2(\text{THF})_4]$.^{16a} Thus our phosphinoselenoic amido strontium complex **10** is another example of a fully structurally characterized strontium complex having direct Sr–Se bond.

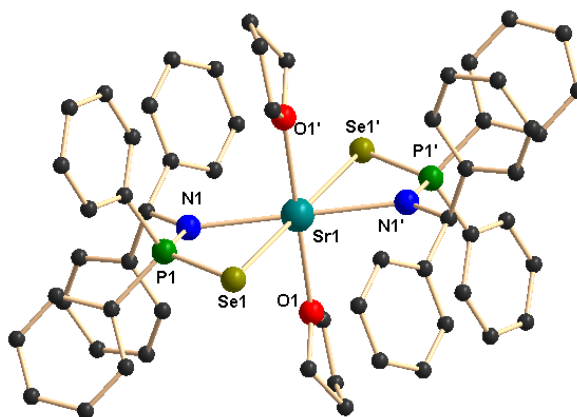


Figure 2.4. Solid state structure of compounds **10**. Hydrogen atoms are omitted for clarity. Selected bond distances (Å) and bond angles (°): Sr1–N1 2.609(3), Sr1–P1 3.4255(15), Sr1–Se1 3.1356(9), Sr1–O1 2.567(3), N1–Sr1–O1 91.72(9), N1–Sr1–P1 26.86(6), P1–Sr1–Se1 37.89(2), Se1–Sr1–N1 64.23(7), O1–Sr1–Oⁱ 180.00(10), Se1–Sr–Se1ⁱ 180.0.

Unlike compounds **9** and **10**, the barium complex **11** crystallizes in the monoclinic space group $P2_1$, having two molecules in the unit cell. The details of the structural parameters are given in Table 2.2. The solid-state structure of complex **11** is given in Figure 2.5. Similar to the calcium and strontium complexes, in the barium complex **11** the coordination polyhedron is formed by two $\{\text{Ph}_2\text{P}(\text{Se})\text{N}(\text{CHPh}_2)\}^-$ ligands and two *trans* THF molecules. The amido nitrogen atom along with the selenium atom of each of the phosphinoselenoic amido ligands coordinates to the barium atoms to adopt a distorted octahedral geometry for the barium atom, considering the $\{\text{Ph}_2\text{P}(\text{Se})\text{N}(\text{CHPh}_2)\}^-$ ligand as bidentate. The Ba–P distance is even larger (3.662(2) Å) compare to that of complexes **9** (3.2737(16) Å) and **10** (3.4255(15) Å), indicating a very weak interaction between the barium atom and phosphorus atom. The Ba–N distances (2.777(6) and 2.778(6) Å) are similar to the values (2.720(4) and 2.706(4) Å) for $[\text{Ba}((\text{Dipp})_2\text{DAD})(\mu\text{-I})(\text{THF})_2)_2]$ reported in the literature.³⁰

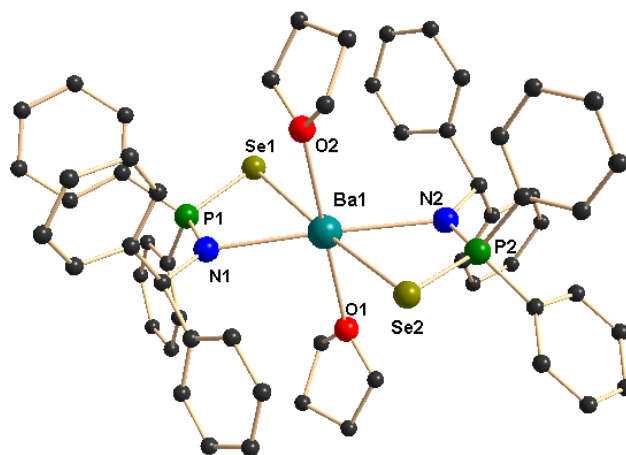
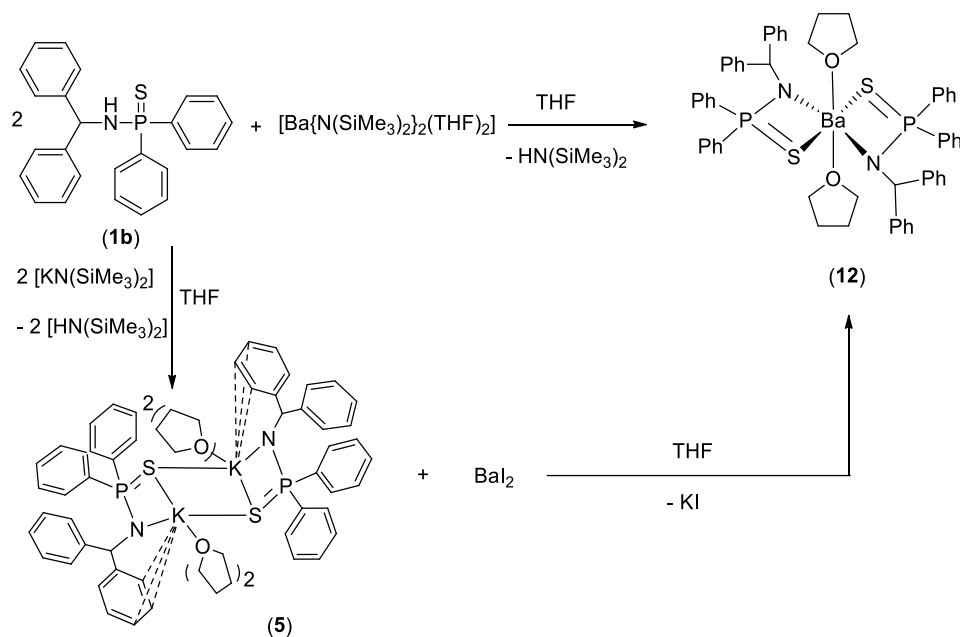


Figure 2.5. Solid state structure of compound **11**. Hydrogen atoms are omitted for clarity. Selected bond distances (Å) and bond angles (°): Ba1–N1 2.777(6), Ba1–P1 3.662(2), Ba1–Se1 3.3553(10), Ba1–O1 2.716(6), Ba1–N2 2.778(6), Ba1–P2 3.665(2), Ba1–Se2 3.3314(10), Ba1–O2 2.734(6), N1–Ba1–O1 91.2(2), N1–Ba1–P1 24.34(15), P1–Ba1–Se1 35.37(4), Se1–Ba1–N1 59.62(15), O1–Ba1–O2 177.3(2), Se1–Ba–Se2 175.66(3), N1–Ba1–N2 175.8(2), N2–Ba1–O2 94.8(2), N2–Ba1–Se2 59.46(15).

The Ba–Se distance (3.3553(1) Å) is the largest among the above mentioned M–Se distances for calcium and strontium complexes (2.9889(8) and 3.1355(9) Å, respectively; vide supra) and can be attributed to the larger ionic radii of the barium atoms compared to calcium and strontium atoms. The Ba–Se distance (3.3553(1) Å) of compound **11** is similar to the reported values of 3.2787(11) Å for the complex [Ba(THF)₄(SeMes*)₂] (Mes* = 2,4,6-*t*Bu₃C₆H₂) and 3.2973(3) Å for [{Ba(Py)₃(THF)(SeTrip)₂}₂] (Trip = 2,4,6-*i*Pr₃C₆H₂) reported by Ruhlandt-Senge and coworkers.²³ Nevertheless complex **11** is a unique example of a barium-seleno complex where two other heteroatoms, nitrogen and phosphorus, coordinate to the barium atom. The P–Se bond (2.152(2) Å) is slightly elongated upon coordination of selenium to the barium atom. A weak interaction between barium and phosphorus (Ba1–P1 3.662(2) and 3.665(2) Å) is also observed. Upon coordination to the barium atom each of the ligand fragments form two three-member metallacycles which are fused together to give a four-member metallacycle Se1–P1–N1–Ba1. The bite angles (Se1–Ba1–N1 59.62(15)° and Se2–Ba1–N2 59.46(15)°, P1–Se1–Ba1 80.11(6)° and 80.77(6)°) indicate a highly strained structure of the molecule.

2.2.3. Barium complex of diphenylphosphinothioic amido ligand

The barium complex **12** was prepared by two synthetic routes. In the first route, known as the silylamide route, the barium bis(trimethylsilyl)amide $[\text{Ba}\{\text{N}(\text{SiMe}_3)_2\}_2(\text{THF})_3]$ was treated with neutral ligand **1b** in 1:2 molar ratio in THF to afford 95% of the product via the elimination of silylamine. In the second method, potassium complex **5** of the diphenylphosphinothioic ligand **1b** was treated with barium diiodide in THF to yield the same product **12** in 85% yields (Scheme 2.2).²⁷



Scheme 2.2. Synthesis of barium complex of phosphinothioic amide ligand.

The complex **12** has been characterized by using standard analytical/spectroscopic techniques and the solid-state structure of **12** was established by using single crystal X-ray diffraction analysis. In FT-IR spectra of the compound **12**, strong absorption at 613 cm^{-1} was observed which can be assigned as characteristic P=S bond stretches and is comparable with the reported values 625 cm^{-1} for P=S (See Chapter 1). In ^1H NMR spectra of the barium complex **12** measured in C_6D_6 , one set of signals were observed indicating the dynamic behavior of compound **12**. The characteristic doublet for the methine proton (δ 5.81 ppm for **12**) is slightly downfield shifted compare to free diphenylphosphinothioicamine **1b** ($\delta = 5.61$ ppm) reported by us (See Chapter 1). The

coupling constant of 23.8 Hz (for **12**) can be observed due to the coupling of α -proton and the phosphorus atom attached to nitrogen. The multiplet signals (3.45 and 1.30 ppm for **12**) could be assigned to resonance of solvated THF molecules coordinated to the barium ion. Additionally, one set of signals for the phenyl protons is also observed which is in the same range to that of ligand **1b**, indicating no significant effects of metal atom on the phenyl groups due to complex formation. $^{31}\text{P}\{^1\text{H}\}$ NMR spectra is more informative as complex **12** shows 73.3 ppm, which is slightly downfield shifted to that of compound **1b** (60.3 ppm) upon addition of barium atom onto the diphenylphosphinothioicamido moiety.

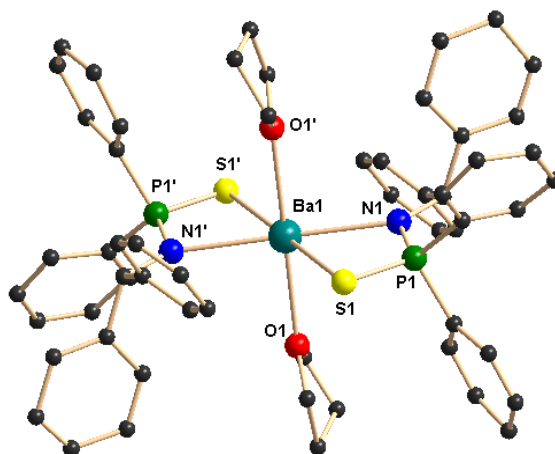


Figure 2.6. Solid state structure of compound **12**. Hydrogen atoms are omitted for clarity. Selected bond distances (Å) and bond angles (°): Ba1-N1 2.744(7), Ba1-P1 3.531(2), Ba1-S1 3.179(2), Ba1-O1 2.737(7), Ba1-N1ⁱ 2.744(7), Ba1-P1ⁱ 3.531(2), Ba1-S1ⁱ 3.179(2), Ba1-O1ⁱ 2.737(7), N1-Ba1-O1 86.1(2), N1-Ba1-P1 25.99(15), P1-Ba1-S1 33.97(5), S1-Ba1-N1 59.50(15), O1-Ba1-O1ⁱ 180.0, S1-Ba1-S1ⁱ 180.0, N1-Ba1-N1ⁱ 180.0, N1ⁱ-Ba1-O1 93.9(2), N1ⁱ-Ba1-S1ⁱ 59.50(15).

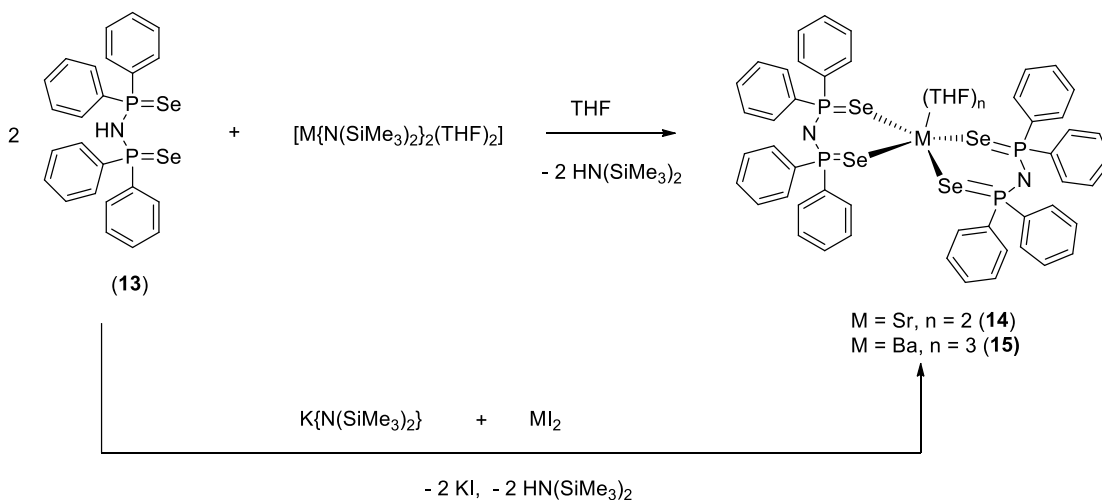
The homoleptic barium phosphinothioic amido complex **12** crystallizes in triclinic space group *P*-1 having one molecule of **12** and one molecule of THF in the unit cell. The details of the structural refinement parameters are given in Table 2.2. The solid state structure of the complex **12** is given in Figure 2.6. In the barium complex **12**, the coordination polyhedron is formed by two {Ph₂P(S)N(CHPh₂)}⁻ ligand and two THF molecules. The Ba1-O1 (2.737(7) Å), and Ba1-N1 (2.744(7) Å) distances of complex **12** are almost similar to that (2.716(6), 2.778(6) Å respectively) of the corresponding values to our previously

observed complex $[\text{Ba}(\text{THF})_2\{\text{Ph}_2\text{P}(\text{Se})\text{N}(\text{CHPh}_2)\}_2]$ (See Figure 2.5). The Ba1-S1 distance 3.179(2) Å is comparable to the Ba-S distance 3.133(2) Å for $[\text{Ba}(\text{THF})_4(\text{S}-2,4,6\text{-}t\text{Bu}_3\text{C}_6\text{H}_2)_2]$ but slightly shorter than that of 3.396(2)-3.629(2) Å for $[\text{Ba}(\text{H}_2\text{O})_4(\text{H}_2,2,4,6\text{-S}_3\text{C}_3\text{N}_3)_2]$ reported by Ruhlandt-Senge and coworkers.²⁶ Thus the central atom barium adopts a distorted octahedral geometry due to coordination from two $\{\text{Ph}_2\text{P}(\text{S})\text{N}(\text{CHPh}_2)\}^-$ ligand moieties and two THF molecules. Two four membered metallacycles Ba1-S1-P1-N1 and Ba1-S1ⁱ-P1ⁱ-N1ⁱ are formed due to ligation of two ligand moieties via sulfur atoms and the amido nitrogen atoms. The P1-Ba1 distance is quite long 3.531(2) Å for complex **12** indicating a very weak interaction from the phosphorus to barium atoms. Similar P-Ba distances (3.662(2) Å) are also observed in $[\text{Ba}(\text{THF})_2\{\text{Ph}_2\text{P}(\text{Se})\text{N}(\text{CHPh}_2)\}_2]$ (Figure 2.5). In complex **12**, the four-membered Ba-S-P-N metallacycle is non-planar and the atoms S1 (0.062 Å and N1 (0.092 Å) are placed above and P1 atom is placed below (0.110 Å) the weighted least-squares best plane having Ba1, S1, P1, N1 atoms. Complex **12** is another example of barium sulfur complex having a barium sulfur direct contact.

2.2.4. Strontium, barium and lithium complexes of diselenoimidodiphosphinato ligand $[\text{HN}(\text{PPh}_2\text{Se})_2]$

In continuation of our study regarding heavier group 2 metal selenoate complexes, we observed that diselenoimidodiphosphinato ligand $[\text{HN}(\text{PPh}_2\text{Se})_2]$ (**13**) is introduced to a wide range of metal coordination sphere including alkali metals,³¹⁻³² group 12,³³ group 13,³⁴⁻³⁵ group 14,^{33,36-37} group 15,³⁸ group 16,³⁹⁻⁴⁰ transition metals (V and Cr,⁴¹ Mn⁴²⁻⁴³ and Re⁴⁴; Ru, Rh, Ir^{32,45-46}; Os,⁴⁷ Co⁴⁸; group 10: Ni,⁴⁹ Pd,⁴⁹⁻⁵² Pt^{32,45,49} and group 11⁵²⁻⁵³ and to rare earth metals⁵⁴⁻⁵⁶ and this can be due to the flexible nature of the ligand moieties to adopt several metallacyclic ring depending upon coordination to the metal center. To our surprise, the reports for heavier alkaline-earth metal diselenoimidodiphosphinato are missing in this series which could give more information about the alkaline-earth metal selenoates and therefore there is a scope to develop the heavier alkaline-earth metal complexes with diselenoimidodiphosphinato ligand. In this chapter, the heavier alkaline-earth metal selenium containing complexes $[\{\eta^2\text{-N}(\text{PPh}_2\text{Se})_2\}_2\text{Sr}(\text{THF})_2]$ (**14**) and $[\{\eta^2\text{-N}(\text{PPh}_2\text{Se})_2\}_2\text{Ba}(\text{THF})_3]$ (**15**) are presented, which can be prepared in good yield and high purity by two synthetic routes. Additionally we also present the synthesis and structure of

lithium complex $[\eta^2\text{-N}(\text{PPh}_2\text{Se})_2\text{Li}(\text{THF})_2]$ (**16**) which were obtained by using ligand **13** and $\text{LiCH}_2\text{SiMe}_3$ in THF solution. The heavier alkaline-earth metal complexes **14** and **15** were prepared in good yield by two synthetic routes. In the first route the diselenoimidodiphosphine (**13**) is treated with alkaline-earth metal bis(trimethylsilyl)amide in THF at ambient temperature to afford the respective strontium and barium complexes of molecular formula $[\{\eta^2\text{-N}(\text{PPh}_2\text{Se})_2\}_2\text{Sr}(\text{THF})_2]$ (**14**) and $[\{\eta^2\text{-N}(\text{PPh}_2\text{Se})_2\}_2\text{Ba}(\text{THF})_3]$ (**15**) via the elimination of volatile bis(trimethylsilyl) amine (Scheme 2.3).²⁷



Scheme 2.3. Synthesis of strontium (**14**) and barium (**15**) complex of $[\text{HN}(\text{PPh}_2\text{Se})_2]$ ligand.

In second method, the compounds **14** and **15** were obtained by the reaction of respective alkaline-earth metal diiodides with potassium salt of diselenoimidodiphosphine $[\text{K}\{\text{N}(\text{Ph}_2\text{PSe})_2\}]$ which was prepared according to the literature procedure involving **13** and potassium bis-trimethylsilylamide as described in chapter 1. The novel alkaline-earth metal complexes **14** and **15** were characterized by analytical/spectroscopic techniques and the molecular structures of both strontium and barium diselenoimidodiphosphinato complexes were determined by single crystal X-ray diffraction analysis.

A strong absorption at 539 cm^{-1} (for **14**), and 538 cm^{-1} (for **15**) in FT-IR spectra indicates the evidence of P=Se bond into the each complex. However, the P=Se bond stretching frequencies for compound **14** and **15** is shifted to lower value compared to the neutral

ligand **13** (595 cm^{-1}) due slight elongation of P=Se bond.⁵⁷ In ^1H NMR spectra, the amino proton of the ligand **13** which was present at 4.42 ppm is absent. The multiplet signals at 3.49 and 1.26 ppm (for **14**) 3.58 and 1.39 ppm (for **15**) can be assigned for resonance of solvated THF molecules coordinated to the metal centre. One set of signals for the phenyl protons are also observed which is in the same range to that of ligand **13** indicating no significant effect of metal atoms onto the phenyl groups due to complex formation. In $^{31}\text{P}\{^1\text{H}\}$ NMR spectra, in complexes **14-15**, all the phosphorus atoms present in the two diselenoimidodiphosphinato moieties are chemically equivalent and show only one signal at 43.3 ppm and 43.7 ppm respectively and these values are significantly high field shifted to that of compound **13** (52.6 ppm) upon coordination of strontium or barium atom onto the selenium atom of the diselenoimidodiphosphinato ligand. This observation is opposite to our previous studies where we noticed a down field shift for the resonance of phosphorus atoms (71.9 ppm for Ca, 71.8 ppm for Sr and 71.9 for Ba respectively; *vide supra*) bound to heavier alkaline-earth metals compared to free phosphinoselenoic amido ligand (58.0 ppm). Although there has been ongoing interest in alkaline-earth organometallics and particularly in the cyclopentadienyl chemistry of these elements,⁵⁸ the complexes **14-15** represents to the best of our knowledge the first diselenoimidodiphosphinato alkaline-earth metal complexes. Therefore, their molecular structures in the solid state were determined by X-ray diffraction analysis.

The strontium complex **14** crystallizes in orthorhombic space group $P bca$ having four molecules in the unit cell. The details of the structural refinement parameters are given in Table 2.3. The molecular structure of compound **14** is shown in Figure 2.7. In the centrosymmetric molecule **14**, the coordination polyhedron is formed by two monoanionic $\{\text{N}(\text{Ph}_2\text{P}(\text{Se}))_2\}^-$ ligands, and two THF molecules which are *trans* to each other. Each $\{\text{N}(\text{Ph}_2\text{P}(\text{Se}))_2\}^-$ ligand coordinates to the strontium atom via chelation of two selenium atoms having a distance of $3.1013(4)\text{ \AA}$.

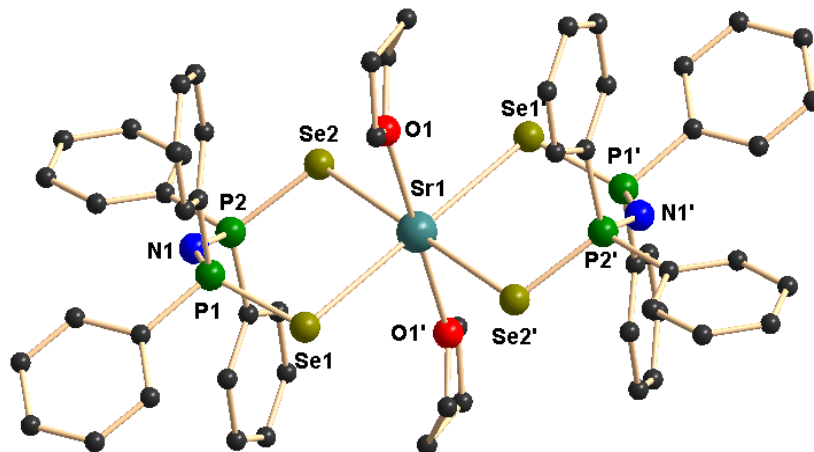


Figure 2.7. Solid state structure of compound **14**. Hydrogen atoms are omitted for clarity. Selected bond distances (Å) and bond angles (°): P1-N1 1.588(3), P2-N1 1.581(3), P1-Se1 2.1515(8), P2-Se2 2.1583(8), P1-C1 1.822(3), P1-C7 1.819(3), P2-C13 1.821(3), P2-C19 1.823(3), Sr1-Se1 3.1013(4), Sr1-Se1ⁱ 3.1013(3), Sr1-Se2 3.1262(3), Sr1-Se2ⁱ 3.1262(3), Sr1-O1 2.523(2) Sr1-O1ⁱ 2.523(2) N1-P1-Se1 120.79(10), N1-P2-Se2 120.01(10), P1-N1-P2 141.44(18), Se1-Sr1-Se2 94.512(9), P1-Se1-Sr1 104.96(2), P2-Se2-Sr1 103.23(2), N1-P1-C1 106.95(14), N1-P1-C7 105.39(14), N1-P2-C13 105.45(14), N1-P2-C19 110.25(14), O1-Sr1-Se1 91.43(6), O1ⁱ-Sr1-Se1 88.57(6), O1ⁱ-Sr1-O1 180.0, O1-Sr1-Se2 86.89(6), O1-Sr1-Se2ⁱ 93.11(6).

The amido nitrogen is not coordinating to the strontium atom as Sr1-N1 distance of 4.422 Å is very high. The Sr1-Se distance (3.1013(4) and 3.1262(3) Å) are within the range of Sr-Se distance 3.1356(9) Å for [Sr(THF)₂{Ph₂P(Se)N(CHPh₂)₂}₂] as described in section 2.2.2, (3.138(7)-3.196(9) Å) for [(THF)₃Sr(Se₂PPh₂)₂] published very recently by Westerhausen et al., and (3.066(1) Å) for the complex [Sr{Se(2,4,6-*t*Bu₃C₆H₂)₂(THF)₄].⁶⁰ The center metal is additionally ligated by two THF molecules having Sr-O distance of 2.523(2) Å to adopt the strontium atom distorted octahedron geometry. The P1-N1-P2 angle of 141.44(18) Å is slightly more than that (130.3(3) and 133.1(3) °) of diselenoimidodiphosphinato cobalt complex [Co{N(Ph₂PSe)₂}₂] reported by Novosad et al.⁶¹ Thus two six-membered metallacycles Sr1-Se1-P1-N1-P2-Se2 and Sr1-Se1ⁱ-P1ⁱ-N1ⁱ-P2ⁱ-Se2ⁱ are formed due to ligation of two ligand moieties via selenium atoms. The plane containing P1, Se1, Sr1 makes a dihedral angle of 28.39 ° with the plane having P2, Se2, Sr1 atoms. The six-membered Sr-Se2-P2-N metallacycle is nonplanar and adopt a twisted

boat conformation. For the metallacycle Sr1-Se1-P1-N1-P2-Se2, the atoms P2 and Se1 reside 0.668 Å and 0.521 Å above the mean plane having Sr1, Se1, P1, N1, P2, Se2 atoms respectively whereas Sr1 (0.076 Å), Se2 (0.092 Å), N1(0.046 Å) and P1(0.312 Å) are located below the mean plane. The P-Se bond distances (2.1515(8) and 2.1583(8) Å) and P-N bond distances (1.588(3) and 1.581(3) Å) are within the range to that of (2.0992(14) and 2.1913(13) Å) and (1.577(7) and 1.609(4) Å) respectively for [Co{N(Ph₂PSe)₂}₂].⁶¹

In contrast to the strontium complex **14**, barium diselenoimidodiphosphinato complex **15** crystallizes in the monoclinic space group *C2/c* having four molecules of **15** in the unit cell. The details of the structural refinement parameters are given in Table 2.3. The solid state structure of the complex **15** is given in Figure 2.8. Similar with strontium complex, in the barium complex **15**, the coordination polyhedron is formed by two {N(Ph₂PSe)₂}⁻ ligands, and three THF molecules. As expected from the larger atomic radius of Ba²⁺, in the compound **15**, Ba1-O (2.707(5), 2.796(8) Å), and Ba1-Se (3.3842(8), 3.3524(8) Å) distances are elongated in comparison with the corresponding values determined for the Sr²⁺ complex **14** (Sr-O 2.523(2) Å and Sr-Se 3.1013(4) and 3.1262(3) Å). However the Ba-O and Ba-Se distances are within the range to that (Ba-O 2.716(6) and Ba-Se 3.3553(10) Å) our previously observed barium compound [Ba(THF)₂{Ph₂P(Se)N(CHPh₂)₂}₂] and also within the range of reported value 3.2787(11) Å for the complex [Ba(THF)₄(SeMes*)₂] (Mes* = 2,4,6-*t*Bu₃C₆H₂) and 3.2973(3) Å for [Ba(Py)₃(THF)(SeTrip)₂]₂] (Trip = 2,4,6-*i*Pr₃C₆H₂) reported by Ruhlandt-Senge et al.¹⁴ Thus the central atom barium adopts a distorted pentagonal bipyramidal geometry due to coordination from two {N(Ph₂P(Se))₂}⁻ moieties and three THF molecules. Two six-membered metallacycles Ba1-Se1-P1-N1-P2-Se2 and Ba1-Se1ⁱ-P1ⁱ-N1ⁱ-P2ⁱ-Se2ⁱ are formed due to ligation of two ligand moieties via selenium atoms. In complex **15**, the six-membered Ba-Se2-P2-N metallacycle is nonplanar and adopts a twisted boat conformation similar to that of strontium complex **14**. For the metallacycle Ba1-Se1-P1-N1-P2-Se2, the atoms P2 and Se1 reside 0.437 Å and 0.527 Å above the mean plane having Ba1, Se1, P1, N1, P2, Se2 atoms respectively whereas Ba1 (0.140 Å), Se2 (0.129 Å), N1(0.083 Å) and P1(0.613 Å) are located below the mean plane.

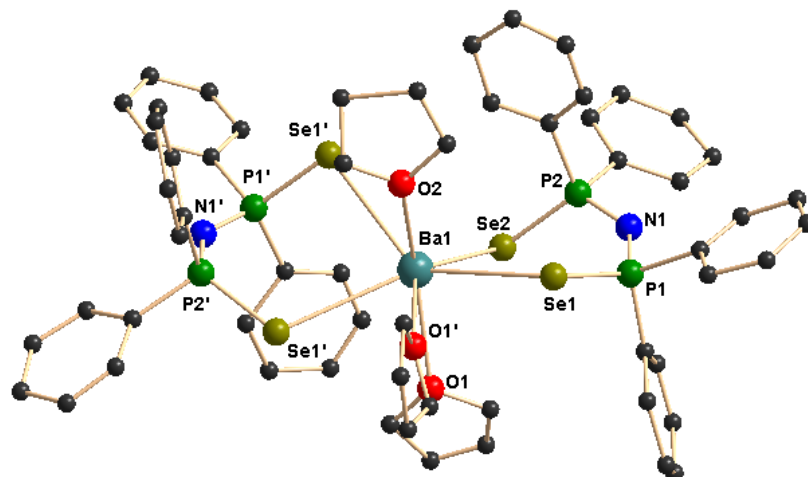
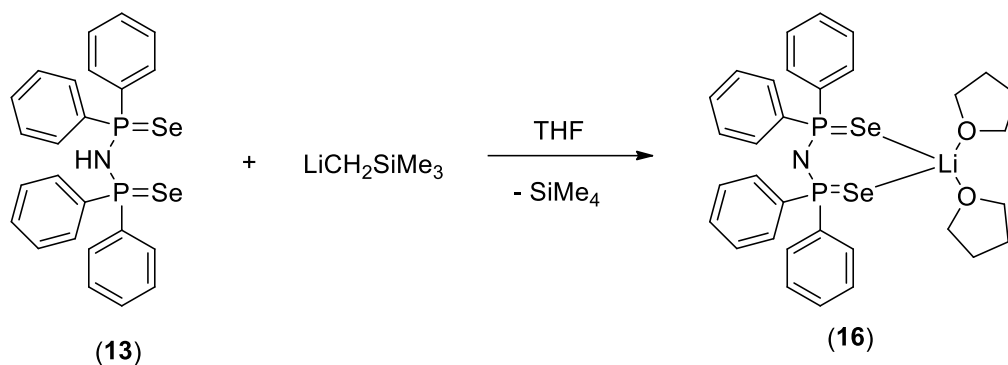


Figure 2.8. Solid state structure of compound **15**. Hydrogen atoms are omitted for clarity. Selected bond distances (Å) and bond angles (°): P1-N1 1.588(5), P2-N1 1.585(5), P1-Se1 2.1393(14), P2-Se2 2.1440(17), P1-C1 1.818(6), P1-C7 1.819(6), P2-C13 1.821(7), P2-C19 1.811(6), Ba1-Se1 3.3842(8), Ba1-Se1ⁱ 3.3842(8), Ba1-Se2 3.3524(8), Ba1-Se2ⁱ 3.3524(8), Ba1-O1 2.796(8), Ba1-O2 2.707(5), Ba1-O2ⁱ 2.707(5), N1-P1-Se1 119.5(2), N1-P2-Se2 121.0(2), P1-N1-P2 135.3(3), Se1-Ba1-Se2 82.371(19), P1-Se1-Ba1 101.68(4), P2-Se2-Ba1 114.06(5), N1-P1-C1 103.8(3), N1-P1-C7 110.1(3), N1-P2-C13 107.9(3), N1-P2-C19 105.0(3), O2-Ba1-O1 76.69(14), O2-Ba1-O2ⁱ 153.4(3), O1-Ba1-Se2 67.253(17), O2-Ba1-Se2 78.68(11).

Similar to strontium complex, no interaction between the amido nitrogen and barium atom was observed. Nevertheless complex **15** is another example of barium seleno complex having barium selenium direct contact.

Lithium complex: Alkali metal salts are important precursors for salt metathesis reaction. Various alkali metal salts of $\{N(PR_2Se)_2\}^-$ ligand are known, however the $[Li\{N(P(i)Pr)_2Se\}_2]$ was prepared by Chivers et al. involving the reaction of *n*-BuLi and $[HN(P(i)Pr)_2Se)_2]$ in the presence of TMEDA at $-78^\circ C$.⁶² Here we describe an alternative method to synthesize the lithium salt of diselenoimidodiphosphinato ligand without using TMEDA. The treatment of **13** with $LiCH_2SiMe_3$ in 1:1 molar ratio in THF at ambient temperature afforded the lithium salt of molecular formula $[\eta^2-N(PPh_2Se)Li(THF)_2]$ (**16**) through the elimination of volatile tetramethylsilane in good yield (Scheme 2.4).



Scheme 2.4. Synthesis of lithium complex **16**

The compound **16** was characterized by analytical/spectroscopic technique and the solid state structure of the complex **16** was determined by single crystal X-ray diffraction analysis. In ^1H NMR spectra of **16**, the resonance of coordinated THF molecules appear at 3.49 and 1.26 ppm as multiplets along with the phenyl protons in the expected range. In the $^{31}\text{P}\{^1\text{H}\}$ NMR spectra, one singlet is observed at 42.9 ppm indicating both the phosphorus atoms are magnetically equivalent. Compound **16** was recrystallized from THF/*n*-pentane (1:2) and crystallizes in monoclinic space group *Cc* having four molecules in the unit cell. The details of the structural refinement parameters are given in Table 2.3. The solid state structure of the complex **16** is given in Figure 2.9. The coordination polyhedron of the complex **16** is formed by the chelation of two selenium atoms of the ligand moiety along with two THF molecules. No interaction between amido

nitrogen and lithium atoms was observed. Li-Se distances 2.598(7) and 2.606(7) Å are within the range to that of (2.556(9) and 2.52(8) Å) previously reported [\square^2 -N(P(*i*Pr)₂Se)Li(TMEDA)] complex.⁶² The Li-O distances of 1.950(7) and 1.932(7) Å are within the reported values. The lithium atom adopts a distorted tetrahedral geometry due to the ligation of two selenium atoms and two THF molecules. The six-membered ring Li1-Se1-P2-N1-P1-Se2 is not coplanar and adopts a twisted boat conformation similar to that of strontium complexes **14** and barium complex **15**.

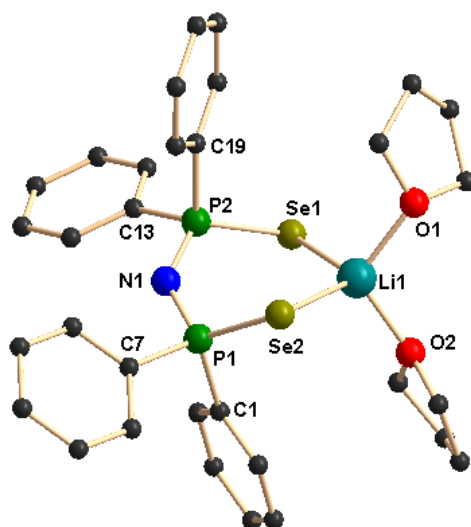


Figure 2.9. Solid state structure of compound **16**. Hydrogen atoms are omitted for clarity. Selected bond distances (Å) and bond angles (°): P1-N1 1.594(3), P2-N1 1.597(3), P1-Se2 2.1453(9), P2-Se1 2.1462(9), P1-C1 1.827(3), P1-C7 1.819(4), P2-C13 1.822(3), P2-C19 1.825(3), Li1-Se1 2.598(7), Li1-Se2 2.606(7), Li1-O1 1.950(7), Li1-O2 1.932(7), N1-P1-Se2 120.19(12), N1-P2-Se1 119.79(11), P1-N1-P2 133.7(2), Se1-Li1-Se2 113.2(2), P1-Se2-Li1 93.27(15), P2-Se1-Li1 98.44(15), N1-P1-C1 108.56(16), N1-P1-C7 103.27(16), N1-P2-C13 104.41(16), N1-P2-C19 108.17(17), O2-Li1-O1 109.7(3), O2-Li1-Se1 105.5(3), O1-Li1-Se1 105.5(3), O2-Li1-Se2 111.9(3).

For the metallacycle Li1-Se1-P2-N1-P1-Se2, the atoms Se2 (0.403 Å), P2 (0.509 Å), N1 (0.013 Å) above the weighted least-squares best plane having Ba1, Se1, P1, N1, P2, Se2 atoms whereas Li1 (0.053 Å), P1 (0.566 Å) and Se1 (0.280 Å) are located below the mean plane.

2.3 Conclusion

We have successfully introduced the amidophosphine chalcogenides (Se and S) into the alkali and alkaline-earth metal coordination chemistry. We have described a series of heavier alkaline-earth metal-selenium complexes having direct metal-selenium bonds via two synthetic routes using phosphinoselenoic amide ligand. In the first method the silylamide route was used to prepare the target compounds, and in the second method the salt metathesis route was used. Due to similar ionic radii, calcium and strontium complexes

are isostructural, and also the M–Se bond distances increase from Ca–Se to Sr–Se and a further increase is observed for the Ba–Se bond. We have also described the missing group 2 metal complexes of diselenoimidodiphosphinato by synthesizing strontium and barium complexes via two synthetic routes using diselenoimidodiphosphinato ligand. Strontium complex **14** adopted distorted octahedral geometry whereas geometry of the larger barium atom in complex **15** can be best described as distorted pentagonal bipyramidal and the M–Se bond distances are increasing from Sr–Se to Ba–Se bond. Finally, synthesis of the lithium diselenoimidodiphosphonato complex was achieved by the deprotonation of the ligand with $\text{LiCH}_2\text{SiMe}_3$, and the molecular structure of the lithium complex obtained was confirmed by the X-ray analysis.

2.4 Experimental procedures

2.4.1. General

All manipulations of air-sensitive materials were performed with the rigorous exclusion of oxygen and moisture in flame-dried Schlenk-type glassware either on a dual manifold Schlenk line, interfaced to a high vacuum (10^{-4} torr) line, or in an argon-filled M. Braun glove box. THF was pre-dried over Na wire and distilled under nitrogen from sodium and benzophenone ketyl prior to use. Hydrocarbon solvents (toluene and *n*-pentane) were distilled under nitrogen from LiAlH_4 and stored in the glove box. ^1H NMR (400 MHz), $^{13}\text{C}\{^1\text{H}\}$ and $^{31}\text{P}\{^1\text{H}\}$ NMR (161.9 MHz) spectra were recorded on a BRUKER AVANCE III-400 spectrometer. BRUKER ALPHA FT-IR was used for FT-IR measurement. Elemental analyses were performed on a BRUKER EURO EA at the Indian Institute of Technology Hyderabad. The starting materials alkaline-earth metal diiodides MI_2 (where M = Ca, Sr and Ba), sodium/potassium bis(trimethyl)silylamides were purchased from Sigma Aldrich and used without further purification. The alkaline-earth metal bis(trimethylsilyl)amides and $\text{LiCH}_2\text{SiMe}_3$ were prepared according to literature procedures.^{63, 64} The NMR solvent C_6D_6 and CDCl_3 were purchased from sigma Aldrich.

2.4.2. Synthesis of $\{[(\text{THF})_2\text{NaPh}_2\text{P}(\text{Se})\text{N}(\text{CHPh}_2)]_2\}$ (**7**)

In a 10 ml sample vial one equivalent (50 mg, 0.112 mmol) of ligand **1c** and one equivalent of sodium bis(trimethylsilyl)amide (20.5 mg, 0.112 mmol) were mixed together with a small amount (2 ml) of toluene. After 6 h, a small amount of THF (2 ml) and *n*-pentane (2 ml) were added to it and kept at $-40\text{ }^{\circ}\text{C}$. After 24 h, colorless crystals of **7** were obtained. Yield (65.2 mg) 95%. ^1H NMR (400 MHz, C_6D_6): δ 7.73–7.67 (m, 4H, ArH), 6.96–6.94 (m, 4H, ArH), 6.84–6.66 (m, 12H, ArH), 5.82–5.76 (dd, 1H, $J_{H-P} = 16.0$ Hz, 6.0, 8.0 Hz CH) ppm. $^{13}\text{C}\{^1\text{H}\}$ NMR (100 MHz, C_6D_6): δ 143.6 (ArC), 143.5 (ArC), 135.4 (P-ArC), 134.5 (P-ArC), 132.3 (P attached *o*-ArC), 132.2 (P attached *o*-ArC), 131.3 (P attached *p*-ArC), 131.2 (P attached *p*-ArC), 128.4 (P attached *m*-ArC), 128.2 (*m*-ArC), 128.0 (*o*-ArC), 127.1 (*p*-ArC), 59.6 (CH) ppm. $^{31}\text{P}\{^1\text{H}\}$ NMR (161.9 MHz, C_6D_6): δ 71.9 ppm. FT-IR (selected frequencies): $\nu = 3365$ (N–H), 1435 (P–C), 894 (P–N), 570 (P=Se) cm^{-1} . Elemental analysis: ($\text{C}_{66}\text{H}_{74}\text{N}_2\text{Na}_2\text{O}_4\text{P}_2\text{Se}_2$) Calcd. C 64.70, H 6.09, N 2.29; Found C 64.15 H 5.82, N 1.76.

2.4.3. Synthesis of $\{[(\text{THF})_2\text{KPh}_2\text{P}(\text{Se})\text{N}(\text{CHPh}_2)]_2\}$ (**8**)

In a 10 ml sample vial, one equivalent (50 mg, 0.112 mmol) of ligand **3** and one equivalent of potassium bis(trimethylsilyl)amide (22.4 mg, 0.112 mmol) were mixed together with 2 ml of toluene. After 6 h, a small amount of THF (2 ml) and *n*-pentane (2 ml) were added to it and kept at $-40\text{ }^{\circ}\text{C}$. After 24 h, colorless crystals of **8** were obtained. Yield (63.4 mg) 90%. ^1H NMR (400 MHz, C_6D_6): δ 7.88–7.82 (m, 4H, ArH), 7.07–7.06 (m, 4H, ArH), 6.96–6.82 (m, 13H, ArH), 5.84–5.78 (dd, 1H, $J = 8.8$ Hz, 6.0 Hz CH) ppm, 3.46 (m, THF), 1.31 (m, THF) ppm. $^{13}\text{C}\{^1\text{H}\}$ NMR (100 MHz, C_6D_6): δ 143.8 (ArC), 143.7 (ArC), 135.9 (P-ArC), 134.9 (P-ArC), 132.2 (P attached *o*-ArC), 132.1 (P attached *o*-ArC), 131.2 (P attached *p*-ArC), 131.1 (P attached *p*-ArC), 128.4 (P attached *m*-ArC), 128.2 (*m*-ArC), 127.9 (*o*-ArC), 127.1 (*p*-ArC), 58.9 (CH) ppm. $^{31}\text{P}\{^1\text{H}\}$ NMR (161.9 MHz, C_6D_6): δ 71.9 ppm. FT-IR (selected frequencies): $\nu = 3373$ (N–H), 1436 (P–C), 931 (P–N), 569 (P=Se) cm^{-1} . Elemental analysis: ($\text{C}_{66}\text{H}_{74}\text{K}_2\text{N}_2\text{O}_4\text{P}_2\text{Se}_2$) Calcd. C 63.04, H 5.93, N 2.23; Found C 62.68, H 5.62, N 1.78.

2.4.4. Synthesis of $[\text{M}(\text{THF})_2\{\text{Ph}_2\text{P}(\text{Se})\text{N}(\text{CHPh}_2)\}_2]$ (M = Ca (**9**), Sr (**10**) and Ba (**11**))

Route 1: In a 10 ml sample vial, two equivalents (100 mg, 0.224 mmol) of ligand **1c** and one equivalent of $[M\{N(\text{SiMe}_3)_2\}_2(\text{THF})_n]$ ($M = \text{Ca}, \text{Sr}, \text{Ba}$) were mixed together with 2 ml of toluene. After 6 h of stirring another 2 ml of THF and *n*-pentane (2 ml) were added to it and kept at -40°C . After 24 h, colorless crystals were obtained.

Route 2: In a 25 ml pre-dried Schlenk flask, potassium salt of ligand **1c** (200 mg, 0.32 mmol) was mixed with CaI_2 (46.8 mg, 0.16 mmol) in 10 ml THF solvent at ambient temperature and stirring continued for 12 h. The white precipitate of KI was filtered off and filtrate was evaporated in *vacuo*. The resulting white compound was further purified by washing with *n*-pentane and crystals suitable for X-ray analysis were grown from THF/*n*-pentane (1:2) mixture at -40°C .

9: Yield: *Route 1.* (204.6 mg) 85% and *Route 2* (192.6 mg) 80%. ^1H NMR (400 MHz, C_6D_6): δ 7.84–7.78 (m, 4H, ArH), 7.07–7.05 (m, 4H, ArH), 6.95–6.78 (m, 12H, ArH), 5.93–5.87 (dd, 1H, $J = 15.3$ Hz, 6.5 Hz, CH) ppm, 3.46 (m, THF), 1.31 (m, THF) ppm. $^{13}\text{C}\{^1\text{H}\}$ NMR (100 MHz, C_6D_6): δ 143.6 (ArC), 143.5 (ArC), 135.4 (P-ArC), 134.5 (P-ArC), 132.3 (P attached *o*-ArC), 132.2 (P attached *o*-ArC), 131.3 (P attached *p*-ArC), 131.2 (P attached *p*-ArC), 128.4 (P attached *m*-ArC), 128.3 (*m*-ArC), 128.0 (*o*-ArC), 127.1 (*p*-ArC), 67.7 (THF) 59.6 (CH), 25.6 (THF) ppm. $^{31}\text{P}\{^1\text{H}\}$ NMR (161.9 MHz, C_6D_6): δ 71.9 ppm. FT-IR (selected frequencies): $\nu = 3381$ (N–H), 1436 (P–C), 930 (P–N), 570 (P=Se) cm^{-1} . Elemental analysis: ($\text{C}_{66}\text{H}_{70}\text{CaN}_2\text{O}_4\text{P}_2\text{Se}_2$) ($7 \cdot 2\text{THF}$) Calcd. C 65.23, H 5.81, N 2.31; Found C 64.88, H 5.32, N 2.11.

10: Yield (196.2 mg) 78%. ^1H NMR (400 MHz, C_6D_6): δ 7.84–7.78 (m, 4H, ArH), 7.33–7.31 (m, 4H, ArH), 6.95–6.79 (m, 12H, ArH), 5.40–5.33 (d, 1H, $J = 27.6$ Hz, CH) ppm, 3.48 (m, THF), 1.27 (m, THF) ppm. $^{13}\text{C}\{^1\text{H}\}$ NMR (100 MHz, C_6D_6): δ 143.6 (ArC), 143.5 (ArC), 135.4 (P-ArC), 134.5 (P-ArC), 132.3 (P attached *o*-ArC), 132.2 (P attached *o*-ArC), 131.3 (P attached *p*-ArC), 131.2 (P attached *p*-ArC), 128.8 (P attached *m*-ArC), 128.4 (*m*-ArC), 127.3 (*o*-ArC), 127.1 (*p*-ArC), 68.1 (THF), 59.6 (CH), 25.5 (THF) ppm. $^{31}\text{P}\{^1\text{H}\}$ NMR (161.9 MHz, C_6D_6): δ 71.9 ppm. FT-IR (selected frequencies): $\nu = 1436$ (P–C), 931 (P–N), 569 (P=Se) cm^{-1} . Elemental analysis: ($\text{C}_{66}\text{H}_{74}\text{N}_2\text{O}_4\text{P}_2\text{Se}_2\text{Sr}$) ($8 \cdot 2\text{THF}$) Calcd. C 62.58, H 5.89, N 2.21; Found C 62.03, H 5.43, N 2.05.

11: Yield (217.9 mg) 83%. ^1H NMR (400 MHz, C_6D_6): δ 7.88–7.83 (m, 4H, ArH), 7.26–7.24 (m, 4H, ArH), 7.06–6.85 (m, 12H, ArH), 5.46–5.39 (d, 1H, $J = 26.1$ Hz, CH) ppm, 3.47 (m, THF), 1.30 (m, THF) ppm. $^{13}\text{C}\{^1\text{H}\}$ NMR (100 MHz, C_6D_6): δ 143.6 (ArC), 143.5 (ArC), 135.4 (P-ArC), 134.5 (P-ArC), 132.3 (P attached *o*-ArC), 132.2 (P attached *m*-ArC), 131.3 (P attached *p*-ArC), 131.2 (P attached *p*-ArC), 128.4 (*o*-ArC), 128.2 (*m*-ArC), 127.1 (*p*-ArC), 67.7 (THF), 59.6 (CH), 25.6 (THF) ppm. $^{31}\text{P}\{^1\text{H}\}$ NMR (161.9 MHz, C_6D_6): δ 71.9 ppm. FT-IR (selected frequencies): $\nu = 1437$ (P–C), 911 (P–N), 569 (P=Se) cm^{-1} . Elemental analysis: ($\text{C}_{58}\text{H}_{58}\text{BaN}_2\text{O}_2\text{P}_2\text{Se}_2$) Calcd. C 59.42, H 4.99, N 2.39; Found C 58.93, H 5.01, N 2.08.

2.4.5. Synthesis of $[\text{Ba}(\text{THF})_2\{\text{Ph}_2\text{P}(\text{S})\text{N}(\text{CHPh}_2)\}_2]$ (**12**)

Route 1: In a 10 ml sample vial two equivalents (200 mg, 0.50 mmol) of ligand **1b** and one equivalent of $[\text{Ba}\{\text{N}(\text{SiMe}_3)_2\}_2(\text{THF})_2]$ (150.5 mg, 0.25 mmol) were mixed together with THF (2 ml). After 12 h of stirring at ambient temperature, *n*-pentane (2 ml) was added and the reaction mixture was kept in -40 °C freezer. After 12 h colorless crystals of **12** were obtained. Yield 256.7 mg (95%).

Route 2: In a 50 ml pre-dried Schlenk flask potassium salt **5** (200 mg, 0.50 mmol) was mixed with BaI_2 (97.8 mg, 0.25 mmol) in THF (10 ml) at ambient temperature and stirred for 12 h. The white precipitate of KI was filtered off and filtrate was dried under *vacuo*. The resulting white compound was further purified by washing with *n*-pentane and crystals suitable for X-ray analysis are grown from THF/*n*-pentane (1:2) mixture solvent at -40 °C. Yield 230.2 mg (85%). ^1H NMR (400 MHz, C_6D_6): δ 7.82–7.87 (m, 4H, ArH), 7.05–7.07 (m, 4H, ArH), 6.80–6.96 (m, 12H, ArH), 5.81 (d, 1H, $J_{\text{H-P}} = 23.8$ Hz, CH) ppm, 3.45 (m, THF), 1.30 (m, THF) ppm. $^{13}\text{C}\{^1\text{H}\}$ NMR (100 MHz, C_6D_6): δ 143.9 (ArC), 143.8 (ArC), 135.9 (P-ArC), 134.9 (P-ArC), 132.3 (P attached *o*-ArC), 132.2 (P attached *o*-ArC), 131.3 (P attached *p*-ArC), 131.2 (P attached *p*-ArC), 128.5 (P attached *m*-ArC), 128.2 (*m*-ArC), 127.8 (*o*-ArC), 127.2 (*p*-ArC), 67.8 (THF), 58.9 (CH), 25.7 (THF) ppm. $^{31}\text{P}\{^1\text{H}\}$ NMR (161.9 MHz, C_6D_6): δ 73.3 ppm. FT-IR (selected frequencies): $\nu = 1436$ (P–C), 955 (P–N), 613 (P=S) cm^{-1} . Elemental analysis: ($\text{C}_{66}\text{H}_{74}\text{BaN}_2\text{O}_4\text{P}_2\text{S}_2$) (1222.71) Calcd. C 64.83, H 6.10, N 2.29; Found C 64.39, H 5.85, N 2.11.

2.4.6. Synthesis of $[\{\eta^2\text{-N}(\text{PPh}_2\text{Se})_2\}_2\text{Sr}(\text{THF})_2]$ (**14**)

Route 1: In a 10 ml sample vial 2 equivalents (200 mg, 0.368 mmol) of ligand **13** and 1 equivalent of $[\text{Sr}\{\text{N}(\text{SiMe}_3)_2\}_2(\text{THF})_2]$ (101.6 mg, 0.184 mmol) are mixed together with 2 ml of THF. After 6 h of stirring, 2 ml of *n*-pentane was added to the top of it and the reaction mixture was placed in - 40 °C freezer. After 12 h, pale green colored crystals of **14** were obtained. Yield 218.3 mg (90%).

Route 2: In a 50 ml pre-dried Schlenk flask potassium salt of ligand **13** $[\text{K}\{\text{N}(\text{Ph}_2\text{PSe})_2\}]$ (200 mg, 0.344 mmol) was mixed with SrI_2 (74.0 mg, 0.172 mmol) in 10 ml of THF solvent at ambient temperature and stirred for 12 h. The white precipitate of KI was filtered off and filtrate was dried under vacuo. The resulting white compound was further purified by washing with *n*-pentane and crystals of **14** suitable for X-ray analysis can be grown from THF/*n*-pentane (1:2) mixture at - 40 °C. Yield 196.3 mg (86%). ^1H NMR (400 MHz, C_6D_6): δ 8.07 (bs, 8H, ArH), 6.90 (bs, 12H, ArH), 3.58 (m, 8H, THF), 1.39 (m, 8H, THF) ppm. $^{13}\text{C}\{^1\text{H}\}$ NMR (100 MHz, C_6D_6): 128.2 (ArC), 127.9 (ArC), 127.7 (ArC), 67.8 (THF), 25.6 (THF) ppm. $^{31}\text{P}\{^1\text{H}\}$ NMR (161.9 MHz, C_6D_6): 43.3 ppm. FT-IR (selected frequencies): 1433 (P-C), 899 (P-N), 539 (P=Se) cm^{-1} . Elemental analysis: $\text{C}_{56}\text{H}_{56}\text{N}_2\text{O}_2\text{P}_4\text{Se}_4\text{Sr}$ (1316.37) Calcd. C 51.09, H 4.29, N 2.13; Found C 50.88, H 4.06, N 2.01.

2.4.7. Synthesis of $[\{\eta^2\text{-N}(\text{PPh}_2\text{Se})_2\}_2\text{Ba}(\text{THF})_2]$ (**15**)

Route 1: in a 10 ml sample vial two equivalents (200 mg, 0.368 mmol) of ligand **13** and 1 equivalent of $[\text{Ba}\{\text{N}(\text{SiMe}_3)_2\}_2(\text{THF})_2]$ (110.8 mg, 0.184 mmol) were mixed together with 2 ml of THF. After 3 h of stirring at ambient temperature, 2 ml of *n*-pentane was added to it and the reaction mixture was kept in - 40 °C freezer. After 12 h pale green colored crystals of **15** were obtained. Yield 225.0 mg (85%).

Route 2: in a 50 ml pre-dried Schlenk flask potassium salt of ligand **13** $[\text{K}\{\text{N}(\text{Ph}_2\text{PSe})_2\}]$ (200 mg, 0.344 mmol) was mixed with BaI_2 (67.3 mg, 0.172 mmol) in 10 ml THF solvent at ambient temperature and stirred for 12 h. The white precipitate of KI was filtered off and filtrate was dried under vacuo. The resulting white compound was further purified by

washing with *n*-pentane and crystals suitable for X-ray analysis are grown from THF/*n*-pentane (1:2) mixture solvent at -40 °C. Yield 202.0 mg (82%). ¹H NMR (400 MHz, C₆D₆): δ 8.16 (bs, 8H, ArH), 6.93-6.98 (m, 12H, ArH), 3.57 (m, 12H, THF), 1.38 (m, 12H, THF) ppm. ¹³C{¹H}NMR (100 MHz, C₆D₆): 131.7 (P attached *o*-ArC), 129.9 (P attached ArC), 128.1 (P attached *p*-ArC), 127.9 (P attached *m*-ArC), 67.8 (THF), 25.6 (THF) ppm. ³¹P{¹H}NMR (161.9 MHz, C₆D₆): 43.7 ppm. FT-IR (selected frequencies): 1434 (P-C), 934 (P-N), 538 (P=Se) cm⁻¹. Elemental analysis: C₆₀H₆₄BaN₂O₃P₄Se₄ (1438.22) calcd. C 50.11, H 4.49, N 1.95; Found C 50.02, H 3.93, N 1.73.

2.4.8. Synthesis of [η²-N(PPh₂Se)Li(THF)₂] (**16**)

In a 10 ml sample vial one equivalent (100 mg, 0.184 mmol) of ligand **13** and one equivalent of LiCH₂SiMe₃ (17.4 mg, 0.184 mmol) were mixed together along with 2 ml of THF. After 6 h of stirring at ambient temperature, 2 ml of *n*-pentane was added onto it and kept in -40 °C. After 3 h, cube shaped colorless crystals of **16** were obtained. Yield 114.8 mg (90%). ¹H NMR (400 MHz, C₆D₆): δ 8.38-8.44 (m, 8H, ArH), 7.04-7.08 (m, 8H, ArH), 6.95-6.99 (m, 4H, ArH), 3.49 (m, 8H, THF), 1.26 (m, 8H, THF) ppm. ¹³C{¹H} NMR (100 MHz, C₆D₆): δ 142.6 (P-ArC), 141.7 (P-ArC), 131.6 (P attached *o*-ArC), 131.5 (P attached *o*-ArC), 129.6 (P attached *p*-ArC), 128.1 (P attached *m*-ArC), 127.6 (P attached *m*-ArC), 68.3 (THF), 25.3 (THF) ppm. ³¹P{¹H}NMR (161.9 MHz, C₆D₆): δ 42.9 ppm. FT-IR (selected frequencies): ν = 1432 (P-C), 931 (P-N), 540 (P=Se) cm⁻¹. Elemental analysis: C₃₂H₃₆LiNO₂P₂Se₂ (693.42) Calcd. C 55.43, H 5.23, N 2.02; Found C 54.99, H 5.01, N 1.87.

2.5 X-ray Crystallographic Studies

In each case a crystal of suitable dimensions was mounted on a CryoLoop (Hampton Research Corp.) with a layer of light mineral oil and placed in a nitrogen stream at 150(2) K. All measurements were made on an Agilent Supernova X-calibur Eos CCD detector

with graphite monochromatic Cu-K α (1.54184 Å) or Mo-K α (0.71069 Å) radiation. Crystal data and structure refinement parameters are summarized in Table 2.1-2.3. The structures were solved by direct methods (SIR92)⁶⁵ and refined on F^2 by full-matrix least-squares methods; using SHELXL-97.⁶⁶ Non-hydrogen atoms were anisotropically refined. H-atoms were included in the refinement on calculated positions riding on their carrier atoms. The function minimized was $[\sum w(F_o^2 - F_c^2)^2]$ ($w = 1 / [\sigma^2(F_o^2) + (aP)^2 + bP]$), where $P = (\text{Max}(F_o^2, 0) + 2F_c^2) / 3$ with $\sigma^2(F_o^2)$ from counting statistics. The function R_1 and wR_2 were $(\sum ||F_o| - |F_c||) / \sum |F_o|$ and $[\sum w(F_o^2 - F_c^2)^2 / \sum (wF_o^4)]^{1/2}$, respectively. The Diamond-3 program was used to draw the molecule. Crystallographic data (excluding structure factors) for the structures described in this chapter have been deposited with the Cambridge Crystallographic Data Centre as a supplementary publication no. CCDC 903850-903855 (**7-11**), 928618(**12**) and 926077-926079 (**14-16**).

2.6 Tables

Table 2.1. Crystallographic data of compounds **7**, **8** and **9**.

Crystal	7	8	9
CCDC No.	903853	903855	903852
Empirical formula	C ₆₆ H ₇₄ N ₂ Na ₂ O ₄ P ₂ Se ₂	C ₆₆ H ₇₂ K ₂ N ₂ O ₄ P ₂ Se ₂	C ₆₆ H ₇₀ CaN ₂ O ₄ P ₂ Se ₂
Formula weight	1225.11	1257.33	1215.18
<i>T</i> (K)	150(2)	150(2)	150(2)
λ (Å)	1.54184	1.54184	1.54184
Crystal system	Triclinic	Triclinic	Triclinic
Space group	<i>P</i> -1	<i>P</i> -1	<i>P</i> -1
<i>a</i> (Å)	10.392(17)	10.4891(10)	10.2981(9)
<i>b</i> (Å)	12.981(2)	13.1334(10)	10.9898(9)
<i>c</i> (Å)	13.463(17)	13.4628(8)	14.4141(13)
α (°)	109.103(13)	67.483(6)	99.955(7)
β (°)	107.189(13)	84.963(6)	101.789(8)
γ (°)	104.478(14)	66.685(8)	103.034(7)
<i>V</i> (Å ³)	1513.8(4)	1568.9(2)	1514.2(2)
<i>Z</i>	1	1	1
<i>D</i> _{calc} g cm ⁻³	1.344	1.331	1.333
μ (mm ⁻¹)	2.549	3.512	3.144
<i>F</i> (000)	636	652	630
Theta range for data collection	3.81 to 70.74 ^o	3.56 to 70.72 ^o	3.22 to 70.99 ^o
Limiting indices	-11 ≤ <i>h</i> ≤ 12, -14 ≤ <i>k</i> ≤ 15, -16 ≤ <i>l</i> ≤ 11	-12 ≤ <i>h</i> ≤ 12, -16 ≤ <i>k</i> ≤ 14, -16 ≤ <i>l</i> ≤ 15	-12 ≤ <i>h</i> ≤ 12, -13 ≤ <i>k</i> ≤ 12, -17 ≤ <i>l</i> ≤ 17
Reflections collected / unique	11164 / 5681 [<i>R</i> (int) = 0.0303]	11473 / 5891 [<i>R</i> (int) = 0.0445]	11585/5710 [<i>R</i> (int) = 0.0533]
Completeness to theta = 71.25	97.5 %	97.9 %	97.6 %
Absorption correction	Multi-Scan	Multi-Scan	Multi-Scan
Max. and min. transmission	0.660 and 0.560	0.685 and 0.585	0.590 and 0.460
Refinement method	Full-matrix least-squares on <i>F</i> ²	Full-matrix least-squares on <i>F</i> ²	Full-matrix least-squares on <i>F</i> ²
Data / restraints / parameters	5681 / 6 / 362	5891 / 6 / 382	5710 / 0 / 349
Goodness-of-fit on <i>F</i> ²	1.036	1.063	1.186
Final <i>R</i> indices [I > 2σ(I)]	<i>R</i> 1 = 0.0379, w <i>R</i> 2 = 0.0987	<i>R</i> 1 = 0.0470, w <i>R</i> 2 = 0.1155	<i>R</i> 1 = 0.0762, w <i>R</i> 2 = 0.1998
<i>R</i> indices (all data)	<i>R</i> 1 = 0.0452, w <i>R</i> 2 = 0.1065	<i>R</i> 1 = 0.0635, w <i>R</i> 2 = 0.1270	<i>R</i> 1 = 0.0897, w <i>R</i> 2 = 0.2068
Largest diff. peak and hole	0.337 and -0.452 e.Å ⁻³	0.586 and -0.741 e.Å ⁻³	1.321. and -0.546 e.Å ⁻³

Table 2.2. Crystallographic data of compounds **10**, **11** and **12**.

Crystal	10	11	12
CCDC No.	903854	903850	928618
Empirical formula	C ₆₆ H ₇₄ N ₂ O ₄ P ₂ Se ₂ Sr	C ₅₈ H ₅₈ Ba ₂ N ₂ O ₂ P ₂ Se ₂	C ₆₆ H ₇₄ BaN ₂ O ₄ P ₂ S ₂
Formula weight	1266.75	1172.26	1222.67
<i>T</i> (K)	150(2)	150(2)	150(2)
λ (Å)	0.71069	1.54184	1.54184
Crystal system	Triclinic	Triclinic	Triclinic
Space group	<i>P</i> -1	<i>P</i> 2 ₁	<i>P</i> -1
<i>a</i> (Å)	10.191(5)	15.7828(7)	10.1569(6)
<i>b</i> (Å)	10.912(5)	11.0357(3)	10.7253(5)
<i>c</i> (Å)	14.641(5)	16.9825(7)	14.9439(9)
α (°)	99.369(5)	90	98.296(4)
β (°)	101.195(5)	117.366(5)	101.989(5)
γ (°)	103.621(5)	90	103.632(4)
<i>V</i> (Å ³)	1514.7(11)	2626.9(2)	1515.24(15)
<i>Z</i>	1	2	1
<i>D</i> _{calc} g cm ⁻³	1.389	1.482	1.340
μ (mm ⁻¹)	2.193	8.372	6.616
<i>F</i> (000)	652	1180	634
Theta range for data collection	1.45 to 25.79°	2.93 to 70.78°	4.33 to 70.84°
Limiting indices	-10 ≤ <i>h</i> ≤ 12, -11 ≤ <i>k</i> ≤ 13, -17 ≤ <i>l</i> ≤ 13	-19 ≤ <i>h</i> ≤ 19, -13 ≤ <i>k</i> ≤ 10, -20 ≤ <i>l</i> ≤ 20	-12 ≤ <i>h</i> ≤ 12, -12 ≤ <i>k</i> ≤ 9, -16 ≤ <i>l</i> ≤ 18
Reflections collected / unique	10504 / 5692 [<i>R</i> (int) = 0.0312]	10905 / 7106 [<i>R</i> (int) = 0.0451]	10949/5688 [<i>R</i> (int) = 0.0512]
Completeness to theta = 71.25	97.8 %	98.4 %	97.4%
Absorption correction	Multi-Scan	Multi-Scan	Multi-Scan
Max. and min. transmission	0.760 and 0.610	0.245 and 0.115	1.000 and 0.142
Refinement method	Full-matrix least-squares on <i>F</i> ²	Full-matrix least-squares on <i>F</i> ²	Full-matrix least-squares on <i>F</i> ²
Data / restraints / parameters	5692 / 0 / 349	7106 / 1 / 604	5688 / 0 / 349
Goodness-of-fit on <i>F</i> ²	1.063	1.026	1.067
Final <i>R</i> indices [I > 2σ(<i>I</i>)]	<i>R</i> 1 = 0.0444, w <i>R</i> 2 = 0.1149	<i>R</i> 1 = 0.0545, w <i>R</i> 2 = 0.1354	<i>R</i> 1 = 0.0854, w <i>R</i> 2 = 0.2360
<i>R</i> indices (all data)	<i>R</i> 1 = 0.0503, w <i>R</i> 2 = 0.1201	<i>R</i> 1 = 0.0583, w <i>R</i> 2 = 0.1396	<i>R</i> 1 = 0.0869, w <i>R</i> 2 = 0.2366
Absolute structure parameter		0.114(5)	
Largest diff. peak and hole	0.818 and -0.625 e.Å ⁻³	1.801 and -1.495 e.Å ⁻³	3.746 and -1.111 e.Å ⁻³

Table 2.3. Crystallographic data of compounds **14**, **15** and **16**.

Crystal	14	15	16
CCDC No.	926079	926077	926078
Empirical formula	C ₅₆ H ₅₆ N ₂ O ₂ P ₄ Se ₄ Sr	C ₆₀ H ₆₀ BaN ₂ O ₃ P ₄ Se ₄	C ₃₂ H ₃₆ LiNO ₂ P ₂ Se ₂
Formula weight	1316.37	1434.15	693.42
<i>T</i> (K)	150(2)	150(2)	150(2)
λ (Å)	1.54184 Å	1.54184	1.54184
Crystal system	Orthorhombic	Monoclinic	Monoclinic
Space group	<i>Pbc</i> a	<i>C</i> 2/ <i>c</i>	<i>C</i> <i>c</i>
<i>a</i> (Å)	10.9194(6)	33.7336(18)	22.0095(5)
<i>b</i> (Å)	17.2140(6)	11.8971(10)	9.1496(2)
<i>c</i> (Å)	29.4632(9)	18.1604(10)	17.3861(5)
α (°)	90	90	90
β (°)	90	104.155	113.821(3)
γ (°)	90	90	90
<i>V</i> (Å ³)	5538.1(4)	7067.1(8)	3202.92(14)
<i>Z</i>	4	4	4
<i>D</i> _{calc} g cm ⁻³	1.579	1.348	1.438
μ (mm ⁻¹)	5.781	7.879	4.052
<i>F</i> (000)	2624	2840	1408
Theta range for data collection	5.03 to 70.77 deg.	3.95 to 70.96 deg.	5.31 to 70.69 deg.
Limiting indices	-4<= <i>h</i> <=13, -15<= <i>k</i> <=20, -35<= <i>l</i> <=28	-41<= <i>h</i> <=40, -14<= <i>k</i> <=11, -22<= <i>l</i> <=19	-26<= <i>h</i> <=26, -11<= <i>k</i> <=10, -20<= <i>l</i> <=21
Reflections collected / unique	14408 / 5242 [<i>R</i> (int) = 0.0423]	14980 / 6696 [<i>R</i> (int) = 0.0392]	6127 / 3804 [<i>R</i> (int) = 0.0200]
Completeness to theta = 71.25	98.6 %	98.0%	97.8 %
Absorption correction	Multi-scan	Multi-scan	Multi-scan
Max. and min. transmission	1.00000 and 0.53975	1.00000 and 0.50182	1.00000 and 0.54515
Refinement method	Full-matrix least-squares on <i>F</i> ²	Full-matrix least-squares on <i>F</i> ²	Full-matrix least-squares on <i>F</i> ²
Data / restraints / parameters	5242 / 0 / 313	6696 / 1 / 335	3804 / 2 / 361
Goodness-of-fit on <i>F</i> ²	1.040	1.085	1.039
Final <i>R</i> indices [<i>I</i> >2σ(<i>I</i>)]	<i>R</i> 1 ^{<i>a</i>} = 0.0370, <i>wR</i> 2 ^{<i>b</i>} = 0.0988	<i>R</i> 1 ^{<i>a</i>} = 0.0688, <i>wR</i> 2 ^{<i>b</i>} = 0.2198	<i>R</i> 1 ^{<i>a</i>} = 0.0292, <i>wR</i> 2 ^{<i>b</i>} = 0.0769
<i>R</i> indices (all data)	<i>R</i> 1 ^{<i>a</i>} = 0.0422, <i>wR</i> 2 ^{<i>b</i>} = 0.1045	<i>R</i> 1 ^{<i>a</i>} = 0.0744, <i>wR</i> 2 ^{<i>b</i>} = 0.2321	<i>R</i> 1 ^{<i>a</i>} = 0.0293, <i>wR</i> 2 ^{<i>b</i>} = 0.0770
Absolute structure parameter			0.025 (19)
Largest diff. peak and hole	0.547 and -0.601 e.Å ⁻³	2.720 and -0.819 e.Å ⁻³	0.538 and -0.642 e.Å ⁻³

References:

- (1) (a) Harder, S. *Chem. Rev.* **2010**, *110*, 3852-3876. (b) Kobayashi, S.; Yamashita, Y. *Acc. Chem. Res.* **2011**, *44*, 58-71.
- (2) (a) Dechy-Cabaret, O.; Martin-Vaca, B.; Bourissou, D. *Chem. Rev.* **2004**, *104*, 6147-6176. (b) O'Keefe, B. J.; Hillmyer, M. A.; Tolman, W. B. *J. Chem. Soc., Dalton Trans.* **2001**, 2215-2225. (c) Wheaton, C. A.; Hayes, P. G.; Ireland, B. *Dalton Trans.* **2009**, 4832-4846. (d) Thomas, C. M. *Chem. Soc. Rev.* **2010**, *39*, 165-173.
- (3) (a) Li, S. M.; Rashkov, I.; Espartero, J. L.; Manolova, N.; Vert, M. *Macromolecules* **1996**, *29*, 57-62. (b) Dobrzyński, P.; Kasperczyk, J.; Bero, M. *Macromolecules* **1999**, *32*, 4735-4737. (c) Zhong, Z.; Dijkstra, P. J.; Birg, C.; Westerhausen, M.; Feijen, J. *Macromolecules* **2001**, *34*, 3863-3868. (d) Westerhausen, M.; Schneiderbauer, S.; Kneifel, A. N.; Sötl, Y.; Mayer, P.; Nöth, H.; Zhong, Z.; Dijkstra, P. J.; Feijen, J. *Eur. J. Inorg. Chem.* **2003**, *18*, 3432-3439. (e) Chisholm, M. H.; Gallucci, J.; Phomphrai, K. *Chem. Commun.* **2003**, 48-49. (f) Hill, M. S.; Hitchcock, P. B. *Chem. Commun.* **2003**, 1758-1759. (g) Chisholm, M. H.; Gallucci, J. C.; Phomphrai, K. *Inorg. Chem.* **2004**, *43*, 6717-6725. (h) Sarazin, Y.; Howard, R. H.; Hughes, D. L.; Humphrey, S. M.; Bochmann, M. *Dalton Trans.* **2006**, 340-350. (i) Darensbourg, D. J.; Choi, W.; Ganguly, P.; Richers, C. P. *Macromolecules* **2006**, *39*, 4374-4379. (j) M. Davidson, G.; O'Hara, C. T.; Jones, M. D.; Keir, C. G.; Mahon, M. F.; Kociok-Köhn, G. *Inorg. Chem.* **2007**, *46*, 7686-7688. (k) Darensbourg, D. J.; Choi, W.; Richers, C. P. *Macromolecules* **2007**, *40*, 3521-3523. (l) Darensbourg, D. J.; Choi, W.; Karroonnirun, O.; Bhuvanesh, N. *Macromolecules* **2008**, *41*, 3493-3502. (m) Poirier, V.; Roisnel, T.; Carpentier, J.-F.; Sarazin, Y. *Dalton Trans.* **2009**, 9820-9827. (n) Xu, X.; Chen, Y.; Zou, G.; Ma, Z.; Li, G. *J. Organomet. Chem.* **2010**, *695*, 1155-1162. (o) Sarazin, Y.; Rosca, D.; Poirier, V.; Roisnel, T.; Silvestru, A.; Maron, L.; Carpentier, J.-F. *Organometallics* **2010**, *29*, 6569-6577. (p) Sarazin, Y.; Liu, B.; Roisnel, T.; Maron, L.; Carpentier, J.-F. *J. Am. Chem. Soc.* **2011**, *133*, 9069-9087.
- (4) (a) Harder, S.; Feil, F.; Knoll, K. *Angew. Chem., Int. Ed.* **2001**, *40*, 4261-4264. (b) Harder, S.; Feil, F. *Organometallics* **2002**, *21*, 2268-2274. (c) Jochmann, P.; Dols, T. S.; Spaniol, T. P.; Perrin, L.; Maron, L.; Okuda, J. *Angew. Chem., Int. Ed.* **2009**, *48*, 5715-5719.
- (5) (a) Barrett, A. G. M.; Crimmin, M. R.; Hill, M. S.; Procopiou, P. A. *Proc. R. Soc. London, Ser. A*, **2010**, *466*, 927-963. (b) Harder, S. *Chem. Rev.* **2010**, *110*, 3852-3876.

- (6) (a) Chisholm, M. H. *Inorg. Chim. Acta* **2009**, *362*, 4284-4290. (b) Saly, M. J.; Heeg, M. J.; Winter, C. H. *Inorg. Chem.* **2009**, *48*, 5303-5312. (c) Chisholm, M. H.; Gallucci, J. C.; Phomphrai, K. *Chem. Commun.* **2003**, 48-49. (d) Chisholm, M. H.; Gallucci, J. C.; Phomphrai, K. *Inorg. Chem.* **2004**, *43*, 6717-6725.
- (7) (a) Crimmin, M. R.; Casely, I. J.; Hill, M. S. *J. Am. Chem. Soc.* **2005**, *127*, 2042-2043. (b) Harder, S.; Brettar, J. *Angew. Chem., Int. Ed.* **2006**, *45*, 3474-3478. (c) Crimmin, M. R.; Arrowsmith, M.; Barrett, A. G. M.; Casely, I. J.; Hill, M. S.; Procopiou, P. A. *J. Am. Chem. Soc.* **2009**, *131*, 9670-9685. (d) Sarish, S. P.; Nembenna, S.; Nagendran, S.; Roesky, H. W. *Acc. Chem. Res.* **2011**, *44*, 157-170. (e) Datta, S.; Roesky, P. W.; Blechert, S. *Organometallics* **2007**, *26*, 4392-4394. (f) Datta, S.; Gamer, M. T.; Roesky, P. W. *Organometallics* **2008**, *27*, 1207-1213.
- (8) (a) Caro, C. F.; Hitchcock, P. B.; Lappert, M. F. *Chem. Commun.* **1999**, 1433-1434. (b) Harder, S. *Organometallics* **2002**, *21*, 3782-3787. (c) Datta, S.; Roesky, P. W.; Blechert, S. *Organometallics* **2007**, *26*, 4392-4394. (d) Datta, S.; Gamer, M. T.; Roesky, P. W. *Organometallics* **2008**, *27*, 1207-1213.
- (9) (a) Jenter, J.; Köppe, R.; Roesky, P. W. *Organometallics* **2011**, *30*, 1404-1413. (b) Hao, H.; Bhandari, S.; Ding, Y.; Roesky, H. W.; Magull, J. H.; Schmidt, G.; Noltemeyer, M.; Cui, C. *Eur. J. Inorg. Chem.* **2002**, 1060-1065. (c) Matsuo, Y.; Tsurugi, H.; Yamagata, T.; Mashima, K. *Bull. Chem. Soc. Jpn.* **2003**, *76*, 1965-1968. (d) Panda, T. K.; Yamamoto, K.; Yamamoto, K.; Kaneko, H.; Yang, Y.; Tsurugi, H.; Mashima, K. *Organometallics* **2012**, *31*, 2286-2301.
- (10) Panda, T. K.; Kaneko, H.; Michel, O.; Tsurugi, H.; Pal, K.; Toernroos, K. W.; Anwander, R.; Mashima, K. *Organometallics* **2012**, *31*, 3178-3184.
- (11) (a) Hubert-Pfalzgraf, L. G. *New J. Chem.* **1987**, *11*, 663. (b) Bradley, D. C. *Chem. Rev.* **1989**, *89*, 1317-1322. (c) Caulton, K. G.; Hubert-Pfalzgraf, L. G. *Chem. Rev.* **1990**, *90*, 969-995.
- (12) (a) Kozlovsky, V. I.; Krysa, A. B.; Korostelin, Y. V.; Shapkin, P. V.; Kalisch, H.; Lünenbürger, M.; Heuken, M. *J. Cryst. Growth* **1998**, *184-185*, 124-128. (b) Hanusa, T. P. *Chem. Rev.* **1993**, *93*, 1023-1036.
- (13) Ruhlandt-Senge, K. *Inorg. Chem.* **1995**, *34*, 3499-3504.
- (14) Ruhlandt-Senge, K.; Davis, K.; Dalai, S.; English, U.; Senge, M. O. *Inorg. Chem.* **1995**, *34*, 2587-2592.
- (15) Ruhlandt-Senge, K.; English, U. *Chem. Eur. J.* **2000**, *6*, 4063-4070.
- (16) English, U.; Ruhlandt-Senge, K. *Z. Anorg. Allg. Chem.* **2001**, *627*, 851-856.

- (17) Kling, C.; Ott, H.; Schwab, G.; Stalke, D. *Organometallics* **2008**, *27*, 5038-5042.
- (18) Gindelberger, D. E.; Arnold, J. *Inorg. Chem.* **1994**, *33*, 6293-6299.
- (19) Al-Shboul, T. M. A.; Volland, G.; Gorls, H.; Krieck, S.; Westerhausen, M. *Inorg. Chem.* **2012**, *51*, 7903-7912.
- (20) Henke, K.; Atwood, D. A. *Inorg. Chem.* **1998**, *37*, 224-227.
- (21) Chadwick, S.; Englich, U.; Ruhlandt-Senge, K. *Chem. Commun.* **1998**, 2149-2150.
- (22) Banbury, F. A.; Davidson, M. G.; Martin, A.; Raithby, P. R.; Snaith, R.; Verhorevoort, K. L.; Wright, D. S. *J. Chem. Soc., Chem. Commun.* **1992**, 1152-1154.
- (23) Mikulcik, P.; Raithby, P. R.; Snaith, R.; Wright, D. S. *Angew. Chem., Int. Ed. Engl.* **1991**, *30*, 428-430.
- (24) Purdy, A. P.; Berry, A. D.; George, C. F. *Inorg. Chem.* **1997**, *36*, 3370-3375.
- (25) Gindelberger, D. E.; Arnold, J. *Inorg. Chem.* **1994**, *33*, 6293-6299.
- (26) Ruhlandt-Senge, K.; Englich, U. *Chem. Eur. J.* **2000**, *6*, 4063-4070.
- (27) The bonding situation in the drawings of the ligand system is simplified for clarity.
- (28) N. N. Greenwood and A. Earnshaw, *Chemistry of the Elements*, Pergamon Press, Oxford, **1984**.
- (29) Panda, T. K.; Kaneko, H.; Michel, O.; Tsurugi, H.; Pal, K.; Törnroos, K. W.; Anwender, R.; Mashima, K. *Organometallics* **2012**, *31*, 3178-3184.
- (30) Panda, T. K.; Yamamoto, K.; Yamamoto, K.; Kaneko, H.; Yang, Y.; Tsurugi, H.; Mashima, K. *Organometallics* **2012**, *31*, 2286-2274.
- (31) Bhattacharyya, P.; Slawin, A. M. Z.; Williams, D. J.; Woollins, J. D. *J. Chem. Soc., Dalton Trans.* **1995**, 2489-2495.
- (32) Robertson, S. D.; Chivers, T. *Dalton Trans.* **2008**, 1765-1772.
- (33) Garcia-Montalvo, V.; Novosad, J.; Kilian, P.; Woollins, J. D.; Slawin, A. M. Z.; Garcia, P. G.; Loepez-Cardoso, M.; Espinosa-Perez, G.; Cea-Olivares, R. *J. Chem. Soc. Dalton Trans.* **1997**, 1025-1029.
- (34) Munoz-Hernandez, M.-A.; Singer, A.; Atwood, D. A.; Cea-Olivares, R. *J. Organomet. Chem.* **1998**, *571*, 15-19.
- (35) Darwin, K.; Gilby, L. M.; Hodge, P. R.; Piggott, B. *Polyhedron* **1999**, *18*, 3729-3733.
- (36) Flores-Santos, L.; Cea-Olivares, R.; Hernandez-Ortega, S.; Toscano, R. A.; Garcia-Montalvo, V.; Novosad, J.; Woollins, J. D. *J. Organomet. Chem.* **1997**, *544*, 37-41.

- (37) Cea-Olivares, R.; Novosad, J.; Woollins, J. D.; Slawin, A. M. Z.; Garcíá-Montalvo, V.; Espinosa-Perez, G.; Garcia, P. G. *Chem. Commun.* **1996**, 519-520.
- (38) Crouch, D. J.; Helliwell, M.; O'Brien, P.; Park, J.-H.; Waters, J.; Williams, D. J. *J. Chem. Soc. Dalton Trans.* **2003**, 1500-1504.
- (39) Cea-Olivares, R.; Canseco-Melchor, G.; Garcia-Montalvo, V.; Hernandez-Ortega, S.; Novosad, J. *Eur. J. Inorg. Chem.* **1998**, 1573-1576.
- (40) Novosad, J.; Lindeman, S.V.; Marek, J.; Woollins, J. D.; Husebye, St. *Heteroatom Chem.* **1998**, *9*, 615-621.
- (41) Bereau, V.; Sekar, P.; McLauchlan, C. C.; Ibers, J. A. *Inorg. Chim. Acta* **2000**, *308*, 91-96.
- (42) German-Acacio, J. M.; Reyes-Lezama, M.; Zuniga-Villarreal, N. *J. Organomet. Chem.* **2006**, *691*, 3223-3231.
- (43) Zuniga-Villarreal, N.; German-Acacio, J. M.; Lemus-Santana, A. A.; Reyes-Lezama, M.; Toscano, R. A. *J. Organomet. Chem.* **2004**, *689*, 2827-2832.
- (44) Rossi, R.; Marchi, A.; Marvell, L.; Magon, L.; Peruzzini, M.; Casellato, U.; Graziani, R. *J. Chem. Soc. Dalton Trans.* **1993**, 723-729.
- (45) Leung, W.-H.; Lau, K.-K.; Zhang, Q.-F.; Wong, W.-T.; Tang, B. *Organometallics* **2000**, *19*, 2084-2089.
- (46) Valderrama, M.; Contreras, R.; Lamata, M. P.; Viguri, F.; Carmona, D.; Lahoz, F. J.; Elipe, S.; Oro, L. A. *J. Organomet. Chem.* **2000**, *607*, 3-11.
- (47) Parr, J.; Smith, M. B.; Elsegood, M. R. *J. Organomet. Chem.* **2002**, *664*, 85-93.
- (48) Novosad, J.; Necas, M.; Marek, J.; Veltsistas, P.; Papadimitriou, Ch.; Haiduc, I.; Watanabe, M.; Woollins, J. D. *Inorg. Chim. Acta* **1999**, *290*, 256-260.
- (49) Papadimitriou, C.; Veltsistas, P.; Novosad, J.; Cea-Olivares, R.; Toscano, A.; Garcia, P. G.; Lopez-Cardoso, M.; Slawin, A. M. Z.; Woollins, J. D. *Polyhedron* **1997**, *16*, 2727-2729.
- (50) Liu, H.; Bandeira, N. A. G.; Calhorda, M. J.; Drew, M. G. B.; Felix, V.; Novosad, J.; Fabrizi de Biani, F.; Zanello, P. *J. Organomet. Chem.* **2004**, *689*, 2808-2819.
- (51) Canales, S.; Crespo, O.; Gimeno, M. C.; Jones, P. G.; Laguna, A.; Silvestru, A.; Silvestru, C. *Inorg. Chim. Acta* **2003**, *347*, 16-22.

- (52) Wilton-Ely, J. D. E. T.; Schier, A.; Schmidbaur, H. *J. Chem. Soc. Dalton Trans.* **2001**, 3647-3651.
- (53) Mikulcik, P.; Raithby, P. R.; Snaith, R.; Wright, D. S. *Angew. Chem. Int. Ed.* **1991**, *30*, 428-430.
- (54) Purdy, A. P.; Berry, A. D.; George, C. F. *Inorg. Chem.* **1997**, *36*, 3370-3375.
- (55) Pernin, C. G.; Ibers, J. A. *Inorg. Chem.* **2000**, *39*, 1222-1226.
- (56) Geissinger, M.; Magull, J. Z. *Anorg. Allg. Chem.* **1997**, *623*, 755-761.
- (57) Bhattacharyya, P.; Novosad, J.; Phillips, J.; Slawin, A. M. Z.; Williams, D. J.; Woollins, J. D. *J. Chem. Soc. Dalton Trans.* **1995**, 1607-1613.
- (58) Hanusa, T. P. in: Crabtree, R. H.; Mingos, M. P. (Eds.), *Comprehensive Organometallic Chemistry III*, vol. 2, Elsevier, Oxford, **2007**, p. 67.
- (59) (a) Hanusa, T. P. *Organometallics* **2002**, *21*, 2559-2571. (b) Hanusa, T. P. *Chem. Rev.* **2000**, *100*, 1023-1036. (c) Hanusa, T. P. *Coord. Chem. Rev.* **2000**, *210*, 329-367.
- (60) Al-Shboul, T. M. A.; Volland, G.; Gorls, H.; Kriek, S.; Westerhausen, M. *Inorg. Chem.* **2012**, *51*, 7903-7912.
- (61) Novosad, J.; Necas, M.; Marek, J.; Veltsistas, P.; Papadimitriou, Ch.; Haiduc, I.; Watanabe, M.; Woollins, J. D. *Inorg. Chim. Acta* **1999**, *290*, 256-260.
- (62) Robertson, S. D.; Chivers, T. *Dalton Trans.* **2008**, 1765-1772.
- (63) Westerhausen, M. *Coord. Chem. Rev.* **1998**, *176*, 157-210.
- (64) George, D.; Vaughn, K.; Alex, K.; Gladysz, J. A. *Organometallics* **1986**, *5*, 936-942.
- (65) M. Sheldrick, SHELXS-97, *Program of Crystal Structure Solution*, University of Göttingen, Germany, **1997**.
- (66) G. M. Sheldrick, SHELXL-97, *Program of Crystal Structure Refinement*, University of Göttingen, Germany, **1997**.

Chapter 3

Novel amidophosphine-boranes into the alkali and heavier alkaline-earth metals coordination sphere: syntheses and structural studies

3.1 Introduction

As described in the previous chapter 2, the organometallic chemistry of the heavier alkaline-earth metals has been changed from obscurity to an exciting, rapidly developing area of chemistry due their large ionic radius, strong negative redox potentials, high oxophilicity and high electropositive character.¹ The homoleptic and heteroleptic alkaline-earth metal complexes have recently been employed in various catalytic applications, including the ring-opening polymerization of various cyclic esters,^{2,3} the polymerization of styrene and dienes,⁴ and the hydroamination and hydrophosphination of alkenes and alkynes.⁵ Determining the structures and reactivities of alkaline-earth metal species is an important step towards the design and development of efficient catalyst; however, the efficiency of catalyst is further dependence on the steric and electronic properties of the chelating ligand system. Therefore, the development of specifically designed donor molecules is one of the major steps in the development of the efficient catalysts. A wide variety of nitrogen-based ancillary ligands, such as tris(pyrazolyl)borates,⁶ aminotroponimines,⁷ β -diketiminates,⁸ iminopyrroles,⁹ and 1,4-diaza-1,3-butadiene,¹⁰ have been introduced to prepare well-defined alkaline-earth-metal complexes. Various P–N systems like monophosphanyl amides (R_2PNR')^{11,12} diphosphanyl amides ($(Ph_2P)_2N$),^{12,13} phosphoraneiminato (R_3PN),¹⁴ phosphiniminomethanides ($(RNPR'_2)_2CH$),^{15–17} phosphiniminomethandiides ($(RNPR'_2)_2C$),^{18,19} and diiminophosphinates ($R_2P(NR')$)²⁰ are well known today as ligands and proved their potency into the transition and f-block metals. Therefore, use of amidophosphines is another alternative way, to stabilize these extremely

oxophilic alkaline-earth metals. We have recently introduced the series of phosphine amines [Ph₂PNHR] (**A**; R = 2,6-Me₂C₆H₃, CHPh₂, CPh₃) and their chalcogen derivatives [Ph₂P(O)NHR] (**NPO**), [Ph₂P(S)NHR] (**NPS**), and [Ph₂P(Se)NHR] (**NPSe**) (Chart 1) into the chemistry of alkali metals and the heavier alkaline-earth metals.[See Chapter 1 and 2]

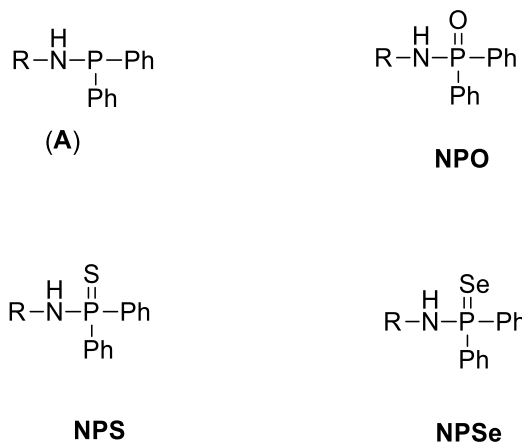


Chart 1. Phosphineamine ligands and their chalcogenides

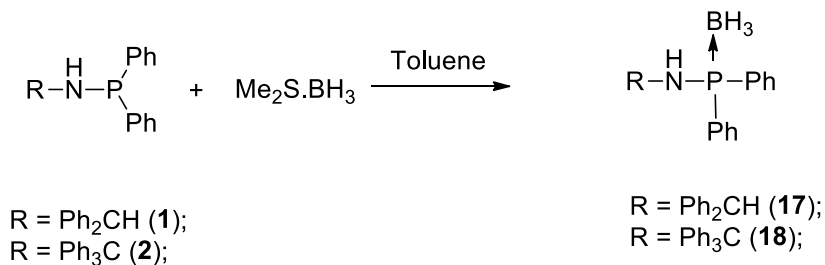
Phosphineamine **A** can coordinate to metals through the nitrogen and phosphorus atoms, resulting in a highly strained three-membered metallacycle, as reported by Roesky and others.^{21,22} The phosphineamine chalcogenides **NPO**, **NPS**, and **NPSe** can form either a four-membered metallacycle, if the nitrogen and the chalcogen atoms (O, S, Se) coordinate to the metal center, or two fused three-membered metallacycles to stabilize the metal complexes, which is what we observed in alkali-metal and heavier alkaline-earth-metal complexes. Thus, due to the presence of three adjacent potential donor atoms, the polymetallacyclic structural motif of the metal complexes was explored. The basicity of the nitrogen atom adjacent to the phosphorus atom in the amidophosphines **A** has remained the driving factor in the ability of the nitrogen and the phosphorus to effectively coordinate to an electron-deficient group. It is well accepted that in acyclic phosphineamines the tricoordinate nitrogen atom assumes a planar configuration with respect to its substituents and thus demonstrates diminished basicity due to enhanced N(pπ)–P(dπ) bonding.^{23–25} From these literature reports and the phosphine amines available to us, we decided to synthesize the amidophosphine–borane adduct to exploit the chelating behavior of amidophosphines in alkali-metal and alkaline-earth metal chemistry. This idea will also

help us to extend our ligand skeleton as **NPB** (*vide infra*) and, in a similar fashion, as **NPO**, **NPS**, and **NPSe** (Chart 1). The complexation of a divalent metal by the **NPB** ligand (**17**) potentially leads to complexes that are isostructural with amidophosphine–chalcogenide divalent complexes of the type $[\{\eta^2\text{-Ph}_2\text{P(X)N}(\text{CHPh}_2)\}_2\text{M}(\text{THF})_2]$. (See Chapter 2) Very recently, Verdaguer and Kolodiazny groups reported a series of chiral aminophosphine–borane compounds and their applications in asymmetric catalysis and hydrogenolysis.²⁶ However, reports of their use as coordinating ligands toward alkali metals and alkaline-earth metals are not available to date. We envision that ligand **17** can be deprotonated to generate the monoanionic compound $\{(\text{Ph}_2\text{CHNP}(\text{BH}_3)\text{Ph}_2)\}^-$, which can coordinate to the metal center. Gaumont and co-workers reported that copper(I) complexes using an anionic phosphido–borane adduct can be used as pre-catalysts for the formation of phosphorus–carbon bonds.²⁷ Most of the structurally characterized complexes in this category can be classified into two classes: In alkali-metal complexes, the hard metal center is chelated by the borane hydrogen atoms of the ligand, and in transition-metal complexes, the soft phosphorus atom shows a preference to bind with the relatively softer metal center.²⁸ It has also been reported that the lithium phosphine–borane complex is diatopic in nature and can be used to reduce aldehydes to generate the corresponding phosphine–borane substituted alcohols at elevated temperatures.²⁹ However, the vast potential of this field of chemistry is still underdeveloped. In this chapter, alkali-metal amidophosphine–borane complexes with the compositions $[(\eta^2\text{-Ph}_2\text{CHNP}(\text{BH}_3)\text{Ph}_2)\text{Li}(\text{THF})_2]$ (**19**), $[\{(\eta^2\text{-Ph}_2\text{C-HNP}(\text{BH}_3)\text{Ph}_2)\text{Na}(\text{THF})_2\}_2]$ (**20**), and $[\{(\eta^2\text{-Ph}_2\text{CHNP}(\text{BH}_3)\text{Ph}_2)\text{K}(\text{THF})_2\}_2]$ (**21**) are presented. The heavier alkaline-earth-metal complexes $[\text{M}(\text{THF})_2\{\text{Ph}_2\text{P}(\text{BH}_3)\text{N}(\text{CHPh}_2)\}_2]$ (M = Ca (**22**), Sr (**23**), Ba (**24**)) are also described herein and can be prepared with high yields and purities by two synthetic routes. The full accounts of two synthetic routes and the solid-state structures of all the complexes are presented.

3.2 Results and Discussion

3.2.1. Synthesis of amidophosphine-borane adducts

The amidophosphine–borane adducts [Ph₂P(BH₃)NH(CHPh₂)] (**17**), [Ph₂P(BH₃)NH(C-Ph₃)] (**18**) were prepared in good yield by Lewis acid base reaction between the corresponding phosphineamine and H₃B.SMe₂ in 1:1 molar ratio in toluene at room temperature and followed by recrystallization either from hot toluene or dichloromethane (Scheme 3.1).³⁰ The compounds **17** and **18** were fully characterized by spectroscopic /analytical techniques and the solid state structures of both the compounds were established by using single crystal X-ray diffraction analysis.



Scheme 3.1. Synthesis of various amidophosphine-borane adducts

The formation of the amidophosphine borane **17** and **18** from the respective phosphineamine [Ph₂PNHR] can easily be followed by ¹H NMR spectroscopy, since an additional resonance is observed for the borane (BH₃) group attached to the phosphorus atom as broad peak at δ 1.17 (**17**) and 0.68 (**18**) ppm respectively. The resonance of the amidophosphine moiety in **17** and **18** are only slightly shifted in comparison to the starting material [Ph₂PNHR] with those reported for the corresponding phosphineamines. (See Chapter 1). The resonance at 5.45 ppm (**17**) as a broad singlet can be assigned to the methine proton of the CH group attached to the nitrogen and this is very close to the that (5.25 ppm) of precursor **1**. In addition, a broad signal at 2.84 (**17**) and 3.45 ppm (**18**) has been observed for the corresponding amine protons of the phosphineamine moieties. In ³¹P{¹H} NMR spectra, a doublet is observed at 57.1 (**17**) and 53.3 ppm (**18**) which is significantly shifted compare to that (35.2 (**1**), 26.3(**2**) ppm) of respective phosphineamines [Ph₂PNHR]. A coupling constant of 85.8 Hz (for **17**) can be observed which can be

assigned as J_{P-B} coupling between the ^{31}P and ^{11}B atoms adjacent to each other. The J_{P-B} is within the range of the reported value (80.1 Hz) for $[(\text{R}_2\text{PBX}_2)_4]$ ($\text{R} = \text{CH}_3$, $\text{X} = \text{H}$).³¹ In $^{11}\text{B}\{^1\text{H}\}$ NMR spectra, we observed a broad peak for the boron atom at -38.1 (**17**) and -36.0 (**18**) ppm. The broadening of the signals for boron resonances can be attributed to the coupling with adjacent phosphorus atom present in the respective amidophosphine-borane adducts. These observations clearly indicate that the BH_3 group forms the phosphine-borane adduct rather than the amido-borane adduct, which is usually formed in homogeneous middle- or late-transition-metal catalysis.³² In FT-IR spectra characteristic signal for P-B bond stretching at 602 (**17**) and 609 (**18**) cm^{-1} was observed along with another characteristic signal at 2383 (**17**) and 2386 (**18**) cm^{-1} assigned for B-H stretching frequency. These values are well agreement with the values reported in literature.³³ To study the molecular structures of **17** and **18** in solid state, the structures of the compound **17** and **18** were established by using single crystal X-ray diffraction analysis.

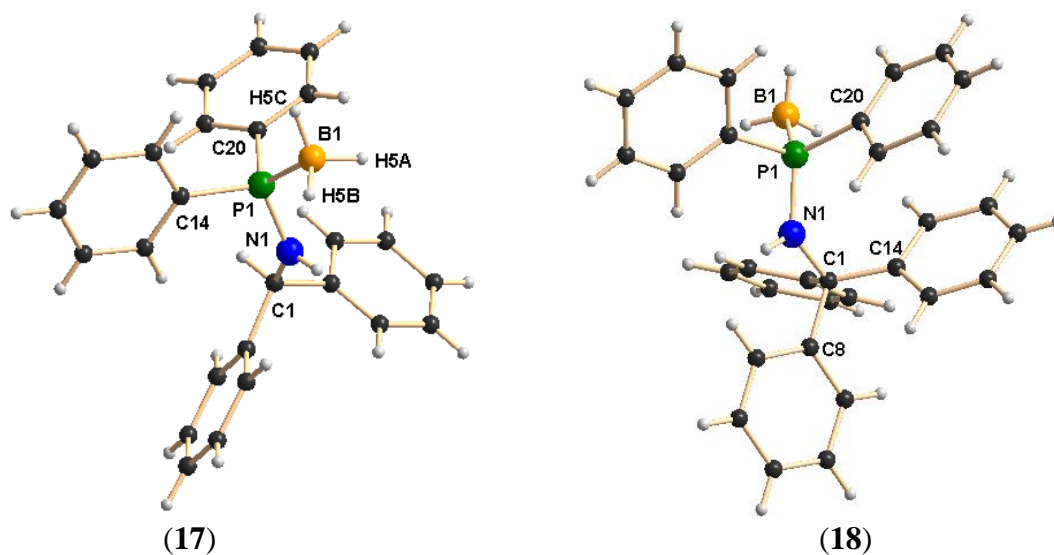


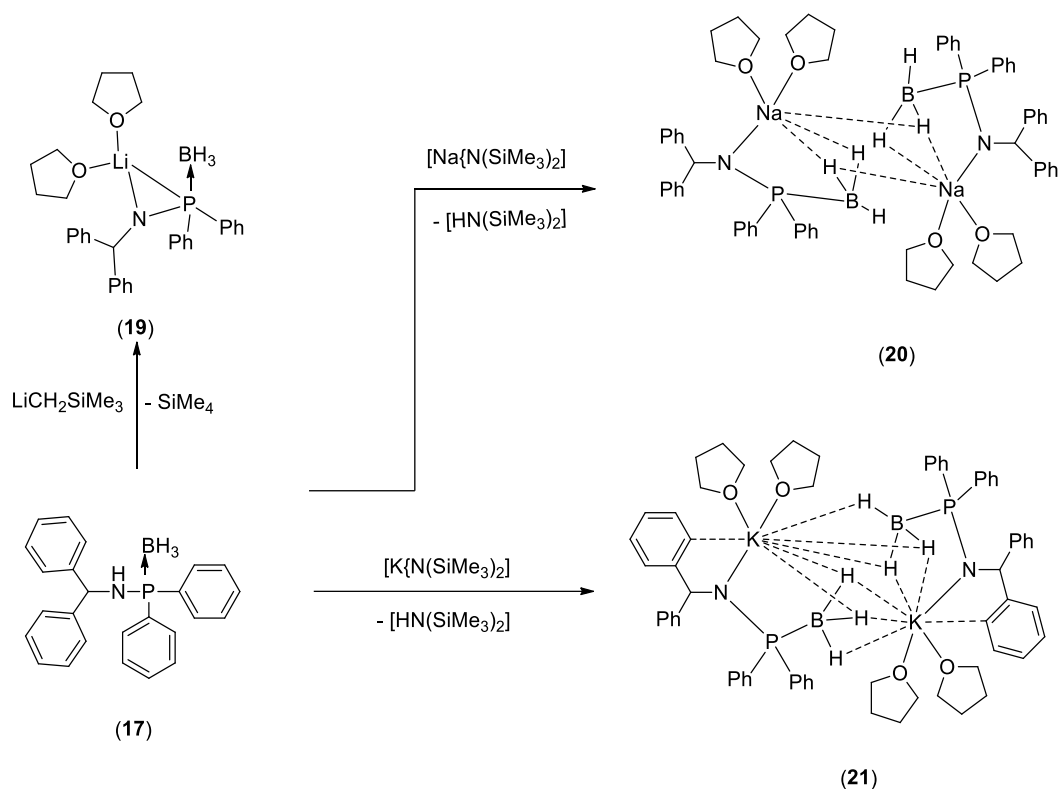
Figure 3.1. Solid state structures of compounds **17** and **18**. Selected bond distances (\AA) and bond angles ($^\circ$): **17**: P1-N1 1.638(3), P1-B1 1.918(6), P1-C14 1.812(4), P1-C20 1.815(4), N1-C1 1.468(5), C1-C2 1.537(6), C1-C8 1.532(6); B1-P1-N1 107.8(3), B1-P1-C14 112.7(3), B1-P1-C20 115.4(3), P1-N1-C1 127.5(3), N1-C1-C8 113.4(3), N1-C1-C2 110.4(3). **18**: P1-N1 1.687(6), P1-B1 1.953(13), P1-C20 1.831(9), P1-C26 1.829(11), N1-C1 1.503(10), C1-C2 1.550(12), C1-C8 1.561(11), C1-C14 1.520(11), B1-P1-N1 119.2(5), B1-P1-C20 111.2(5), B1-P1-C26 109.5(6), P1-N1-C1 126.5(5),

N1–C1–C2 109.9(6), N1–C1–C8 107.4(6), N1–C1–C14 109.2(6), N1–P1–C20 112.2(4), N1–P1–C26 99.1(4).

Compound **17** crystallizes in the triclinic space group $P-1$ and has two independent molecules in the unit cell (Figure 3.1). The details of the structural parameters of compound **17** are given in the Table 3.1. The P1–B1 bond distance in compound **17** (1.918(6) Å) is in agreement with the reported value of 2.1019(8) Å for $[\{\text{Ph}_2\text{P}(\text{BH}_3)\}_2\text{CH}_2]$ and can be considered a phosphorus–boron dative bond. The bond distances P1–N1 (1.638(3) Å) and C1–N1 (1.468(5) Å) are also similar to those of the phosphineamine compound $[\text{Ph}_2\text{PNH}(\text{CHPh}_2)]$ (P1–N1 = 1.673(6) Å and C1–N1 = 1.453(8) Å), as we previously observed. Compound **18** crystallizes in the monoclinic space group $P2_1/c$ having four independent molecules in the unit cell (Figure 3.1). The P1–B1 bond distance (1.953(13) Å for **18**), is almost similar and slightly shorter than the reported values 2.1019(8) Å for $[\{\text{Ph}_2\text{P}(\text{BH}_3)\}_2\text{CH}_2]$ and can be consider as phosphorus boron dative bond.^{33b} Thus the molecular structures of both the aminophosphine-borane compounds clearly indicate that enhanced basicity upon the phosphorus atom to coordinate compare to that of adjacent nitrogen atom in the respective aminophosphines. P1–N1 bond distance (1.687(6) Å for **18**), C1–N1 distance (1.503(10) Å for **18**), are also similar to that of phosphineamine compound $[\text{Ph}_2\text{PNHCHPh}_2]$ (P1–N1 1.673(6) Å and C1–N1 1.453(8) Å) previously observed by us (Chapter 1). The angles C1–N1–P1 (126.5(5)° (**18**)), is slightly widened upon coordination of BH_3 onto the phosphorus [118.24(4)° (**1**)] but similar range with compound **17** (127.5(3)°). The solid state structures of both the aminophosphine-borane compounds confirmed the dynamic nature of the molecules observed in multinuclear NMR spectra (*vide supra*).

3.3 Synthesis and characterization of the alkali-metal complexes

Diphenylphosphineamido-borane ligand **17** was reacted with (trimethylsilyl)-methylolithium in THF at ambient temperature in a 1:1 molar ratio to afford a lithium amidophosphine–borane complex with the composition $[\{\eta^2\text{-Ph}_2\text{CHNP}(\text{BH}_3)\text{Ph}_2\}\text{Li}(\text{THF})_2]$ (**19**) through the elimination of the volatile tetramethylsilane (Scheme 3.2).³⁰



Scheme 3.2. Synthesis of Alkali-metal complexes

Compound **19** was recrystallized from THF and *n*-pentane (1:2 ratio) and was found to crystallize in the monoclinic space group $P2_1/c$, which has four molecules in the unit cell. The solid-state structure of complex **19** is given in Figure 3.2. The details of the structural parameters are given in the Table 3.1. The lithium coordination polyhedron of complex **19** is formed by the chelation of the amido nitrogen, the phosphorus atom of the ligand moiety, and two THF molecules. Notably, the borane group does not participate in the coordination to the lithium metal, which can be explained as being due to the smaller size of the lithium metal in comparison to the other metals used in this work. The Li1–N1 distance of 1.971(3) Å is very similar to the lithium–amido bond distances reported in the literature.³⁴ The Li1–O1 (1.945(3) Å) and Li1–O2 (1.929(3) Å) bond distances are also consistent with reported values. The Li1–P1 distance of 2.925(3) Å is slightly greater than the distances of 2.611(6) and 2.527(3) Å reported for $[[\{(\text{Me}_3\text{Si})_2\text{CH}\}\text{P}(\text{BH}_3)(\text{C}_6\text{H}_4\text{-2-SMe})\}\text{Li}(\text{THF})]_2$ in the literature³⁴ and can be termed as a very weak interaction between the phosphorus and lithium atoms.

Thus, a three-membered metallacycle, Li1–N1–P1, is formed that has the bond angles Li1–P1–N1 39.61(7)°, N1–Li1–P1 31.50(6)°, and Li1–N1–P1 108.88(11)°. Similar three-membered lithium metallacycles can be found in the literature.³⁴ The P1–B1 distance (1.9199(18) Å) remained unchanged in comparison to that of ligand **17** (1.918(6) Å).

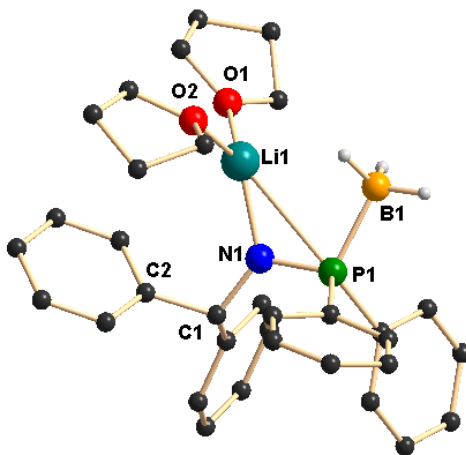


Figure 3.2. Solid state structure of lithium-complex **19**. Selected bond distances (Å) and bond angles (°): P1–N1 1.638(3), P1–B1 1.918(6), P1–C14 1.812(4), P1–C20 1.815(4), N1–C1 1.468(5), C1–C2 1.537(6), C1–C8 1.532(6); B1–P1–N1 107.8(3), B1–P1–C14 112.7(3), B1–P1–C20 115.4(3), P1–N1–C1 127.5(3), N1–C1–C8 113.4(3), N1–C1–C2 110.4(3).

The ^1H , $^{31}\text{P}\{^1\text{H}\}$, and $^{11}\text{B}\{^1\text{H}\}$ NMR spectra also confirmed the solid-state structure of **19**. In the ^1H NMR spectra, a doublet at 5.41 ppm can be assigned to the methine proton of ligand moiety **17** having a coupling constant ($^3J_{\text{H-P}}$) of 21.5 Hz. The three protons of the free BH_3 group gave a broad signal at 1.45 ppm, which is similar to the signal from compound **17**. Coordinated THF signals are also observed as two broad singlets at 3.32 and 1.17 ppm. The proton-decoupled $^{31}\text{P}\{^1\text{H}\}$ NMR spectrum shows a doublet at 71.1 ppm, which exhibits a significant low-field shift in comparison to the corresponding signal of ligand **17** (56.8 ppm). The $^{11}\text{B}\{^1\text{H}\}$ NMR spectrum is also informative and shows a doublet signal at –36.1 ppm, which is shifted slightly to low field in comparison to that of the free ligand **17** (–38.1 ppm).

The dimeric sodium and potassium amidophosphine–borane complexes with molecular formulas $[\{(\eta^2\text{-Ph}_2\text{CHNP}(\text{BH}_3)\text{Ph}_2)\text{Na}(\text{THF})_2\}_2]$ (**20**) and $[\{(\eta^2\text{-Ph}_2\text{CHNP}(\text{BH}_3)\text{Ph}_2)\text{K}(\text{THF})_2\}_2]$ (**21**) were prepared via the reaction of ligand **17** and sodium bis(trimethylsilyl)amide (or potassium bis(trimethylsilyl)amide in the case of **21**) in THF at ambient temperature through the elimination of volatile bis(trimethylsilyl)amine (Scheme 3.2). Both of the complexes were characterized by spectroscopic and analytical techniques, and the solid-state structures of complexes **20** and **21** were established by single-crystal X-ray diffraction analyses. In the ^1H NMR spectra of **20** and **21**, the resonance signals are similar, due to their similar structural properties. The characteristic doublet at 5.46 ppm for **20** (5.73 ppm for **21**) can be assigned to the methine proton of the CH group attached to the nitrogen having coupling constants ($^3J_{\text{P-H}}$) of 25.0 Hz (for **20**) and 21.5 Hz (for **21**), and they are shifted slightly to low field in comparison to the corresponding signal (5.45 ppm) of ligand **17**. In the $^{31}\text{P}\{^1\text{H}\}$ NMR spectra, a doublet is observed at 46.2 ppm for **20** (73.2 ppm for **21**). Thus, for complex **20**, the resonance for the phosphorus is shifted slightly to high field, whereas in complex **21**, the resonance of the phosphorus atom is shifted significantly to low field in comparison to that (56.8 ppm) of **17**. This result can be attributed to the fact that the phosphorus atom is highly influenced by the electron-deficient borane (BH_3) group attached to it. The doublet signal is caused by the coupling between the ^{31}P and ^{11}B atoms adjacent to each other, and a coupling constant (135.9 Hz for **20**) is observed. In the $^{11}\text{B}\{^1\text{H}\}$ NMR spectra, we obtained a broad doublet signal at -34.2 ppm for **20** (-37.4 ppm for **21**), and the broadening is presumably caused by the coupling to the adjacent phosphorus atom. In the FT-IR spectra, the characteristic signal for the P–B bond stretching at 610 cm^{-1} for **20** (607 cm^{-1} for complex **21**) was observed along with another characteristic signal at 2379 cm^{-1} for **20** (2380 cm^{-1} for **21**) assigned as the B–H stretching frequency. These values correspond well with the values (602 and 2383 cm^{-1}) of the neutral ligand **17** as well (*vide supra*). Single crystals of the sodium and potassium salts **20** and **21** were obtained from a mixture of THF and *n*-pentane, and in the solid state, both the complexes crystallized in the triclinic space group *P*-1 and had one molecule in the unit cell. The solid-state structures of complexes **20** and **21** are given in Figure 3.3 and 3.4 respectively. All of the hydrogen atoms were located in the Fourier difference map and were subsequently refined.

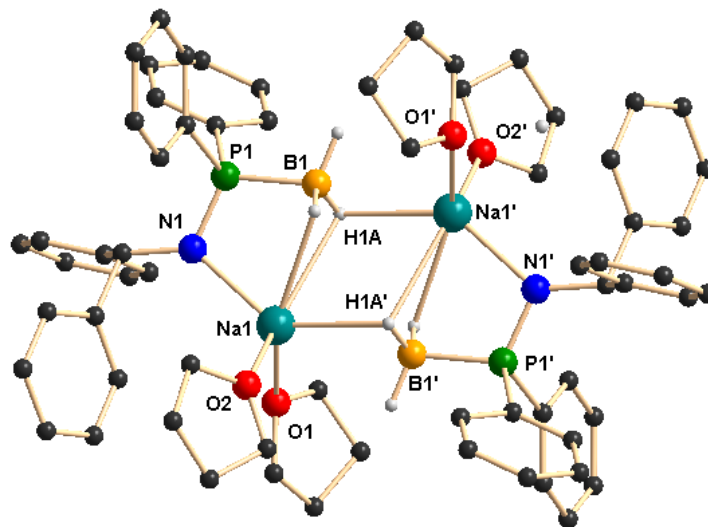


Figure 3.3. Solid state structure of sodium-complex **20**. Hydrogen atoms (except H1a, H1b; H, and H1aⁱ, H1bⁱ, Hⁱ) are omitted for clarity. Selected bond distances (Å) and bond angles (°): P1–N1 1.6060(19), P1–B1 1.921(3), P1–Na1 3.2078(11), B1–Na1 2.949(3), B1ⁱ–Na1 2.862(3), N1–Na1 2.387(2), Na1–O1 2.337(2), Na1–O2 2.377(2), B1–H 1.15(3), B1–H1a 1.07(3), B1–H1b 1.10(3), Na1–H 2.57(3); B1–P1–N1 110.35(11), P1–B1–Na1 79.34(10), P1–B1–Na1ⁱ 170.67(15), P1–N1–Na1 105.23(9), O1–Na1–O2 106.96(8), B1–Na1–N1 64.87(7), B1–Na1–P1 36.05(5), P1–Na1–N1 28.89(5), O1–Na1–B1 127.09(9), O2–Na1–B1 125.71(9), O1–Na1–P1 118.68(6), O2–Na1–P1 122.16(6), N1–Na1–H 75.5(6), B1–Na1–H 22.7(6), P1–Na1–H 48.5(6), H–B1–H1a 110(2), H–B1–H1b 115(2), H1a–B1–H1b 112(2), Na1–B1–Naⁱ 94.27(9), B1–Na1–B1ⁱ 85.73(9).

In the centrosymmetric molecule **20**, two amidophosphine–borane ligands coordinate to two sodium atoms by one BH₃ group, one phosphorus atom, and one amido nitrogen atom and exhibit a diamond-shaped Na₂(BH₃)₂ core with the mean bond angles B1–Na1–B1ⁱ 85.73(9)° and Na1–B1–Na1ⁱ 94.27(9)°. The BH₃ borane groups of the two ligands coordinate to the sodium atom in a η² fashion with a Na1–B1 bond distance of 2.949(3) Å and a Na1–B1ⁱ bond distance of 2.862(3) Å. The P1–Na1 distance of 3.2078(11) Å is slightly longer than the bond distances of 2.9661(17) and 2.9474(16) Å reported for [[{(Me₃Si)₂CH}P(BH₃)(C₆H₄-2-SMe)]Na(tmeda)]_∞ by Izod and co-workers,^{34c,d} and is also larger than the sum of the covalent radii (3.00 Å) of sodium and phosphorus. Thus, it can be concluded that no interaction between the phosphorus and sodium atoms can be

observed. In complex **20**, two additional THF molecules are also coordinated to each sodium atom, and the geometry of each sodium atom can best be described as a distorted trigonal bipyramidal having two THF molecules in the apical position. The bond distances Na1–N1 2.387(2) Å, Na1–O1 2.337(2) Å, and Na1–O2 2.4377(2) Å are in the range of the previously reported values (Chapter 1 and 2). The P1–B1 distance [1.921(3) Å] remains almost unchanged compared to that of the free ligand **17** (1.918(6) Å). If the BH₃ group is considered monodentate, the entire structure consists of three four-membered rings forming a trimetallacyclo [4.2.0.0^{2,5}]-octane structure. To the best of our knowledge, this is the first example of that type of structural motif in sodium complexes using borane groups.³⁵

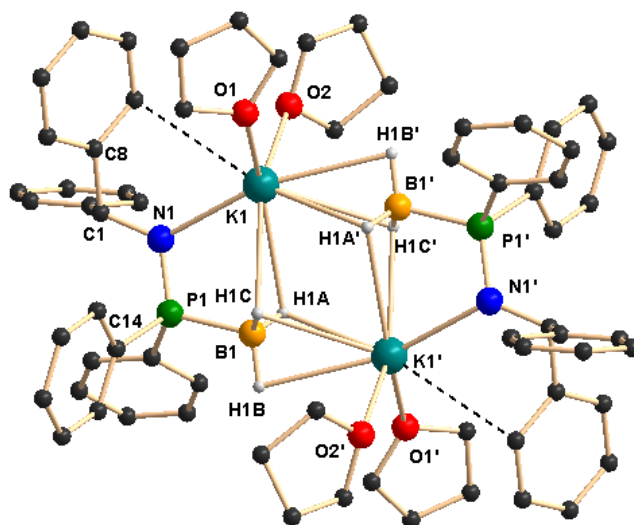


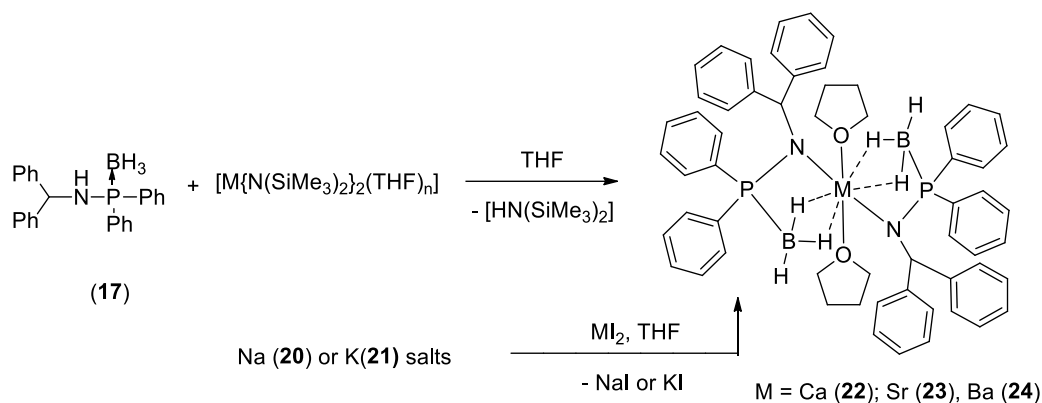
Figure 3.4. Solid state structure of potassium-complex **21**. Hydrogen atoms (except H1a, H1b, H1c and H1aⁱ, H1bⁱ and H1cⁱ) are omitted for clarity. Selected bond lengths (Å) and bond angles (°): P1–N1 1.604(2), P1–B1ⁱ 1.920(3), P1–K1 3.5148(10), B1ⁱ–K1 3.192(4), B1–K1 3.043(3), N1–K1 2.691(2), K1–O1 2.713(3), K1–O2 2.651(3), K1–C13 3.468(3), B1–H1a 1.09(4), B1–H1b 1.15(4), B1–H1c 1.16(3), K1–H1a 2.69(4), K1–H1b 2.93(3), K1–H1c 3.01(3), K1–K1ⁱ 4.5732(13); B1ⁱ–P1–N1 110.73(14), P1ⁱ–B1–K1ⁱ 82.86(12), P1–N1–K1 107.11(11), O1–K1–O2 105.99(9), B1ⁱ–K1–N1 58.44(8), B1ⁱ–K1–P1 32.82(6), P1–K1–N1 25.86(5), B1–K1–B1ⁱ 85.68(9), B1–K1–O1 94.50(9), B1–K1–O2 89.70(9), H1a–B1–H1b 106(3), H1a–B1–H1c 112(3), H1b–B1–H1c 112(2), K1–B1–K1ⁱ 94.32(9).

The potassium complex **21** is centrosymmetric and dimeric in nature, where each potassium atom is coordinated by two amidodiphenylphosphine–borane ligands **17** via one phosphorus atom and one amido nitrogen atom along with one BH₃ group. It exhibits a diamond-shaped K₂(BH₃)₂ core with a mean B1–K1–B1ⁱ bond angle of 85.68(4)° and a mean K1–B1–K1ⁱ bond angle of 94.32(9)°. Each BH₃ borane group of the two ligands coordinates to two potassium atoms in a η³ fashion with a K1–B1 bond length of 3.043(3) Å and a K1–B1ⁱ bond length of 3.193(4) Å. The P1–K1 bond distance of 3.5148(10) Å is even more elongated in comparison to the P1–Na1 distance (3.2078(11) Å) and is also longer than the sum of the covalent radii (3.45 Å) of potassium and phosphorus.^{34d, 35} Each potassium atom is bound to two THF molecules, having the bond distances K1–O1 2.713(3) Å and K1–O2 2.651(3) Å. The P1–B1 distance (1.917(4) Å) remains almost unperturbed in comparison to that of ligand **17** (1.920(3) Å). A short contact between the potassium and one of the phenyl carbon atoms (K1⋯C13 (3.469(3) Å)) is observed, which can be attributed to a remote or secondary M–C interaction. However, in solution, all phenyl protons appear to be equivalent, as observed in the ¹H NMR study, presumably due to the dynamic behavior of the complex. Thus, in the solid state, the two additional five-membered metallacycles K1–N1–C1–C8–C13 and K1ⁱ–N1ⁱ–C1ⁱ–C8ⁱ–C13ⁱ are formed.

3.4 Synthesis and characterization of the alkaline-earth-metal complexes

The reaction of ligand **17** with alkaline-earth metal bis(trimethylsilyl)amides [M{N(SiMe₃)₂}₂(THF)_n] (M = Ca, Sr, Ba) in a 2:1 molar ratio in THF followed by crystallization from THF and *n*-pentane yields the respective heavier alkaline-earth metal amidophosphine–borane complexes [M(THF)₂{Ph₂P(BH₃)N(CHPh₂)₂}₂] (M = Ca (**22**), Sr (**23**), Ba (**24**)) at ambient temperatures with the loss of bis(trimethylsilyl)amine, [(Me₃Si)₂NH]. The same alkaline-earth metal complexes, **22–24**, can also be prepared by a salt metathesis reaction involving **20** or **21** with alkaline-earth metal diiodides in THF at ambient temperature (Scheme 3.3).³⁰ The silylamide route was followed for all three complexes **22–24**, whereas both routes were used to prepare the calcium complex **22**. The silylamide route gave higher purity metal complexes in comparison to the salt metathesis reaction.³⁶ All of the new complexes **22–24** were characterized using standard analytical and spectroscopic techniques, and the solid-state structures were established by single-

crystal X-ray diffraction analyses. A strong absorption at 610 cm^{-1} (for **22**), 610 cm^{-1} (for **23**), and 603 cm^{-1} (for **24**) in the FT-IR spectra is evidence of the P–B bond in each complex. The ^1H NMR spectra of **22–24** in C_6D_6 are very similar to the spectra recorded for complexes **20** and **21** (*vide supra*) and reveals time-averaged C_s symmetry in solution. The presence of solvated THF is also indicated by two broad signals: 3.32 and 1.17 ppm for **22**; 3.45 and 1.29 ppm for **23**; 3.38 and 1.24 ppm for **24**. The doublet signals due to the resonance of the methine protons (5.49 ppm for **22**, 5.53 ppm for **23**, and 5.48 ppm for **24**) in the ^1H NMR spectra of complexes **22–24** remained almost unaffected in comparison to the signals of the free ligand (5.45 ppm) after complex formation with the metals.



Scheme 3.3. Synthesis of alkaline-earth metal complexes **22**, **23** and **24**.

The coupling between the phosphorus and the methane proton is also evident from their respective coupling constants (23.3 Hz for **22**, 24.5 Hz for **23**, and 22.3 Hz for **24**), which are within the range reported in the literature.³⁷ The resonances of the three protons attached to the boron atom appeared as a broad signal (1.62 ppm for **22**, 1.63 ppm for **23**, and 1.72 ppm for **24**) in the ^1H NMR spectra. In the proton-decoupled $^{31}\text{P}\{^1\text{H}\}$ NMR spectra, complexes **22–24** show only one doublet signal at 46.9 ppm for **22**, 46.3 ppm for **23**, and 46.9 ppm for **24**, respectively, and these values are shifted significantly to high field in comparison to the value for compound **17** (56.8 ppm) upon the coordination of calcium, strontium, or barium atoms to the amidophosphine–borane ligand. The phosphorus atoms present in the two $\{\text{Ph}_2\text{P}(\text{BH}_3)\text{N}(\text{CHPh}_2)\}^-$ moieties are chemically equivalent. Although there has been ongoing interest in alkaline-earth organometallics^{38a} and particularly in the cyclopentadienyl chemistry of these elements,^{38b} complexes **22–24**

represent, to the best of our knowledge, the first amidophosphine–borane alkaline-earth metal complexes containing three hetero atoms, N, P, and B, adjacent to each other in the ligand. Therefore, their molecular structures in the solid state were determined by X-ray diffraction analysis. The calcium and strontium complexes **22** and **23** crystallize in the triclinic space group *P*-1 and have one molecule of either **22** or **23** and two THF molecules as solvent in the unit cell. The details of the structural parameters are given in the Table 3.2 & 3.3 respectively. The solid-state structures of complexes **28** and **29** are shown in Figures 3.5 and 3.6, respectively.

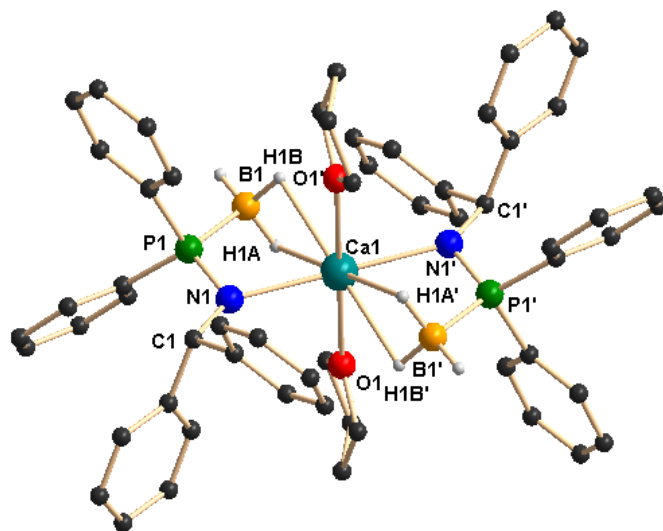


Figure 3.5. Solid state structure of complex **22**. Hydrogen atoms (except H1a, H1b, H3 and H1aⁱ, H1bⁱ, H3ⁱ) are omitted for clarity. Selected bond lengths (Å) and bond angles (°): P1–N1 1.6217(14), P1–B1 1.921(2), P1–Ca1 3.2308(4), N1–Ca1 2.4534(14), B1–Ca1 2.850(2), Ca1–O1 2.5111(12), Ca1–H1a 2.4961, Ca1–H1b 2.4651, B1–H3 1.0598, B1–H1b 1.1340, B1–H1a 1.1547; O1–Ca1–O1ⁱ 180.0, N1–Ca1–B1 65.15(5), N1–Ca1–P1 29.28(3), P1–Ca1–B1 36.15(4), N1–P1–B1 108.18(8), H1a–B1–H1b 105.3, N1–Ca1–H1a 74.4, N1–Ca1–H1b 77.3, P1–Ca1–H1a 50.0, P1–Ca1–H1b 49.2, B1–Ca1–H1a 23.8, B1–Ca1–H1b 23.2, H1b–Ca1–H1b 43.0, P1–Ca1–P1ⁱ 180.000(14), N1–Ca1–N1ⁱ 180.0, B1–Ca1–B1ⁱ 180.000(1).

Complexes **22** and **23** are isostructural with each other, due to the similar ionic radii for the metal ions (1.00 and 1.18 Å) for a coordination number of 6.³⁹ In the centrosymmetric molecule **22**, the metal coordination polyhedron is formed by two monoanionic

$\{\text{Ph}_2\text{P}(\text{BH}_3)\text{N}(\text{CHPh}_2)\}^-$ ligand moieties and two THF molecules, which are *trans* to each other. Each of the $\{\text{Ph}_2\text{P}(\text{BH}_3)\text{N}(\text{CHPh}_2)\}^-$ ligands coordinates to the calcium atom via the chelation of one of the amido nitrogen atoms and the BH_3 group. The P–Ca distance of 3.2308(4) Å in **22** is significantly larger than the sum of the covalent radii (3.07 Å) of phosphorus and calcium, which indicates that there is no interaction between these two atoms. The borane (BH_3) group coordinates through the hydrogen atoms in a η^2 fashion and has a Ca1–B1 bond length of 2.850(2) Å. Thus, the $\{\text{Ph}_2\text{P}(\text{BH}_3)\text{N}(\text{CHPh}_2)\}^-$ group can be considered a pseudo-bidentate ligand. The Ca1–B1 distance is slightly longer than the 2.751(2) Å distance reported for $[[(\text{Me}_3\text{Si})_2\{\text{Me}_2(\text{BH}_3)\text{P}\}\text{C}]_2\text{Ca}(\text{THF})_4]$.⁴⁰ The central atom, calcium, adopts a distorted-octahedral geometry due to the coordination of two $\{\text{Ph}_2\text{P}(\text{BH}_3)\text{N}(\text{CHPh}_2)\}^-$ moieties and two THF molecules. The N1, P1, B1, and Ca1 atoms are not coplanar; rather, a dihedral angle of 10.11° is observed between the planes containing the P1, N1, and Ca1 atoms and the P1, B1, and Ca1 atoms. The Ca1–N1 distance of 2.4534(14) Å is slightly elongated in comparison with the calcium–nitrogen covalent bond distances (2.361(2) and 2.335(2) Å) reported for $[\text{Ca}(\text{Dipp}_2\text{DAD})(\text{THF})_4]$ (Dipp₂DAD = N,N'-bis(2,6-diisopropylphenyl)-1,4-diaza-1,3-butadiene) in the literature¹⁹ but is close to the corresponding distance (2.479(5) Å) of our recently reported complex $[\text{Ca}(\text{THF})_2\{\text{Ph}_2\text{P}(\text{Se})\text{N}(\text{CHPh}_2)\}_2]$ using the analogous phosphine selenoicamido ligand (See Chapter 2). It is noteworthy that the P1–B1 distance (1.921(2) Å) remains almost unperturbed in comparison to that of the ligand **17** (1.918(6) Å), even after the coordination of the BH_3 group to the calcium center.

In compound **23**, the strontium atom is hexa-coordinated by two borane groups, two amido nitrogen atoms of two **17** ligands, and two coordinating THF molecules. The solvated THF molecules are *trans* to each other, and the strontium atom adopts a distorted-octahedral geometry.

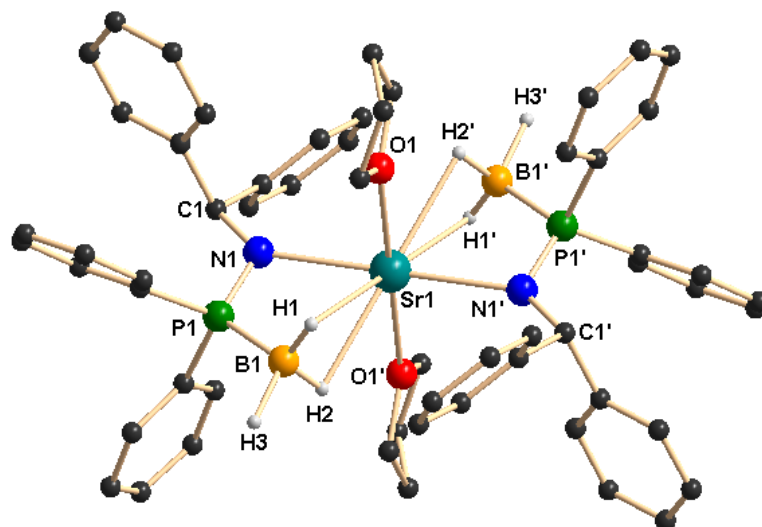


Figure 3.6. Solid state structure of complex **23**. Hydrogen atoms (except H1, H2, H3 and H1ⁱ, H2ⁱ, H3ⁱ) are omitted for clarity. Selected bond lengths (Å) and bond angles (°): P1–N1 1.623(5), P1–B1 1.915(7), P1–Sr1 3.3849(13), N1–Sr1 2.591(4), B1–Sr1 2.995(6), Sr1–O1 2.626(4), Sr1–H1 2.70(6), Sr1–H2 2.60(7), B1–H1 1.11(6), B1–H2 1.12(7), B1–H3 1.14(7); O1–Sr1–O1ⁱ 180.0, N1–Sr1–B1 61.60(16), N1–Sr1–P1 27.65(10), P1–Sr1–B1 34.24(13), N1–P1–B1 108.8(3), H1–B1–H2 104(4), H1–B1–H3 111(5), H2–B1–H3 110(5), B1–Sr1–H1 21.6(13), B1–Sr1–H2 21.5(15), P1–Sr1–H1 49.2(12), P1–Sr1–H2 45.2(14), N1–Sr1–H1 73.1(12), N1–Sr1–H2 71.7(14), P1–Sr1–P1ⁱ 180.00(5), N1–Sr1–N1ⁱ 180.0, B1–Sr1–B1ⁱ 180.0(2).

In comparison to the P–Ca distance (3.2308(4) Å) in compound **22**, the considerably elongated P–Sr distance of 3.385(2) Å, which is also longer than the sum of the covalent radii (3.25 Å) of the phosphorus and strontium atoms, indicates no interaction between the phosphorus and the metal atom. A dihedral angle of 10.65° is observed between the planes formed by the P1, B1, and Sr1 and the P1, N1, and Sr1 atoms, which indicates a slight deviation from coplanarity by the P1, B1, N1, and Sr1 atoms. The strontium–nitrogen bond distance (2.591(14) Å) corresponds well with the distances (2.6512(2) and 2.669(2) Å) in our previously reported strontium complex [(ImpDipp)₂Sr(THF)₃] (ImpDipp = 2,6-ⁱPr₂C₆H₃N=CHC₄H₃N).^{18d} The borane (BH₃) group is coordinated through the hydrogen atoms in a η² fashion and has a Sr1–B1 bond length of 2.995(6) Å, which is longer than in the calcium complex (2.850(2) Å) due to the greater ionic radius of strontium in

comparison to calcium. However, the Sr1–B1 distance (2.995(6) Å) is slightly longer than the reported values [2.893(4) and 2.873(4) Å] observed for $[(\text{Me}_3\text{Si})_2\{\text{Me}_2(\text{BH}_3)\text{P}\}\text{C}]_2\text{Sr}(\text{THF})_5$.⁴⁰

In accordance with complexes **22** and **23**, the barium amidophosphine–borane complex **24** also crystallizes in the triclinic space group *P*-1 having one molecule of **24** and two THF molecules in the unit cell. The details of the structural parameters are given in the Table 3.3. The solid-state structure of complex **24** is given in Figure 3.7.

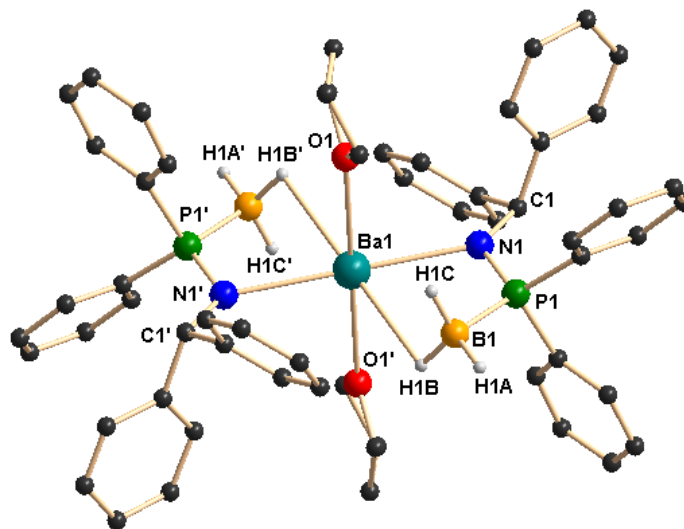


Figure 3.7. Solid state structure of complex **24**. Hydrogen atoms (except H1a, H1b, H1c and H1aⁱ, H1bⁱ, H1cⁱ) are omitted for clarity. Selected bond lengths (Å) and bond angles (°): P1–N1 1.617(6), P1–B1 1.927(8), P1–Ba1 3.5273(18), N1–Ba1 2.733(6), B1–Ba1 3.159(9), Ba1–O1 2.790(5), Ba1–H1b 1.77(7), B1–H1a 1.21(7), B1–H1b 1.13(8), B1–H1c 1.19(10); O1–Ba1–O1ⁱ 180.0, N1–Ba1–B1 58.78(19), N1–Ba1–P1 26.22(12), P1–Ba1–B1 32.92(15), N1–P1–B1 110.4(3), P1–B1–Ba1 84.1(3), P1–B1–H1a 113(3), P1–B1–H1b 107(4), N1–Ba1–H1b 70.3(15), H1a–B1–H1c 105(6), H1b–B1–H1c 115(6), P1–Ba1–P1ⁱ 180.0, N1–Ba1–N1ⁱ 180.0, B1–Ba1–B1ⁱ 179.999(1).

Similar to the calcium and strontium complexes, the coordination polyhedron of the barium complex **24** is formed by two $\{\text{Ph}_2\text{P}(\text{BH}_3)\text{N}(\text{CHPh}_2)\}^-$ ligands and two *trans* THF molecules. As expected because of the larger atomic radius of Ba(II)^{41,42} the Ba1–N1 (2.733(6) Å), Ba1–O1 (2.790(5) Å), and Ba1–P1 (3.527(2) Å) distances are elongated in comparison with the corresponding values determined for the Ca²⁺ and Sr²⁺ complexes **22**

and **23**, respectively. The considerably elongated P–Ba distance of 3.527(2) Å in **24**, which is greater than the sum of the covalent radii of barium and phosphorus (3.34 Å), indicates that barium and phosphorus have no interaction between themselves. Thus, the central atom barium adopts a distorted-pseudo-octahedral geometry due to the ligation from two **17** moieties and two THF molecules. This high distortion can be mainly attributed to the coordination of adjacent atoms present in the ligand and is indicated by the large N1–Ba1–B1 angle of 58.78(19)°. The borane (BH₃) group is coordinated through the hydrogen atoms in a η¹ fashion and has a Ba1–B1 bond length of 3.159(9) Å. In complex **24**, a dihedral angle of 12.24° is observed between the planes containing P1, B1, and Ba1 and P1, N1, and Ba1 atoms, which indicates a slight deviation from planarity by the P1, N1, B1, and Ba1 atoms. The slight increase in the dihedral angle (12.24°) for **24** in comparison to **22** (10.11°) and **23** (10.65°) can be attributed to the larger ionic radius of barium in comparison to the calcium and the strontium atoms. The Ba1–N1 distance of 2.733(6) Å is similar to the barium–nitrogen covalent bond lengths of 2.720(4) and 2.706(4) Å reported for [Ba((Dipp)₂DAD)(μ-I)(THF)₂]₂ (Dipp₂DAD = bis(2,6-diisopropylphenyl)-1,4-diaza-1,3-butadiene) in the literature¹⁹ and is also similar to that (2.776(6) Å) of our recently described complex [Ba(THF)₂{Ph₂P(Se)N(CHPh₂)₂}₂] using the analogous phosphine selenoicamido ligand. (see Chapter 2) It is noteworthy that the P1–B1 distance (1.927(8) Å) remains almost unperturbed in comparison to that of the ligand **17** (1.918(6) Å) even after the coordination of the BH₃ group to the barium center. The Ba1–B1 bond length of 3.159(9) Å is the longest among the metal–B distances of **19–24** due to barium having the largest ionic radius among Ca, Sr, and Ba. However, the Ba1–B1 distance (3.159(9) Å) is similar to the reported values (3.027(8) and 3.023(8) Å) observed for [[(Me₃Si)₂{Me₂(BH₃)P}C]₂Ba(THF)₅].⁴⁰

3.5 Conclusion

We have successfully synthesized and characterized the novel amidophosphine-borane ligands by using single crystal X-ray diffraction analysis and spectroscopic/analytical techniques and we have successfully introduced these borane ligands into the alkali metals as well as to the heavier alkaline-earth metal coordination sphere by synthesizing various alkali and alkaline-earth metal complexes using diphenylphosphinoamido borane ligand

17. The strong electron-donating capacity of the N, P, and BH₃ moieties effectively stabilizes the unusual three-membered or four-membered metallacycles. The alkaline-earth metal complexes obtained by amidophosphino-borane ligand are useful as good reducing agent.

3.6 Experimental Procedures

3.6.1. General

All manipulations of air-sensitive materials were performed with the rigorous exclusion of oxygen and moisture in flame-dried Schlenk-type glassware either on a dual manifold Schlenk line, interfaced to a high vacuum (10⁻⁴ torr) line, or in an argon-filled M. Braun glove box. THF was pre-dried over Na wire and distilled under nitrogen from sodium and benzophenone ketyl prior to use. Hydrocarbon solvents (toluene and *n*-pentane) were distilled under nitrogen from LiAlH₄ and stored in the glove box. ¹H NMR (400 MHz), ¹³C{¹H} and ³¹P{¹H} NMR (161.9 MHz) spectra were recorded on a BRUKER AVANCE III-400 spectrometer. BRUKER ALPHA FT-IR was used for FT-IR measurement. Elemental analyses were performed on a BRUKER EURO EA at the Indian Institute of Technology Hyderabad. The aminophosphines [Ph₂PNH(CHPh₂)] (**1**), [Ph₂PNH(CPh₃)] (**2**) were prepared as described in the Chapter 1 and [M{N(SiMe₃)₂}₂(THF)_n] (M = Ca, Sr and Ba) and LiCH₂SiMe₃ were synthesized according to the literature procedure.^{43,44} The starting materials chlorodiphenylphosphine, benzdihydramine, triphenylmethylamine, borane-dimethylsulfide, sodium/potassium bis(trimethyl)-silylamides and metal diiodides MI₂ (M = Ca, Sr and Ba) were purchased from Sigma Aldrich and used without further purification. The NMR solvent C₆D₆ and CDCl₃ were purchased from sigma Aldrich.

3.6.2. Synthesis of [Ph₂P(BH₃)NH(CHPh₂)] (**17**)

In a pre-dried schlenk flask 1.0 g (2.72 mmol) of N-benzhydryl 1,1diphenylphosphinamine (**1**) in 10 ml toluene was taken and to this borane-dimethylsulfide (0.26 ml, 2.72 mmol) in 5 ml of toluene was added drop wise under the stirring at room temperature. Stirring continued for 12 h. White precipitate was formed, and it was filtered through G4-frit and dried in vacuo. Pure compound was obtained after washing with *n*-pentane. (Yield: 1.20 g,

(100%). The title compound $\text{Ph}_2\text{P}(\text{BH}_3)\text{NHCHPh}_2$ (**17**) is soluble in CDCl_3 , CH_2Cl_2 , THF and hot toluene. The compound **17** was re-crystallized from hot toluene. ^1H NMR (400 MHz, CDCl_3): δ 7.44-7.49 (m, 4H, ArH), 7.34-7.38 (m, 2H, ArH), 7.24-7.28 (m, 4H, ArH), 7.05-7.19 (m, 10H, ArH), 5.45 (d, 1H, $J = 9.4$ Hz, CH), 2.83 (br, 1H, NH), 1.17 (br, 3H, BH_3) ppm. $^{13}\text{C}\{^1\text{H}\}$ NMR (100 MHz, CDCl_3): δ 143.5 (ArC), 143.4 (ArC), 132.1 (P attached ArC), 131.9 (P attached ArC), 131.2 (P attached o-ArC), 131.1 (P attached o-ArC), 128.5 (P attached p-ArC), 128.4 (P attached m-ArC), 128.3 (m-ArC), 127.3 (o-ArC), 127.1 (p-ArC), 60.8 (CH) ppm. $^{31}\text{P}\{^1\text{H}\}$ NMR (161.9 MHz, CDCl_3): δ 56.8 (d, $J = 85.8$ Hz) ppm. $^{11}\text{B}\{^1\text{H}\}$ NMR (128.4 MHz, CDCl_3): $\delta = -38.1$ (br) ppm. FT-IR (selected frequencies): $\nu = 3338$ (N-H), 1434 (P-C), 999 (P-N), 2383 (B-H), 602 (P-B) cm^{-1} . Elemental analysis: $\text{C}_{25}\text{H}_{25}\text{BNP}$ (381.24): Calcd. (%) C 78.76, H 6.61, N 3.67; Found C 78.30, H 6.38, N 3.22.

3.6.3. Synthesis of $[\text{Ph}_2\text{P}(\text{BH}_3)\text{NHCPh}_3]$ (**18**)

Same as above for **17**. Yield is 1.2 gm, (90%). ^1H NMR (400 MHz, CDCl_3): δ 7.43–7.48 (m, 4H, ArH), 7.29–7.33 (m, 2H, ArH), 7.20–7.25 (m, 4H, ArH), 7.16–7.19 (m, 6H, ArH), 7.08–7.11 (m, 9H, ArH), 3.45 (s, 1H, NH), 0.68 (br, 3H, BH_3) ppm. $^{13}\text{C}\{^1\text{H}\}$ NMR (100 MHz, CDCl_3): δ 145.5 (ArC), 145.4 (ArC), 134.3 (P-ArC), 133.7 (P-ArC), 131.9 (P attached o-ArC), 131.8 (P attached o-ArC), 130.8 (P attached p-ArC), 130.7 (P attached p-ArC), 129.5 (o-ArC), 128.4 (P attached m-ArC), 128.3 (P attached m-ArC), 127.8 (m-ArC), 127.2 (p-ArC), 71.8 (CH) ppm. $^{31}\text{P}\{^1\text{H}\}$ NMR (161.9 MHz, CDCl_3): δ 53.3 (br, s) ppm. $^{11}\text{B}\{^1\text{H}\}$ NMR (128.4 MHz, CDCl_3): $\delta - 36.0$ (br) ppm. FT-IR (selected frequencies): $\nu = 3212$ (N-H), 1436 (P-C), 999 (P-N), 2386 (B-H), 609 (P-B) cm^{-1} . Elemental analysis: $\text{C}_{31}\text{H}_{29}\text{BNP}$ (457.33): Calcd (%) C 81.41, H 6.39, N 3.06; Found C 80.97, H 6.13, N 2.82.

3.6.4. Synthesis of $[(\eta^2\text{-Ph}_2\text{CHNP}(\text{BH}_3)\text{Ph}_2)\text{Li}(\text{THF})_2]$ (**19**)

In a 10 ml sample vial 1 equiv (100 mg, 0.264 mmol) of ligand **17** and 1 equiv of $\text{LiCH}_2\text{SiMe}_3$ (25.0 mg, 0.264 mmol) were mixed together with a small amount of THF (2 ml). After 6 h of stirring, a small amount of *n*-pentane (2 ml) was added to the solution, and it was stored at -40 °C. After 12 h, colorless crystals of **19** were obtained. Yield: 120

mg (85%). $^1\text{H NMR}$ (400 MHz, C_6D_6): δ 7.53–7.58 (m, 4H, ArH), 7.06–7.10 (m, 4H, ArH), 6.81–6.90 (m, 12H, ArH), 5.41 (d, $J_{\text{H-P}} = 21.5$ Hz, 1H, CH), 1.45 (br, 3H, BH_3), 3.32 (br, THF), 1.17 (br, THF) ppm. $^{13}\text{C}\{^1\text{H}\}$ NMR (100 MHz, C_6D_6): δ 146.8 (ArC), 146.7 (ArC), 135.7 (P attached ArC), 135.2 (P attached ArC), 132.9 (P attached *o*-ArC), 129.8 (P attached *p*-ArC), 129.1 (P attached *m*-ArC), 128.5 (*m*-ArC), 127.8 (*o*-ArC), 126.5 (*p*-ArC), 68.4 (THF), 66.1 (CH), 25.7 (THF) ppm. $^{31}\text{P}\{^1\text{H}\}$ NMR (161.9 MHz, C_6D_6): δ 71.1 (d) ppm. $^{11}\text{B}\{^1\text{H}\}$ NMR (128.4 MHz, C_6D_6): δ -36.06 (d) ppm. FT-IR (selected frequencies): $\nu = 3373$ (N–H), 2382 (B–H), 1447 (P–C), 931 (P–N), 617 (P–B) cm^{-1} . Elemental analysis: $\text{C}_{33}\text{H}_{40}\text{BLiNO}_2\text{P}$ (531.40): Calcd. C 74.59, H 7.59, N 2.64, Found: C 74.19, H 7.44, N 2.43.

3.6.5. Synthesis of $[\{(\eta^3\text{-Ph}_2\text{CHNP}(\text{BH}_3)\text{Ph}_2)\text{Na}(\text{THF})_2\}_2]$ (**20**)

In a 10 ml sample vial, 50 mg (0.132 mmol) of ligand **17** and 24.2 mg (0.132 mmol) of sodium bis(trimethylsilyl)amide were mixed together with a small amount of THF (2 ml), and the mixture was then stirred for 6 h. A small amount of *n*-pentane (2 ml) was added on top of the solution, and it was stored at -40 °C. After 24 h, colorless crystals of **20** were obtained. Yield: 65 mg (90%). $^1\text{H NMR}$ (400 MHz, C_6D_6): δ 7.65–7.70 (m, 4H, ArH), 7.21–7.23 (d, 4H, ArH), 6.95–7.00 (m, 12H, ArH), 5.46 (d, 1H, $J_{\text{H-P}} = 25.0$ Hz, CH), 3.35 (br, THF), 0.94–1.49 (m, 3H, BH_3), 1.22 (br, THF) ppm. $^{13}\text{C}\{^1\text{H}\}$ NMR (100 MHz, C_6D_6): δ 148.3 (ArC), 148.2 (ArC), 136.7 (P attached ArC), 136.3 (P attached ArC), 130.1 (P attached *o*-ArC), 126.5 (P attached *p*-ArC), 125.9 (P attached *m*-ArC), 125.3 (*m*-ArC), 125.1 (*o*-ArC), 123.2 (*p*-ArC), 65.4 (THF), 62.8 (CH), 22.9 (THF) ppm. $^{31}\text{P}\{^1\text{H}\}$ NMR (161.9 MHz, C_6D_6): δ 46.2 (d, $J_{\text{P-B}} = 135.9$ Hz) ppm. $^{11}\text{B}\{^1\text{H}\}$ NMR (128.4 MHz, C_6D_6): δ -34.2 (d) ppm. FT-IR (selected frequencies): $\nu = 3330$ (N–H), 2379 (B–H), 1440 (P–C), 929 (P–N), 610 (P–B) cm^{-1} . Elemental analysis: $\text{C}_{66}\text{H}_{80}\text{B}_2\text{N}_2\text{Na}_2\text{O}_4\text{P}_2$ (1094.86): Calcd. C 72.40, H 7.36, N 2.56, Found: C 71.98, H 7.05, N 2.43.

3.6.6. Synthesis of $[\{(\eta^3\text{-Ph}_2\text{CHNP}(\text{BH}_3)\text{Ph}_2)\text{K}(\text{THF})_2\}_2]$ (**21**)

In a 10 ml sample vial, 1 equiv of ligand **17** (50 mg, 0.132 mmol) and 1 equiv of potassium bis(trimethylsilyl)amide (26.2 mg, 0.132 mmol) were mixed together with a small amount of THF (2 ml). After 6 h, a small amount of *n*-pentane (2 ml) was added to the solution,

and it was stored at $-40\text{ }^{\circ}\text{C}$. After 24 h, colorless crystals of **21** were obtained. Yield: 66.9 mg (90%). ^1H NMR (400 MHz, C_6D_6): δ 7.58 (m, 6H, ArH), 6.96–7.01 (m, 14H, ArH), 5.73 (d, $J_{\text{H-P}} = 21.5$ Hz, 1H, CH), 3.55 (br, THF), 1.42 (br, THF), 1.82 (br m, 3H, BH_3) ppm. $^{13}\text{C}\{^1\text{H}\}$ NMR (100 MHz, C_6D_6): δ 146.4 (ArC), 144.3 (ArC), 132.3 (P-ArC), 132.2 (P-ArC), 130.7 (P attached *o*-ArC), 128.4 (P attached *p*-ArC), 128.3 (P attached *m*-ArC), 128.2 (*m*-ArC), 127.9 (*o*-ArC), 127.2 (*p*-ArC), 67.6 (THF), 59.9 (CH) 25.6 (THF) ppm. $^{31}\text{P}\{^1\text{H}\}$ NMR (161.9 MHz, C_6D_6): δ 73.2 ppm. $^{11}\text{B}\{^1\text{H}\}$ NMR (128.4 MHz, C_6D_6): δ -37.4 (d) ppm. FT-IR (selected frequencies): $\nu = 3328$ (N–H), 2380 (B–H), 1435 (P–C), 999 (P–N), 607 (P–B) cm^{-1} . Elemental analysis: $\text{C}_{66}\text{H}_{80}\text{B}_2\text{K}_2\text{N}_2\text{O}_4\text{P}_2$ (1126): Calcd. C 70.33, H 7.15, N 2.49. Found: C 70.03, H 6.89, N 2.21.

3.6.7. Synthesis of $[\text{M}(\text{THF})_2\{\text{Ph}_2\text{P}(\text{BH}_3)\text{N}(\text{CHPh}_2)\}_2]$ (M = Ca (**22**), Sr (**23**) and Ba (**24**))

Complex 22: Route 1: In a 10 ml sample vial, 2 equiv of ligand **17** (100 mg, 0.264 mmol) and 1 equiv of $[\text{Ca}(\text{N}(\text{SiMe}_3)_2(\text{THF})_2)]$ (40.4 mg, 0.132 mmol) were mixed together with a small amount of THF (2 ml). After 12 h, a small amount of *n*-pentane (2 ml) was added, and it was stored in a $-40\text{ }^{\circ}\text{C}$ freezer. After 24 h, colorless crystals of **22** were obtained. Yield: 123 mg (86%).

Route 2. In a 25 ml predried Schlenk flask, a potassium salt of ligand **17** (200 mg, 0.32 mmol) was mixed with CaI_2 (46.8 mg, 0.16 mmol) in 10 ml of THF solvent at ambient temperature, and the solution was continuously stirred for 12 h. The white precipitate of KI was filtered off, and the filtrate was dried in vacuo. The resulting white compound was further purified by washing it with *n*-pentane, and crystals suitable for X-ray analysis were grown from a THF and *n*-pentane solvent mixture (1:2) at $-40\text{ }^{\circ}\text{C}$. Yield: 160 mg (92%). ^1H NMR (400 MHz, C_6D_6): δ 7.60–7.65 (m, 4H, ArH), 7.35–7.37 (d, 4H, ArH), 6.80–6.98 (m, 12H, ArH), 5.49 (d, 1H, $J_{\text{H-P}} = 23.3$ Hz, CH), 1.62 (br, 3H, BH_3), 3.32 (br, THF), 1.17 (br, THF) ppm. $^{13}\text{C}\{^1\text{H}\}$ NMR (100 MHz, C_6D_6): δ 148.7 (ArC), 148.6 (ArC), 136.3 (P attached ArC), 135.8 (P attached ArC), 132.9 (P attached *o*-ArC), 132.8 (P attached *o*-ArC), 129.8 (P attached *p*-ArC), 128.5 (P attached *m*-ArC), 128.2 (*m*-ArC), 127.9 (*o*-ArC), 125.9 (*p*-ArC), 68.2 (THF) 66.1 (CH), 25.3 (THF) ppm. $^{31}\text{P}\{^1\text{H}\}$ NMR (161.9 MHz, C_6D_6): δ 46.9 (d, $J_{\text{P-B}} = 121.4$ Hz) ppm. $^{11}\text{B}\{^1\text{H}\}$ NMR (128.4 MHz, C_6D_6): δ -31.8 (d) ppm. FT-IR (selected frequencies): $\nu = 3373$ (N–H), 1443 (P–C), 972 (P–N), 2380 (B–H), 610

(P–B) cm^{-1} . Elemental analysis: $\text{C}_{66}\text{H}_{80}\text{B}_2\text{CaN}_2\text{O}_4\text{P}_2$ (1088.96): Calcd. C 72.79, H 7.40, N 2.57. Found: C 72.57, H 7.24, N 2.21.

Complex 23: In a 10 ml sample vial, 2 equiv of ligand **17** (100 mg, 0.264 mmol) and 1 equiv of $[\text{Sr}(\text{N}(\text{SiMe}_3)_2(\text{THF})_2)]$ (53.9 mg, 0.132 mmol) were mixed together with a small amount of THF (2 ml). After 12 h, a small amount of *n*-pentane (2 ml) was added to it, and it was stored in a $-40\text{ }^\circ\text{C}$ freezer. After 24 h, colorless crystals of **23** were obtained. Yield: 136 mg (91%). ^1H NMR (400 MHz, C_6D_6): δ 7.63–7.68 (m, 4H, ArH), 7.24–7.26 (d, 4H, ArH), 6.82–6.96 (m, 12H, ArH), 5.53 (d, 1H, $J_{\text{H-P}} = 24.5$ CH), 1.63 (br, 3H, BH_3), 3.45 (br, THF), 1.29 (br, THF) ppm. $^{13}\text{C}\{^1\text{H}\}$ NMR (100 MHz, C_6D_6): δ 144.1 (ArC), 144.0 (ArC), 133.1 (P-ArC), 133.0 (P-ArC), 132.5 (P attached *o*-ArC), 132.3 (P attached *o*-ArC), 131.1 (P attached *p*-ArC), 131.0 (P attached *p*-ArC), 128.6 (P attached *m*-ArC), 128.3 (*m*-ArC), 128.0 (*o*-ArC), 127.2 (*p*-ArC), 68.4 (THF) 61.1 (CH), 25.7 (THF) ppm. $^{31}\text{P}\{^1\text{H}\}$ NMR (161.9 MHz, C_6D_6): δ 46.3 ppm. $^{11}\text{B}\{^1\text{H}\}$ NMR (128.4 MHz, C_6D_6): δ - 31.7 (d) ppm. FT-IR (selected frequencies): $\nu = 3376$ (N–H), 1444 (P–C), 930 (P–N), 2380 (B–H), 610 (P–B) cm^{-1} . Elemental analysis: $\text{C}_{66}\text{H}_{80}\text{B}_2\text{N}_2\text{O}_4\text{P}_2\text{Sr}$ (1136.50): Calcd. C 69.75, H 7.09, N 2.46. Found: C 69.35, H 6.86, N 2.32.

Complex 24: In a 10 ml sample vial, 2 equiv of ligand **17** (100 mg, 0.264 mmol) and 1 equiv of $[\text{Ba}\{\text{N}(\text{SiMe}_3)_2\}(\text{THF})_2]$ (79.5 mg, 0.132 mmol) were mixed together with a small amount of THF (2 ml). After 12 h of stirring, a small amount of *n*-pentane (2 ml) was added to the reaction mixture, and it was stored in a $-40\text{ }^\circ\text{C}$ freezer. After 24 h, colorless crystals of **24** were obtained. Yield: 147 mg (94%). ^1H NMR (400 MHz, C_6D_6): δ 7.58–7.63 (m, 4H, ArH), 7.25–7.26 (d, 4H, ArH), 7.02–7.06 (m, 12H, ArH), 5.48 (d, 1H, $J_{\text{H-P}} = 22.3$ Hz, CH), 1.72 (br, 3H, BH_3), 3.38 (br, THF), 1.24 (br, THF) ppm. $^{13}\text{C}\{^1\text{H}\}$ NMR (100 MHz, C_6D_6): δ 148.7 (ArC), 134.5 (P attached ArC), 132.8 (P attached *o*-ArC), 132.6 (P attached *o*-ArC), 129.4 (P attached *p*-ArC), 128.9 (P attached *m*-ArC), 128.1 (*m*-ArC), 127.6 (*o*-ArC), 126.1 (*p*-ArC), 68.2 (THF) 66.5 (CH), 25.3 (THF) ppm. $^{31}\text{P}\{^1\text{H}\}$ NMR (161.9 MHz, C_6D_6): δ 46.9 ppm. $^{11}\text{B}\{^1\text{H}\}$ NMR (128.4 MHz, C_6D_6): δ - 30.9 (d) ppm. FT-IR (selected frequencies): $\nu = 3328$ (N–H), 1449 (P–C), 929 (P–N), 2378 (B–H), 603 (P–B) cm^{-1} . Elemental analysis: $\text{C}_{66}\text{H}_{80}\text{B}_2\text{BaN}_2\text{O}_4\text{P}_2$ (1186.22): Calcd. C 66.82, H 6.80, N 2.36. Found: C 66.44, H 6.33, N 2.09.

3.7 X-ray Crystallographic Studies

In each case a crystal of suitable dimensions was mounted on a CryoLoop (Hampton Research Corp.) with a layer of light mineral oil and placed in a nitrogen stream at 150(2) K. All measurements were made on an Agilent Supernova X-calibur Eos CCD detector with graphite monochromatic Cu-K α (1.54184 Å) or Mo-K α (0.71069 Å) radiation. Crystal data and structure refinement parameters are summarized in Table 3.1-3.3. The structures were solved by direct methods (SIR92)⁴⁵ and refined on F^2 by full-matrix least-squares methods; using SHELXL-97.⁴⁶ Non-hydrogen atoms were anisotropically refined. H-atoms were included in the refinement on calculated positions riding on their carrier atoms. The function minimized was $[\sum w(F_o^2 - F_c^2)^2]$ ($w = 1 / [\sigma^2(F_o^2) + (aP)^2 + bP]$), where $P = (\text{Max}(F_o^2, 0) + 2F_c^2) / 3$ with $\sigma^2(F_o^2)$ from counting statistics. The function R_1 and wR_2 were $(\sum ||F_o| - |F_c||) / \sum |F_o|$ and $[\sum w(F_o^2 - F_c^2)^2 / \sum (wF_o^4)]^{1/2}$, respectively. The Diamond-3 program was used to draw the molecule. Crystallographic data (excluding structure factors) for the structures described in this chapter have been deposited with the Cambridge Crystallographic Data Centre as a supplementary publication no. CCDC 923124 (**17**), 927524 (**18**), 923127 (**19**), 923125 (**20**), 923129 (**21**), 923123 (**22**), 923126 (**23**), 923128 (**24**).

3.8 Tables

Table 3.1. Crystallographic data of compounds **17**, **18** and **19**

Crystal	17	18	19
CCDC No.	923124	927524	923127
Empirical formula	C ₂₅ H ₂₅ BNP	C ₃₁ H ₂₉ BNP	C ₃₃ H ₄₀ BLiNO ₂ P
Formula weight	381.24	457.33	531.38
<i>T</i> (K)	150(2)	293(2)	150(2)
λ (Å)	1.54184	1.54184	1.54184
Crystal system	Triclinic,	Monoclinic	Monoclinic
Space group	<i>P</i> -1	<i>P</i> 2 ₁ / <i>c</i>	<i>P</i> 2 ₁ / <i>c</i>
<i>a</i> (Å)	9.1468(10)	14.0654(9)	15.4438(5)
<i>b</i> (Å)	10.0257(19)	14.3444(7)	13.1276(8)
<i>c</i> (Å)	12.941(2)	13.8285(8)	19.1155(11)
α (°)	73.657(16)	90	90
β (°)	71.578(14)	114.495(7)	127.859(3)
γ (°)	82.298(13)	90	90
<i>V</i> (Å ³)	1079.1(3)	2538.9(3)	3059.8(3)
<i>Z</i>	2	4	4
<i>D</i> _{calc} g cm ⁻³	1.173	1.196	1.154
μ (mm ⁻¹)	1.178	1.087	1.007
<i>F</i> (000)	404	968	1136
Theta range for data collection	3.72 to 70.80 deg.	3.45 to 49.99 deg.	3.62 to 70.95 deg.
Limiting indices	-7<= <i>h</i> <=11, -12<= <i>k</i> <=11, -13<= <i>l</i> <=15	-13<= <i>h</i> <=11, -14<= <i>k</i> <=9, -13<= <i>l</i> <=13	-17<= <i>h</i> <=18, -14<= <i>k</i> <=16, -23<= <i>l</i> <=16
Reflections collected / unique	7294 / 4027 [<i>R</i> (int) = 0.0423]	6688 / 2603 [<i>R</i> (int) = 0.0283]	13134 / 5780 [<i>R</i> (int) = 0.0287]
Completeness to theta = 71.25	97.1 %	100.0%	98.1 %
Absorption correction	Multi-scan	Multi-scan	Multi-scan
Max. and min. transmission	0.850 and 0.795	1.000 and 0.750	0.855 and 0.790
Refinement method	Full-matrix least-squares on <i>F</i> ²	Full-matrix least-squares on <i>F</i> ²	Full-matrix least-squares on <i>F</i> ²
Data / restraints / parameters	4027 / 0 / 265	2603 / 0 / 323	5780 / 0 / 364
Goodness-of-fit on <i>F</i> ²	1.092	2.318	1.035
Final <i>R</i> indices [I>2σ(I)]	<i>R</i> 1 ^{<i>a</i>} = 0.0800, w <i>R</i> 2 ^{<i>b</i>} = 0.2450	<i>R</i> 1 ^{<i>a</i>} = 0.1530, w <i>R</i> 2 ^{<i>b</i>} = 0.4625	<i>R</i> 1 = 0.0426, w <i>R</i> 2 = 0.1115
<i>R</i> indices (all data)	<i>R</i> 1 ^{<i>a</i>} = 0.1117, w <i>R</i> 2 ^{<i>b</i>} = 0.2652	<i>R</i> 1 ^{<i>a</i>} = 0.1578, w <i>R</i> 2 ^{<i>b</i>} = 0.4685	<i>R</i> 1 = 0.0500, w <i>R</i> 2 = 0.1190
Largest diff. peak and hole	0.956 and -0.341 e.Å ⁻³	3.348 and -0.622 e.Å ⁻³	0.411 and -0.245 e.Å ⁻³

Table 3.2. Crystallographic data of compounds **20**, **21** and **22**

Crystal	20	21	22
CCDC No.	923125	923129	923123
Empirical formula	C ₆₆ H ₈₀ B ₂ N ₂ Na ₂ O ₄ P ₂	C ₆₆ H ₈₀ B ₂ K ₂ N ₂ O ₄ P ₂	C ₆₆ H ₈₀ B ₂ CaN ₂ O ₄ P ₂
Formula weight	1094.86	1127.08	1088.96
<i>T</i> (K)	150(2) K	150(2) K	150(2)
λ (Å)	1.54184	1.54184	1.54184
Crystal system	Triclinic	Triclinic	Triclinic
Space group	<i>P</i> -1	<i>P</i> -1	<i>P</i> -1
<i>a</i> (Å)	10.1516(10)	10.1635(10)	10.3720(4)
<i>b</i> (Å)	12.2992(12)	12.5894(13)	10.7801(5)
<i>c</i> (Å)	13.0193(13)	13.2261(12)	14.3830(6)
α (°)	76.553(9)	76.773(8)	100.239(4)
β (°)	77.197(9)	75.288(8)	102.076(4)
γ (°)	86.976(8)	85.431(8)	101.623(4)
<i>V</i> (Å ³)	1541.7(3)	1593.0(3)	1499.20(11)
<i>Z</i>	1	1	1
<i>D</i> _{calc} g cm ⁻³	1.179	1.175	1.206
μ (mm ⁻¹)	1.146	2.146	1.780
<i>F</i> (000)	584	600	582
Theta range for data collection	3.57 to 70.82 deg.	3.54 to 69.97 deg.	3.23 to 70.73 deg.
Limiting indices	-11<= <i>h</i> <=12, -14<= <i>k</i> <=14, -11<= <i>l</i> <=15	-12<= <i>h</i> <=9, -15<= <i>k</i> <=11, -16<= <i>l</i> <=16	-12<= <i>h</i> <=11, -13<= <i>k</i> <=12, -17<= <i>l</i> <=17
Reflections collected / unique	10676 / 5798 [<i>R</i> (int) = 0.0350]	11636 / 5952 [<i>R</i> (int) = 0.0418]	10728 / 5632 [<i>R</i> (int) = 0.0266]
Completeness to theta = 71.25	97.6 %	98.4 %	97.9 %
Absorption correction	Multi-scan	Multi-scan	Multi-scan
Max. and min. transmission	0.846 and 0.811	0.715 and 0.598	0.741 and 0.641
Refinement method	Full-matrix least-squares on <i>F</i> ²	Full-matrix least-squares on <i>F</i> ²	Full-matrix least-squares on <i>F</i> ²
Data / restraints / parameters	5798 / 0 / 372	5952 / 0 / 374	5632 / 0 / 349
Goodness-of-fit on <i>F</i> ²	1.046	1.050	1.046
Final <i>R</i> indices [I>2σ(I)]	<i>R</i> 1 = 0.0557, <i>wR</i> 2 = 0.1446	<i>R</i> 1 = 0.0769, <i>wR</i> 2 = 0.2055	<i>R</i> 1 = 0.0443, <i>wR</i> 2 = 0.1210
<i>R</i> indices (all data)	<i>R</i> 1 = 0.0689, <i>wR</i> 2 = 0.1562	<i>R</i> 1 = 0.0908, <i>wR</i> 2 = 0.2253	<i>R</i> 1 = 0.0480, <i>wR</i> 2 = 0.1244
Largest diff. peak and hole	0.380 and -0.442 e.Å ⁻³	0.801 and -0.596 e.Å ⁻³	0.415 and -0.399 e.Å ⁻³

Table 3.3. Crystallographic data of compounds **23** and **24**

Crystal	23	24
CCDC No.	923126	923128
Empirical formula	C ₆₆ H ₈₀ B ₂ N ₂ O ₄ P ₂ Sr	C ₆₆ H ₇₈ B ₂ BaN ₂ O ₄ P ₂
Formula weight	1136.50	1186.22
<i>T</i> (K)	150(2)	150(2)
λ (Å)	0.71069	1.54184
Crystal system	Triclinic	Triclinic
Space group	<i>P</i> -1	<i>P</i> -1
<i>a</i> (Å)	10.2490(5)	10.1805(7)
<i>b</i> (Å)	10.6953(5)	10.6809(6)
<i>c</i> (Å)	14.7358(9)	15.0344(10)
α (°)	98.806(4)	98.317(5)
β (°)	102.559(5)	102.864(6)
γ (°)	102.225(4)	102.762(5)
<i>V</i> (Å ³)	1506.93(14)	1521.75(17)
<i>Z</i>	1	1
<i>D</i> _{calc} g cm ⁻³	1.252	1.294
μ (mm ⁻¹)	2.116	5.940
<i>F</i> (000)	600	618
Theta range for data collection	3.14 to 69.98 deg.	3.08 to 69.98 deg.
Limiting indices	-12<= <i>h</i> <=8, -13<= <i>k</i> <=12, -16<= <i>l</i> <=18	-12<= <i>h</i> <=11, -12<= <i>k</i> <=9, -18<= <i>l</i> <=18
Reflections collected / unique	10490 / 5496 [<i>R</i> (int) = 0.0673]	10422 / 5580 [<i>R</i> (int) = 0.0661]
Completeness to theta = 71.25	96.2 %	96.7%
Absorption correction	Multi-scan	Multi-scan
Max. and min. transmission	0.725 and 0.540	0.395 and 0.287
Refinement method	Full-matrix least-squares on <i>F</i> ²	Full-matrix least-squares on <i>F</i> ²
Data / restraints / parameters	5496 / 0 / 361	5580 / 0 / 361
Goodness-of-fit on <i>F</i> ²	1.053	1.059
Final <i>R</i> indices [<i>I</i> >2σ(<i>I</i>)]	<i>R</i> 1 = 0.0832, <i>wR</i> 2 = 0.2065	<i>R</i> 1 = 0.0702, <i>wR</i> 2 = 0.1878
<i>R</i> indices (all data)	<i>R</i> 1 = 0.0901, <i>wR</i> 2 = 0.2092	<i>R</i> 1 = 0.0834, <i>wR</i> 2 = 0.2054
Largest diff. peak and hole	2.432 and -0.61 e.Å ⁻³	3.290 and -1.480 e.Å ⁻³

References:

- (1) (a) Harder, S. *Chem. Rev.* **2010**, *110*, 3852-3876. (b) Kobayashi, S.; Yamashita, Y. *Acc. Chem. Res.* **2011**, *44*, 58-59.
- (2) (a) Dechy-Cabaret, O.; Martin-Vaca, B.; Bourissou, D. *Chem. Rev.* **2004**, *104*, 6147-6176. (b) O'Keefe, B.; Hillmyer, J. M. A.; Tolman, W. B. *J. Chem. Soc. Dalton Trans.* **2001**, 2215-2224. (c) Wheaton, C. A.; Hayes, P. G.; Ireland, B. *Dalton Trans.* **2009**, 4832-4846. (d) Thomas, C. M. *Chem. Soc. Rev.* **2010**, *39*, 165-173.
- (3) (a) Li, S. M.; Rashkov, I.; Espartero, J. L.; Manolova, N.; Vert, M. *Macromolecules* **1996**, *29*, 57-62. (b) Dobrzyński, P.; Kasperczyk, J.; Bero, M. *Macromolecules* **1999**, *32*, 4735-4737. (c) Zhong, Z.; Dijkstra, P. J.; Birg, C.; Westerhausen, M.; Feijen, J. *Macromolecules* **2001**, *34*, 3863-3868. (d) Westerhausen, M.; Schneiderbauer, S.; Kneifel, A. N.; Sörtl, Y.; Mayer, P.; Nöth, H.; Zhong, Z.; Dijkstra, P. J.; Feijen, J. *Eur. J. Inorg. Chem.* **2003**, 3432-3439. (e) Chisholm, M. H.; Gallucci, J.; Phomphrai, K. *Chem. Commun.* **2003**, 48-49. (f) Hill, M. S.; Hitchcock, P. B. *Chem. Commun.* **2003**, 1758-1759. (g) Chisholm, M. H.; Gallucci, J. C.; Phomphrai, K. *Inorg. Chem.* **2004**, *43*, 6717-6725. (h) Sarazin, Y.; Howard, R. H.; Hughes, D. L.; Humphrey, S. M.; Bochmann, M. *Dalton Trans.* **2006**, 340-350. (i) Darensbourg, D. J.; Choi, W.; Ganguly, P.; Richers, C. P. *Macromolecules* **2006**, *39*, 4374-4379. (j) Davidson, M. G.; O'Hara, C. T.; Jones, M. D.; Keir, C. G.; Mahon, M. F.; Kociok-Köhn, G. *Inorg. Chem.* **2007**, *46*, 7686-7688. (k) Darensbourg, D. J.; Choi, W.; Richers, C. P. *Macromolecules* **2007**, *40*, 3521-3523. (l) Darensbourg, D. J.; Choi, W.; Karroonnirun, O.; Bhuvanesh, N. *Macromolecules* **2008**, *41*, 3493-3502. (m) Poirier, V.; Roisnel, T.; Carpentier, J.-F.; Sarazin, Y. *Dalton Trans.* **2009**, 9820-9827. (n) Xu, X.; Chen, Y.; Zou, G.; Ma, Z.; Li, G. *J. Organomet. Chem.* **2010**, *695*, 1155-1162. (o) Sarazin, Y.; Rosca, D.; Poirier, V.; Roisnel, T.; Silvestru, A.; Maron, L.; Carpentier, J.-F. *Organometallics* **2010**, *29*, 6569-6577. (p) Sarazin, Y.; Liu, B.; Roisnel, T.; Maron, L.; Carpentier, J.-F. *J. Am. Chem. Soc.* **2011**, *133*, 9069-9087.
- (4) (a) Harder, S.; Feil, F.; Knoll, K. *Angew. Chem., Int. Ed.* **2001**, *40*, 4261-4264. (b) Harder, S.; Feil, F. *Organometallics* **2002**, *21*, 2268-2274. (c) Jochmann, P.; Dols, T. S.; Spaniol, T. P.; Perrin, L.; Maron, L.; Okuda, J. *Angew. Chem., Int. Ed.* **2009**, *48*, 5715-5719.
- (5) (a) Barrett, A. G. M.; Crimmin, M. R.; Hill, M. S.; Procopiou, P. A. *Proc. R. Soc. London, Ser. A* **2010**, *466*, 927-963. (b) Harder, S. *Chem. Rev.* **2010**, *110*, 3852-3876.

- (6) (a) Chisholm, M. H. *Inorg. Chim. Acta* **2009**, *362*, 4284-4290. (b) Saly, M. J.; Heeg, M. J.; Winter, C. H. *Inorg. Chem.* **2009**, *48*, 5303-5312. (c) Chisholm, M. H.; Gallucci, J. C.; Phomphrai, K. *Chem. Commun.* **2003**, 48-49. (d) Chisholm, M. H.; Gallucci, J. C.; Phomphrai, K. *Inorg. Chem.* **2004**, *43*, 6717-6725.
- (7) (a) Crimmin, M. R.; Casely, I. J.; Hill, M. S. *J. Am. Chem. Soc.* **2005**, *127*, 2042-2043. (b) Harder, S.; Brettar, J. *Angew. Chem., Int. Ed.* **2006**, *45*, 3474-3478. (c) Crimmin, M. R.; Arrowsmith, M. A.; Barrett, G. M.; Casely, I. J.; Hill, M. S.; Procopiou, P. A. *J. Am. Chem. Soc.* **2009**, *131*, 9670-9685. (d) Sarish, S. P.; Nembenna, S.; Nagendran, S.; Roesky, H. W. *Acc. Chem. Res.* **2011**, *44*, 157-170. (e) Datta, S.; Roesky, P. W.; Blechert, S. *Organometallics* **2007**, *26*, 4392-4394. (f) Datta, S.; Gamer, M. T.; Roesky, P. W. *Organometallics* **2008**, *27*, 1207-1213.
- (8) (a) Caro, C. F.; Hitchcock, P. B.; Lappert, M. F. *Chem. Commun.* **1999**, 1433-1434. (b) Harder, S. *Organometallics* **2002**, *21*, 3782-3787. (c) Datta, S.; Roesky, P. W.; Blechert, S. *Organometallics* **2007**, *26*, 4392-4394.
- (9) (a) Jenter, J.; Köppe, R.; Roesky, P. W. *Organometallics* **2011**, *30*, 1404-1413. (b) Hao, H.; Bhandari, S.; Ding, Y.; Roesky, H. W.; Magull, J.; Schmidt, H. G.; Noltemeyer, M.; Cui, C. *Eur. J. Inorg. Chem.* **2002**, 1060-1065. (c) Matsuo, Y.; Tsurugi, H.; Yamagata, T.; Mashima, K. *Bull. Chem. Soc. Jpn.* **2003**, *76*, 1965-1968. (d) Panda, T. K.; Yamamoto, K.; Yamamoto, K.; Kaneko, H.; Yang, Y.; Tsurugi, H.; Mashima, K. *Organometallics* **2012**, *31*, 2286-2301.
- (10) Panda, T. K.; Kaneko, H.; Michel, O.; Tsurugi, H.; Pal, K.; Toernroos, K. W.; Anwander, R.; Mashima, K. *Organometallics* **2012**, *31*, 3178-3184.
- (11) Fenske, D.; Maczek, B.; Maczek, K. *Z. Anorg. Allg. Chem.* **1997**, *623*, 1113-1120.
- (12) (a) Köhl, O.; Koch, T.; Somoza Jr., F. B.; Junk, P. C.; Hey-Hawkins, E.; Plat, D.; Eisen, M. S. *J. Organomet. Chem.* **2000**, *604*, 116-125. (b) Wetzelschell, T.G.; Dehnen, S.; Roesky, P.W. *Angew. Chem.* **1999**, *111*, 1155-1158. (c) Wetzelschell, T.G.; Dehnen, S.; Roesky, P.W. *Angew. Chem. Int. Ed.* **1999**, *38*, 1086-1088.
- (13) (a) Roesky, P. W.; Gamer, M. T.; Puchner, M.; Greiner, A. *Chem. Eur. J.* **2002**, *8*, 5265-5271. (b) Braunstein, P.; Durand, J.; Kickelbick, G.; Knorr, M.; Morise, X.; Pugin, R.; Tiripicchio, A.; Ugozzoli, F. *J. Chem. Soc. Dalton Trans.* **1999**, 4175-4186. (c) Knoerr, M.; Strohmman, C. *Organometallics* **1999**, *18*, 248-257. (d) Braunstein, P.; Cossy, J.; Knorr, M.; Strohmman, C.; Vogel, P. *New J. Chem.* **1999**, *23*, 1215-1222.

- (14) (a) Dehnicke, K.; Weller, F. *Coord. Chem. Rev.* **1997**, *158*, 103–169. (b) Dehnicke, K.; Krieger, M.; Massa, W. *Coord. Chem. Rev.* **1999**, *182*, 19–65.
- (15) (a) Panda, T. K.; Roesky, P. W. *Chem. Soc. Rev.* **2009**, *38*, 2782–2804. (b) Imhoff, P.; Guelpen, J. H.; Vrieze, K.; Smeets, W. J. J.; Spek, A. L.; Elsevier, C. J. *Inorg. Chim. Acta* **1995**, *235*, 77–88.
- (16) (a) Avis, M. W.; Boom, M. E. V.; Elsevier, C. J.; Smeets, W. J. J.; Spek, A. L. *J. Organomet. Chem.* **1997**, *527*, 263–276. (b) Avis, M. W.; Elsevier, C. J.; Ernsting, J. M.; Vrieze, K.; Veldman, N.; Spek, A. L.; Katti, K. V.; Barnes, C. L. *Organometallics* **1996**, *15*, 2376–2392.
- (17) (a) Ong, C. M.; McKarns, P.; Stephan, D. W. *Organometallics* **1999**, *18*, 4197–4208. (b) Gamer, M. T.; Dehnen, S.; Roesky, P. W. *Organometallics* **2001**, *20*, 4230–4236. (c) Aharonian, G.; Feghali, K.; Gambarotta, S.; Yap, G. P. A. *Organometallics* **2001**, *20*, 2616–2622.
- (18) (a) Cavell, R. G.; Kamalesh Babu, R. P.; Aparna, K. *J. Organomet. Chem.* **2001**, *617–618*, 158–169. (b) Kamalesh Babu, R. P.; McDonald, R.; Cavell, R. G. *Chem. Commun.* **2000**, 481–482. (c) Aparna, K.; Kamalesh Babu, R. P.; McDonald, R.; Cavell, R. G. *Angew. Chem.* **2001**, *113*, 4535–4537. (d) Aparna, K.; Kamalesh Babu, R. P.; McDonald, R.; Cavell, R. G. *Angew. Chem. Int. Ed.* **2001**, *40*, 4400–4402.
- (19) (a) Kasani, A.; Kamalesh Babu, R. P.; McDonald, R.; Cavell, R. G. *Organometallics* **1999**, *18*, 3775–3777. (b) Aparna, K.; McDonald, R.; Ferguson, M.; Cavell, R. G. *Organometallics* **1999**, *18*(21), 4241–4243.
- (20) (a) Edelmann, F. T. *Top. Curr. Chem.* **1996**, *179*, 113–148. (b) Reissmann, U.; Poremba, P.; Noltemeyer, M.; Schmidt, H.-G.; Edelmann, F. T. *Inorg. Chim. Acta* **2000**, *303*, 156–162. (c) Recknagel, A.; Steiner, A.; Noltemeyer, M.; Brooker, S.; Stalke, D.; Edelmann, F. T. *J. Organomet. Chem.* **1991**, *414*, 327–335. (d) Recknagel, A.; Witt, M.; Edelmann, F. T. *J. Organomet. Chem.* **1989**, *371*, C40–C44.
- (21) (a) Wiecko, M.; Gimt, D.; Rastatter, M.; Panda, T. K.; Roesky, P. W. *Dalton Trans.* **2005**, *36*, 2147–2150. (b) Panda, T. K.; Gamer, M. T.; Roesky, P. W. *Inorg. Chem.* **2006**, *45*, 910–916.
- (22) (a) Agarwal, S.; Mast, C.; Dehnicke, K.; Greiner, A. *Macromol. Rapid Commun.* **2000**, *21*, 195–212. (b) Ravi, P.; Groeb, T.; Dehnicke, K.; Greiner, A. *Macromolecules* **2001**, *34*, 8649–8653. (c) Halcovitch, N. R.; Fryzuk, M. D. *Dalton Trans.* **2012**, *41*, 1524–1528.
- (23) (a) Cowley, A. H.; Lattman, M.; Stricklen, P. M.; Verkade, J. G. *Inorg. Chem.* **1982**, *21*, 543–549. (b) Gonbeau, D.; Sanchez, M.; Pfister-Guillouzo, G. *Inorg. Chem.* **1981**, *20*, 1966–1973. (c)

- Worley, S. D.; Hargis, J. H.; Chang, L.; Mattson, G. A.; Jennings, W. B. *Inorg. Chem.* **1979**, *18*, 3581-3585.
- (24) (a) Kroshefsky, R. D.; Weiss, R.; Verkade, J. G. *Inorg. Chem.* **1979**, *18*, 469-472. (b) Kroshefsky, R. D.; Verkade, J. G.; Pipal, J. R. *Phosphorus Sulfur Relat. Elem.* **1979**, *6*, 377-389. (c) Kroshefsky, R. D.; Verkade, J. G. *Phosphorus Sulfur Relat. Elem.* **1979**, *6*, 391-395.
- (25) (a) Vande Griend, L. J.; Verkade, J. G.; Pennings, J. F. M.; Buck, H. M. *J. Am. Chem. Soc.* **1977**, *99*, 2459-2463. (b) Hodaes, R. V.; Houle, F. A.; Beauchamp, J. L.; Montag, R. A.; Verkade, J. G. *J. Am. Chem. Soc.* **1980**, *102*, 932-935. (c) Lee, T. H.; Jolly, W. L.; Bakke, A. A.; Weiss, R.; Verkade, J. G. *J. Am. Chem. Soc.* **1980**, *102*, 2631-2636.
- (26) (a) Reves, M.; Ferrer, C.; Leon, T.; Doran, S.; Etayo, P.; Ferran, A. V.; Riera, A.; Verdaguer, X. *Angew. Chem., Int. Ed.* **2010**, *49*, 9452-9455. (b) Kolodiazhnyi, O. I.; Gryshkun, E. V.; Andrushko, N. V.; Freytag, M. P.; Jones, G.; Schmutzler, R. *Tetrahedron: Asymmetry* **2003**, *14*, 181-183.
- (27) Abdellah, I.; Bernoud, E.; Lohier, J.-F.; Alayrac, C.; Toupet, L.; Lepetit, C.; Gaumont, A.-C. *Chem. Commun.* **2012**, *48*, 4088-4090.
- (28) (a) Müller, G.; Brand, J. *Organometallics*. **2003**, *22*, 1463-1467. (b) Dornhaus, F.; Bolte, M.; Lerner, H.-W.; Wagner, M. *Eur. J. Inorg. Chem.* **2006**, 1777-1785. (c) Dornhaus, F.; Bolte, M.; Lerner, H.-W.; Wagner, M. *Eur. J. Inorg. Chem.* **2006**, 5138-5147.
- (29) Consiglio, G. B.; Queval, P.; Harrison-Marchand, A.; Mordini, A.; Lohier, J.-F.; Delacroix, O.; Gaumont, A.-C.; Gérard, H.; Maddaluno, J.; Oulyadi, H. *J. Am. Chem. Soc.* **2011**, *133*, 6472-6480.
- (30) The bonding situation in the drawing of the ligand system is simplified for clarity.
- (31) Sens, M. A.; Odom, J. D.; Goodrow, M. H. *Inorg. Chem.* **1976**, *15*(11), 2825-2830.
- (32) (a) Jaska, C. A.; Temple, K.; Lough, A. J.; Manners, I. *Chem. Commun.* **2001**, 962-963. (b) Denney, M. C.; Pons, V.; Heinekey, D. M.; Goldberg, K. I. *J. Am. Chem. Soc.* **2006**, *128*, 12048-12049. (c) Keaton, R. J.; Blacquiere, J. M.; Baker, R. T. *J. Am. Chem. Soc.* **2007**, *129*, 1844-1845. (d) Dietrich, B. L.; Goldberg, K. I.; Heinekey, D. M.; Autrey, T.; Linehan, J. C. *Inorg. Chem.* **2008**, *47*, 8583-8585. (e) Douglas, T. M.; Chaplin, A. M.; Weller, A. S. *J. Am. Chem. Soc.* **2008**, *130*, 14432-14433. (f) Blacquiere, N.; Diallo-Garcia, S.; Gorelsky, S. I.; Black, D. A.; Fagnou, K. *J. Am. Chem. Soc.* **2008**, *130*, 14034-14035. (g) Käß, M.; Friedrich, A.; Drees, M.; Schneider, S. *Angew. Chem., Int. Ed.* **2009**, *48*, 905-907. (h) Friedrich, A.; Drees, M.; Schneider, S. *Chem. Eur. J.* **2009**, *15*, 10339-10342. (i) Douglas, T. M.; A. Chaplin, M. A.; Weller, S.; Yang, X.; Hall, M. B. *J. Am. Chem. Soc.*

- 2009**, *131*, 15440-15456. (j) Jiang, Y.; Berke, H. *Chem. Commun.* **2007**, 3571-3573. (k) Chaplin, A. B.; Weller, A. S. *Inorg. Chem.* **2010**, *49*, 1111-1121. (l) Clark, T. J.; Lee, K.; Manners, I. *Chem. Eur. J.* **2006**, *12*, 8634-8648. (m) Stevens, C. J.; Allanegra, R. D.; Chaplin, A. B.; Weller, A. S.; Macgregor, S. A.; Ward, B.; McKay, D.; Alcaraz, G.; Sabo-Etienne, S. *Chem. Eur. J.* **2011**, *17*, 3011-3020.
- (33) (a) Odom, J. D.; Hudgens, B. A.; Durig, J. R. *J. Phys. Chem.* **1973**, *77*, 1972-1977. (b) Hubert, S.; Stützer, A.; Bissinger, P.; Schier, A. Z. *Anorg. Allg. Chem.* **1993**, *619*, 1519-1525.
- (34) (a) Briand, G. G.; Chivers, T.; Parvez, M.; Schatte, G. *Inorg. Chem.* **2003**, *42*, 525-531. (b) Izod, K.; Watson, J. M.; Clegg, W.; Harrington, R. W. *Dalton Trans.* **2011**, *40*, 11712-11718. (c) Izod, K.; Watson, J. M.; Clegg, W.; Harrington, R. W. *Eur. J. Inorg. Chem.* **2012**, 1696-1701. (d) Housecroft, C. E.; Sharpe, A. G. *Inorganic Chemistry*, 2nd ed.; Prentice Hall: Englewood Cliffs, N.J, **2005**, p 135.
- (35) Köese, D. A.; Zümreoglu-Karan, B.; Hökelek, T.; Sahin, E. Z. *Allg. Anorg. Chem.* **2009**, *635*, 563-566.
- (36) Anwander, R. *In Topics in Organometallic Chemistry*; Kobayashi, S., Ed.; Springer: Berlin, **1998**; Vol. 2, p 16.
- (37) Izod, K.; Watson, J. M.; Clegg, W.; Harrington, R. W. *Inorg. Chem.* **2013**, *52*, 1466-1475.
- (38) (a) Hanusa, T. P. *In Comprehensive Organometallic Chemistry III*; Crabtree, R. H., Mingos, M. P., Eds.; Elsevier: Oxford, U.K., **2007**; Vol. 2, p 67. (b) Hanusa, T. P. *Organometallics* **2002**, *21*, 2559-2571. (c) Hanusa, T. P. *Chem. Rev.* **2000**, *100*, 1023-1036. (d) Hanusa, T. P. *Coord. Chem. Rev.* **2000**, *210*, 329-367.
- (39) Greenwood, N. N.; Earnshaw, A. *Chemistry of the Elements*; Pergamon Press: Oxford, U.K., **1984**.
- (40) Izod, K.; Wills, C.; Clegg, W.; Harrington, R. W. *Inorg. Chem.* **2007**, *46*, 4320-4325.
- (41) Panda, T. K.; Zulys, A.; Gamer, M. T.; Roesky, P. W. *J. Organomet. Chem.* **2005**, *690*, 5078-89.
- (42) Shannon, R. D. *Acta Crystallogr. Sect. A* **1976**, *32*, 751-767.
- (43) (a) Brady, E. D.; Hanusa, T. P.; Pink, M., Jr.; Young, V. G., Jr. *Inorg. Chem.* **2000**, *39*, 6028-6037. (b) Panda, T. K.; Hrib, C. G.; Jones, P. G.; Jenter, J.; Roesky, P. W.; Tamm, M. *Eur. J. Inorg. Chem.* **2008**, 4270-4279.
- (44) George, D.; Vaughn, K.; Alex, K.; Gladysz, J. A. *Organometallics* **1986**, *5*, 936-942.

- (45) Sheldrick, M. SHELXS-97, *Program of Crystal Structure Solution; University of Göttingen, Göttingen, Germany, 1997.*
- (46) Sheldrick, G. M. SHELXL-97, *Program of Crystal Structure Refinement; University of Göttingen, Göttingen, Germany, 1997.*

Chapter 4

Bis(phosphinoselenoicamides) as versatile chelating ligands for alkaline earth metal (Mg, Ca, Sr and Ba) complexes: syntheses, structure and ϵ -caprolactone polymerization

4.1 Introduction

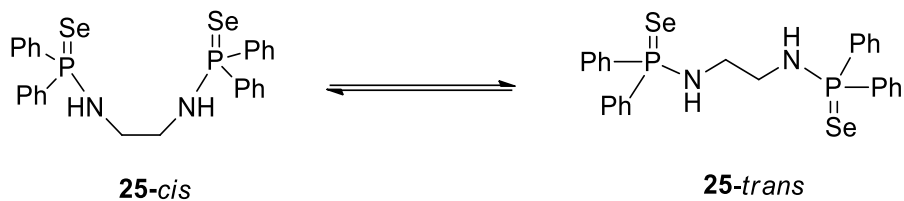
Aliphatic polyesters are currently considered as alternatives to synthetic petrochemical-based polymers and are attractive to the researcher, since the starting materials for their synthesis can be obtained from annually renewable resources. Their biodegradable and biocompatible nature along with their mechanical and physical properties make them prospective thermoplastics with broad commercial applications (e.g., single-use packaging materials, medical sutures and drug delivery systems).^{1,2} It is well established that polymer properties are highly dependent on their intrinsic structural parameters, such as polymer composition, molecular weight, polydispersity, tacticity, and polymer chain ends.^{3,4} Ring-opening polymerisation (ROP) of cyclic esters promoted, for example, by metal initiators, proved to be the most efficient manner for preparing polyesters with controlled molecular weight and microstructure and narrow molecular-weight distribution.⁵⁻⁷ This makes for the design and synthesis of new, well-defined, single-site catalysts that exhibit good activity, productivity and selectivity for cyclic ester polymerisation and allow crucial polymer architecture control. Group 2 metal complexes have attracted considerable attention as initiators for the ROP of cyclic esters, and some of them have demonstrated impressive results.⁸ Recently, we described the synthesis of alkaline-earth metal complexes with iminopyrrolyl and amidopyrrolyl ligands and they proved to be highly active for the ROP of ϵ -caprolactone, affording high-molecular-weight poly(ϵ -caprolactone)s.⁹ We have continuously studied the complexation reaction of amidophosphine-chalcogen-based ligands to alkaline-earth metal precursors; for example, synthesis of homoleptic alkaline-earth metal complexes of composition $[M(\text{THF})_2\{\text{Ph}_2\text{P}(\text{Se})\text{N}(\text{CHPh}_2)\}_2]$ ($M = \text{Ca}, \text{Sr}$,

Ba).(Chapter 2) We also described the amidophosphine-borane complexes of $[M(\text{THF})_2\{\text{Ph}_2\text{P}(\text{BH}_3)\text{N}(\text{CHPh}_2)\}_2]$ ($M = \text{Ca}$ (**22**), Sr (**23**), Ba (**24**)).(Chapter 3) All these ligands are monoanionic and form homoleptic mono-nuclear complexes. To explore the chemistry of heavier alkaline-earth metal and their application in ϵ -caprolactone polymerization, we focused on the dianionic system *N,N'*-(ethane-1,2-diyl)bis(*P,P'*-diphenylphos-phinoselenoicamide) $[\text{Ph}_2\text{P}(\text{Se})\text{NCH}_2\text{CH}_2\text{NPh}_2(\text{Se})]^{2-}$ (**25**) which was recently prepared by Woollins et al.¹⁰ However, their detailed study of alkaline-earth metal chemistry has not been available so far. In this chapter, the synthetic and structural details of bis(phosphinoselenoicamide) alkaline-earth metal complexes with the compositions $[(\text{THF})_3\text{M}\{\text{Ph}_2\text{P}(\text{Se})\text{NCH}_2\text{CH}_2\text{NPPH}_2(\text{Se})\}]$ [$M = \text{Ca}$ (**26**), Sr (**27**), Ba (**28**) and Mg (**29**)] are presented. We also describe the ROP study of ϵ -caprolactone using complexes **26–28** as catalysts. In addition, we described the synthesis and structure of the bis(amidophosphino borane) ligand $[\text{Ph}_2\text{P}(\text{BH}_3)\text{NHCH}_2\text{CH}_2\text{NHPPH}_2(\text{BH}_3)]$ (**30**) and the corresponding dimeric barium complex $[(\text{THF})_2\text{Ba}\{\text{Ph}_2\text{P}(\text{BH}_3)\text{NCH}_2\text{CH}_2\text{NPPH}_2(\text{BH}_3)\}]_2$ (**31**).

4.2 Results and Discussion

4.2.1. Bis(phosphinoselenoicamide) ligand

N,N'-(ethane-1,2-diyl)bis(*P,P'*-diphenylphos-phinoselenoicamide) was prepared according to the method prescribed by Woollins et al. by the reaction of bis(diphenylphosphino)ethane-1,2-diamine, $[\text{Ph}_2\text{PNHCH}_2\text{CH}_2\text{NHPPH}_2]$ and elemental selenium in 1:2 molar ratio at room temperature in THF.¹⁰ The spectroscopic data for compound **25** was in full agreement with the reported values. The solid-state structure of compound **25** was established using single crystal X-ray diffraction analysis. When compound **25** was re-crystallised from a mixture of THF/*n*-pentane (1:2) at -35°C , a *trans* product (**25-trans**) was obtained. However, crystallisation from dichloromethane at room temperature afforded a *cis* product (**25-cis**). This indicates that there is equilibrium between *cis* and *trans* forms in solution (see Scheme 4.1).



Scheme 4.1. *Cis* and *trans* forms of ligand **25**.

Ligand **25-trans** crystallises in orthorhombic space group $P bca$, with one molecule of **25-trans** and THF in the asymmetric unit. In contrast, **25-cis** crystallises in monoclinic space group $C 2/c$, with four isolated molecules in the unit cell. The molecular structure of **25-cis** and **25-trans** are shown in Figures 4.1 and 4.2 respectively. The details of the structural parameters are given in the Table 4.2.

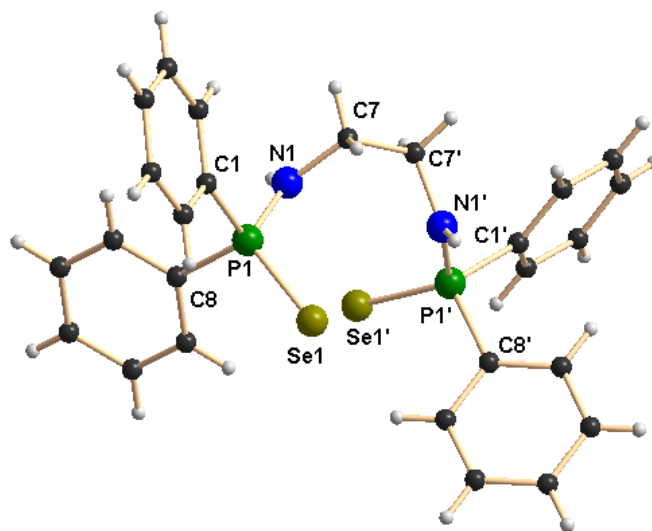


Figure 4.1. Solid-state structure of compound **25-cis**. Selected bond lengths (Å) and bond angles(°): P1–N1 1.665(2), P1–Se1 2.1194(7), P1–C1 1.810(3), P1–C8 1.810(3), N1–C7 1.468(3), C7–C7ⁱ 1.512(5), C7ⁱ–C7–N1 112.9(2), N1–P1–C8 102.55(12), N1–P1–Se1 116.97(8), N1–P1–C1 104.95(12), P1–N1–C7 120.73(18), Se1–P1–C8 113.29(10), Se1–P1–C1 111.36(9).

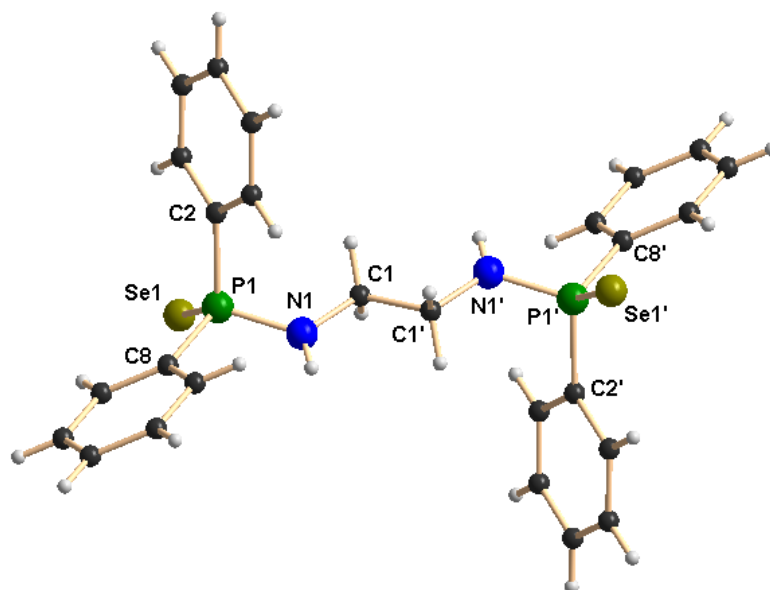
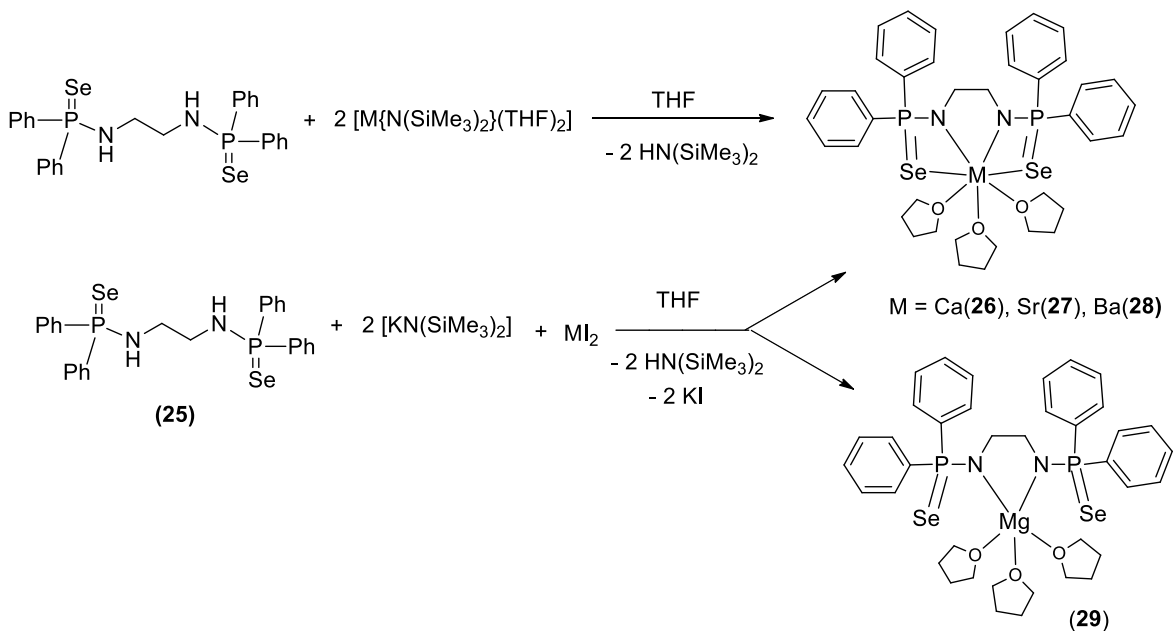


Figure 4.2. Solid-state structure of compound **25-trans**. Selected bond lengths (Å) and bond angles (°): P1–N1 1.6660(18), P1–Se1 2.1057(5), P1–C2 1.817(2), P1–C8 1.816(2), N1–C1 1.468(3), C1–C1ⁱ 1.507(4), C1ⁱ–C1–N1 109.4(2), N1–P1–C8 101.65(9), N1–P1–Se1 118.10(7), N1–P1–C2 102.72(10), P1–N1–C1 117.58(14), Se1–P1–C8 112.19(7), Se1–P1–C2 112.45(7).

The P–Se bond distances [2.1194(7) Å for **25-cis** and 2.1057(5) Å for **25-trans**] are in the range similar to that of [Ph₂P(Se)NH(CHPh₂)] [2.1086(12) Å], [Ph₂P(Se)NH(CPh₃)] [2.1166(8) Å] and [Ph₂P(Se)NH(2,6-Me₂C₆H₃)] [2.1019(8) Å], previously we described to consider as phosphorus–selenium bond as double bond.¹¹ P1–N1 bond distances of 1.665(2) Å and 1.116(2) Å for **25-cis** and **25-trans** respectively are in the expected range, as reported for other phosphinoselenoic amido compounds in the literature.¹¹ In the centrosymmetric **25-trans** form, C1–N1 and C1ⁱ–N1ⁱ bonds are trans to each other. The compound **25-cis** also possesses a centre of inversion *i* in the middle of the C7–C7ⁱ bond. C7–N1 and C7ⁱ–N1ⁱ bonds are *cis* to each other and a dihedral angle of 67.09° is formed by the planes containing C7, N1, P1 and C7ⁱ, N1ⁱ, P1ⁱ atoms. Thus, planes containing the N1, P1, Se1 and N1ⁱ, P1ⁱ, Se1ⁱ atoms are not coplanar, but almost orthogonal (86.90°) to each other.

4.2.2. Alkaline-earth metal complexes

The title compounds $[(\text{THF})_3\text{M}\{\text{Ph}_2\text{P}(\text{Se})\text{NCH}_2\text{CH}_2\text{NPPh}_2(\text{Se})\}]$ [$\text{M} = \text{Ca}$ (**26**), Sr (**27**), Ba (**28**) and Mg (**29**)] can be obtained by two different synthetic approaches. Both the approaches were used for the calcium complex **26**, whereas the other complexes were obtained using a one-pot reaction only. In the first approach, the well-established compound $[(\text{THF})_2\text{Ca}\{\text{N}(\text{SiMe}_3)_2\}_2]$,^{12,13} was made to react with compound **25** in a 1:1 molar ratio in THF at room temperature to afford the corresponding bis(diphenylphosphinoselenoicamide) complex **26** via the elimination of volatile bis(trimethylsilyl)amine (see Scheme 4.2). However, the most convenient approach to obtaining complexes **26–29** is a one-pot reaction, in which the ligand, $[\text{Ph}_2\text{P}(\text{Se})\text{NHCH}_2\text{CH}_2\text{NHP}(\text{Se})\text{Ph}_2]$, is made to react with anhydrous potassium bis(trimethylsilyl)amide in a 1:2 molar ratio in THF to generate *in situ* potassium salt of ligand **25**, followed by the addition of anhydrous alkaline-earth metal diiodide to the reaction mixture (see Scheme 4.2).¹⁴



Scheme 4.2. Syntheses of alkaline-earth metal phosphinoselenoic amide complexes **26–29**.

The corresponding magnesium complex $[(\text{THF})_3\text{Mg}\{\text{Ph}_2\text{P}(\text{Se})\text{NCH}_2\text{CH}_2\text{NPPH}_2(\text{Se})\}]$ (**29**) was obtained by the second route, using ligand **25** and $[\text{KN}(\text{SiMe}_3)_2]$, followed by addition of magnesium diiodide in THF solvent (see Scheme 4.2). The new complexes were characterised using standard analytical and spectroscopic techniques, and the solid-state structures of all four alkaline earth metal complexes were established by single crystal X-ray diffraction analysis. A strong absorption band at 550 cm^{-1} (for complex **26**), 552 cm^{-1} (for complex **27**), 555 cm^{-1} (for complex **28**) and 551 cm^{-1} (for complex **29**) in FT-IR spectra indicates a P=Se bond in the each complex. The P=Se stretching frequencies are within the range reported by us.¹¹ The ^1H NMR spectra of the diamagnetic compounds **26–29** show a multiplet signal [δ 3.39 ppm (complex **26**), 2.87 ppm (complex **27**), 3.14 ppm (complex **28**) and 3.09 ppm (complex **29**)] for the four methylene protons and this is very close to resonance signal (δ 3.16 ppm) of the analogous methylene protons present in free ligand **25**. Each of the complexes **26–29** shows a sharp signal in the $^{31}\text{P}\{^1\text{H}\}$ NMR spectra [δ 71.8 (complex **26**), 71.9 (complex **27**), 73.3 ppm (complex **28**) and 43.7 ppm (complex **29**)], which is significantly low field shifted for complexes **26–28** and high field shifted for the complex **29** and to free ligand **25** (δ 59.6 ppm),¹⁰ showing that both the phosphorous atoms in each complex are chemically equivalent in solution. All three complexes are coordinated to THF molecules, as is evident from the typical multiplet signals at 3.65–3.55 ppm and 1.35–1.33 ppm observed in ^1H NMR spectra. Although there is ongoing interest in alkaline-earth organometallics¹⁵ and particularly in the cyclopentadienyl chemistry of these elements,¹⁶ complexes **26–29** represent, to the best of our knowledge, the first alkaline earth metal complexes containing a bis(diphenylphosphinoselenoicamide) ligand having two sets of three heteroatom, N, P and Se, adjacent to each other in the ligand. Therefore, their molecular structures in the solid state were determined by X-ray diffraction analysis.

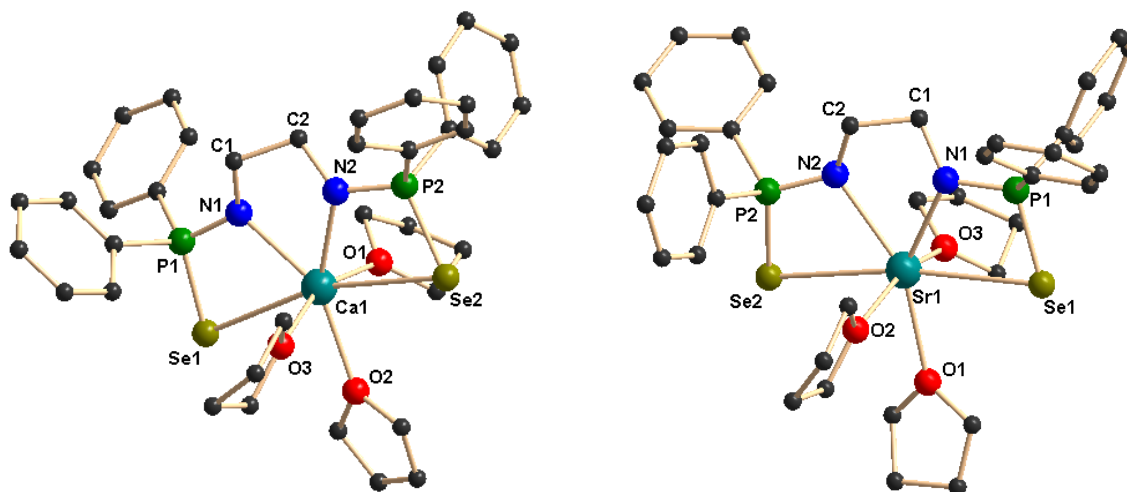


Figure 4.3. Solid-state structures of compounds **26** and **27**. Hydrogen atoms are omitted for clarity. Selected bond lengths (Å) and bond angles (°):

26: P1–N1 1.592(8), P1–Se1 2.148(3), P1–C9 1.824(10), P1–C3 1.832(10), N1–C1 1.450(13), P2–N2 1.595(8), P2–Se2 2.155(3), P2–C15 1.833(9), P2–C21 1.824(10), N2–C2 1.433(13), C1–C2 1.526(13), Ca1–N1 2.386(8), Ca1–Se1 3.252(2), Ca1–P1 3.359(3), Ca1–N2 2.418(8), Ca1–Se2 3.300(2), Ca1–P2 3.364(3), Ca1–O1 2.374(7), Ca1–O2 2.429(7), Ca1–O3 2.385(7), C2–C1–N1 108.0(8), N1–P1–C9 112.3(4), N1–P1–Se1 108.4(3), N1–P1–C3 111.0(4), P1–N1–C1 123.0(7), Se1–P1–C9 110.3(3), Se1–P1–C3 111.3(3), C1–C2–N2 109.2(8), N2–P2–C15 111.9(4), N2–P2–Se2 108.8(3), N2–P2–C21 112.4(5), P2–N2–C2 123.6(7), Se2–P2–C15 111.8(3), Se2–P2–C21 110.1(3), N1–Ca1–Se1 63.3(2), N1–Ca1–N2 68.6(3), Se1–Ca1–Se2 165.42(7), O1–Ca1–O2 79.6(3), O1–Ca1–O3 159.1(3), O2–Ca1–O3 80.4(3), P1–Se1–Ca1 73.76(8), P2–Se2–Ca1 72.76(8).

27: P1–N1 1.592(5), P1–Se1 2.1548(17), P1–C9 1.823(7), P1–C3 1.826(7), N1–C1 1.465(7), P2–N2 1.589(5), P2–Se2 2.1559(17), P2–C15 1.837(6), P2–C21 1.819(6), N2–C2 1.463(7), C1–C2 1.524(8), Sr1–N1 2.517(5), Sr1–Se1 3.2788(10), Sr1–P1 3.4456(18), Sr1–N2 2.540(5), Sr1–Se2 3.3259(10), Sr1–P2 3.4521(16), Sr1–O1 2.568(5), Sr1–O2 2.529(5), Sr1–O3 2.537(5), C2–C1–N1 108.4(5), N1–P1–C9 111.3(3), N1–P1–Se1 109.13(19), N1–P1–C3 112.7(3), P1–N1–C1 122.7(4), Se1–P1–C9 110.3(2), Se1–P1–C3 109.1(2), C1–C2–N2 109.3(5), N2–P2–C15 112.2(3), N2–P2–Se2 108.72(19), N2–P2–C21 112.6(3), P2–N2–C2 123.4(4), Se2–P2–C15 111.2(2), Se2–P2–C21 109.8(2), N1–

Sr1–Se1 62.35(11), N1–Sr1–N2 65.80(15), Se1–Sr1–Se2 170.54(2), O1–Sr1–O2 80.67(18), O1–Sr1–O3 80.37(17), O2–Sr1–O3 159.22(17), P1–Se1–Sr1 75.57(5), P2–Se2–Sr1 74.67(5).

The calcium, strontium bis(diphenylphosphinoselenoicamido) complexes **26** and **27** crystallise in the triclinic space group *P*-1, with two molecules of **26** and **27** in the unit cell respectively. The slightly larger barium compound **28** also crystallises in the triclinic space group *P*-1, with two independent molecules of complex **28** in the asymmetric unit. The details of the structural parameters are given in the Table 4.2 & 4.3. The solid-state structures of complexes **26–28** are shown in the figure 4.3 & 4.4 respectively. Complexes **26–28** are isostructural to each other due to the similar ionic radii of the metal ions (1.00 Å, 1.18 Å and 1.35 Å respectively) for a coordination number of 6.¹⁷ In all three complexes, the coordination polyhedron is formed by dianionic bis(diphenylphosphinoselenoicamide) [Ph₂P(Se)NCH₂CH₂NP(Se)Ph₂]²⁻ ligands, and three THF molecules which are present as solvates to provide the metal ion seven-fold coordination.

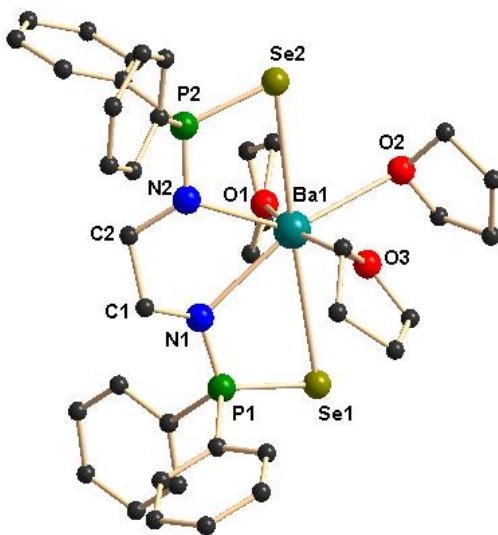


Figure 4.4. Solid-state structure of compound **28**. Hydrogen atoms are omitted for clarity. Selected bond lengths (Å) and bond angles (°): P1–N1 1.585(6), P1–Se1 2.1583(19), P1–C14 1.834(7), P1–C3 1.835(7), N1–C1 1.458(9), P2–N2 1.591(6), P2–Se2 2.1490(18), P2–C15 1.833(7), P2–C21 1.837(7), N2–C2 1.478(8), C1–C2 1.517(9), Ba1–N1 2.657(5), Ba1–Se1 3.4706(9), Ba1–P1 3.6129(17), Ba1–N2 2.654(6), Ba1–Se2 3.4071(9), Ba1–P2 3.5929(18), Ba1–O1 2.716(5), Ba1–O2 2.812(5), Ba1–O3 2.721(5), C2–C1–N1 110.6(6),

N1–P1–C14 112.6(3), N1–P1–Se1 110.1(2), N1–P1–C3 111.6(3), P1–N1–C1 122.3(5), Se1–P1–C14 109.4(2), Se1–P1–C3 110.0(2), C1–C2–N2 108.8(6), N2–P2–C15 111.8(3), N2–P2–Se2 109.5(2), N2–P2–C21 112.3(3), P2–N2–C2 121.9(5), Se2–P2–C15 110.4(2), Se2–P2–C21 110.0(3), N1–Ba1–Se1 58.71(12), N1–Ba1–N2 63.45(17), Se1–Ba1–Se2 175.44(2), O1–Ba1–O2 74.26(18), O1–Ba1–O3 155.90(19), O2–Ba1–O3 85.91(18), P1–Se1–Ba1 75.90(5), P2–Se2–Ba1 76.91(5).

The ligand **25** coordinates to the alkaline earth metal ion via chelation of two amido nitrogen atoms and two selenium atoms attached to the phosphorus atoms. The phosphorus-metal distances (3.365 and 3.359 Å for complex **26**, 3.452 and 3.446 Å for complex **27**, and 3.593 and 3.613 Å for complex **28**) are significantly greater than the sum of the covalent radii of the respective metal ion and phosphorus atom (3.07 Å for complex **26**, 3.25 Å for complex **27** and 3.34 Å for complex **28**). This indicates that the metal ion and phosphorous have no interaction between themselves. Thus, in each case, the central metal ion adopts a distorted pentagonal bi-pyramidal geometry around it, with two selenium atoms, two nitrogen atoms of ligand **25**, along with one oxygen atom from THF molecule, which is in the basal plane, whereas two remaining THF molecules occupy the apical positions. In complex **26-28**, the M–N distances [2.386(8) Å and 2.418(8) Å for complex **26**, 2.517(5) Å and 2.540(5) Å for complex **27**, and 2.657(5) Å and 2.654(6) Å for complex **28**] and M–Se distances [3.252(2) and 3.300(2) for complex **26**, 3.2788(1) Å and 3.3259(1) Å for complex **27** and 3.4706(9) Å and 3.4071(9) Å for complex **28**] indicate a slight asymmetrical attachment of the tetra-dentate ligand **25** to the alkaline earth metal ion. This is due to the presence of four phenyl rings attached to two phosphorus atoms. However, similar M–N distances and M–Se distances were observed in our previously reported complexes [(THF)₂M{Ph₂P(Se)N(CHPh₂)₂}₂] (M = Ca, Sr, Ba) (Chapter 2) and heavier alkaline earth metal complexes reported by other groups.¹⁸ Thus, we observe that bis(diphenylphos-phinoselenoicamide **25** behaves as a tetra-dentate chelating ligand to form a five-member metallacycle M1–N1–C1–C2–N2, where two four-membered metallacycles M1–Se1–P1–N1 and M1–Se2–P2–N2 are fused together to construct a polymetallacyclic motif tricyclometalla[5.2.0.0^{1,4}]nonane structure. To the best of our knowledge, this is the first example of such a structural motif in alkaline earth metal complexes, with three adjacent hetero donor atoms—selenium, phosphorus and nitrogen.

Among the three M–O distances for each complex, M–O distance [2.429(7) Å for complex **26**, 2.568(5) Å for complex **27**, 2.812(5) Å for complex **28**], the THF molecule resides in the basal plane of the distorted pentagonal bi-pyramidal structure and is slightly elongated compared to the remaining M–O distances [2.374(7) Å, 2.385(7) Å for complex **26**, 2.537(5) Å, 2.568(5) Å for complex **27**, 2.716(5) Å and 2.721(5) Å for complex **28**] measured for the THF molecules placed in apical position. This slight elongation can be explained by the extensive electron release from the two anionic basal nitrogen atoms opposite the THF molecule in the metal complex.

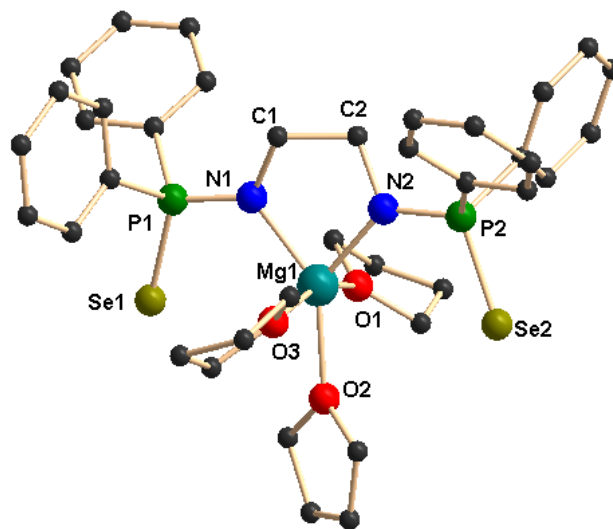


Figure 4.5. Solid-state structure of compound **29**. Hydrogen atoms are omitted for clarity. Selected bond lengths (Å) and bond angles(°): P1–N1 1.606(3), P1–Se1 2.1308(10), P1–C3 1.831(3), P1–C9 1.825(3), N1–C1 1.477(4), P2–N2 1.612(3), P2–Se2 2.1240(10), P2–C15 1.833(3), P2–C21 1.834(3), N2–C2 1.482(4), C1–C2 1.524(4), Mg1–N1 2.083(3), Mg1–N2 2.066(3), Mg1–O1 2.124(3), Mg1–O2 2.137(2), Mg1–O3 2.106(2), C2–C1–N1 108.9(3), N1–P1–C9 112.57(15), N1–P1–Se1 110.69(10), N1–P1–C3 111.46(15), P1–N1–C1 121.0(2), Se1–P1–C9 109.18(11), Se1–P1–C3 111.65(11), C1–C2–N2 109.0(3), N2–P2–C15 111.99(15), N2–P2–Se2 111.98(11), N2–P2–C21 110.05(15), P2–N2–C2 118.6(2), Se2–P2–C15 109.14(11), Se2–P2–C21 110.70(11), N1–Mg1–N2 83.40(12), O1–Mg1–O2 80.49(10), O1–Mg1–O3 160.13(11), O2–Mg1–O3 80.11(10), N1–Mg1–O1 94.85(11), N2–Mg1–O1 99.30(11), N1–Mg1–O3 97.76(11), N2–Mg1–O2 134.70(12), N2–Mg1–O1 99.30(11), N2–Mg1–O3 97.36(11).

The magnesium ion has the smallest ionic radius among the Mg^{2+} to Ba^{2+} ions and thus different coordination behaviours can be anticipated.¹⁹ As we have observed that ligand **25** is acting as tetra-dentate chelating ligand towards moderately larger ions (Ca^{2+} to Ba^{2+}) it would be interesting to study its solid-state structure to learn more about its flexible nature. The magnesium compound **29** was crystallized from THF/*n*-pentane mixture as a colourless solid. Compound **29** crystallizes in the triclinic space group *P*-1, with two molecules in the unit cell. Table 4.3 contains the details of structural refinement parameters for compound **29** and its solid-state structure is shown in Figure 4.5. In contrast to compounds **26–28**, it is observed that for complex **29**, a five magnesia-metallacycle Mg1–N1–C1–C2–N2 is formed by the chelation of two amido nitrogen atoms of ligand **25**. Two selenium atoms, which coordinated to Ca, Sr and Ba ions to make two four-membered rings in complexes **26–28**, are unable to interact with the smaller magnesium ion (Mg1–Se1 3.661 Å and Mg1–Se2 3.769 Å). This is an instance of flexibility of the chelating ligand **25**, switching from tetra-dentate to bi-dentate fashion depending upon the nature of the metal ion. As three THF molecules are chelated to magnesium ion, the geometry around it is best described as a distorted trigonal bi-pyramidal geometry, having the amido nitrogens and one THF at the equatorial position and two THF molecules in the apical position. As expected, the Mg–N bond distances [2.066(3) Å and 2.083(3) Å] are among the shortest with respect to M–N distances [2.386(8) and 2.418(8) Å for Ca, 2.517(5) and 2.540(5) Å for Sr, and 2.657(5) and 2.654(6) Å for Ba]. Five-membered magnesium metallacycles are reported in the literature.²⁰

4.2.3. Bis(amidodiphenylphosphene borane) ligand

In the chapter 3 we have introduced a novel amidophosphine-borane adduct as a ligand and exploited its chelating behaviour in alkali metal and alkaline earth metal chemistry. The amidophosphine-borane [$Ph_2P(BH_3)NHR$] acts as a monoanionic ligand and coordinates to the metal ions through amido nitrogen and borane hydrogens. We intended to extend the idea of amidophosphine-borane to bis(amidodiphenylphosphene-borane) by introducing one spacer of ethylene bridge. Thus, bis(amidodiphenylphosphene-borane) would form a dianion and act as a tetra-dentate ligand towards metal ions. In this chapter we present the synthesis and structure of bis(amidophosphine-orane) ligand

$[\text{Ph}_2\text{P}(\text{BH}_3)\text{NHCH}_2\text{CH}_2\text{NHPPh}_2(\text{BH}_3)]$ (**30**) and the corresponding dimeric barium complex $[(\text{THF})_2\text{Ba}\{\text{Ph}_2\text{P}(\text{BH}_3)\text{N-CH}_2\text{CH}_2\text{NPPh}_2(\text{BH}_3)\}]_2$ (**31**) to demonstrate our concept of versatility of the amidophosphine backbone. The bis(amidodiphenylphosphine-borane) ligand $[\text{Ph}_2\text{P}(\text{BH}_3)\text{NHCH}_2\text{CH}_2\text{NHPPh}_2(\text{BH}_3)]$ (**30**) was isolated as a white precipitate from the reaction between bis(phosphineamine) $[\text{Ph}_2\text{PNHCH}_2\text{CH}_2\text{NHPPh}_2]$ and the borane adduct $[\text{H}_3\text{B.SMe}_2]$ at room temperature in a 1:2 molar ratio in toluene as the solvent (see Scheme 4.3).¹⁴



Scheme 4.3. Synthesis of the bis(amidodiphenylphosphine-borane) ligand **30**

The formation of the amidophosphine-borane ligand **30** from $[\text{Ph}_2\text{PNHCH}_2\text{CH}_2\text{NHPPh}_2]$ can easily be followed by ^1H NMR spectroscopy measured in CDCl_3 , since additional resonances for the two chemically equivalent borane (BH_3) groups attached to the phosphorus atoms appear as a broad signal at δ 1.4 ppm. In the ^1H NMR spectra, the resonances of the amidophosphine moiety in ligand **30** are only slightly shifted in comparison to the starting material with those reported for the phosphine amines.²¹ The multiplet signals at 2.78 ppm can be assigned to the four methylene protons of ligand **30** in which both the hydrogen atoms are diastereotopic to each other. This indicates that methylene signals are slightly high field shifted compared to the selenium analogue **25** (3.16 ppm). Another broad signal at 3.02 ppm corresponding to the two NH protons of ligand **30** is observed and also shifted to the higher field (3.24 ppm) compared to **25**. Ligand **30** shows a doublet signal in the $^{31}\text{P}\{^1\text{H}\}$ NMR spectrum at 58.8 ppm with a coupling constant of 67.9 Hz due to coupling with adjacent boron atom. In $^{11}\text{B}\{^1\text{H}\}$ NMR spectrum, the signal at -38.1 ppm can be assigned to the BH_3 group attached with phosphorus. This observation is in agreement with our previously reported values. (See Chapter 3) In the FT-IR spectra, a characteristic signal for P–B bond stretching at 606 cm^{-1} was observed along with another characteristic signal at 2380 cm^{-1} assigned to the B–H stretching frequency. These values are in agreement with those reported in literature.²² The molecular structure

of ligand **30** was established using single crystal X-ray diffraction analysis. It crystallizes in the monoclinic space group *Cc*, with four independent molecules in the unit cell (see Figure 4.6). The details of the structural parameters are given in Table 4.4. The P1–B1 bond distances in **30** [1.9091(2) Å and 1.916(1) Å] are almost similar and in agreement with reported values 1.918(6) Å for [Ph₂P(BH₃)NH(CHPh₂)], 2.1019(8) Å for [{Ph₂P(BH₃)}₂CH₂] and 1.921(3) Å for [(CH₂-*o*-CF₃C₆H₄)-(Ph)P(BH₃)C₄H₈P(BH₃)(Ph)(CH₂-*o*-CF₃C₆H₄)] to be considered as the phosphorus–boron dative bond reported by us and others.^{17,23} The P1–N1 bond ranges from 1.659(1) Å to 1.660(9) Å and C1–N1 bond distances of 1.443(1) Å and 1.480(1) are also similar to those reported by us previously: P1–N1 1.673(6) Å and C1–N1 1.453(8) Å for Ph₂PNH(CHPh₂) (Chapter 1) and P1–N1 1.638(3) Å and C1–N1 1.468(5) Å for [Ph₂P(BH₃)NH(CHPh₂)]. (See Chapter 3).

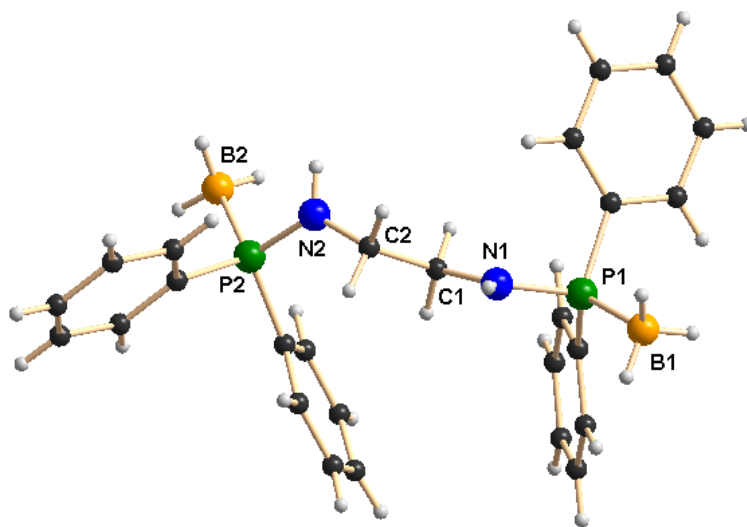
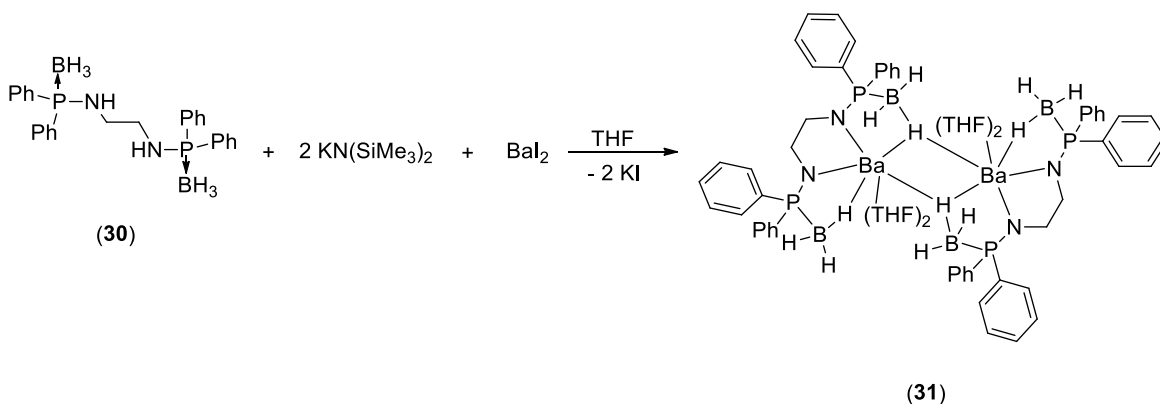


Figure 4.6. Solid-state structure of compound **30**. Selected bond lengths (Å) and bond angles(°): P1–N1 1.668(3), P1–B1 1.920(5), P1–C3 1.805(4), P1–C9 1.815(4), N1–C1 1.463(5), C1–C2 1.523(5), C2–N2 1.437(5), P2–N2 1.660(3), P2–B2 1.896(5), P2–C15 1.810(4), P2–C21 1.817(4), B1–H1c 0.9600, B2–H2c 0.9600, B1–P1–N1 110.0(2), C3–P1–B1 110.3(2), C9–P1–B1 117.1(2), N1–P1–C3 106.20(19), N1–P1–C9 107.62(17), P1–N1–C1 121.4(3), N1–C1–C2 110.3(3), C1–C2–N2 111.9(3), C2–N2–P2 128.8(3), B2–P2–N2 106.7(2), B2–P2–C15 111.7(2), B2–P2–C21 116.8(2), N2–P2–C15 108.20(18), N2–P2–C21 107.85(17).

4.2.4. Bis(amidodiphenylphosphene-borane) barium complex

Ligand **30** was made to react with $[K\{N(SiMe_3)_2\}]$ in THF at an ambient temperature in a 1:2 molar ratio followed by addition of barium diiodide to afford the dimeric barium bis(amidodiphenylphosphene-borane) complex $[(THF)_2Ba\{Ph_2P(BH_3)NCH_2CH_2NPPh_2(BH_3)\}]_2$ (**31**) through the elimination of KI and volatile tetramethylsilane (see Scheme 4.4).¹⁴



Scheme 4.4. Synthesis of barium complex **31**

In FT-IR spectra, strong absorption band at 605 cm^{-1} is assigned to the P–B bond of complex **31**, which is in the range of that of ligand **30** (606 cm^{-1}). The ^1H NMR spectrum of complex **31** in C_6D_6 is very similar to the spectra recorded for compound **30** and reveals time-averaged C_s -symmetry in solution. The four methylene protons in the ligand backbone appear as a multiplet at 2.69 ppm. The resonances of the three protons attached to the boron atom appear as a multiplet at 1.38 ppm in the ^1H NMR spectra. In the proton decoupled ^{31}P NMR spectra, complex **31** shows only one doublet signal at 70.8 ppm and these values are significantly low-field shifted compared to the value for compound **30** (58.8 ppm) upon the coordination of barium atoms to the bis(amidophosphine-borane) ligand. The phosphorus atoms present in the $[\text{Ph}_2\text{P}(\text{BH}_3)\text{NCH}_2\text{CH}_2\text{NPPh}_2(\text{BH}_3)]^{2-}$ moieties are chemically equivalent. A broad signal at -37.6 ppm was observed in the $^{11}\text{B}\{^1\text{H}\}$ NMR spectra of complex **31**.

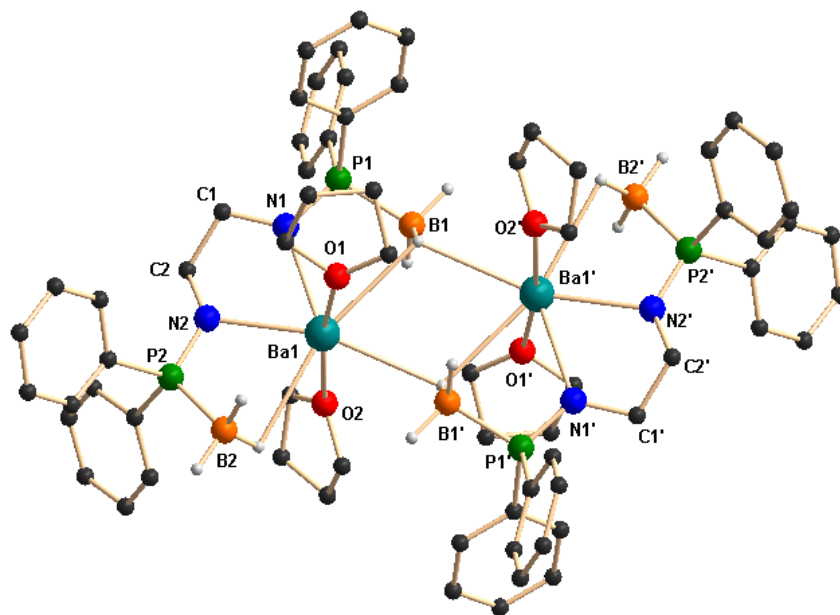


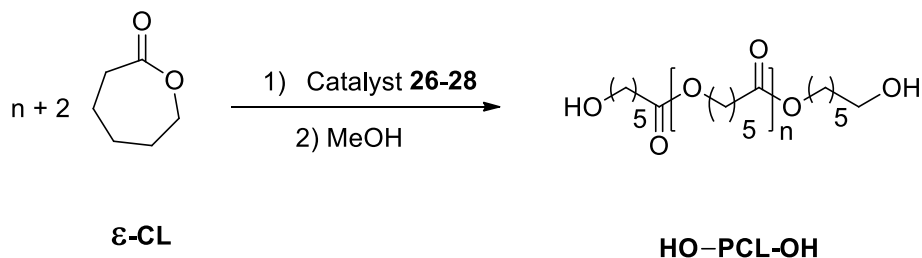
Figure 4.7. Solid state structure of compound **31**. Hydrogen atoms are omitted for clarity except for borane atoms. Selected bond lengths (Å) and bond angles(°): P1–N1 1.595(5), P1–B1 1.938(7), C1–N1 1.468(7), C1–C2 1.531(8), C2–N2 1.475(7), P2–N2 1.596(5), P2–B2 1.943(8), B1–Ba1ⁱ 3.245(7) , B1–H2aa 1.16(6), B1–H2bb 1.07(7), B1–H2cc 1.10(5), B2–H1aa 1.10(5), B2–H1bb 1.12(6), B1–H1cc 1.11(6), Ba1–N1 2.671(5), Ba1–N2 2.647(5), Ba1–B1 3.332(6), Ba1–B2 3.251(7), Ba1–P1 3.6169(16), Ba1–P2 3.5540(16), Ba1–O1 2.730(5), Ba1–O2 2.744(5), Ba1–B1ⁱ 3.245(7), Ba1–H1bb 2.90(6), Ba1–H2bb 2.95(7), B1–P1–N1 107.2(3), P1–N1–C1 125.3(4), N1–Ba1–N2 62.32(15), O1–Ba1–O2 169.80(14), N1–C1–C2 109.1(5), C1–C2–N2 109.2(5), N2–P2–B2 108.1(3).

Compound **31** was re-crystallised from THF and *n*-pentane (1:2 ratio) and was found to crystallize in the triclinic space group *P*-1, which has two molecules in the unit cell. The solid-state structure of complex **31** is given in Figure 4.7. The details of the structural parameters are given in Table 4.4 Compound **31** is dimeric and two barium ions are coordinated by four amido nitrogen atoms and four BH₃ groups of two ligands **30**. Out of four borane groups, two are in mode to coordinate to the two barium ions. Each of the borane (BH₃) group coordinates through the hydrogen atoms in a η¹ fashion and has a Ba1–B1 bond length of 3.332(6) and Ba1–B2 3.251(7) Å. Thus, ligand **30** can be considered a tetra-dentate ligand, similar to what was observed for ligand **25** in the Ca–Ba complexes (see above). Additionally, two THF molecules are coordinated to each barium ion and the

geometry around each barium ion is best described as distorted pentagonal bi-pyramidal. It is noteworthy that the P–B distances [1.938(7) and 1.943(8) Å] are slightly elongated compared to that of the ligand, **30**, [1.920(5) and 1.896(5) Å] even after the coordination of the BH₃ group to the barium centre. The Ba–N [2.671(5), 2.647(5) Å], Ba1–O1 [2.730(5) and 2.744(5) Å] distances are in the range similar to that of the previously described barium complex in chapter 3.

4.3 Ring-Opening Polymerization study

Catalytic activities of the calcium, strontium and barium complexes **26**, **27** and **28** were performed (see Scheme 4.5). Polymerization studies were typically conducted in toluene, with various monomer/catalyst ratios at 25 °C. Selected data obtained with respect to complexes **26**, **27** and **28** are given in Table 4.1.



Scheme 4.5. ROP of ϵ -CL in toluene with calcium, strontium and barium complexes **26–28**.

The catalytic ability of the newly synthesised mono-nuclear calcium complex **26** to promote the ROP of ϵ -CL was first evaluated (Table 4.1, entries 1–4). Indeed, the sluggish reactivity of the calcium complexes is very similar to that observed in some previously reported studies using other calcium complexes for ROP of ϵ -caprolactone.⁸ Since the larger strontium derivatives have been reported to be more active than the calcium congeners in ROP,^{24,25} we tested compound **27** as a catalyst and observed enhanced rate of the polymerisation (Table 4.1, entries 5–8). In both cases, higher reactivity was observed for conversion of ϵ -caprolactone to poly-caprolactone and up to 500 ϵ -CL units were

successfully converted in high yields (90 per cent and 80 per cent) within 15 and 10 minutes respectively at 25 °C.

Table 4.1. Polymerization of ϵ -Caprolactone initiated by alkaline earth metal complexes of type $[\text{MC}_2\text{H}_4(\text{NPh}_2\text{P}=\text{Se})_2(\text{THF})_3]$ (where M = Ca, Sr, Ba)^[a]

Entry	[M]	$[\epsilon\text{CL}]_0/[\text{M}]_0$	Reac. time ^[b] [min]	Conv. ^[c] [%]	$Mn_{(\text{theo})}$ ^[d] [g mol ⁻¹]	$Mn_{(\text{GPC})}$ ^[e] [g mol ⁻¹]	$Mw_{(\text{GPC})}$ ^[e] [g mol ⁻¹]	Mw/Mn ^[f]
1	Ca	200	10	75	15000	17065	11658	1.473
2	Ca	300	15	96	28872	31027	17769	1.746
3	Ca	400	20	89	35689	27238	19883	1.370
4	Ca	500	20	64	32080	33618	24744	1.359
5	Sr	100	10	99	17759	28789	17338	1.660
6	Sr	200	10	98	35159	50353	44198	1.139
7	Sr	300	10	95	51125	60384	53266	1.134
8	Sr	400	10	72	28872	29925	22051	1.357
9	Sr	500	15	80	40100	31590	22461	1.406
10	Ba	200	5	82	16441	24947	18278	1.365
11	Ba	300	5	94	28270	29965	20262	1.479
12	Ba	400	5	85	34085	35033	25045	1.399
13	Ba	500	5	70	35087	43215	34650	1.247

^[a] Results are representative of at least two experiments. ^[b] Reaction times were not necessarily optimized.

^[c] Monomer conversions were determined by ¹H NMR spectroscopy. ^[d] Theoretical molar mass values calculated from the relation: $[\text{monomer}]_0/[\text{M}]_0 \times \text{monomer conversion}$ where $[\text{M}]^0 = 8.76 \times 10^{-3}$ mmol and Monomer weight of ϵ -CL = 114 g mol⁻¹. ^[e] Experimental molar masses were determined by GPC versus polyethylene glycol standards. ^[f] Molar mass distribution was calculated from GPC.

The control over the ROP process was rather good, affording PCLs, featuring a good match between the observed (as determined by GPC) and calculated molar mass values, as well as moderate dispersity data ($\text{PDI} = \text{Mw}/\text{Mn} < 1.80$). The overall efficiency of the calcium initiator **26** towards the ROP of ϵ -CL was weaker than that of the strontium analogue **27**. Being the largest ionic radius of the barium atom, it was anticipated that complex **28** would show the highest reactivity among all the three alkaline earth metal complexes.^{26,27} In

reality we observed that up to 500 ϵ -CL units were successfully converted in good yields (70 per cent) within 5 minutes at 25 °C (Table 4.1, entries 10–13). The poly-caprolactone produced by the use of the barium catalyst was a good match between the observed and calculated molar mass values, and we observed a relatively narrow poly-dispersity data (PDI up to 1.25, entry 13 in Table 4.1). Thus, among three metal complexes **26**, **27** and **28**, the barium complex showed the highest activity for ROP of ϵ -caprolactone.

4.4 Conclusion

We have demonstrated a series of alkaline earth metal complexes with bis(phosphinoselenoicamine) ligand via two synthetic routes. In the solid-state structures of Ca–Ba complexes, the bis(phosphinoselenoicamine) acts as a tetra-dentate ligand by the chelation of two amido nitrogen and two selenium atoms, whereas due to the smaller size of magnesium, the same ligand behaves as a bidentate ligand through chelation of two amido-nitrogen atoms only, showing its flexible nature. We have also introduced another poly-dentate ligand bis(amidodiphenylphosphine borane) in barium chemistry to prepare the barium dimeric complex. We have tested complexes **26–28** as catalysts for the ROP of ϵ -caprolactone and observed that the barium complex, being the largest ionic radius, acts as best catalyst among the three analogues complexes.

4.5. Experimental Procedures

4.5.1. General

All manipulations of air-sensitive materials were performed with the rigorous exclusion of oxygen and moisture in flame-dried Schlenk-type glassware either on a dual manifold Schlenk line, interfaced to a high vacuum (10^{-4} torr) line, or in an argon-filled M. Braun glove box. THF was pre-dried over Na wire and distilled under nitrogen from sodium and benzophenone ketyl prior to use. Hydrocarbon solvents (toluene and *n*-pentane) were distilled under nitrogen from LiAlH₄ and stored in the glove box. ¹H NMR (400 MHz), ¹³C{¹H} and ³¹P{¹H} NMR (161.9 MHz) spectra were recorded on a BRUKER AVANCE III-400 spectrometer. BRUKER ALPHA FT-IR was used for FT-IR measurement.

Elemental analyses were performed on a BRUKER EURO EA at the Indian Institute of Technology Hyderabad. Metal iodides (MgI_2 , CaI_2 , SrI_2 and BaI_2), $\text{KN}(\text{SiMe}_3)_2$, $\text{Me}_2\text{S}\cdot\text{BH}_3$ and ϵ -caprolactone were purchased from Sigma Aldrich and used as such. The bis(phosphinamine) [$\text{Ph}_2\text{PNHCH}_2\text{CH}_2\text{NHPPh}_2$], and bis(phosphinoselenoicamine) [$\text{Ph}_2\text{P}(\text{Se})\text{NHCH}_2\text{CH}_2\text{NHPPh}_2(\text{Se})$] (**25**) were prepared according to procedure prescribed in the literature.^{10,21} The NMR solvent C_6D_6 was purchased from Sigma Aldrich and dried under Na/K alloy prior to use.

4.5.2. Preparation of $[(\text{THF})_3\text{Ca}\{\text{Ph}_2\text{P}(\text{Se})\text{NCH}_2\text{CH}_2\text{NPPh}_2(\text{Se})\}]$ (**26**)

In a 50 ml dry Schlenk flask ligand **25** (200 mg, 0.34 mmol), $\text{KN}(\text{SiMe}_3)_2$ (136 mg, 0.68 mmol) and CaI_2 (100 mg, 0.34 mmol) were mixed together in 10 ml of THF at an ambient temperature and stirred for 14 hours. The precipitate of KI was filtered using a filter dropper and filtrate was dried in *vacuo*. The resulting white compound was further purified by washing with *n*-pentane and crystals of compound **26** suitable for X-ray analysis were grown from THF/*n*-pentane (1:2) mixture solvent at -40°C . Yield 202.0 mg (70.6 %). ^1H NMR (400 MHz, C_6D_6): $\delta = 8.04\text{-}7.99$ (m, 8H, ArH), $7.10\text{-}7.05$ (m, 12H, ArH), $3.77\text{-}3.74$ (m, THF), 3.39 (m, 4H, CH_2), $1.36\text{-}1.33$ (m, THF) ppm; $^{13}\text{C}\{^1\text{H}\}$ NMR (100 MHz, C_6D_6): $\delta = 133.1$ (P-ArC), 131.9 (*o*-ArC), 131.8 (*m*-ArC), 129.7 (*p*-ArC), 68.5 (THF), 42.9 (CH_2), 25.3 (THF) ppm; $^{31}\text{P}\{^1\text{H}\}$ NMR (161.9 MHz, C_6D_6): $\delta = 71.8$ ppm; FT-IR (selected frequencies): 3052 (ArC-H), 2920 (C-H), 1435 (P-C), 969 (P-N), 550 (P=Se) cm^{-1} . Elemental analysis: $\text{C}_{38}\text{H}_{48}\text{CaN}_2\text{O}_3\text{P}_2\text{Se}_2$ (840.74). Calcd. C 54.29, H 5.75, N 3.33. Found: C 53.83, H 5.39, N 2.98.

4.5.3. Preparation of $[(\text{THF})_3\text{Sr}\{\text{Ph}_2\text{P}(\text{Se})\text{NCH}_2\text{CH}_2\text{NPPh}_2(\text{Se})\}]$ (**27**)

In a 50 ml dry Schlenk flask ligand **25** (130 mg, 0.23 mmol), $\text{KN}(\text{SiMe}_3)_2$ (89 mg, 0.45 mmol) and SrI_2 (100 mg, 0.23 mmol) were mixed together in 10 ml of THF at an ambient temperature and stirred for 14 hours. The precipitate of KI was filtered using a filter dropper

and filtrate was dried in *vacuo*. The resulting white compound was further purified by washing with *n*-pentane and crystals suitable for X-ray analysis were grown from THF/*n*-pentane (1:2) mixture solvent at $-40\text{ }^{\circ}\text{C}$. Yield 176.5 mg (87.8 %). ^1H NMR (400 MHz, C_6D_6): $\delta = 8.05\text{--}7.99$ (m, 8H, ArH), $7.12\text{--}6.97$ (m, 12H, ArH), $3.57\text{--}3.53$ (m, THF), 2.87 (m, 4H, CH_2), $1.41\text{--}1.37$ (m, THF) ppm; $^{13}\text{C}\{^1\text{H}\}$ NMR (100 MHz, C_6D_6): $\delta = 133.8$ (P-ArC), 132.9 (P-ArC), 131.0 (*o*-ArC), 130.8 (*m*-ArC), 130.2 (*p*-ArC), 66.4 (THF), 40.9 (CH_2), 24.4 (THF) ppm; $^{31}\text{P}\{^1\text{H}\}$ NMR (161.9 MHz, C_6D_6): $\delta = 71.9$ ppm; FT-IR (selected frequencies): 3052 (Ar C-H), 2922 (C-H), 1435 (P-C), 998 (P-N), 552 (P=Se) cm^{-1} . Elemental analysis: $\text{C}_{38}\text{H}_{48}\text{N}_2\text{O}_3\text{P}_2\text{Se}_2\text{Sr}$ (888.26): Calcd. C 51.38, H 5.45, N 3.15. Found: C 50.65, H 5.08, N 3.01.

4.5.4. Preparation of $[(\text{THF})_3\text{Ba}\{\text{Ph}_2\text{P}(\text{Se})\text{NCH}_2\text{CH}_2\text{NPPh}_2(\text{Se})\}]$ (**28**)

In a 50 ml dry Schlenk flask ligand **25** (150 mg, 0.256 mmol), $\text{KN}(\text{SiMe}_3)_2$ (102 mg, 0.512 mmol) and BaI_2 (100 mg, 0.256 mmol) were mixed together in 10 ml of THF at ambient temperature and stirred for 14 hours. The precipitate of KI was filtered using a filter dropper and filtrate was dried in *vacuo*. The resulting white residue was further purified by washing with *n*-pentane and crystals suitable for X-ray analysis were grown from THF/*n*-pentane (1:2) mixture solvent at $-40\text{ }^{\circ}\text{C}$. Yield 210.0 mg (87.5 %). ^1H NMR (400 MHz, C_6D_6): $\delta = 8.14\text{--}8.02$ (m, 8H, ArH), $7.11\text{--}7.03$ (m, 12H, ArH), $3.57\text{--}3.53$ (m, THF), 3.14 (m, 4H, CH_2), $1.41\text{--}1.38$ (m, THF) ppm; $^{13}\text{C}\{^1\text{H}\}$ NMR (100 MHz, C_6D_6): $\delta = 133.1$ (P-ArC), 132.8 (P-ArC), 131.5 (*o*-ArC), 131.3 (*m*-ArC), 130.7 (*p*-ArC), 67.5 (THF), 48.5 (CH_2), 25.5 (THF) ppm; $^{31}\text{P}\{^1\text{H}\}$ NMR (161.9 MHz, C_6D_6): $\delta = 73.3$ ppm; FT-IR (selected frequencies): 3052 (Ar C-H), 2951 (C-H), 1434 (P-C), 997 (P-N), 555 (P=Se) cm^{-1} . Elemental analysis: $\text{C}_{38}\text{H}_{48}\text{BaN}_2\text{O}_3\text{P}_2\text{Se}_2$ (937.97): Calcd. C 48.66, H 5.16, N 2.99. Found: C 47.88, H 4.72, N 2.69.

4.5.5. Preparation of $[(\text{THF})_3\text{Mg}\{\text{Ph}_2\text{P}(\text{Se})\text{NCH}_2\text{CH}_2\text{NPPh}_2(\text{Se})\}]$ (**29**)

In a 50 ml dry Schlenk flask ligand **25** (210 mg, 0.36 mmol), $\text{KN}(\text{SiMe}_3)_2$ (143 mg, 0.72 mmol) and MgI_2 (100 mg, 0.36 mmol) were mixed together in 10 ml of THF at an ambient temperature and stirred for 14 hours. The precipitate of KI was filtered using a filter dropper

and filtrate was dried in *vacuo*. The resulting white compound was further purified by washing with *n*-pentane and crystals suitable for X-ray analysis were grown from THF/*n*-pentane (1:2) mixture solvent at $-40\text{ }^{\circ}\text{C}$. Yield 202.0 mg (70.6 %). ^1H NMR (400 MHz, C_6D_6): $\delta = 7.92\text{--}7.87$ (m, 8H, ArH), $7.01\text{--}6.90$ (m, 12H, ArH), $3.61\text{--}3.58$ (m, THF), 3.09 (m, 4H, CH_2), $1.32\text{--}1.26$ (m, THF) ppm; $^{13}\text{C}\{^1\text{H}\}$ NMR (100 MHz, C_6D_6): $\delta = 132.1$ (P-ArC), 131.9 (P-ArC), 131.7 (*o*-ArC), 131.6 (*m*-ArC), 129.6 (*p*-ArC), 68.1 (THF) 29.9 (CH_2), 25.4 (THF) ppm; $^{31}\text{P}\{^1\text{H}\}$ NMR (161.1 MHz, C_6D_6): $\delta = 43.7$ ppm; FT-IR (selected frequencies): 3052 (Ar C-H), 2917 (C-H), 1435 (P-C), 997 (P-N), 551 (P=Se) cm^{-1} . Elemental analysis: $\text{C}_{38}\text{H}_{48}\text{MgN}_2\text{O}_3\text{P}_2\text{Se}_2$ (824.95): Calcd. C 55.32, H 5.86, N 3.40. Found: C 54.83, H 5.49, N 3.18.

4.5.6. Preparation of $[\text{Ph}_2\text{P}(\text{BH}_3)\text{NHCH}_2\text{CH}_2\text{NHPPH}_2(\text{BH}_3)]$ (**30**)

To a stirring solution of ethylenediamine (325.2 mg, 5.4 mmol) and triethylamine (1.09 g, 1.5 ml, 10.8 mmol) in THF/ CH_2Cl_2 mixture solvent (10 ml), was added a solution of chlorodiphenylphosphine (2.39 g, 10.8 mmol) in THF (5 ml), drop-wise, and stirred for 3 hours. The precipitate formed was filtered and the solvent removed in *vacuo*. To this residue, 20 ml of dry toluene and two equivalents of borane-dimethyl sulphide (822.2 mg, 10.8 mmol) was added and stirred for another 12 hours. The title compound was formed as a white precipitate and it was further purified by washing several times with *n*-hexane. Crystals suitable for X-ray diffraction analysis were obtained from THF/*n*-pentane combination in 1:2 ratio. Yield 1.45 g (58.7 %). ^1H NMR (400 MHz, CDCl_3): $\delta = 7.66\text{--}7.57$ (m, 8H, ArH), $7.55\text{--}7.32$ (m 12H, ArH), $3.03\text{--}3.01$ (m, 2H, $\text{P}(\text{BH}_3)\text{NH}$), $2.81\text{--}2.75$ (m, 4H, CH_2), $1.87\text{--}0.95$ (m, 6H, BH_3) ppm; $^{13}\text{C}\{^1\text{H}\}$ NMR (100 MHz, CDCl_3): $\delta = 134.3$ (P-ArC), 134.2 (P-ArC), 132.9 (*o*-ArC), 132.8 (*o*-ArC), 132.2 (*p*-ArC), 132.1 (*p*-ArC), 131.4 (*m*-ArC), 131.2 (*m*-ArC), 44.2 (CH_2) ppm; $^{31}\text{P}\{^1\text{H}\}$ NMR (161.9 MHz, CDCl_3): $\delta = 58.8$ (d, $J_{\text{P-B}} = 67.9$ Hz) ppm; $^{11}\text{B}\{^1\text{H}\}$ NMR (128.4 MHz, CDCl_3): $\delta -38.1$ ppm. FT-IR (selected frequencies): 3366 (N-H), 3056 (Ar C-H), 2960 (C-H), 2380 (B-H), 1436 (P-C), 935 (P-N), 606 (P-B) cm^{-1} . Elemental analysis: $\text{C}_{26}\text{H}_{32}\text{B}_2\text{N}_2\text{P}_2$ (456.10). Calcd. C 68.46, H 7.07, N 6.14. Found: C 67.98, H 6.79, N 5.88.

4.5.7. Preparation of $[(\text{THF})_2\text{Ba}\{\text{Ph}_2\text{P}(\text{BH}_3)\text{NCH}_2\text{CH}_2\text{NPPH}_2(\text{BH}_3)\}]_2$ (**31**)

In a 50 ml dry Schlenk flask, ligand **6** (116.8 mg, 0.256 mmol), KN(SiMe₃)₂ (102 mg, 0.512 mmol) and BaI₂ (100 mg, 0.256 mmol) were mixed together in 10 ml of THF at an ambient temperature and stirred for 14 hours. The precipitate of KI was filtered using a filter dropper and filtrate was dried in *vacuo*. The resulting white compound was further purified by washing with *n*-pentane and crystals suitable for X-ray analysis were grown from THF/*n*-pentane (1:2) mixture solvent at -40 °C. Yield 153.0 mg (85.0 %). ¹H NMR (400 MHz, C₆D₆): δ = 7.59–7.54 (m, 8H, ArH), 7.15–7.01 (m, 12H, ArH), 2.71–2.67 (m, 4H, CH₂), 1.96–0.80 (m, 6H, BH₃) ppm; ¹³C{¹H} NMR (100 MHz, C₆D₆): δ = 133.3 (P-ArC), 132.6 (P-ArC), 132.2 (o-ArC), 132.1 (o-ArC), 131.3 (p-ArC), 131.2 (p-ArC), 128.8 (m-ArC), 128.7 (m-ArC), 44.4 (CH₂) ppm; ³¹P{¹H} NMR (161.9 MHz, C₆D₆): δ = 70.8 (d, *J*_{P-B} = 62.4 MHz) ppm; ¹¹B{¹H} NMR (128.4 MHz, C₆D₆): δ -37.6 ppm. FT-IR (selected frequencies): 3056 (Ar C-H), 2957 (C-H), 2375 (B-H), 1434 (P-C), 996 (P-N), 605 (P-B) cm⁻¹. Elemental analysis: (C₃₄H₄₆B₂BaN₂O₂P₂) (735.62). Calcd. C 55.51, H 6.30, N 3.81; Found: C 54.92, H 6.02, N 3.31.

4.5.8. Typical polymerisation experiment

In a glove box under argon atmosphere, the catalyst was dissolved in the appropriate amount (1.0 ml) of dry toluene. ε-caprolactone in 1.0 ml of toluene was then added under vigorous stirring. The reaction mixture was stirred at room temperature for 5–20 minutes, after which the reaction mixture was quenched by addition of a small amount of (1.0 ml) methanol and then added acidified methanol little excess. The polymer was precipitated in excess methanol and it was filtered and dried under vacuum. The final polymer was then analysed by NMR and SEC.

4.6 X-Ray crystallographic studies

Single crystals of compounds **26–29** and **31** were grown from THF and *n*-pentane mixture at -40 °C under inert atmosphere. The single crystal of **25-cis**, **25-trans** and **30** suitable for X-ray measurement were grown at room temperature. For compounds **26–29** and **31**, a crystal of suitable dimensions was mounted on a CryoLoop (Hampton Research Corp.)

with a layer of light mineral oil and placed in a nitrogen stream at 150(2) K. However for compounds **25-cis**, **25-trans** and **30**, the data were collected at 293 K. All measurements were made on an Agilent Supernova X-calibur Eos CCD detector with graphite-monochromatic Cu-K α (1.54184 Å) radiation. Crystal data and structure refinement parameters are summarised in Table 4.1-4.3. The structures were solved by direct methods (SIR92)²⁸ and refined on F² by full-matrix least-squares methods; using SHELXL-97.²⁹ Non-hydrogen atoms were anisotropically refined. H atoms were included in the refinement in calculated positions riding on their carrier atoms. For compounds **26** and **29**, two carbon atoms which are part of two coordinated THF molecules are slightly thermally disorder and treated anisotropically. The function minimised was $[\sum w(F_o^2 - F_c^2)^2]$ ($w = 1 / [\sigma^2(F_o^2) + (aP)^2 + bP]$), where $P = (\text{Max}(F_o^2, 0) + 2F_c^2) / 3$ with $\sigma^2(F_o^2)$ from counting statistics. The function R_1 and wR_2 were $(\sum ||F_o| - |F_c||) / \sum |F_o|$ and $[\sum w(F_o^2 - F_c^2)^2 / \sum (wF_o^4)]^{1/2}$, respectively. The Diamond-3 program was used to draw the molecule. Crystallographic data (excluding structure factors) for the structures reported in this paper have been deposited with the Cambridge Crystallographic Data Centre CCDC 987282-987289.

4.7 Tables

Table 4.2. Crystallographic data of compounds **25-cis**, **25-trans** and **26**

Crystal	25-cis	25-trans	26
CCDC No.	987282	987283	987285
Empirical formula	C ₂₆ H ₂₆ N ₂ P ₂ Se ₂	C ₃₄ H ₄₀ N ₂ O ₂ P ₂ Se ₂	C ₃₈ H ₄₈ CaN ₂ O ₃ P ₂ Se ₂
Formula weight	586.35	728.54	840.72
<i>T</i> (K)	293(2)	293(2)	150(2)
λ (Å)	1.54184	1.54184	1.54184
Crystal system	Monoclinic,	Orthorhombic	Triclinic
Space group	<i>C</i> 2/ <i>c</i>	<i>P</i> <i>b</i> <i>c</i> <i>a</i>	<i>P</i> -1
<i>a</i> (Å)	23.2423(12)	16.5026(5)	9.8642(10)
<i>b</i> (Å)	12.0610(7)	11.4432(3)	13.4955(12)
<i>c</i> (Å)	9.2715(5)	18.3315(5)	16.8868(12)
α (°)	90	90	106.675(7)
β (°)	102.372(6)	90	101.705(8)
γ (°)	90	90	106.697(9)
<i>V</i> (Å ³)	2538.7(2)	3461.77(17)	1960.4(3)
<i>Z</i>	4	4	2
<i>D</i> _{calc} g cm ⁻³	1.534	1.398	1.424
μ (mm ⁻¹)	4.957	3.790	4.567
<i>F</i> (000)	1176	1488	864
Theta range for data collection	3.89 to 70.74 deg.	4.82 to 70.73 deg.	2.87 to 65.00 deg.
Limiting indices	-28<= <i>h</i> <=27, -14<= <i>k</i> <=14, -8<= <i>l</i> <=11	-15<= <i>h</i> <=20, -13<= <i>k</i> <=13, -17<= <i>l</i> <=22	-11<= <i>h</i> <=11, -14<= <i>k</i> <=15, -19<= <i>l</i> <=14
Reflections collected / unique	4948 / 2396 [<i>R</i> (int) = 0.0296]	8871 / 3273 [<i>R</i> (int) = 0.0251]	12666 / 6651 [<i>R</i> (int) = 0.0738]
Completeness to theta = 71.25	98.2 %	98.3 %	99.6 %
Absorption correction	Multi-scan	Multi-scan	Multi-scan
Max. and min. transmission	1.000 and 0.634	1.000 and 0.659	1.000 and 0.179
Refinement method	Full-matrix least-squares on <i>F</i> ²	Full-matrix least-squares on <i>F</i> ²	Full-matrix least-squares on <i>F</i> ²
Data / restraints / parameters	2396 / 0 / 145	3273 / 0 / 193	6651 / 0 / 433
Goodness-of-fit on <i>F</i> ²	1.041	1.080	1.104
Final <i>R</i> indices [<i>I</i> >2σ(<i>I</i>)]	<i>R</i> 1 = 0.0340, <i>wR</i> 2 = 0.0859	<i>R</i> 1 = 0.0329, <i>wR</i> 2 = 0.0888	<i>R</i> 1 = 0.0674, <i>wR</i> 2 = 0.2624
<i>R</i> indices (all data)	<i>R</i> 1 = 0.0426, <i>wR</i> 2 = 0.0938	<i>R</i> 1 = 0.0346, <i>wR</i> 2 = 0.0903	<i>R</i> 1 = 0.0974, <i>wR</i> 2 = 0.2936
Largest diff. peak and hole	0.417 and -0.48 e.Å ⁻³	0.475 and -0.458 e.Å ⁻³	0.164 and -1.222 e.Å ⁻³

Table 4.3. Crystallographic data of compounds **27**, **28** and **29**

Crystal	27	28	29
CCDC No.	987287	987284	987289
Empirical formula	C ₃₈ H ₄₈ N ₂ O ₃ P ₂ Se ₂ Sr	C ₃₈ H ₄₈ BaN ₂ O ₃ P ₂ Se ₂	C ₃₈ H ₄₈ MgN ₂ O ₃ P ₂ Se ₂
Formula weight	888.26	937.97	824.95
<i>T</i> (K)	150(2)	150(2)	150(2)
λ (Å)	1.54184	1.54184	1.54184
Crystal system	Triclinic	Triclinic,	Triclinic
Space group	<i>P</i> -1	<i>P</i> -1	<i>P</i> -1
<i>a</i> (Å)	9.8678(11)	9.6600(5)	9.6053(11)
<i>b</i> (Å)	13.4550(14)	17.2064(10)	13.3939(14)
<i>c</i> (Å)	17.0933(17)	25.4384(14)	16.644(3)
α (°)	106.687(9)	105.952(5)	107.905(13)
β (°)	101.184(9)	90.358(4)	99.522(12)
γ (°)	106.567(10)	102.056(5)	105.115(10)
<i>V</i> (Å ³)	1987.4(4)	3966.6(4)	1895.5(5)
<i>Z</i>	2	4	2
<i>D</i> _{calc} g cm ⁻³	1.484	1.571	1.445
μ (mm ⁻¹)	5.028	10.938	3.701
<i>F</i> (000)	900	1872	848
Theta range for data collection	3.68 to 70.77 deg.	3.62 to 71.13 deg.	2.90 to 70.69 deg.
Limiting indices	-10<= <i>h</i> <=12, -16<= <i>k</i> <=16, -20<= <i>l</i> <=15	-11<= <i>h</i> <=11, -21<= <i>k</i> <=18, -21<= <i>l</i> <=31	-10<= <i>h</i> <=11 -16<= <i>k</i> <=11 -20<= <i>l</i> <=20
Reflections collected / unique	14710 / 7443 [<i>R</i> (int) = 0.0610]	31367 / 14953 [<i>R</i> (int) = 0.0555]	13867 / 7151 [<i>R</i> (int) = 0.0400]
Completeness to theta = 71.25	97.5 %	97.4 %	98.0 %
Absorption correction	Multi-scan	Multi-scan	Multi-scan
Max. and min. transmission	1.000 and 0.586	1.000 and 0.564	1.000 and 0.849
Refinement method	Full-matrix least-squares on <i>F</i> ²	Full-matrix least-squares on <i>F</i> ²	Full-matrix least-squares on <i>F</i> ²
Data / restraints / parameters	7443 / 0 / 433	14953 / 0 / 865	7151 / 0 / 433
Goodness-of-fit on <i>F</i> ²	1.277	1.088	1.045
Final <i>R</i> indices [<i>I</i> >2σ(<i>I</i>)]	<i>R</i> 1 = 0.0497, w <i>R</i> 2 = 0.1484	<i>R</i> 1 = 0.0572, w <i>R</i> 2 = 0.1524	<i>R</i> 1 = 0.0415, w <i>R</i> 2 = 0.0979
<i>R</i> indices (all data)	<i>R</i> 1 = 0.0773, w <i>R</i> 2 = 0.1581	<i>R</i> 1 = 0.0799, w <i>R</i> 2 = 0.1694	<i>R</i> 1 = 0.0555, w <i>R</i> 2 = 0.1080
Largest diff. peak and hole	0.553 and -0.617 e.Å ⁻³	1.769 and -1.288 e.Å ⁻³	0.872 and -0.605 e.Å ⁻³

Table 4.4. Crystallographic data of compounds **30** and **31**

Crystal	30	31
CCDC No.	987288	987286
Empirical formula	C ₂₆ H ₃₂ B ₂ N ₂ P ₂	C ₃₄ H ₄₆ B ₂ BaN ₂ O ₂ P ₂
Formula weight	456.10	735.62
<i>T</i> (K)	293(2)	150(2)
λ (Å)	1.54184	1.54184
Crystal system	Monoclinic	Triclinic
Space group	<i>C</i> <i>c</i>	<i>P</i> -1
<i>a</i> (Å)	12.7050(6)	9.2659(9)
<i>b</i> (Å)	13.7069(7)	14.0750(13)
<i>c</i> (Å)	14.7809(7)	14.9320(15)
α (°)	90	111.894(9)
β (°)	91.387(4)	91.583(8)
γ (°)	90	101.013(8)
<i>V</i> (Å ³)	2573.3(2)	1763.2(3)
<i>Z</i>	4	2
<i>D</i> _{calc} g cm ⁻³	1.177	1.386
μ (mm ⁻¹)	1.640	9.855
<i>F</i> (000)	968	752
Theta range for data collection	4.75 to 70.77 deg.	3.71 to 70.77deg.
Limiting indices	-15<= <i>h</i> <=15, -10<= <i>k</i> <=16, -15<= <i>l</i> <=18	-8<= <i>h</i> <=11, -17<= <i>k</i> <=15, -18<= <i>l</i> <=15
Reflections collected / unique	4908 / 3221 [<i>R</i> (int) = 0.0330]	13627 / 6641 [<i>R</i> (int) = 0.0755]
Completeness to theta = 71.25	97.9 %	97.7 %
Absorption correction	Multi-scan	Multi-scan
Max. and min. transmission	1.000 and 0.790	1.000 and 0.527
Refinement method	Full-matrix least-squares on <i>F</i> ²	Full-matrix least-squares on <i>F</i> ²
Data / restraints / parameters	3221 / 2 / 292	6641 / 0 / 412
Goodness-of-fit on <i>F</i> ²	1.073	1.010
Final <i>R</i> indices [<i>I</i> >2sigma(<i>I</i>)]	<i>R</i> 1 = 0.0456, <i>wR</i> 2 = 0.1263	<i>R</i> 1 = 0.0527, <i>wR</i> 2 = 0.1148
<i>R</i> indices (all data)	<i>R</i> 1 = 0.0491, <i>wR</i> 2 = 0.1312	<i>R</i> 1 = 0.0768, <i>wR</i> 2 = 0.1350
Largest diff. peak and hole	0.195 and -0.235 e.Å ⁻³	1.068 and -1.276 e.Å ⁻³

References:

- (1) (a) Vert, M. *Biomacromolecules* **2005**, *6*, 538–546. (b) Nair, L. S.; Laurencin, C. T. *Prog. Polym. Sci.* **2007**, *32*, 762–798. (c) Sudehsh, K.; Abe H.; Doi, Y. *Prog. Polym. Sci.* **2000**, *25*, 1503–1555. (d) Ikada, Y.; Tsuji, H. *Macromol. Rapid Commun.* **2000**, *21*, 117–132. (e) Albertsson, A.-C.; Varma, I. K. *Biomacromolecules* **2003**, *4*, 1466–1486.
- (2) (a) Stridsberg, K. M.; Ryner, M.; Albertsson, A.-C. *Adv. Polym. Sci.* **2002**, *157*, 42–65. (b) Albertsson, A. -C.; Varma, I. K. *Biomacromolecules* **2002**, *3*, 1–41. (c) Rokicki, G. *Prog. Polym. Sci.* **2000**, *25*, 259–342. (d) Dove, A. P. *Chem. Commun.* **2008**, 6446–6470.
- (3) Meimaroglou, D.; Kiparissides, C. *Macromolecules* **2010**, *43*, 5820–5832.
- (4) Nunes, R. W.; Martin, J. R.; Johnson, J. F. *Polym. Eng. Sci.* **1982**, *2*, 205–228.
- (5) (a) Yasuda, H. *J. Organomet. Chem.* **2002**, *647*, 128–138. (b) Hou, Z.; Wakatsuki, Y. *Coord. Chem. Rev.* **2002**, *231*, 1–22. (c) Yasuda, H. *Prog. Polym. Sci.* **2000**, *25*, 573–626. (d) Agarwal, S.; Mast, C.; Denicke, K.; Greiner, A. *Macromol. Rapid Commun.* **2000**, *21*, 195–212. (e) Wu, J.; Yu, T. L.; Chen, C. T.; Lin, C. C. *Coord. Chem. Rev.* **2006**, *250*, 602–626. (f) O’Keefe, B. J.; Hillmyer, M. A.; Tolman, W. B. *J. Chem. Soc. Dalton Trans.* **2001**, 2215–2224.
- (6) (a) Dechy-Cabaret, O.; Martin-Vaca, B.; Bourissou, D. *Chem. Rev.* **2004**, *104*, 6147–6176. (b) O’Keefe, B. J.; Hillmyer, M. A.; Tolman, W. B. *J. Chem. Soc. Dalton Trans.* **2001**, 2215–2224. (c) Wheaton, C. A.; Hayes, P. G.; Ireland, B. *Dalton Trans.* **2009**, 4832–4846. (d) Thomas, C. M. *Chem. Soc. Rev.* **2010**, *39*, 165–173.
- (7) (a) Li, S. M.; Rashkov, I.; Espartero, J. L.; Manolova, N.; Vert, M. *Macromolecules* **1996**, *29*, 57–62. (b) Dobrzyński, P.; Kasperczyk, J.; Bero, M. *Macromolecules* **1999**, *32*, 4735–4737. (c) Zhong, Z.; Dijkstra, P. J.; Birg, C.; Westerhausen, M.; Feijen, J. *Macromolecules* **2001**, *34*, 3863–3868. (d) Westerhausen, M.; Schneiderbauer, S.; Kneifel, A. N.; Sörtl, Y.; Mayer, P.; Nöth, H.; Zhong, Z.; Dijkstra, P. J.; Feijen, J. *Eur. J. Inorg. Chem.* **2003**, 3432–3439. (e) Chisholm, M. H.; Gallucci, J.; Phomphrai, K. *Chem. Commun.* **2003**, 48–49. (f) Hill, M. S.; Hitchcock, P. B. *Chem. Commun.* **2003**, 1758–1759. (g) Chisholm, M. H.; Gallucci, J. C.; Phomphrai, K. *Inorg. Chem.* **2004**, *43*, 6717–6725. (h) Sarazin, Y.; Howard, R. H.; Hughes, D. L.; Humphrey, S. M.; Bochmann, M. *Dalton Trans.* **2006**, 340–350.
- (8) Kuzdrowska, M.; Annunziata, L.; Marks, S.; Schmid, M.; Jaffredo, C. G.; Roesky, P. W.; Guillaume, S. M.; Maron, L. *Dalton Trans.* **2013**, *42*, 9352–9360.

- (9) Panda, T. K.; Yamamoto, K.; Yamamoto, K.; Kaneko, H.; Yang, Y.; Tsurugi, H.; Mashima, K. *Organometallics* **2012**, *31*, 2268–2274.
- (10) Ahmed, R.; Altieri, A.; D'Souza, D. M.; Leigh, D. A.; Mullen, K. M.; Papmeyer, M. A.; Slawin, M. Z.; Wong, J. K. Y.; Woollins, J. D. *J. Am. Chem. Soc.* **2011**, *133*, 12304–12310.
- (11) Naktode, K.; Kottalanka, R. K.; Panda, T. K. *New J. Chem.* **2012**, *36*, 2280–2285.
- (12) Boncella, J. M.; Coston, C. J.; Cammack, J. K. *Polyhedron* **1991**, *10*, 769–770.
- (13) Tanner, P. S.; Burkey, D. J.; Hanusa, T. P. *Polyhedron* **1995**, *14*, 331–333.
- (14) The bonding situation in the drawing of the ligand system is simplified for clarity.
- (15) Hanusa, T. P. *In Comprehensive Organometallic Chemistry III*, ed. Crabtree, R. H.; Mingos, M. P. Elsevier, Oxford. **2007**, vol. 2, p. 67.
- (16) (a) Hanusa, T. P. *Organometallics* **2002**, *21*, 2559–2571. (b) Hanusa, T. P. *Chem. Rev.* **2000**, *100*, 1023–1036. (c) Hanusa, T. P. *Coord. Chem. Rev.* **2000**, *210*, 329–367.
- (17) N. N. Greenwood and A. Earnshaw, *Chemistry of the Elements*, Pergamon Press, *Oxford, U.K.*, **1984**.
- (18) (a) Panda, T. K.; Kaneko, H.; Michael, O.; Tsurugi, H.; Pal, K.; Tömroos, W.; Anwander, R.; Mashima, K. *Organometallics* **2012**, *31*, 3178–3184. (b) Barrett, A. G. M.; Crimmin, M. R.; Hill, M. S.; Hitchcock, P. B.; Kociok-Köhn, G.; Procopiou, P. A. *Inorg. Chem.* **2008**, *47*, 7366–7376.
- (19) (a) Grignard, V. C. R. *Acad. Sci.* **1900**, *130*, 1322–1324. (b) Grignard, V. *Ann. Chim.* **1901**, *24*, 433–490. (c) Seyferth, D. *Organometallics* **2009**, *28*, 1598–1605. (d) Bickelhaupt, F. *J. Organomet. Chem.* **1994**, *475*, 1–14.
- (20) (a) Bradley, D. C.; Frigo, D. M.; Harding, I. S.; Motevalli, M. *Eur. J. Solid State Inorg. Chem.* **1993**, *30*, 241–258. (b) Xia, A.; Heeg, M. J.; Winter, C. H. *Organometallics* **2002**, *21*, 4718–4725. (c) Michel, O.; Yamamoto, K.; Tsurugi, H.; Maichle-Mössmer, C.; Tömroos, K. W.; Mashima, K.; Anwander, R. *Organometallics* **2011**, *30*, 3818–3825.
- (21) Dolinskya, M. C. B.; Lina, W. O.; Dias, M. L. *J. Mol. Catal. A: Chem.* **2006**, *258*, 267–274.
- (22) Odom, J. D.; Hudgens, B. A.; Durig, J. R. *J. Phys. Chem.* **1973**, *77*, 1972–1977.

- (23) (a) Anderson, B. J.; Glueck, D. S.; DiPasquale, A. G.; Rheingold, A. L. *Organometallics* **2008**, *27*, 4992–5001. (b) Hubert, S.; Stützer, A.; Bissinger, P.; Schier, A. Z. *Anorg. Allg. Chem.* **1993**, *619*, 1519–1525.
- (24) Liu, B.; Roisnel, T.; Guegan, J.-P.; Carpentier, J.-F.; Sarazin, Y. *Chem. Eur. J.* **2012**, *18*, 6289–6301.
- (25) Sarazin, Y.; Liu, B.; Maron, L.; Carpentier, J.-F. *J. Am. Chem. Soc.* **2011**, *133*, 9069–9087.
- (26) Davidson, M. G.; O'Hara, C. T.; Jones, M. D.; Keir, C. G.; Mahon, M. F.; Kociok-Köhn, G. *Inorg. Chem.* **2007**, *46*, 7686–7688.
- (27) (a) Palard, I.; Soum, A.; Guillaume, S. M. *Chem. Eur. J.* **2004**, *10*, 4054–4062. (b) Jenter, J.; Roesky, P. W.; Ajellal, N.; Guillaume, S. M.; Susperregui, N.; Maron, L. *Chem. Eur. J.* **2010**, *16*, 4629–4638.
- [28]. M. Sheldrick, SHELXS-97. *Program of Crystal Structure Solution, University of Göttingen, Germany, 1997.*
- [29]. G. M. Sheldrick, SHELXL-97. *Program of Crystal Structure Refinement, University of Göttingen, Germany, 1997.*

Chapter 5

Novel alkaline-earth metal complexes having chiral phosphinoselenoic amides and boranes in the coordination sphere: chiral alkaline earth metal complexes having M-Se direct bond (M = Mg, Ca, Sr, Ba)

5.1 Introduction

Efficient synthesis of optically active compounds is one of the most important tasks in synthetic organic chemistry. The most promising methodology is catalytic asymmetric synthesis using chiral metal center. Among many useful metal species, alkaline-earth metals have long been recognized as belonging to less toxic and less harmful metals.¹⁻⁵ However, besides the potential high utility of alkaline-earth species as homogeneous catalyst for ring-opening polymerization of various cyclic esters,^{6,7} polymerization of styrene and dienes,⁸ and hydroamination and hydrophosphination reactions of alkenes and alkynes,⁹ their use in synthetic organic chemistry, especially in asymmetric synthesis as chiral catalyst, has been quite limited compared with that of transition metal catalysts.¹⁻⁵ Recently it was revealed that several catalytic asymmetric carbon-carbon bond-forming and related reactions proceeded smoothly in high enantioselectivities using the chiral Ca, Sr, and Ba catalysts.¹⁰⁻²⁰ Their strong Brønsted basicity and mild Lewis acidity are promising and attractive characteristics and can influence their catalytic activity as well as their chiral modification capability in a positive manner. Bearing these characteristic features in mind and our on-going interest on highly electropositive alkaline-earth metals, catalytic activity and vast potentiality of the field in asymmetric synthesis, we have planned to synthesize various novel chiral alkaline-earth metal complexes stabilized by chiral amidophosphine selenoids and boranes to explore the chemistry of alkaline-earth metals in asymmetric synthesis. To achieve our target compounds with high-purity and good yield, we have chosen chiral phosphineamines $\text{HN}(R\text{-*CHMePh})(\text{PPh}_2)$ and $\text{HN}(S\text{-*CHMePh})(\text{PPh}_2)$ were originally introduced by Brunner into coordination chemistry of

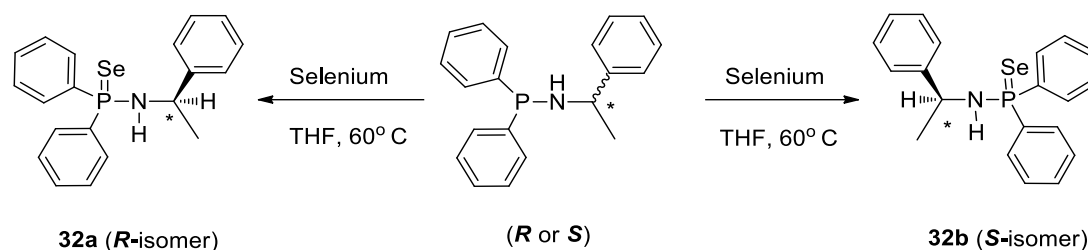
the late transition metals.²¹ Peter W. Roesky *et al.* introduced the same ligands into the zirconium chemistry,²² Group 3 and lanthanide chemistry.²³ We have synthesized the corresponding enantiomeric pure amidophosphine-selenoids [HN(*R*-*CHMePh)P(Se)Ph₂] (**32a**) and [HN(*S*-*CHMe Ph)P(Se)Ph₂] (**32b**) in a similar fashion as we described in the Chapter 1 and we have successfully introduced into the alkaline-earth metal chemistry. These ligands typically coordinate through the amido nitrogen atom, and selenium atom and hence forming four membered mettallacycle with centre metal atom.

In this chapter, detailed synthetic and structural features of the chiral phosphinoselenoic amide ligands {HN(*R*-*CHMePh)P(Se)Ph₂} (**32a**) and {HN(*S*-*CHMePh)P(Se)Ph₂} (**32b**) and the corresponding homoleptic complexes of alkaline-earth metals of molecular composition [M{N(*R*-*CHMePh)P(Se)Ph₂}₂(THF)₂] [M = Mg(**34a**), Ca(**35a**), Sr(**36a**) and Ba (**37a**)] and [M{N(*S*-*CHMePh)P(Se)Ph₂}₂(THF)₂] [M = Mg (**34b**), Ca (**35b**), Sr (**36b**) and Ba (**37b**)] were described. In addition, we described the synthesis and structures of the chiral amidophosphine-borane ligands {HN(*R*-*CHMePh)P(BH₃)Ph₂} (**38a**) and {HN(*S*-*CHMePh)P(BH₃)Ph₂} (**38b**) and the corresponding homoleptic barium complexes of composition [Ba{N(*R*-*CHMePh)P(BH₃)Ph₂}₂(THF)₂] (**39a**) and [Ba{N(*R*-*CHMePh)P(BH₃)Ph₂}₂(THF)₂] (**39b**) are described.

5.2 Results and Discussion

5.2.1 Synthesis of chiral phosphinoselenoicamides

The chiral phosphinoselenoicamides {HN(*R*-*CHMePh)(Ph₂P(Se))} (**32a**) and {HN(*S*-*CHMePh)(Ph₂P(Se))} (**32b**) were prepared in enantiomeric pure forms in a similar fashion as [Ph₂P(Se)NHCHPh₂] (**1c**) and [Ph₂P(Se)NHCPh₃] (**2c**) were synthesised in quantitative yield by the treatment of the respective 1,1-diphenyl-*N*-(1-phenylethyl)phosphinamines {HN(*R*-*CHMePh)(Ph₂P)} and {HN(*S*-*CHMePh)(Ph₂P)} with excess elemental selenium in 1:1.2 molar ratio at ambient temperature in THF solvent (Scheme 5.1).^{24,25} Both enantiomeric pure compounds **32a** and **32b** have been characterized by using standard analytical/spectroscopic techniques and the solid-state structures were established by single crystal X-ray diffraction analysis.



Scheme 5.1. Synthesis of chiral-phosphinoselenoicamide ligands.

The enantiomeric pure compounds **32a** and **32b** shows strong absorption at 559 cm^{-1} in their FT-IR spectrum can be assigned as characteristic P=Se bond stretching frequency and it is comparable with the previously observed values 568 cm^{-1} for $[\text{Ph}_2\text{P}(\text{Se})\text{NHCHPh}_2]$ (**1c**), 599 cm^{-1} for $[\text{Ph}_2\text{P}(\text{Se})\text{NHCPh}_3]$ (**2c**) (See Chapter 2) and 535 cm^{-1} for $[\text{Ph}_2\text{P}(\text{Se})\text{NHC}(\text{CH}_3)_3]$ reported by our group.²⁶ ^1H NMR spectrum of both the enantiomers (**32a** and **32b**) shows doublet resonance signals at δ 1.42 ppm ($J_{\text{H-H}} = 6.76\text{ Hz}$) and multiplates at 4.52 ppm corresponds to the methyl protons and CH proton attached to the α position of amine nitrogen atom respectively. A broad resonance signal at δ 2.57 ppm represents the amine N-H proton of the ligand moiety. These values are observed as slightly downfield shifted when compared to free chiral phosphineamine $[\text{Ph}_2\text{PNH}\{R\text{-*CHMePh}\}]$ or $[\text{Ph}_2\text{PNH}\{S\text{-*CHMePh}\}]$ due to addition of the selenium atom on to the phosphorous atom.^{21a} The solid state structures of **32a** and **32b** were confirmed by single crystal X-ray diffraction analysis. The details of the structural parameters are given in Table 5.1. The solid-state structures of both enantiomers and selected bond lengths and bond angles were shown in Figure 5.1. From the molecular structure of two compounds, it is clear that both enantiomers are non-superimposable mirror images and crystalizes in the triclinic space group *P1* having one molecule in the unit cell. The P=Se bond distance is found to be $2.1219(15)\text{ \AA}$ (for **32a**) and $2.126(2)\text{ \AA}$ (for **32b**) are in good agreement with values reported by us previously: $2.1019(8)\text{ \AA}$ for $[\text{Ph}_2\text{P}(\text{Se})\text{NH}(2,6\text{-Me}_2\text{C}_6\text{H}_4)]$,²⁵ $2.1086(12)\text{ \AA}$ for $[\text{Ph}_2\text{P}(\text{Se})\text{NHCHPh}_2]$ (**1c**), $2.1166(8)\text{ \AA}$ for $[\text{Ph}_2\text{P}(\text{Se})\text{NHCPh}_3]$ (**2c**) and $2.1187(8)\text{ \AA}$ for $[\text{Ph}_2\text{P}(\text{Se})\text{NHC}(\text{CH}_3)_3]$. P1-N1 distance ($1.671(5)$ for **32a** and $1.645(5)\text{ \AA}$ for **32b**) and C1-N1 distance ($1.454(7)$ for **32a** and $1.470(9)\text{ \AA}$ for **32b**) are also similar to those of phosphinoselenoicamides $[\text{Ph}_2\text{P}(\text{Se})\text{NHR}]$, which we previously reported: P1-N1 $1.656(3)\text{ \AA}$, C1-N1 $1.441(4)\text{ \AA}$ for $R = 2,6\text{-Me}_2\text{C}_6\text{H}_4$, P1-N1 $1.642(4)\text{ \AA}$, C1-N1 $1.459(6)\text{ \AA}$ for R

= CHPh₂, P1–N1 1.664(2) Å, C1–N1 1.496(4) Å for R = CPh₃ and P1–N1 1.655(3) Å, C1–N1 1.494(4) Å).(See Chapter 1)

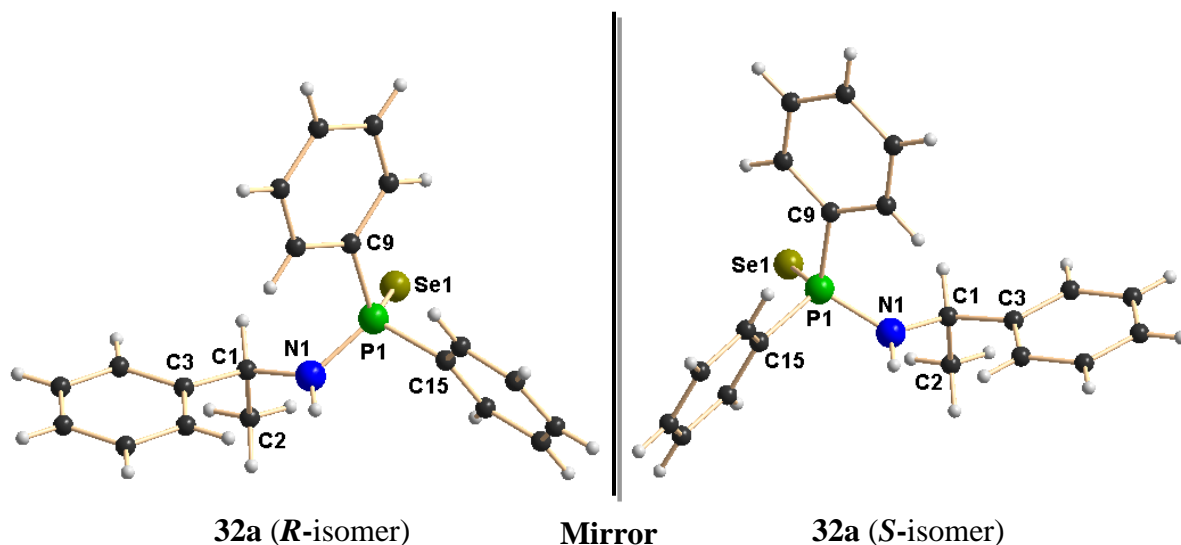


Figure 5.1. Solid state structures of ligands **32a** and **32b**. Selected bond lengths (Å) and bond angles (°):

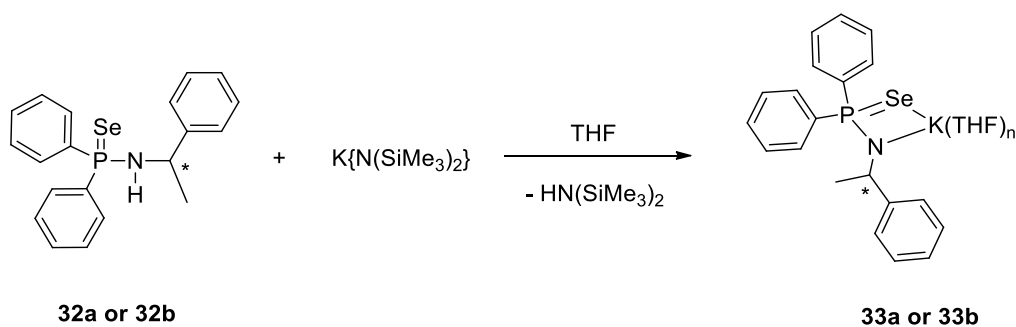
32a: P1–Se1 2.1219(15), P1–N1 1.671(5), P1–C9 1.818(6), P1–C15 1.815(6), C1–N1 1.454(7), C1–C2 1.551(10), C1–C3 1.517(9), N1–P1–Se1 116.4(2), C9–P1–C15 106.5(3), C9–P1–Se1 111.0(2), C15–P1–Se1 112.8(2), C9–P1–N1 105.7(3), C15–P1–N1 103.6(3), P1–N1–C1 120.8(4), N1–C1–C2 110.7(6), N1–C1–C3 112.4(5), C2–C1–C3 109.7(5).

32b: P1–Se1 2.126(2), P1–N1 1.645(5), P1–C9 1.808(7), P1–C15 1.802(7), C1–N1 1.470(9), C1–C2 1.532(11), C1–C3 1.521(10), N1–P1–Se1 116.0(2), C9–P1–C15 106.5(3), C9–P1–Se1 110.5(3), C15–P1–Se1 112.9(3), C9–P1–N1 106.2(3), C15–P1–N1 104.1(3), P1–N1–C1 121.5(5), N1–C1–C2 110.4(7), N1–C1–C3 111.9(6), C2–C1–C3 110.2(6)

5.2.2. Chiral phosphineamidoseleuoicamide potassium complexes

The potassium salt of molecular composition [K{N(*R*-*CHMePh)(Ph₂P(Se))}{THF}_n] (**33a**) or [K{N(*S*-*CHMePh)(Ph₂P(Se))}{THF}_n] (**33b**) were readily prepared by the reaction of compound **32a** or **32b** and potassium bis(trimethylsilyl)amide in THF solvent through the elimination of volatile bis(trimethylsilyl)amine (see Scheme 5.2).²⁴ The complexes **33a-b** were characterized by spectroscopic and analytical techniques. However

crystals suitable for X-ray diffraction analysis were not obtained due to high solubility of the compound (**33a,b**) in THF solvent. In FT-IR spectra, compound (**33a,b**) showed a strong absorption band at 570 cm^{-1} which can be best assigned to characteristic P=Se bond stretching and it is in good agreement with our previously described potassium salts of phosphinoselenoicamides: 569 cm^{-1} for $[\{(\text{THF})_2\text{KPh}_2\text{P}(\text{Se})\text{N}(\text{CHPh}_2)\}_2]$ (See Chapter 2) and 570 cm^{-1} for $[\text{K}(\text{THF})_2\{\text{Ph}_2\text{P}(\text{Se})\text{N}(\text{CMe}_3)\}]_n$.^[26] $^{31}\text{P}\{^1\text{H}\}$ NMR spectra of compounds (**33a,b**) show a sharp singlet resonance signal at δ 48.6 ppm, which is upfield shifted to that of ligand moiety (56.1 ppm), is a clear evidence for the formation of potassium salt. The multiplet signals in the region of 3.50-3.53 ppm and 1.37-1.40 ppm in ^1H spectra also confirm the coordinated THF molecules present in the complex **33a,b**. One set of signals were observed for compound (**33a,b**) in the ^1H and $^{13}\text{C}\{^1\text{H}\}$ NMR spectra similar to free ligand moiety due to the dynamic behaviour of the complexes in the solution state.

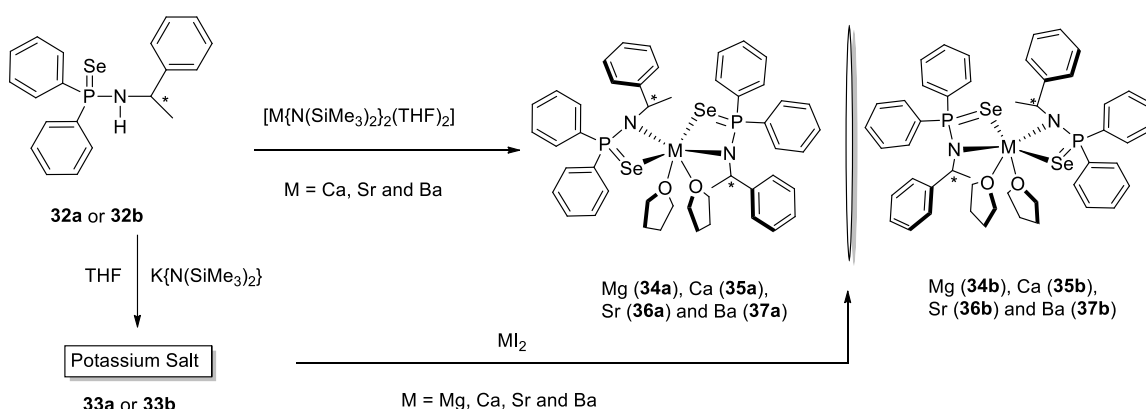


Scheme 5.2. Synthesis of potassium salts of chiral phosphinoselenoicamides.

5.2.3. Synthesis of alkaline-earth metal complexes

The enantiomeric pure chiral alkaline-earth metal complexes of composition $[(\text{THF})_2\text{M}\{\text{Ph}_2\text{P}(\text{Se})\text{N}(\text{R}-^*\text{CHMePh})_2\}]$ (M = Mg (**34a**), Ca (**35a**), Sr (**36a**) and Ba (**37a**)) and $[(\text{THF})_2\text{M}\{\text{Ph}_2\text{P}(\text{Se})\text{N}(\text{S}-^*\text{CHMePh})_2\}]$ (M = Mg (**34b**), Ca (**35b**), Sr (**36b**) and Ba (**37b**)) were prepared by two synthetic methods. In the first method, the ligands **32a** or **32b** were treated with alkaline-earth metal bis(trimethylsilyl)amides $[\text{M}\{\text{N}(\text{SiMe}_3)_2\}_2(\text{THF})_n]$ (M = Ca, Sr and Ba) in 2:1 molar ratio at ambient temperature in THF solvent through the elimination of volatile trimethylsilylamine (see Scheme 5.3).²⁴ The second method involves a salt metathesis reaction in which alkaline-earth metal diiodides MI_2 (M = Mg,

Ca, Sr and Ba) are treated with potassium salt $[K\{N(R\text{-*CHMePh})(Ph_2P(Se))\}\{THF\}_n]$ (**33a**) or $[K\{N(S\text{-*CHMePh})(Ph_2P(Se))\}\{THF\}_n]$ (**33b**) in 1:2 molar ratio (which can be obtained *in situ* by reaction involving potassium bis(trimethylsilyl)amide and chiral phosphinoselenoic amides **32a** or **32b**) at ambient temperature in THF solvent (see Scheme 5.3).²⁴ The compounds **35a,b-37a,b** were recrystallized from THF/*n*-pentane mixture solvents in 1:2 ratio at -40°C . The solid-state structures of all the compounds **35a,b-37a,b** were established by single crystal X-ray diffraction analysis and fully characterized by standard analytical/spectroscopic techniques.



Scheme 5.3.

Synthesis of alkaline-earth metal complexes of chiral phosphinoselenoic amides.

A strong absorption at 562 cm^{-1} for **34a,b**, 559 cm^{-1} for **35a,b**, 552 cm^{-1} for **36a,b** and 553 cm^{-1} for **37a,b** in FT-IR spectra indicates the evidence of P=Se bond into the each metal complex. The resonance of the methine proton (CH) α to amido nitrogen were observed as multiplets (δ 4.58-4.62 ppm for **34a,b**, 4.26-4.34 ppm for **35a,b**, 4.47-4.55 ppm for **36a,b** and 4.21-4.29 ppm for **37a,b**) in the ^1H NMR spectra of the diamagnetic complexes **34-37** and are unaffected due to complex formation. Doublet signals at δ 1.86 for **34a,b**, 1.68 for **35a,b**, 1.20 for **36a,b** and 1.48 ppm for **37a,b** were observed with coupling constants of range $J_{\text{H-H}} = 6.20\text{-}6.85\text{ Hz}$ in the ^1H NMR spectra can be assigned to methyl protons ($-\text{CH}_3$) group attached to the chiral carbon atom in each complex. In $^{31}\text{P}\{^1\text{H}\}$ NMR spectra, complexes **34a,b** showed sharp resonance signal at 45.1 ppm which is upfield shifted compared to free ligands **32a** or **32b**, whereas the complexes **35a,b-37a,b** showed one resonance signal at δ 68.9 ppm which is significantly downfield shifted compared to that

of free ligands **32a** or **32b** (δ 56.1 ppm) upon coordination of calcium, strontium or barium atom onto the selenium atom of the chiral phosphinoselenoicamido ligand. This can be endorsed because of high electropositive character of heavier alkaline-earth metals compared to magnesium.²⁷ Both the phosphorus atoms present in the two $\{\text{Ph}_2\text{P}(\text{Se})\text{N}(\text{*CHMePh})\}^-$ moieties are chemically equivalent. The structures of all the complexes **35a,b-37a,b** were confirmed by the single crystal X-ray diffraction analysis in the solid-state. The details of the structural parameters are given in the Table 5.1-5.3. As a result of the similar ionic radii of the alkaline-earth metals, the solid state structures of compounds **35a-37a** are isostructural, whereas **35b-37b** forms the corresponding enantiomers (Figures 5.2-5.4). All the compounds crystallize in the monoclinic space group $P2_1$ having two molecules in the unit cell. The coordination polyhedron is formed by the two $\{\text{N}(\text{*CHMePh})(\text{P}(\text{Se})\text{Ph}_2)\}^-$ ligands and two THF molecules. The $\{\text{N}(\text{*CHMePh})(\text{P}(\text{Se})\text{Ph}_2)\}^-$ ligand is coordinated to the metal atom in a similar fashion to $\{\text{Ph}_2\text{P}(\text{Se})\text{N}(\text{CHPh}_2)\}^-$ ligand as we described in chapter 2. Thus, the $\{\text{N}(\text{*CHMePh})(\text{P}(\text{Se})\text{Ph}_2)\}^-$ ligand coordinates to the center metal atom through amido nitrogen atom (N) and the selenium atom (Se) forming a four membered metallacycle M-Se-P-N. In contrast to our previous results described in chapter 2 such as $[\text{M}\{\text{Ph}_2\text{P}(\text{Se})\text{NCHPh}_2\}_2(\text{THF})_2]$ (M = Ca, Sr and Ba) and $[\text{M}\{\text{Ph}_2\text{P}(\text{Se})\text{NC}(\text{CH}_3)_3\}(\text{THF})_2]$ (M = Mg and Ca) reported by our group,²⁶ the compounds **35a,b-37a,b** are non-centrosymmetric in the solid-state and the orientation of two ligand moieties are almost perpendicular to each other.

In the calcium complexes **35a** and **35b**, the central calcium atom in each case adopts a distorted octahedral geometry due to coordination from two $\{\text{N}(\text{*CHMePh})\text{P}(\text{Se})\text{Ph}_2\}^-$ moieties and two THF molecules. Each ligand $\{\text{N}(\text{R-}*CHMePh)\text{P}(\text{Se})\text{Ph}_2\}^-$ (for **35a**) and $\{\text{N}(\text{S-}*CHMePh)\text{P}(\text{Se})\text{Ph}_2\}^-$ (for **35b**) coordinates through the amido nitrogen atom and one selenium atom. Thus the $\{\text{N}(\text{*CHMePh})\text{P}(\text{Se})\text{Ph}_2\}^-$ ligand group can be considered as pseudo-bidentate ligand. The Ca–N distances (2.441(3) and 2.426(3) Å) for **35a** and (2.444(5) and 2.430(5) Å) for **35b** are in good agreement with our structurally characterized calcium complexes: 2.479(5) Å for $[\text{Ca}\{\text{Ph}_2\text{P}(\text{Se})\text{NCHPh}_2\}_2(\text{THF})_2]$ (**9**) (Chapter 2), 2.4534(14) Å for $[\text{Ca}\{\text{Ph}_2\text{P}(\text{BH}_3)\text{NCHPh}_2\}_2(\text{THF})_2]$ (**22**) (Chapter 3), 2.451(3) Å for $[\text{Ca}\{\text{Ph}_2\text{P}(\text{Se})\text{NC}(\text{CH}_3)_3\}_2(\text{THF})_2]$ ²⁶ and 2.386(8) Å for $[\text{Ca}\{\text{C}_2\text{H}_4(\text{N}-\text{Ph}_2\text{P}=\text{Se})_2\}(\text{THF})_3]$

(**26**) (Chapter 4). The observed calcium-nitrogen bond distances are slightly elongated compare to the calcium–nitrogen covalent bond (2.361 (2) and 2.335(2) Å) reported for [Ca(Dipp₂DAD)(THF)₄] (Dipp₂DAD = *N,N'*-bis(2,6-diisopropylphenyl)-1,4-diaza-1,3-butadiene in the literature.²⁸ The observed Ca–Se bond distances of 3.0303(9) and 3.0794(9) Å for **35a** and 3.0327(15) and 3.0817(14) Å for **35b** were slightly elongated but within the range of the reported Ca–Se distance of 2.9889(8) Å for structurally characterized complex [Ca{Ph₂P(Se)NCHPh₂}₂(THF)₂] (**9**) and 2.9619(3) Å for the complex [Ca{Ph₂P(Se)NC(CH₃)₃}₂(THF)₂]²⁶ and 3.252(2) Å for the complex [Ca{C₂H₄(N-Ph₂P=Se)₂}₂(THF)₃] (**26**) we have described in the Chapters 2 and 4 respectively. In the literature, we have found 2.945(1) Å reported for [(THF)₂Ca{(PyCH)(Se)PPh₂}₂],²⁹ 2.93 Å to 3.00 Å reported for [(THF)₄Ca(SeMes')₂] and 2.958(2) Å to 3.001(2) Å reported for [(THF)₂Ca(Se₂PPh₂)₂].^{30,31} The considerably elongated Ca-P distance of [3.2960(13), 3.3013(11) Å in **35a** and 3.295(2), 3.3069(19) Å in **35b**], were greater than the sum of the covalent radii of calcium and phosphorus (3.07 Å), indicates that calcium and phosphorus have no interaction between themselves. The P–Se distances (2.1444(10), 2.1389(10) Å for **35a** and 2.1443(17), 2.1420(16) Å for **35b**) are slightly elongated but within the same range as that of free ligand **32a** (2.1219(15) Å) indicating no impact on P–Se bond upon coordination of the calcium atom to the selenium atom. P-N distances (1.603(3), 1.607(3) Å for **35a** and 1.611(5), 1.602(5) Å for **35b**) are slightly shortened compared to free ligand **32a** (1.671(5) Å). The central calcium atom is additionally ligated by two THF molecules having Ca-O distance of 2.400(3), 2.444(3) Å for **35a** and 2.440(5), 2.394(5) Å for **35b** to adopt the calcium atom distorted octahedron geometry. Thus two four-membered metallacycles Ca1-Se1-P1-N1 and Ca1-Se2-P2-N2 are formed due to ligation of two ligand moieties via selenium and amide nitrogen atoms. The plane containing N1, P1, Se1 and Ca1 makes a dihedral angle of 82.02° (for **35a**) and 82.38° (for **35b**) with the plane having N2, P2, Se2 and Ca1 indicating that two four-membered metallacycles are almost perpendicular to each other. O1-Ca1-O2 bond angle is found to be 79.03(13)° for **35a** and 78.8(2)° for **35b**. Thus the enantiomeric pure compounds **35a** and **35b** are known to be fully structurally characterized calcium complexes and best of our knowledge these are the first examples of chiral calcium complexes having calcium-selenium direct bond.

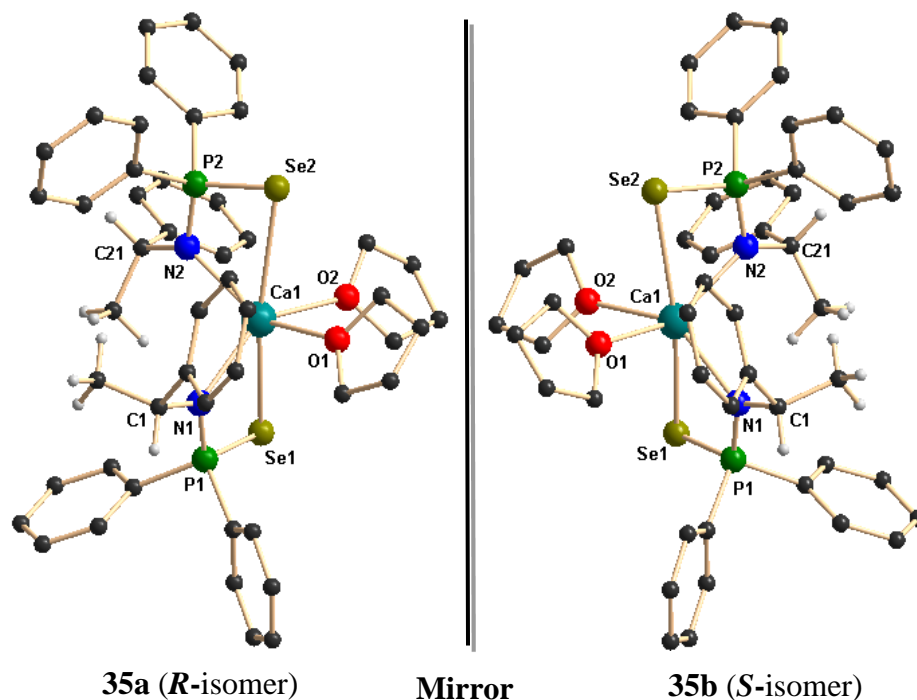


Figure 5.2. Solid state structures of calcium complexes **35a** and **35b**. Hydrogen atoms are omitted for clarity except methyl and methine hydrogen atoms. Selected bond lengths (Å) and bond angles (°):

35a: P1-Se1 2.1444(10), P1-N1 1.603(3), P1-C9 1.829(4), P1-C15 1.831(4), C1-N1 1.489(5), C1-C2 1.536(6), C1-C3 1.523(5), P2-Se2 2.1389(10), P2-N2 1.607(3), P2-C35 1.840(4), C21-N2 1.488(4), C21-C22 1.527(5), C21-C23 1.531(6), Ca1-Se1 3.0303(9), Ca1-N1 2.441(3), Ca1-O1 2.400(3), Ca1-O2 2.444(3), Ca1-Se2 3.0794(9), Ca1-N2 2.426(3), N1-P1-Se1 108.33(12), C1-N1-P1 119.8(2), C2-C1-N1 111.9(3), C9-P1-C15 99.44(17), N1-Ca1-Se1 166.88(8), O1-Ca1-O2 79.03(13), N2-Ca1-Se2 66.15(7), N2-P2-Se2 108.42(12), C21-N2-P2 116.9(3), N1-Ca1-N2 104.74(11), Se1-Ca1-Se2 162.60(3).

35b: P1-Se1 2.1443(17), P1-N1 1.611(5), P1-C9 1.835(6), P1-C15 1.825(6), C1-N1 1.482(8), C1-C2 1.527(9), C1-C3 1.526(8), P2-Se2 2.1420(16), P2-N2 1.602(5), P2-C35 1.838(7), C21-N2 1.498(7), C21-C22 1.533(8), C21-C23 1.510(10), Ca1-Se1 3.0327(15), Ca1-N1 2.444(5), Ca1-O1 2.440(5), Ca1-O2 2.394(5), Ca1-Se2 3.0817(14), Ca1-N2 2.430(5), N1-P1-Se1 108.3(2), C1-N1-P1 119.8(4), C2-C1-N1 111.9(5), C9-P1-C15

99.8(3), N1-Ca1-Se1 66.92(13), O1-Ca1-O2 78.8(2), N2-Ca1-Se2 66.19(11), N2-P2-Se2 108.7(2), C21-N2-P2 117.1(4), N1-Ca1-N2 104.37(18), Se1-Ca1-Se2 162.75(5).

The strontium complex **36a** is isostructural to calcium complex **35a** due to similar ionic radii of the metal centers ($\text{Ca}^{2+} = 1.00 \text{ \AA}$; $\text{Sr}^{2+} = 1.18 \text{ \AA}$ for CN = 6)²⁷ and the strontium complex **36b** forms the corresponding enantiomer (see Figure 5.3). The details of the structural parameters are given in the Table 5.2 and the solid-state structures of strontium complexes **36a** and **36b** are shown in the Figure 5.3. In the enantiomeric pure strontium complexes **36a** and **36b** the coordination polyhedron was formed by the two monoanionic $\{\text{N}(\text{*CHMePh})\text{P}(\text{Se})\text{Ph}_2\}^-$ ligands and two THF molecules. Each ligand $\{\text{N}(\text{*CHMePh})\text{P}(\text{Se})\text{Ph}_2\}^-$ coordinates through the amido nitrogen atom and one selenium atom. The central strontium atom adopts a distorted octahedral geometry due to coordination from two $\{\text{N}(\text{*CHMePh})\text{P}(\text{Se})\text{Ph}_2\}^-$ moieties and two THF molecules. The Sr–N distances [(2.570(7) and 2.542(7) \AA) for **36a** and (2.564(5) and 2.569(5) \AA) for **36b**] well fit with our previously reported strontium-nitrogen bond distances: 2.609(3) \AA for the complex $[\text{Sr}\{\text{Ph}_2\text{P}(\text{Se})\text{NCHPh}_2\}_2(\text{THF})_2]$ (**10**) and 2.591(4) \AA for $[\text{Sr}\{\text{Ph}_2\text{P}(\text{BH}_3)\text{NCHPh}_2\}_2(\text{THF})_2]$ (**23**) and 2.540(5) \AA for $[\text{Sr}\{\text{C}_2\text{H}_4(\text{NPh}_2\text{P}=\text{Se})_2\}(\text{THF})_3]$ (**27**) (See Chapter 2-4). The Sr–Se bond distances of 3.1726(10) and 3.2141(10) \AA for **36a**, 3.2151(8) and 3.1722(9) \AA for **36b** are observed, which are quite long, compared to the calcium analogue [3.0327(15) to 3.0817(14) \AA] due to the larger ionic radius of the Sr^{2+} ion. The observed Sr–Se distance in the compounds **36a** and **36b** are within the range of Sr–Se distances (3.138(7) to 3.196(9) \AA) of structurally characterized complex $[(\text{THF})_3\text{Sr}(\text{Se}_2\text{PPh}_2)_2]$ published by Westerhausen and coworkers^{32b} and 3.066(1) \AA for the complex $[\text{Sr}\{\text{Se}(2,4,6\text{-}^i\text{Bu}_3\text{C}_6\text{H}_2)\}_2(\text{THF})_4]$ [32a] and 3.1356(9) \AA for the complex $[\text{Sr}\{\text{Ph}_2\text{P}(\text{Se})\text{NCHPh}_2\}_2(\text{THF})_2]$ (**10**) and 3.2788(10) \AA for the complex $[\text{Sr}\{\text{C}_2\text{H}_4(\text{NPh}_2\text{P}=\text{Se})_2\}(\text{THF})_3]$ (**27**) reported by us (See chapter 2 & 4). The considerably elongated Sr–P distance of [3.449(2), 3.4586(19) \AA in **36a** and 3.4520(17), 3.4539(15) \AA in **36b**], were greater than the sum of the covalent radii of strontium and phosphorus (3.25 \AA), indicates that strontium and phosphorus have no interaction between themselves. The central strontium metal ion is additionally ligated by two THF molecules to adopt the distorted octahedron geometry around the Sr^{2+} ion. Therefore, two four-membered metallacycles Sr1–Se1–P1–N1 and Sr1–Se2–P2–N2 are formed due to ligation of two ligand

moieties via selenium and amido nitrogen atoms. The plane containing N1, P1, Se1 and Sr1 makes a dihedral angle of 81.13° (for **36a**) and 81.14° (for **36b**) with the plane having N2, P2, Se2 and Sr1 indicating that two four-membered metallacycles are almost perpendicular to each other as we observed in the calcium case (**35a** and **35b**). Thus the enantiomeric pure compounds **36a** and **36b** are known to be new and best of our knowledge these are the first examples for chiral strontium complexes having strontium-selenium direct bond.

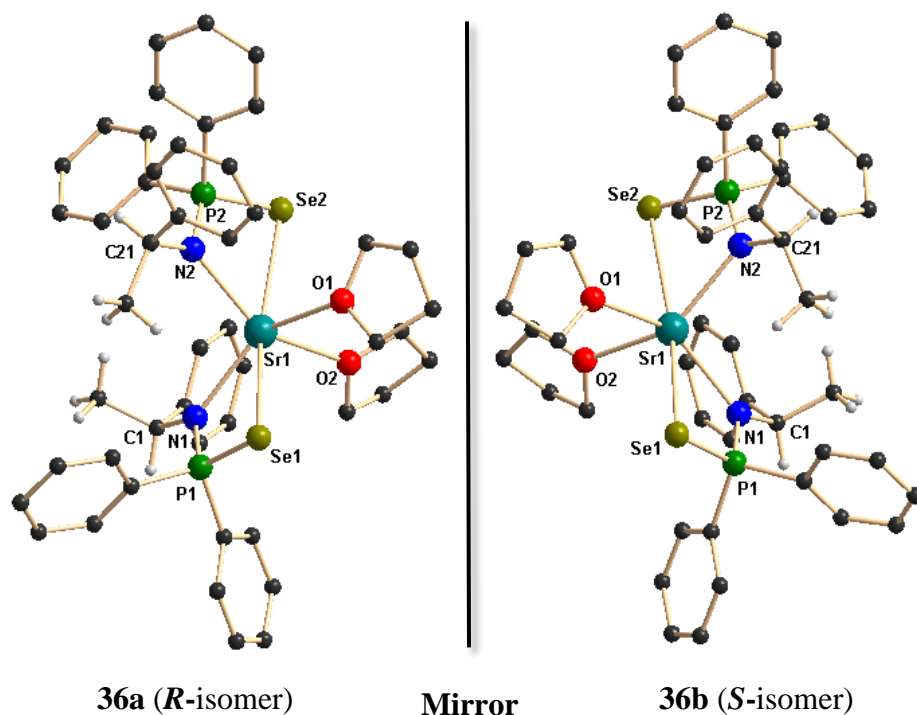


Figure 5.3. Solid state structures of strontium complexes **36a** and **36b**. Hydrogen atoms are omitted for clarity except methyl and methine hydrogen atoms. Selected bond lengths (Å) and bond angles (°):

36a: P1-Se1 2.149(2), P1-N1 1.611(7), P1-C9 1.829(9), P1-C15 1.839(8), C1-N1 1.492(10), C1-C2 1.550(12), C1-C3 1.550(12), P2-Se2 2.153(2), P2-N2 1.607(7), P2-C35 1.838(8), C21-N2 1.492(10), C21-C22 1.545(11), C21-C23 1.528(12), Sr1-Se1 3.1726(10), Sr1-N1 2.570(7), Sr1-O1 2.579(6), Sr1-O2 2.553(6), Sr1-Se2 3.2141(10), Sr1-N2 2.542(7), N1-P1-Se1 108.5(3), C1-N1-P1 119.1(5), C2-C1-N1 110.2(7), C9-P1-C15 103.1(4), N1-Sr1-Se1 63.56(15), O1-Sr1-O2 78.2(2), N2-Sr1-Se2 63.16(14), N2-P2-Se2 108.5(3), C21-N2-P2 118.9(5), N1-Sr1-N2 103.6(2), Se1-Sr1-Se2 166.47(3).

36b: P1-Se1 2.1537(17), P1-N1 1.597(5), P1-C9 1.825(7), P1-C15 1.826(6), C1-N1 1.480(7), C1-C2 1.529(8), C1-C3 1.528(9), P2-Se2 2.1459(18), P2-N2 1.604(5), P2-C35 1.829(6), C21-N2 1.504(8), C21-C22 1.535(10), C21-C23 1.503(9), Sr1-Se1 3.2151(8), Sr1-N1 2.564(5), Sr1-O1 2.585(5), Sr1-O2 2.544(4), Sr1-Se2 3.1722(9), Sr1-N2 2.569(5), N1-P1-Se1 109.1(2), C1-N1-P1 120.6(4), C2-C1-N1 109.3(5), C9-P1-C15 102.3(3), N1-Sr1-Se1 63.06(11), O1-Sr1-O2 78.24(15), N2-Sr1-Se2 63.44(11), N2-P2-Se2 108.59(19), C21-N2-P2 118.9(4), N1-Sr1-N2 103.50(16), Se1-Sr1-Se2 166.41(3).

Similar to calcium and strontium complexes (**35a,b-36a,b**), the analogous chiral barium complexes **37a** and **37b** were also crystallize in monoclinic space group $P2_1$ having two molecules in the unit cell. The details of the structural parameters are given in the Table 5.3. Figure 5.4 shows the both enantiometric forms of the barium complexes **37a** and **37b** along with selected bond angles and selected bond lengths. The coordination sphere of the central barium ion of each enantiomer was occupied by the two monoanionic $\{N(*CHMePh)P(Se)Ph_2\}^-$ ligand moieties where each ligand coordinating via amido nitrogen and one selenium atom and two THF molecules coordinating through oxygen atoms. Therefore, the central Ba^{2+} ion in the each enantiomer is having distorted octahedral geometry. The Ba-N bond distances of 2.693(4) and 2.679(5) Å for **37a** and 2.693(6) and 2.672(7) Å for **37b** were observed which are quite long when compared to analogous calcium (2.441(3) to 2.430(5) Å) and strontium (2.542(7) to 2.570(7) Å) complexes. The observed Ba-N distances are similar to our previously reported values 2.777(6) and 2.778(6) Å for $[Ba\{Ph_2P(Se)NCHPh_2\}_2(THF)_2]$ (**11**), 2.733(6) Å for $[Ba\{Ph_2P(BH_3)NCHPh_2\}_2(THF)_2]$ (**24**), (2.657(5) and 2.654(6) Å) for $[Ba\{C_2H_4(NPh_2P=Se)_2\}(THF)_3]$ (**28**) (See Chapters 2-4), (2.774(5) Å, 2.790(5) and 2.789(5) Å) for polymeric ate complex of $[K(THF)Ba\{Ph_2P(Se)N(CMe_3)\}_3]_n$ reported by us²⁶ and 2.706(4) Å for $[Ba((Dip)_2DAD)(\mu-I)(THF)_2]_2$ reported in the literature.²⁸ The Ba-Se bond distances of [3.3181(6) and 3.3524(7) Å for **37a** and 3.3172(9) and 3.3537(9) Å for **37b**] were observed and these are within the range of the Ba-Se distances [3.366(1) Å and 3.324(1) Å] for the complex $[Ba\{4,5-(P(Se)Ph_2)_2tz\}_2(thf)_7]$ reported by Raymundo Cea-Olivares et al.,³³ 3.2787(11) Å for $[Ba(THF)_4(SeMes^*)_2]$ ($Mes^* = 2,4,6-t-Bu_3C_6H_2$) and 3.2973(3) Å for $[Ba(Py)_3(THF)(SeTrip)_2]_2$ ($Trip = 2,4,6-i-Pr_3C_6H_2$) reported by Ruhlandt-Senge et al.,³⁴ [3.3553(10) and 3.3314(10) Å] for

[Ba{Ph₂P(Se)NCHPh₂}₂(THF)₂], 3.3842(8) Å for [{η²-N(PPh₂Se)₂}₂Ba(THF)₃] and [3.3274(7) Å, 3.3203(7) Å (See Chapters 2 & 4) and 3.3518(7) Å] for [K(THF)Ba{Ph₂P(Se)N(CMe₃)₃}₃]_n previously reported by us.²⁶

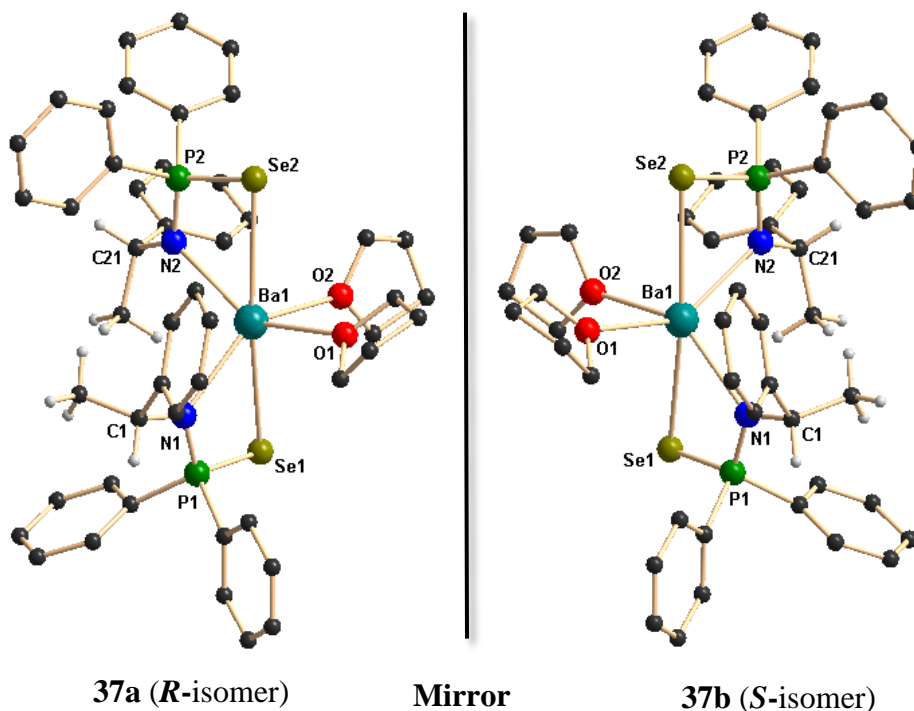


Figure 5.4. Solid state structures of barium complexes **37a** and **37b**. Hydrogen atoms are omitted for clarity except methyl and methine hydrogen atoms. Selected bond lengths (Å) and bond angles (°):

37a: P1-Se1 2.1447(15), P1-N1 1.597(5), P1-C9 1.833(5), P1-C15 1.832(6), C1-N1 1.483(7), C1-C2 1.533(9), C1-C3 1.511(8), P2-Se2 2.1514(15), P2-N2 1.607(5), P2-C35 1.823(7), C21-N2 1.486(6), C21-C22 1.535(8), C21-C23 1.515(9), Ba1-Se1 3.3181(6), Ba1-N1 2.693(4), Ba1-O1 2.690(5), Ba1-O2 2.719(5), Ba1-Se2 3.3524(7), Ba1-N2 2.679(5), N1-P1-Se1 109.88(17), C1-N1-P1 120.0(4), C2-C1-N1 111.3(5), C9-P1-C15 103.1(2), N1-Ba1-Se1 60.56(10), O1-Ba1-O2 78.94(19), N2-Ba1-Se2 60.19(9), N2-P2-Se2 109.23(18), C21-N2-P2 120.6(4), N1-Ba1-N2 103.52(15), Se1-Ba1-Se2 168.708(19).

37b: P1-Se1 2.144(2), P1-N1 1.601(6), P1-C10 1.826(8), P1-C16 1.837(7), C1-N1 1.481(10), C1-C3 1.534(11), C1-C4 1.511(11), P2-Se2 2.150(2), P2-N2 1.612(7), P2-C35 1.826(9), C2-N2 1.486(9), C2-C22 1.530(11), C2-C23 1.523(12), Ba1-Se1 3.3172(9), Ba1-

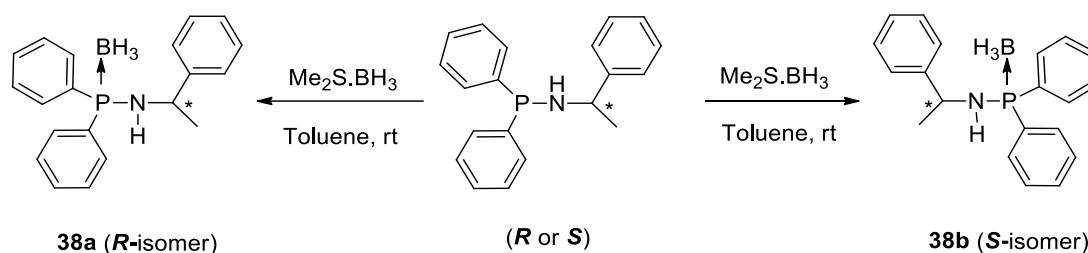
N1 2.693(6), Ba1-O1 2.729(7), Ba1-O2 2.696(7), Ba1-Se2 3.3537(9), Ba1-N2 2.672(7), N1-P1-Se1 109.9(2), C1-N1-P1 119.7(5), C3-C1-N1 110.8(6), C10-P1-C16 102.9(3), N1-Ba1-Se1 60.64(13), O1-Ba1-O2 79.2(3), N2-Ba1-Se2 60.23(14), N2-P2-Se2 109.1(3), C2-N2-P2 120.0(6), N1-Ba1-N2 103.4(2), Se1-Ba1-Se2 168.72(3).

The considerably elongated Ba-P distance of [3.5838(13), 3.5959(15) Å in **37a** and 3.5837(18), 3.595(2) Å in **37b**], were greater than the sum of the covalent radii of barium and phosphorus (3.34 Å), indicates that barium and phosphorus have no interaction between themselves. The Ba²⁺ ion is additionally ligated by two THF molecules to adopt the distorted octahedron geometry around the Ba²⁺ ion. Therefore, two four-membered metallacycles Ba1-Se1-P1-N1-Ba1 and Ba1-Se2-P2-N2-Ba1 are formed due to ligation of two ligand moieties via selenium and amide nitrogen atoms. The plane containing N1, P1, Se1 and Ba1 makes a dihedral angle of 81.37° (for **37a**) and 81.29° (for **37b**) with the plane having N2, P2, Se2 and Ba1 indicating that two four-membered metallacycles are almost perpendicular to each other as we observed in the case of calcium (**35a** and **35b**) and strontium (**36a** and **36b**). Thus the enantiomeric pure compounds **37a** and **37b** are known to be new class of alkaline-earth metal molecules and best of our knowledge these are the first examples for chiral barium complexes having barium-selenium direct bond.

5.2.4. Chiral amidophosphine-borane ligands

In the Chapter 3 & 4, we have introduced an monoanionic amidophosphine-borane {Ph₂P(BH₃)NR}⁻ (R = CHPh₂ and CPh₃) and dianionic bis(amidodiphenylphosphine-borane) {Ph₂P(BH₃)NCH₂CH₂NP(BH₃)Ph₂}²⁻ as a chelating ligand and exploited their chelating behaviour in alkali metal and alkaline-earth metal chemistry. The monoanionic amidophosphine-borane {Ph₂P(BH₃)NR}⁻ act as bidentate ligand and coordinates to the metal ions through amido nitrogen and borane hydrogens. Whereas bis(amidodiphenylphosphine-borane) would form a dianion and act as a tetradentate ligand towards metal ion. To extend our research work on amidophosphine-boranes and demonstrate the versatility of the amidophosphine-boranes mainly in the alkaline-earth metals, here we have described the synthesis and structures of chiral amidophosphine-borane ligands {HN(*R*-*CHMePh)(P(BH₃)Ph₂)} (**38a**) and {HN(*S*-*CHMePh)(P(BH₃)Ph₂)} (**38b**) and the corresponding homoleptic barium complexes [Ba{N(*R*-*CHMePh)-

$P(BH_3)Ph_2)_2(THF)_2]$ (**39a**) and $[Ba\{N(R-^*CHMePh)P(BH_3)Ph_2\}_2(THF)_2]$ (**39b**) to demonstrate our concept of versatility of the amidophosphine backbone. The chiral amidophosphine-borane ligands $\{HN(R-^*CHMePh)(P(BH_3)Ph_2)\}$ (**38a**) and $\{HN(S-^*CHMePh)(P(BH_3)Ph_2)\}$ (**38b**) was isolated as a white precipitate from the reaction between chiral phosphineamines $\{HN(R-^*CHMePh)(PPh_2)\}$ and $\{HN(S-^*CHMePh)(PPh_2)\}$ and the borane adduct $[H_3B \bullet SMe_2]$ at room temperature in a 1:1 molar ratio in toluene as the solvent (see Scheme 5.4).²⁴



Scheme 5.4. Synthesis of chiral amidophosphine-boranes.

The formation of the chiral amidophosphine-borane ligands **38a** and **38b** from $\{HN(R-^*CHMePh)(PPh_2)\}$ and $\{HN(S-^*CHMePh)(PPh_2)\}$ can easily be followed by 1H NMR spectroscopy measured in $CDCl_3$, since additional resonances for the two chemically equivalent borane (BH_3) groups attached to the phosphorus atoms appear as a broad signal at δ 0.96 ppm. In the 1H NMR spectra, the resonances of the amidophosphine moiety in ligand **38a,b** are only slightly shifted in comparison to the starting material with those reported for the phosphineamines.^{21a} The multiplet signals at δ 4.47-4.37 ppm can be assigned to the methine proton ($-CH$) α to amino nitrogen of ligand **38a,b**. Another broad signal at δ 2.48 ppm corresponding to the NH proton of ligand **38a,b** is observed and also shifted to the higher field (3.24 ppm) compared to **32a,b**. Ligand **38a,b** shows a doublet signal at δ 1.40 ppm with coupling constant of $J_{H-H} = 6.76$ Hz corresponds to the methyl ($-CH_3$) protons of the ligand **38a,b**. In the $^{31}P\{^1H\}$ NMR spectra, the doublet resonance signal at δ 54.9 ppm with a coupling constant of $J_{P-B} = 80.95$ Hz can be attributed to coupling of phosphorus atom with adjacent boron atom. In $^{11}B\{^1H\}$ NMR spectrum, the

broad signal at -37.9 ppm can be assigned to the BH_3 group attached to the phosphorus atom. This observation is in agreement with our previously reported values (See Chapter 3 and 4). In the FT-IR spectra, a characteristic signal for P–B bond stretching at 608 cm^{-1} was observed along with another characteristic signal at 2379 cm^{-1} assigned to the B–H stretching frequency. These values are in agreement with those reported in literature. (See Chapter 3 and 4).

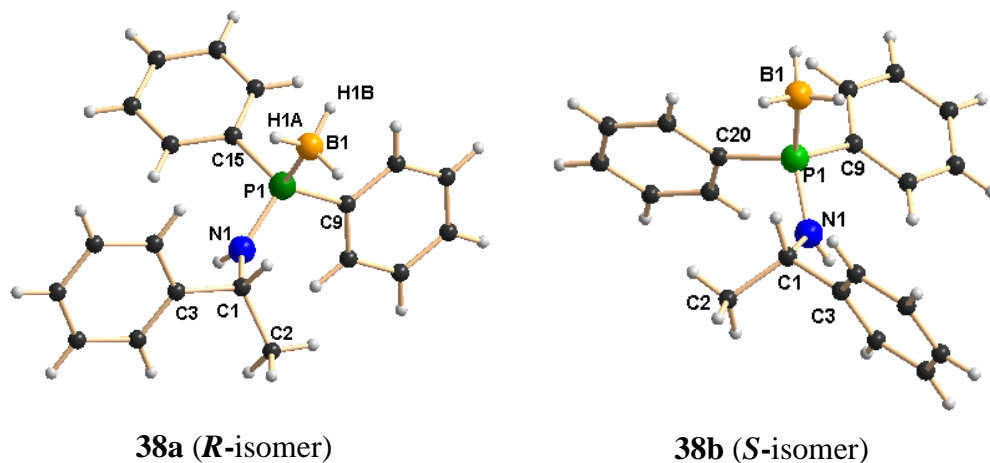


Figure 5.5. Solid state structures of two enantiomers **38a** and **38b**. Selected bond lengths (Å) and bond angles (°):

38a: P1-B1 1.915(5), P1-N1 1.638(3), P1-C9 1.817(3), P1-C15 1.818(4), C1-N1 1.466(4), C1-C2 1.531(5), C1-C3 1.530(4), B1-H1A 0.9600, B1-H1B 0.9600, B1-H1C 0.9600, N1-P1-B1 113.73(19), C9-P1-C15 104.54(14), C9-P1-B1 110.97(19), C15-P1-B1 112.8(2), C9-P1-N1 109.58(16), C15-P1-N1 104.62(16), P1-N1-C1 125.8(3), N1-C1-C2 109.3(3), N1-C1-C3 109.8(3), C2-C1-C3 114.3(3), H1A-B1-H1B 109.5.

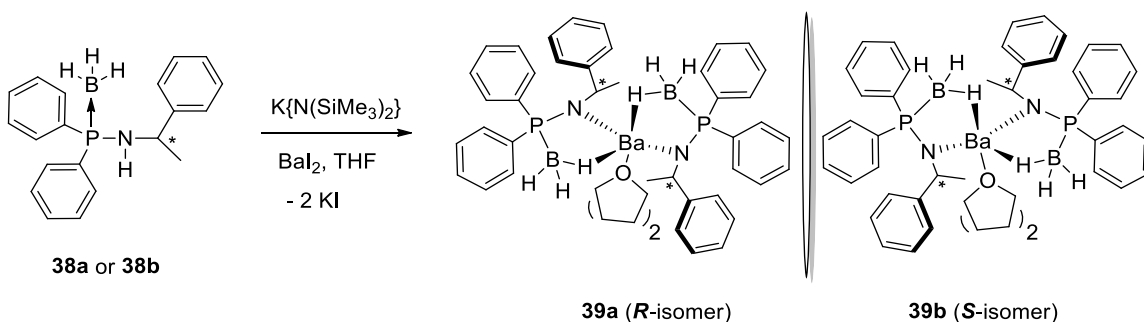
38b: P1-B1 1.892(3), P1-N1 1.653(2), P1-C9 1.802(3), P1-C20 1.816(2), C1-N1 1.478(3), C1-C2 1.528(4), C1-C3 1.502(4), B1-H1B 0.9600, B1-H1C 0.9600, B1-H1D 0.9600, N1-P1-B1 116.4(2), C9-P1-C20 104.94(12), C9-P1-B1 111.89(15), C20-P1-B1 112.13(13), C9-P1-N1 105.00(12), C20-P1-N1 109.45(12), N1-C1-C2 110.2(3), N1-C1-C3 110.8(2), C2-C1-C3 113.0(3).

The solid state structures of enantiomers **38a** and **38b** were established by using single crystal X-ray diffraction analysis. *R*-isomer (**38a**) crystallizes in the monoclinic space group

$P2_1$, with two independent molecules in the unit cell, whereas the corresponding *S*-isomer (**38b**) crystallizes in orthorhombic space group $P2_12_12_1$ having 8 independent molecules in the unit cell (see Figure 5.5). The details of the structural parameters are given in Table 5.4. The P1–B1 bond distances [1.915(5) Å (**38a**) and 1.892(3) Å (**38b**)] are almost similar and in full agreement with reported values-1.918(6) Å for [Ph₂P(BH₃)NH(CHPh₂)] (**17**), 1.9091(2) and 1.916(1) Å for [{Ph₂P(BH₃)N-CH₂-CH₂-NP(BH₃)Ph₂}] (**30**) (See Chapters 3 and 4) and 2.1019(8) Å for [{Ph₂P(BH₃)}₂CH₂] and 1.921(3) Å for [(CH₂-*o*-CF₃C₆H₄)-(Ph)P(BH₃)C₄H₈P(BH₃)(Ph)-(CH₂-*o*-CF₃C₆H₄)] to be considered as the phosphorus–boron dative bond reported by us and others.³⁵ The P1–N1 bond ranges from 1.638(3) Å to 1.653(2) Å and C1–N1 bond distances of 1.466(4) Å and 1.478(3) are also similar to those reported by us previously: P1–N1 1.673(6) Å and C1–N1 1.453(8) Å for [Ph₂PNH(CHPh₂)] (**1**) and P1–N1 1.638(3) Å and C1–N1 1.468(5) Å for [Ph₂P(BH₃)NH(CHPh₂)] (**17**) (See Chapters 1 and 3).

5.2.5. Chiral-amidophosphine-borane barium complexes

Ligand **38a** or **38b** was made to react with [K{N(SiMe₃)₂}] in THF at an ambient temperature in a 1:1 molar ratio followed by addition of barium diiodide to afford the barium complexes [(THF)₂Ba{N(*R*-*CHMePh)(P(BH₃)Ph₂)}₂] (**39a**) and [(THF)₂Ba{N(*S*-*CHMePh)(P(BH₃)Ph₂)}₂] (**39b**) through the elimination of KI and volatile tetramethylsilane (see Scheme 5.5).²⁴



Scheme 5.5. Synthesis of barium complexes **39a** and **39b** of chiral amidophosphine-boranes.

In FT-IR spectra, strong absorption band at 602 cm⁻¹ is assigned to the P–B bond of complexes **39a,b** which is in the range to that of ligand **38a** or **38b** (608 cm⁻¹). The ¹H

NMR spectra of complex **39a,b** in C₆D₆ are very similar to the spectra recorded for ligand **38a** or **38b** and reveals time-averaged C_s-symmetry in solution. Methyl protons in the ligand backbone appear as a doublet at δ 1.40 ppm with coupling constant of 6.76 Hz. The resonances of the three protons attached to the boron atom appear as multiplets at δ 1.22 ppm in the ¹H NMR spectra. Methine proton of the anionic ligand in the barium complex **39a,b** observed as multiplet signal in the region of δ 4.39-4.48 in the ¹H NMR spectra. In the proton decoupled ³¹P NMR spectra, complexes **39a,b** show only one doublet signal at δ 46.9 ppm and this value is significantly up-field shifted compared to the value for compound **38a** or **38b** (54.9 ppm) upon the coordination of barium atoms to the ligand **38a** or **38b**. The phosphorus atoms present in the {N(*CHMePh)P(BH₃)Ph₂}⁻ moieties are chemically equivalent. A broad signal at □ -34.9 ppm was observed in the ¹¹B{¹H} NMR spectra of complexes **39a,b**. Compounds **39a** and **39b** were re-crystallised from THF and *n*-pentane (1:2) and was found to crystallize in the monoclinic space group *P*2₁ having two molecules in the unit cell. The solid-state structures of complex **39a,b** are given in Figure 5.6. The details of the structural parameters are given in Table 5.4. The enantiomeric pure barium compounds **39a,b** were non-centrosymmetric and each barium ion in **39a** and **39b** were coordinated by two amido nitrogen atoms and two BH₃ groups of two ligands **38a** or **39b**.

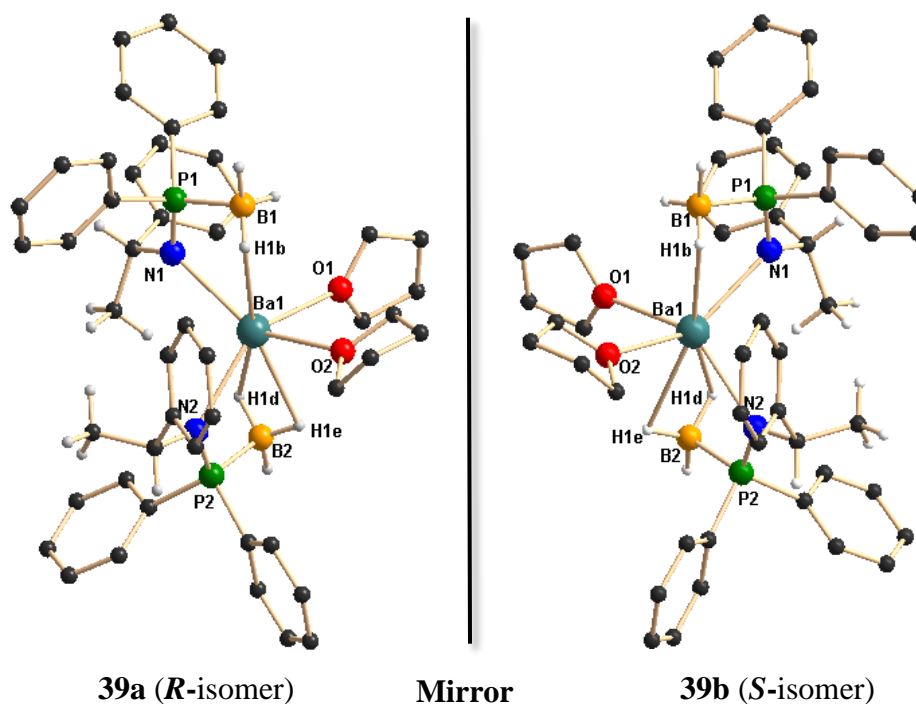


Figure 5.6. Solid state structures of enantiomeric pure barium complexes **39a** and **39b**. Hydrogen atoms are omitted for clarity except for methyl, methine as well as for borane hydrogen atoms. Selected bond lengths (Å) and bond angles (°):

39a: P1-B1 1.929(6), P1-N1 1.610(4), P1-C9 1.826(5), P1-C15 1.826(5), C1-N1 1.482(6), C1-C2 1.527(7), C1-C3 1.523(7), P2-B2 1.924(6), P2-N2 1.604(4), P2-C29 1.839(5), C21-N2 1.486(6), C21-C22 1.534(7), C21-C23 1.514(6), Ba1-B1 3.221(6), Ba1-N1 2.674(4), Ba1-O1 2.759(4), Ba1-O2 2.697(4), Ba1-B2 3.155(6), Ba1-N2 2.684(4), Ba1-H1b 2.68(6), Ba2-H1d 2.87(6), B1-H1b 1.03(6), B2-H1d 1.14(6), N1-P1-B1 110.8(2), C1-N1-P1 119.3(3), C2-C1-N1 108.9(4), C9-P1-C15 103.8(2), N1-Ba1-B1 58.48(13), O1-Ba1-O2 82.20(14), N2-Ba1-B2 58.90(13), N2-P2-B2 110.2(2), C21-N2-P2 121.4(3), N1-Ba1-N2 104.51(12), B1-Ba1-B2 167.87(15), H1b-Ba1-H1d 162.4(17), P1-Ba1-H1b 44.3(13), P2-Ba1-H1d 45.8(12), N1-Ba1-H1b 70.0(13), N2-Ba1-H1d 69.1(12).

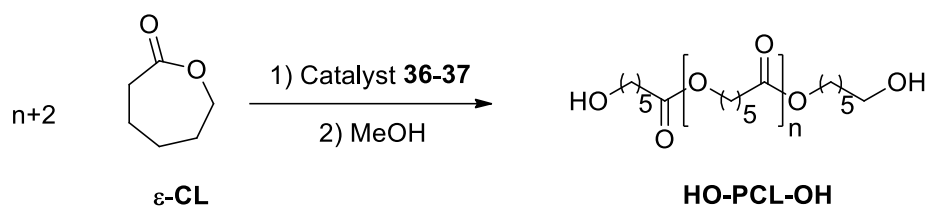
39b: P1-B1 1.920(5), P1-N1 1.608(4), P1-C9 1.823(4), P1-C15 1.835(5), C1-N1 1.477(5), C1-C2 1.534(6), C1-C3 1.520(6), P2-B2 1.920(5), P2-N2 1.607(4), P2-C29 1.819(4), C21-N2 1.475(5), C21-C22 1.537(6), C21-C23 1.521(6), Ba1-B1 3.228(5), Ba1-N1 2.677(3), Ba1-O1 2.694(3), Ba1-O2 2.778(4), Ba1-B2 3.153(5), Ba1-N2 2.683(3), Ba1-H1b 2.69(5), Ba2-H1d 2.90(5), B1-H1b 1.12(5), B2-H1d 1.01(6), N1-P1-B1 111.0(2), C1-N1-P1 119.5(3), C2-C1-N1 108.4(4), C9-P1-C15 103.5(2), N1-Ba1-B1 58.22(12), O1-Ba1-O2 81.96(12), N2-Ba1-B2 58.96(12), N2-P2-B2 110.4(2), C21-N2-P2 121.2(3), N1-Ba1-N2 104.66(11), B1-Ba1-B2 167.70(14), H1b-Ba1-H1d 156.8(13), P1-Ba1-H1b 44.8(10), P2-Ba1-H1d 46.4(11), N1-Ba1-H1b 70.3(10), N2-Ba1-H1d 70.4(11).

One of the borane (BH₃) group coordinates through the hydrogen atoms in a η^1 fashion and has a Ba1–B1 bond length of 3.221(6) Å. the second borane (BH₃) group coordinates in η^2 fashion and has Ba1–B2 bond distance of 3.155(6) Å. Thus, ligand **38a** or **38b** can be considered as pseudo bi-dentate ligand, similar to {Ph₂P(BH₃)N(CHPh₂)} which is previously introduced into the alkaline-earth metal chemistry by us (See Chapter 3). Additionally, two THF molecules are coordinated to each barium ion and the geometry around each barium ion is best described as distorted octahedral. It is noteworthy that the P–B distances [1.929(6) and 1.924(6) Å] are slightly elongated compared to that of the

ligands, **38a** [1.915(5)] and **38b** [1.892(3 Å)] even after the coordination of the BH₃ group to the barium centre. The Ba–N [2.674(4), 2.684(4) Å], Ba1–O1 [2.759(4) and 2.697(4) Å] distances are in the range similar to that of the reported complexes (See Chapters 2-4).

5.3 Ring-opening polymerisation study

Catalytic activities of the chiral strontium and barium complexes **36a** or **36b** and **37a** or **37b** were performed (see Scheme 5.6). Polymerisation studies were typically conducted in toluene, with various monomer/catalyst ratios at 25 °C. Selected data obtained with respect to complexes **36** and **37** are given in Table 5.



Scheme 5.6. Ring-opening polymerisation of ϵ -CL with strontium (**36a,b**) and barium (**37a,b**) complexes

The catalytic ability of the newly synthesised enantiomeric pure mono-nuclear strontium complexes **36a** or **36b** to promote the ROP of ϵ -CL was first evaluated (Table 5, entries 1–5). Indeed, the moderate reactivity of the strontium complexes is very similar to that observed in previously reported studies using other strontium complexes for ROP of ϵ -caprolactone.³⁶ Since the larger ion radius barium complexes have been reported to be more active than the calcium and strontium congeners in ROP,^{37,38} we tested compound **37a** or **37b** as a catalyst and observed an enhanced rate of polymerisation (Table 5, entries 6–10). In the case of strontium, higher reactivity was observed for conversion of ϵ -caprolactone to poly-caprolactone and up to 500 ϵ -CL units were successfully converted in high yields (75–90 per cent), within 15 and 10 minutes respectively, at 25 °C. The control over the ROP process was rather good, affording PCLs, featuring a considerable match between the observed (as determined by GPC) and calculated molar mass values, as well as moderate dispersity data (PDI = Mw/Mn < 1.94). However, the overall efficiency of the strontium

Table 5. Polymerization of ϵ -caprolactone initiated by alkaline earth metal complexes of type $[(\text{THF})_2\text{M}\{\text{Ph}_2\text{P}(\text{Se})\text{N}(\text{R}/\text{S}-*\text{CHMePh})\}_2]$ (where $\text{M} = \text{Sr}, \text{Ba}$)^a

Entry	[M]	$[\epsilon\text{CL}]_0/[\text{M}]_0$	Reac. time ^[b] [min]	Conv. ^[c] [%]	$Mn_{(\text{theo})}^{[d]}$ [g mol ⁻¹]	$Mn_{(\text{GPC})}^{[e]}$ [g mol ⁻¹]	$Mw_{(\text{GPC})}^{[e]}$ [g mol ⁻¹]	$Mw/Mn^{[f]}$
1	Sr	100	15	90	9001	8797	17108	1.94
2	Sr	200	15	80	16603	10515	17153	1.63
3	Sr	300	15	73	21904	12717	19707	1.54
4	Sr	400	15	82	32807	20492	32065	1.56
5	Sr	500	15	75	37508	22261	24295	1.09
6	Ba	100	10	98	9802	8829	11512	1.30
7	Ba	200	10	90	18003	10351	14450	1.39
8	Ba	300	10	85	25505	11735	17467	1.48
9	Ba	400	10	80	32007	12620	19581	1.55
10	Ba	500	10	83	43509	32338	37336	1.15

^[a] Results are representative of at least two experiments. ^[b] Reaction times were not necessarily optimized.

^[c] Monomer conversions were determined by ¹H NMR spectroscopy. ^[d] Theoretical molar mass values calculated from the relation: $[\text{monomer}]_0/[\text{M}]_0 \times \text{monomer conversion}$ where $[\text{M}]^0 = 8.76 \times 10^{-3}$ mmol and Monomer weight of $\epsilon\text{-CL} = 114$ g mol⁻¹, ^[e] Experimental molar masses were determined by GPC versus polyethylene glycol standards. ^[f] Molar mass distribution was calculated from GPC.

initiator **36a,b** towards the ROP of $\epsilon\text{-CL}$ was weaker than that of the barium analogue **37a,b**. Being the largest ionic radius of the barium atom, it was anticipated that complex **37a,b** would show the highest reactivity among all the three alkaline earth metal complexes.^{39,40} In reality we observed that up to 500 $\epsilon\text{-CL}$ units were successfully converted in good yields (80–98 per cent) within 10 minutes at 25 °C (Table 5, entries 6–10). The polycaprolactone produced by the use of the barium catalyst was a considerable match between the observed and calculated molar mass values, and we observed a relatively narrow poly-dispersity data (PDI up to 1.55, entry 9 in Table 5). Thus, among strontium and barium metal complexes, the barium complexes **37a,b** showed the highest activity for ROP of $\epsilon\text{-caprolactone}$.

5.4 Conclusion

We have synthesized two enantiomeric pure chiral phosphinoselenoic amides and these enantiomeric pure ligands were successfully introduced into the alkaline-earth metal chemistry. In each complex, the monoanionic ligand coordinates to metal centre through the amido nitrogen and selenium atoms indicates chiral phosphinoselenoic amide act as pseudo-bidentate ligand can able to stabilize highly electropositive metal centers. Thus the enantiomeric pure compounds **34-37** are known to be new class of alkaline-earth metal molecules and best of our knowledge these are the first examples for chiral alkaline earth metal complexes having metal-selenium direct bond. We have also introduced chiral amidophosphine-boranes into the barium metal chemistry where a mixed ligation η^1 and η^2 from BH_3 groups are observed.

5.5 Experimental Procedures

5.5.1. General

All manipulations of air-sensitive materials were performed with the rigorous exclusion of oxygen and moisture in flame-dried Schlenk-type glassware either on a dual manifold Schlenk line, interfaced to a high vacuum (10^{-4} torr) line, or in an argon-filled M. Braun glove box. THF was pre-dried over Na wire and distilled under nitrogen from sodium and benzophenone ketyl prior to use. Hydrocarbon solvents (toluene and *n*-pentane) were distilled under nitrogen from LiAlH_4 and stored in the glove box. ^1H NMR (400 MHz), $^{13}\text{C}\{^1\text{H}\}$ and $^{31}\text{P}\{^1\text{H}\}$ NMR (161.9 MHz) spectra were recorded on a BRUKER AVANCE III-400 spectrometer. BRUKER ALPHA FT-IR was used for FT-IR measurement. Elemental analyses were performed on a BRUKER EURO EA at the Indian Institute of Technology Hyderabad. Metal diiodides (MgI_2 , CaI_2 , SrI_2 and BaI_2), $\text{KN}(\text{SiMe}_3)_2$, selenium and $\text{Me}_2\text{S}\cdot\text{BH}_3$ were purchased from Sigma Aldrich and used as such. The chiral-aminophosphines $[\text{HN}(\text{R}-*\text{CHMePh})(\text{PPh}_2)]$, $[\text{HN}(\text{S}-*\text{CHMePh})(\text{PPh}_2)]$ were prepared according to procedure prescribed in the literature.^{21a} The NMR solvent C_6D_6 and CDCl_3 were purchased from Sigma Aldrich and dried under Na/K alloy prior to use.

5.5.2. Synthesis of [Ph₂P(Se)HN(*R*-*CHMePh)] (**32a**):

1,1-diphenyl-*N*-(*R*-1-phenylethyl)phosphinamine (1.0 g, 3.27 mmol) and elemental selenium (392 mg, 4.91 mmol) were heated to 60 °C in THF (10 ml) solvent for 12 h. Excess selenium metal was filtered through a G4 frit to collect the yellow colour filtrate. After evaporation of solvent from filtrate in *vacuo*, a light yellow solid residue was obtained which was further purified by washing with *n*-hexane. Compound **32a** was recrystallized from THF at room temperature. ¹H NMR (400 MHz, CDCl₃): δ 7.88-7.94 (m, 2H, ArH), 7.71-7.77 (m, 2H, ArH), 7.30-7.39 (m, 4H, ArH), 7.12-7.25 (m, 7H, ArH), 4.43-4.52 (m, 1H, CH), 2.57 (br, 1H, NH), 1.42 (d, *J*_{H-H} = 6.76 Hz, 3H, CH₃) ppm. ¹³C{¹H} NMR (100 MHz, CDCl₃): δ 144.7 (ArC), 132.0 (P-ArC), 131.8 (P attached *o*-ArC), 131.6 (*o*-ArC), 128.5 (P attached *m*-ArC), 128.3 (*m*-ArC), 127.1 (*p*-ArC), 126.3 (P attached *p*-ArC), 52.7 (CH), 25.2 (CH₃) ppm. ³¹P{¹H} NMR (161.9 MHz, CDCl₃): δ 56.1 ppm. FT-IR (selected frequencies): ν = 3501 (N-H), 1434 (P-C), 954 (P-N), 556 (P=Se) cm⁻¹. Elemental analysis: C₂₀H₂₀NPSe (385.05): Calcd. C 62.50, H 5.25, N 3.64. Found C 61.89, H 5.13, N 3.29

5.5.3. Synthesis of [Ph₂P(Se)HN(*S*-*CHMePh)] (**32b**): Same as above for **32a**

¹H NMR (400 MHz, CDCl₃): δ 7.88-7.94 (m, 2H, ArH), 7.71-7.77 (m, 2H, ArH), 7.30-7.39 (m, 4H, ArH), 7.12-7.25 (m, 7H, ArH), 4.43-4.52 (m, 1H, CH), 2.57 (br, 1H, NH), 1.42 (d, *J*_{H-H} = 6.76 Hz, 3H, CH₃) ppm. ¹³C{¹H} NMR (100 MHz, CDCl₃): δ 144.7 (ArC), 132.0 (P-ArC), 131.8 (P attached *o*-ArC), 131.6 (*o*-ArC), 128.5 (P attached *m*-ArC), 128.3 (*m*-ArC), 127.1 (*p*-ArC), 126.3 (P attached *p*-ArC), 52.7 (CH), 25.2 (CH₃) ppm. ³¹P{¹H} NMR (161.9 MHz, CDCl₃): δ 56.1 ppm. FT-IR (selected frequencies): ν = 3501 (N-H), 1434 (P-C), 954 (P-N), 556 (P=Se) cm⁻¹. Elemental analysis: C₂₀H₂₀NPSe (385.05): Calcd. C 62.50, H 5.25, N 3.64. Found C 61.91, H 5.12, N 3.32

5.5.4. Synthesis of [K{N(*R*-*CHMePh)(Ph₂P(Se))}(THF)_n] (**33a**)

In a 50 ml pre-dried Schlenk flask, one equivalent (1.00 g, 2.60 mmol) of ligand **32a** and one equivalent of potassium bis(trimethylsilyl)amide (520 mg, 2.60 mmol) were mixed together with 10 ml of dry THF. After 6h of stirring THF solvent was evaporated in *vacuo* and dry compound was further purified by washing with *n*-pentane (5 ml) twice. The title compound **33a** was obtained as light orange powder. Yield: 1.24 g, (90%) (**33a**) and Yield:

1.20 g (86 %) (**33b**). ^1H NMR (400 MHz, C_6D_6): δ 7.92-8.08 (m, 4H, ArH), 7.34 (bs, 2H, ArH), 7.01-7.19 (m, 9H, ArH), 4.31-4.37 (m, 1H, CH), 3.50-3.53 (m, THF), 1.37-1.40 (m, THF), 1.30 (d, $J_{\text{H-H}} = 6.20$ Hz, 3H, CH_3) ppm. $^{13}\text{C}\{^1\text{H}\}$ NMR (100 MHz, C_6D_6): δ 144.7 (ArC), 132.0 (P-ArC), 131.8 (P attached *o*-ArC), 131.6 (*o*-ArC), 128.7 (P attached *m*-ArC), 128.4 (*m*-ArC), 127.7 (*p*-ArC), 126.7 (P attached *p*-ArC), 67.6 (THF), 52.7 (CH), 26.1 (CH_3), 25.6 (THF) ppm. $^{31}\text{P}\{^1\text{H}\}$ NMR (161.9 MHz, C_6D_6): δ 42.7 ppm. FT-IR (selected frequencies): $\nu = 1435$ (P-C), 955 (P-N), 550 (P=Se) cm^{-1} . Elemental analysis: $\text{C}_{28}\text{H}_{35}\text{KNO}_2\text{PSe}$ (567.12): Calcd. C 59.35, H 6.23, N 2.47. Found C 58.84, H 5.99, N 2.23.

5.5.5. Synthesis of $\{[(\text{THF})_2\text{Mg}\{\text{Ph}_2\text{P}(\text{Se})\text{N}(\text{R}-*\text{CHMePh})_2\}]_2\}$ (**34a**) :

Route 2: In a 25 ml pre-dried Schlenk flask, potassium salt of ligand **32a** (304 mg, 0.72 mmol) was mixed with MgI_2 (100 mg, 0.36 mmol) in 10 ml THF solvent at ambient temperature and stirring continued for 12 hours. The white precipitate of KI was filtered off and filtrate was evaporated in *vacuo*. The resulting white residue was further purified by washing with *n*-pentane and crystals suitable for X-ray analysis were grown from THF/*n*-pentane (1: 2) mixture at -40°C . Yield: 154.0 mg, (90%) (**34a**) and Yield: 125 mg (80%) (**34b**). ^1H NMR (400 MHz, C_6D_6): δ 8.06-8.12 (m, 1H, ArH), 7.91-7.98 (m, 2H, ArH), 7.76-7.82 (m, 1H, ArH), 7.40-7.42 (m, 1H, ArH), 6.89-7.11 (m, 10H, ArH), 4.58-4.62 (m, 1H, CH), 3.68-3.74 (m, THF), 1.86 (d, $J_{\text{H-H}} = 6.72$ Hz, 3H, CH_3), 1.42-1.44 (m, THF) ppm. $^{13}\text{C}\{^1\text{H}\}$ NMR (100 MHz, C_6D_6): δ 144.7 (ArC), 132.0 (P-ArC), 131.8 (P attached *o*-ArC), 131.6 (*o*-ArC), 128.5 (P attached *m*-ArC), 128.3 (*m*-ArC), 127.1 (*p*-ArC), 126.3 (P attached *p*-ArC), 52.7 (CH), 25.2 (CH_3) ppm. $^{31}\text{P}\{^1\text{H}\}$ NMR (161.9 MHz, C_6D_6): δ 45.1 ppm. FT-IR (selected frequencies): $\nu = 1435$ (P-C), 955 (P-N), 562 (P=Se) cm^{-1} . Elemental analysis: $\text{C}_{38}\text{H}_{48}\text{MgN}_2\text{O}_3\text{P}_2\text{Se}_2$ (826.13): Calcd. C 55.32, H 5.86, N 3.40. Found C 54.93, H 5.62, N 3.13.

5.5.6. Synthesis of $\{[(\text{THF})_2\text{Ca}\{\text{Ph}_2\text{P}(\text{Se})\text{N}(\text{R}-*\text{CHMePh})_2\}]_2\}$ (**35a**) :

Route 1: In a 10 ml sample vial, two equivalents (200 mg, 0.52 mmol) of ligand **35a** and one equivalent of $[\text{Ca}\{\text{N}(\text{SiMe}_3)_2\}_2(\text{THF})_2]$ (130.8 mg, 0.26 mmol) were mixed together with 5 ml of THF. After 6 hours of stirring, 2 ml of *n*-pentane (2 ml) was added to it and

kept at -40° C freezer. After one day, colourless crystals suitable for X-ray diffraction analysis were obtained.

Route 2: In a 25 ml pre-dried Schlenk flask, compound **33a** (288 mg, 0.68 mmol) was mixed with CaI_2 (100 mg, 0.34 mmol) in 10 ml THF solvent at ambient temperature and stirring continued for 12 hours. The white precipitate of KI was filtered off and filtrate was evaporated in *vacuo*. The resulting white residue was further purified by washing with *n*-pentane and crystals suitable for X-ray analysis were grown from THF/*n*-pentane (1: 2) mixture at -40° C. Yield: 154.0 mg, (90%) (**35a**) and Yield: 149 mg (86%) (**35b**). ^1H NMR (400 MHz, C_6D_6): δ 7.95-8.00 (m, 2H, ArH), 7.63-7.94 (m, 2H, ArH), 7.43-7.45 (m, 2H, ArH), 6.85-7.06 (m, 9H, ArH), 4.26-4.34 (d, 1H, CH), 3.63 (m, THF), 1.68 (d, $J_{\text{H-H}} = 6.56$ Hz, 3H, CH_3), 1.21 (m, THF) ppm. $^{13}\text{C}\{^1\text{H}\}$ NMR (100 MHz, C_6D_6): δ 150.2 (ArC), 150.1 (ArC), 132.6 (P-ArC), 132.4 (P attached *o*-ArC), 130.2 (*o*-ArC), 129.9 (P attached *m*-ArC), 128.6 (*m*-ArC), 126.6 (*p*-ArC), 125.9 (P attached *p*-ArC), 69.0 (THF), 58.7 (CH), 30.0 (CH_3), 25.5 (THF) ppm. $^{31}\text{P}\{^1\text{H}\}$ NMR (161.9 MHz, C_6D_6): δ 69.8 ppm. FT-IR (selected frequencies): $\nu = 1435$ (P-C), 954 (P-N), 559 (P=Se) cm^{-1} . Elemental analysis: $\text{C}_{48}\text{H}_{54}\text{CaN}_2\text{O}_2\text{P}_2\text{Se}_2$ (950.87): Calcd. C 60.63, H 5.72, N 2.95. Found C 59.36, H 5.66, N 2.86.

5.5.7. Synthesis of $[(\text{THF})_2\text{Sr}\{\text{Ph}_2\text{P}(\text{Se})\text{N}(\text{R}-*\text{CHMePh})_2\}]$ (**36a**) :

Route 1: In a 10 ml sample vial, two equivalents (200 mg, 0.52 mmol) of ligand **32a** and one equivalent of $[\text{Sr}\{\text{N}(\text{SiMe}_3)_2\}_2(\text{THF})_2]$ (143.6 mg, 0.26 mmol) were mixed together with 5 ml of THF. After 6 hours of stirring, 2 ml of *n*-pentane was added to it and kept at -40° C freezer. After 24 hours, colourless crystals suitable for X-ray diffraction analysis were obtained.

Route 2: In a 25 ml pre-dried Schlenk flask, compound **33a** (245 mg, 0.58 mmol) was mixed with SrI_2 (100 mg, 0.29 mmol) in 10 ml THF solvent at ambient temperature and stirring continued for 12 hours. The white precipitate of KI was filtered off and filtrate was evaporated in *vacuo*. The resulting white residue was further purified by washing with *n*-pentane (3 ml) and crystals suitable for X-ray analysis were grown from THF/*n*-pentane (1: 2) mixture at -40° C. Yield: 154.0 mg, (90%) (**36a**) and Yield 145 mg (85%) (**36b**).

^1H NMR (400 MHz, C_6D_6): δ 7.98-8.03 (m, 2H, ArH), 7.78-7.84 (m, 4H, ArH), 6.90-6.97 (m, 2H, ArH), 6.78-87 (m, 7H, ArH), 4.47-4.55 (m, 1H, CH), 3.45-3.48 (m, THF), 1.29-1.32 (m, THF), 1.20 (d, $J_{\text{H-H}} = 6.80$ Hz, 3H, CH_3) ppm. $^{13}\text{C}\{^1\text{H}\}$ NMR (100 MHz, C_6D_6): δ 145.4 (ArC), 145.3 (ArC), 135.4 (P-ArC), 134.5 (P-ArC), 132.3 (P attached *o*-ArC), 131.2 (*o*-ArC), 128.1 (P attached *m*-ArC), 127.9 (*m*-ArC), 127.7 (*p*-ArC), 126.4 (P attached *p*-ArC), 67.6 (THF), 52.5 (CH), 25.6 (THF), 25.1 (CH_3) ppm. $^{31}\text{P}\{^1\text{H}\}$ NMR (161.9 MHz, C_6D_6): δ 69.8 ppm. FT-IR (selected frequencies): $\nu = 1434$ (P-C), 955 (P-N), 552 (P=Se) cm^{-1} . Elemental analysis: $\text{C}_{48}\text{H}_{54}\text{N}_2\text{O}_2\text{P}_2\text{Se}_2\text{Sr}$ (998.41): Calcd. C 57.74, H 5.45, N 2.81. Found C 56.32, H 4.97, N 2.61.

5.5.8. Synthesis of $\{[(\text{THF})_2\text{Ba}\{\text{Ph}_2\text{P}(\text{Se})\text{N}(\text{R}-*\text{CHMePh})_2\}]_2\}$ (**37a**) :

Route 1: In a 10 ml sample vial, two equivalents (200 mg, 0.52 mmol) of ligand **33a** and one equivalent of $[\text{Ba}\{\text{N}(\text{SiMe}_3)_2\}_2(\text{THF})_3]$ (156.7 mg, 0.26 mmol) were mixed together with 5 ml of THF. After 6 hours of stirring, 2 ml of *n*-pentane was added to it and kept at -40°C freezer. After 24 hours, colourless crystals suitable for X-ray diffraction analysis were obtained.

Route 2: In a 25 ml pre-dried Schlenk flask, compound **33a** (216 mg, 0.52 mmol) was mixed with BaI_2 (100 mg, 0.26 mmol) in 10 ml THF solvent at ambient temperature and stirring continued for 12 hours. The white precipitate of KI was filtered off and filtrate was evaporated in *vacuo*. The resulting white residue was further purified by washing with *n*-pentane and crystals suitable for X-ray analysis were grown from THF/*n*-pentane (1: 2) mixture at -40°C . Yield: 154.0 mg, (90%) (**37a**) and Yield 156 g, (91%) (**37b**). ^1H NMR (400 MHz, C_6D_6): δ 7.96-7.99 (m, 2H, ArH), 7.62-7.66 (m, 2H, ArH), 7.19-7.29 (m, 4H, ArH), 6.90-7.06 (m, 7H, ArH), 4.21-4.29 (m, 1H, CH), 3.54-3.57 (m, THF), 1.48 (d, $J_{\text{H-H}} = 6.20$ Hz, 3H, CH_3), 1.35-1.38 (m, THF) ppm. $^{13}\text{C}\{^1\text{H}\}$ NMR (100 MHz, C_6D_6): δ 144.7 (ArC), 132.1 (P-ArC), 130.2 (P attached *o*-ArC), 129.5 (*o*-ArC), 127.8 (P attached *m*-ArC), 126.8 (*m*-ArC), 126.4 (*p*-ArC), 126.3 (P attached *p*-ArC), 68.0 (THF), 52.7 (CH), 25.2 (CH_3), 25.6 (THF) ppm. $^{31}\text{P}\{^1\text{H}\}$ NMR (161.9 MHz, C_6D_6): δ 69.8 ppm. FT-IR (selected frequencies): $\nu = 1435$ (P-C), 956 (P-N), 553 (P=Se) cm^{-1} . Elemental analysis: $\text{C}_{48}\text{H}_{54}\text{BaN}_2\text{O}_2\text{P}_2\text{Se}_2$ (1048.12): Calcd. C 55.00, H 5.19, N 2.67. Found C 54.32, H 4.96, N 2.41.

5.5.9. Synthesis of [Ph₂P(BH₃)HN(*R*-*CHMePh)] (38a):

In a predried Schlenk flask was placed 1.0 g (3.27 mmol) of 1,1-diphenyl-N-(*R*-1-phenylethyl)phosphinamine in 10 ml of toluene, and to this solution, borane–dimethyl sulfide (0.30 ml, 3.27 mmol) in 5 ml of toluene was added drop wise with constant stirring at room temperature. The reaction mixture was then stirred for another 12 h. A white precipitate was formed and was filtered through a G4 frit and dried in *vacuo*. Pure compound was obtained after washing with *n*-pentane. Yield: 1.20 g (100%). Compound **38a** was soluble in CDCl₃, CH₂Cl₂, THF, and hot toluene. It was recrystallized from hot toluene. ¹H NMR (400 MHz, CDCl₃): δ 7.60-7.54 (m, 4H, ArH), 7.45-7.30 (m, 6H, ArH), 7.24-7.15 (m, 5H, ArH), 4.47-4.37 (m, 1H, CH), 2.48 (br, 1H, NH), 1.40 (d, *J*_{H-H} = 6.76 Hz, 3H, CH₃), 1.17-0.75 (br, 3H, BH₃) ppm. ¹³C{¹H} NMR (100 MHz, CDCl₃): δ 145.1 (ArC), 132.4 (P-ArC), 131.9 (P attached *o*-ArC), 131.1 (*o*-ArC), 128.5 (P attached *m*-ArC), 128.3 (*m*-ArC), 127.0 (*p*-ArC), 125.8 (P attached *p*-ArC), 53.1 (CH), 25.9 (CH₃) ppm. ³¹P{¹H} NMR (161.9 MHz, CDCl₃): δ 54.9 (d, *J*_{P-B} = 80.95 Hz) ppm. ¹¹B{¹H} NMR (128.4 MHz, CDCl₃): δ -37.9 (br) ppm. FT-IR (selected frequencies): ν 3438 (N–H), 1436 (P–C), 909 (P–N), 2379 (B–H), 608 (P–B) cm⁻¹. Elemental analysis: C₂₀H₂₃BNP (319.17): Calcd. C 75.26, H 7.26, N 4.39. Found C 74.14, H 6.86, N 3.99.

5.5.10. Synthesis of [Ph₂P(BH₃)HN(*S*-*CHMePh)] (38b): Same as above for **38a**.

¹H NMR (400 MHz, CDCl₃): δ 7.60-7.54 (m, 4H, ArH), 7.45-7.30 (m, 6H, ArH), 7.24-7.15 (m, 5H, ArH), 4.47-4.37 (m, 1H, CH), 2.48 (br, 1H, NH), 1.40 (d, *J*_{H-H} = 6.76 Hz, 3H, CH₃), 1.17-0.75 (br, 3H, BH₃) ppm. ¹³C{¹H} NMR (100 MHz, CDCl₃): δ 145.1 (ArC), 132.4 (P-ArC), 131.9 (P attached *o*-ArC), 131.1 (*o*-ArC), 128.5 (P attached *m*-ArC), 128.3 (*m*-ArC), 127.0 (*p*-ArC), 125.8 (P attached *p*-ArC), 53.1 (CH), 25.9 (CH₃) ppm. ³¹P{¹H} NMR (161.9 MHz, CDCl₃): δ 54.9 (d, *J*_{P-B} = 80.95 Hz) ppm. ¹¹B{¹H} NMR (128.4 MHz, CDCl₃): δ -37.9 (d, *J*_{B-P} = 62.91 Hz) ppm. FT-IR (selected frequencies): ν 3438 (N–H), 1436 (P–C), 909 (P–N), 2379 (B–H), 608 (P–B) cm⁻¹. Elemental analysis: C₂₀H₂₃BNP (319.17): Calcd. C 75.26, H 7.26, N 4.39. Found C 74.23, H 6.89, N 3.92.

5.5.11. Synthesis of $[(\text{THF})_2\text{Ba}\{\text{Ph}_2\text{P}(\text{BH}_3)\text{N}(\text{R}-^*\text{CHMePh})\}_2]$ (**39a**) :

Route 1: In a 25 ml pre-dried Schlenk flask, ligand **38a** or **38b**, potassium bis(trimethylsilyl)amide and BaI_2 (100 mg, 0.26 mmol) were mixed in 10 ml THF solvent at ambient temperature and stirring continued for 12 hours. The white precipitate of KI was filtered off and filtrate was evaporated in *vacuo*. The resulting white residue was further purified by washing with *n*-pentane and crystals suitable for X-ray analysis were grown from THF/*n*-pentane (1: 2) mixture at -40°C . Yield: 154.0 mg, (90%) (**39a**) and Yield 156 g, (91%) (**39b**). ^1H NMR (400 MHz, C_6D_6): δ 7.60-7.54 (m, 4H, ArH), 7.45-7.30 (m, 6H, ArH), 7.24-7.15 (m, 5H, ArH), 4.48-4.39 (m, 1H, CH), 2.48 (br, 1H, NH), 1.40 (d, $J_{\text{H-H}} = 6.76$ Hz, 3H, CH_3), 1.49-0.94 (br, 3H, BH_3) ppm. $^{13}\text{C}\{^1\text{H}\}$ NMR (100 MHz, C_6D_6): δ 144.7 (ArC), 132.0 (P-ArC), 131.8 (P attached *o*-ArC), 131.6 (*o*-ArC), 128.5 (P attached *m*-ArC), 128.3 (*m*-ArC), 127.1 (*p*-ArC), 126.3 (P attached *p*-ArC), 52.7 (CH), 25.2 (CH_3) ppm. $^{31}\text{P}\{^1\text{H}\}$ NMR (161.9 MHz, C_6D_6): δ 46.9 ppm. $^{11}\text{B}\{^1\text{H}\}$ NMR (128.4 MHz, C_6D_6): δ -34.9 (d) ppm. FT-IR (selected frequencies): ν 1434 (P-C), 999 (P-N), 2383 (B-H), 602 (P-B) cm^{-1} . Elemental analysis: $\text{C}_{48}\text{H}_{60}\text{B}_2\text{BaN}_2\text{O}_2\text{P}_2$ (917.87): Calcd. C 62.81, H 6.59, N 3.05. Found C 61.94, H 6.20, N 2.83.

5.6 X-Ray crystallographic studies

Single crystals of compounds **35–39** were grown from THF and *n*-pentane mixture at -40°C under inert atmosphere. The single crystals of **32a,b** and **38a,b** suitable for X-ray measurement were grown from $\text{CH}_2\text{Cl}_2/\text{THF}$ at room temperature. For compounds **32–39**, a crystal of suitable dimensions was mounted on a CryoLoop (Hampton Research Corp.) with a layer of light mineral oil and placed in a nitrogen stream at 150(2) K. However for compounds **32a,b** and **38a,b**, the data were collected at 293 K. All measurements were made on an Agilent Supernova X-calibur Eos CCD detector with graphite-monochromatic $\text{Cu-K}\alpha$ (1.54184 Å) radiation. Crystal data and structure refinement parameters are summarised in Table 5.1-5.4. The structures were solved by direct methods (SIR92)⁴¹ and refined on F^2 by full-matrix least-squares methods; using SHELXL-97.⁴² Non-hydrogen atoms were anisotropically refined. H atoms were included in the refinement in calculated positions riding on their carrier atoms. The function minimised was $[\sum w(F_o^2 - F_c^2)^2]$ ($w =$

$1 / [\sigma^2 (Fo^2) + (aP)^2 + bP]$, where $P = (\text{Max}(Fo^2, 0) + 2Fc^2) / 3$ with $\sigma^2(Fo^2)$ from counting statistics. The function $R1$ and $wR2$ were $(\Sigma|Fo| - |Fc|) / \Sigma|Fo|$ and $[\Sigma w(Fo^2 - Fc^2)^2 / \Sigma(wFo^4)]^{1/2}$, respectively. The Diamond-3 program was used to draw the molecule.

5.7 Tables

Table 5.1. Crystallographic data of compounds **32a**, **32b** and **35a**

Crystal	32a	32b	35a
CCDC No.			
Empirical formula	C ₂₀ H ₂₀ NPSe	C ₂₀ H ₂₀ NPSe	C ₄₈ H ₅₄ CaN ₂ O ₂ P ₂ Se ₂
Formula weight	384.30	384.30	950.87
<i>T</i> (K)	293(2)	293(2)	150(2)
λ (Å)	1.54184	1.54184	1.54184
Crystal system	Triclinic	Triclinic	Monoclinic
Space group	<i>P</i> 1	<i>P</i> 1	<i>P</i> 2 ₁
<i>a</i> (Å)	6.0159(11)	6.0127(12)	13.0607(5)
<i>b</i> (Å)	9.3867(17)	9.368(3)	14.5382(5)
<i>c</i> (Å)	9.5866(17)	9.581(3)	13.6308(6)
α (°)	106.872(16)	106.91(3)	90
β (°)	107.869(16)	107.98(2)	118.032(5)
γ (°)	103.345(15)	103.26(2)	90
<i>V</i> (Å ³)	461.65(14)	459.9(2)	2284.57(15)
<i>Z</i>	1	1	2
<i>D</i> _{calc} g cm ⁻³	1.382	1.388	1.382
μ (mm ⁻¹)	3.545	3.558	3.971
<i>F</i> (000)	196	196	980
Theta range for data collection	5.26 to 70.94 deg.	5.27 to 71.98 deg.	3.67 to 70.76 deg.
Limiting indices	-7<= <i>h</i> <=7 -11<= <i>k</i> <=8 -11<= <i>l</i> <=11	-7<= <i>h</i> <=6 -11<= <i>k</i> <=11 -11<= <i>l</i> <=11	-14<= <i>h</i> <=15 -9<= <i>k</i> <=17 -16<= <i>l</i> <=16
Reflections collected / unique	3019 / 2114 [<i>R</i> (int) = 0.0216]	3475 / 2382 [<i>R</i> (int) = 0.0218]	9628 / 6006 [<i>R</i> (int) = 0.0310]
Completeness to theta = 71.25	96.6 % (70.94)	95.2 % (71.98)	97.9 % (70.76)
Absorption correction	Multi-scan	Multi-scan	Multi-scan
Max. and min. transmission	1.00000 and 0.25106	1.00000 and 0.78826	1.00000 and 0.62045
Refinement method	Full-matrix least-squares on <i>F</i> ²	Full-matrix least-squares on <i>F</i> ²	Full-matrix least-squares on <i>F</i> ²
Data / restraints / parameters	2114 / 3 / 210	2382 / 3 / 211	6006 / 1 / 517
Goodness-of-fit on <i>F</i> ²	1.086	1.015	1.025
Final <i>R</i> indices [<i>I</i> >2σ(<i>I</i>)]	<i>R</i> 1 = 0.0544, <i>wR</i> 2 = 0.1402	<i>R</i> 1 = 0.0542, <i>wR</i> 2 = 0.1610	<i>R</i> 1 = 0.0342, <i>wR</i> 2 = 0.0874
<i>R</i> indices (all data)	<i>R</i> 1 = 0.0547, <i>wR</i> 2 = 0.1417	<i>R</i> 1 = 0.0552, <i>wR</i> 2 = 0.1657	<i>R</i> 1 = 0.0359, <i>wR</i> 2 = 0.0895
Absolute structure parameter	0.00(5)	0.01(5)	0.002(13)
Largest diff. peak and hole	0.885 and -0.394 e.Å ⁻³	0.618 and -0.735 e.Å ⁻³	0.455 and -0.607 e.Å ⁻³

Table 5.2. Crystallographic data of compounds **35b**, **36a** and **36b**

Crystal	35b	36a	36b
CCDC No.			
Empirical formula	C ₄₈ H ₅₄ CaN ₂ O ₂ P ₂ Se ₂	C ₄₈ H ₅₄ N ₂ O ₂ P ₂ Se ₂ Sr	C ₄₈ H ₅₄ N ₂ O ₂ P ₂ Se ₂ Sr
Formula weight	950.87	998.41	998.41
<i>T</i> (K)	150(2)	150(2)	150(2)
λ (Å)	1.54184	1.54184	1.54184
Crystal system	Monoclinic	Monoclinic	Monoclinic
Space group	<i>P</i> 2 ₁	<i>P</i> 2 ₁	<i>P</i> 2 ₁
<i>a</i> (Å)	13.0797(10)	12.5000(7)	12.4934(6)
<i>b</i> (Å)	14.5246(8)	14.6217(4)	14.6187(7)
<i>c</i> (Å)	13.6284(14)	13.9074(8)	13.9134(6)
α (°)	90	90	90
β (°)	117.984(11)	115.038(7)	115.041(5)
γ (°)	90	90	90
<i>V</i> (Å ³)	2286.4(3)	2303.0(2)	2302.25(19)
<i>Z</i>	2	2	2
<i>D</i> _{calc} g cm ⁻³	1.381	1.440	1.439
μ (mm ⁻¹)	3.968	4.391	4.393
<i>F</i> (000)	980	1016	1014
Theta range for data collection	3.67 to 70.73 deg.	3.51 to 70.58 deg.	3.51 to 70.63 deg.
Limiting indices	-11<= <i>h</i> <=15 -17<= <i>k</i> <=10 -16<= <i>l</i> <=15	-14<= <i>h</i> <=15 -17<= <i>k</i> <=17 -17<= <i>l</i> <=16	-15<= <i>h</i> <=14 -13<= <i>k</i> <=17 -16<= <i>l</i> <=16
Reflections collected / unique	6276 / 4644 [R(int) = 0.0327]	10051 / 6833 [R(int) = 0.0397]	11230 / 6302 [R(int) = 0.0424]
Completeness to theta = 71.25	83.8 % (70.73)	97.8 % (70.58)	98.2 % (70.63)
Absorption correction	Multi-scan	Multi-scan	Multi-scan
Max. and min. transmission	1.00000 and 0.64464	1.00000 and 0.71299	1.00000 and 0.52179
Refinement method	Full-matrix least-squares on F ²	Full-matrix least-squares on F ²	Full-matrix least-squares on F ²
Data / restraints / parameters	4644 / 1 / 517	6833 / 1 / 517	6302 / 1 / 517
Goodness-of-fit on F ²	1.052	1.049	1.032
Final R indices [I > 2σ(I)]	R1 = 0.0425, wR2 = 0.1123	R1 = 0.0602, wR2 = 0.1622	R1 = 0.0402, wR2 = 0.0979
R indices (all data)	R1 = 0.0456, wR2 = 0.1169	R1 = 0.0650, wR2 = 0.1697	R1 = 0.0464, wR2 = 0.1032
Absolute structure parameter	-0.05(3)	0.00(3)	0.00(2)
Largest diff. peak and hole	0.381 and -0.530 e.Å ⁻³	1.680 and -0.805 e.Å ⁻³	0.722 and -0.756 e.Å ⁻³

Table 5.3. Crystallographic data of compounds **37a**, **37b** and **38a**

Crystal	37a	37b	38a
CCDC No.			
Empirical formula	C ₄₈ H ₅₄ BaN ₂ O ₂ P ₂ Se ₂	C ₄₈ H ₅₄ BaN ₂ O ₂ P ₂ Se ₂	C ₂₀ H ₂₃ BNP
Formula weight	1048.12	1048.12	319.17
<i>T</i> (K)	150(2)	150(2)	293(2)
λ (Å)	1.54184	1.54184	1.54184
Crystal system	Monoclinic	Monoclinic	Monoclinic
Space group	<i>P</i> 2 ₁	<i>P</i> 2 ₁	<i>P</i> 2 ₁
<i>a</i> (Å)	12.5451(2)	12.5571(3)	11.3581(10)
<i>b</i> (Å)	14.6496(3)	14.6478(3)	6.1729(5)
<i>c</i> (Å)	14.0905(2)	14.0913(4)	13.3347(12)
α (°)	90	90	90
β (°)	115.323(2)	115.305(3)	90.752(8)
γ (°)	90	90	90
<i>V</i> (Å ³)	2340.73(7)	2343.16(10)	934.85(14)
<i>Z</i>	2	2	2
<i>D</i> _{calc} g cm ⁻³	1.487	1.486	1.134
μ (mm ⁻¹)	9.319	9.309	1.264
<i>F</i> (000)	1052	1052	340
Theta range for data collection	3.47 to 70.86 deg.	3.47 to 71.12 deg.	3.31 to 70.69 deg.
Limiting indices	-14<= <i>h</i> <=15 -14<= <i>k</i> <=17 -16<= <i>l</i> <=17	-13<= <i>h</i> <=15 -12<= <i>k</i> <=17 -16<= <i>l</i> <=17	-13<= <i>h</i> <=13 -7<= <i>k</i> <=7 -16<= <i>l</i> <=13
Reflections collected / unique	9480 / 6551 [R(int) = 0.0284]	10629 / 6444 [R(int) = 0.0436]	3685 / 2609 [R(int) = 0.0280]
Completeness to theta = 71.25	98.2 % (70.86)	98.1 % (71/12)	97.7 %
Absorption correction	Multi-scan	Multi-scan	Multi-scan
Max. and min. transmission	1.00000 and 0.39804	1.00000 and 0.31944	1.00000 and 0.86951
Refinement method	Full-matrix least-squares on F ²	Full-matrix least-squares on F ²	Full-matrix least-squares on F ²
Data / restraints / parameters	6551 / 1 / 519	6444 / 1 / 516	2609 / 1 / 211
Goodness-of-fit on F ²	1.031	1.061	1.044
Final R indices [I>2σ(I)]	R1 = 0.0391, wR2 = 0.1042	R1 = 0.0538, wR2 = 0.1402	R1 = 0.0478, wR2 = 0.1179
R indices (all data)	R1 = 0.0394, wR2 = 0.1047	R1 = 0.0543, wR2 = 0.1412	R1 = 0.0573, wR2 = 0.1285
Absolute structure parameter	-0.009(3)	-0.004(4)	0.00(4)
Largest diff. peak and hole	1.081 and -1.064 e.Å ⁻³	1.568 and -1.383 e.Å ⁻³	0.140 and -0.297 e.Å ⁻³

Table 5.4. Crystallographic data of compounds **38b**, **39a** and **39b**

Crystal	38b	39a	39b
CCDC No.			
Empirical formula	C ₂₀ H ₂₃ BNP	C ₄₈ H ₆₀ B ₂ BaN ₂ O ₂ P ₂	C ₄₈ H ₆₀ B ₂ BaN ₂ O ₂ P ₂
Formula weight	319.17	917.87	917.87
<i>T</i> (K)	293(2)	150(2)	150(2)
λ (Å)	1.54184	1.54184	1.54184
Crystal system	Orthorhombic	Monoclinic	Monoclinic
Space group	<i>P</i> 2 ₁ 2 ₁ 2 ₁	<i>P</i> 2 ₁	<i>P</i> 2 ₁
<i>a</i> (Å)	8.8785(2)	13.1696(9)	13.1465(5)
<i>b</i> (Å)	18.0839(4)	14.8039(4)	14.7929(3)
<i>c</i> (Å)	23.6013(6)	13.7579(9)	13.7413(7)
α (°)	90	90	90
β (°)	90	117.394(9)	117.316(5)
γ (°)	90	90	90
<i>V</i> (Å ³)	3789.38(15)	2381.5(2)	2374.34(16)
<i>Z</i>	8	2	2
<i>D</i> _{calc} g cm ⁻³	1.119	1.280	1.284
μ (mm ⁻¹)	1.247	7.403	7.425
<i>F</i> (000)	1360	948	948
Theta range for data collection	3.08 to 70.72 deg.	3.62 to 70.75 deg.	3.62 to 70.78 deg.
Limiting indices	-9<= <i>h</i> <=10 -18<= <i>k</i> <=21 -28<= <i>l</i> <=26	-16<= <i>h</i> <=12 -16<= <i>k</i> <=18 -10<= <i>l</i> <=16	-16<= <i>h</i> <=15, -10<= <i>k</i> <=17, -15<= <i>l</i> <=16
Reflections collected / unique	10266 / 5991 [<i>R</i> (int) = 0.0257]	10805 / 7370 [<i>R</i> (int) = 0.0310]	11397 / 6453 [<i>R</i> (int) = 0.0320]
Completeness to theta = 71.25	98.0 % (70.72)	98.1 % (70.75)	97.5 %
Absorption correction	Multi-scan	Multi-scan	Multi-scan
Max. and min. transmission	1.00000 and 0.66265	1.00000 and 0.66652	1.00000 and 0.51058
Refinement method	Full-matrix least-squares on <i>F</i> ²	Full-matrix least-squares on <i>F</i> ²	Full-matrix least-squares on <i>F</i> ²
Data / restraints / parameters	5991 / 0 / 420	7370 / 1 / 540	6453 / 1 / 541
Goodness-of-fit on <i>F</i> ²	1.034	1.004	1.021
Final <i>R</i> indices [<i>I</i> >2σ(<i>I</i>)]	<i>R</i> ₁ = 0.0418, <i>wR</i> ₂ = 0.1102	<i>R</i> ₁ = 0.0357, <i>wR</i> ₂ = 0.0905	<i>R</i> ₁ = 0.0333, <i>wR</i> ₂ = 0.0843
<i>R</i> indices (all data)	<i>R</i> ₁ = 0.0482, <i>wR</i> ₂ = 0.1183	<i>R</i> ₁ = 0.0387, <i>wR</i> ₂ = 0.0935	<i>R</i> ₁ = 0.0338, <i>wR</i> ₂ = 0.0850
Absolute structure parameter	0.000(19)	-0.021(4)	-0.019(4)
Largest diff. peak and hole	0.212 and -0.286 e.Å ⁻³	0.611 and -1.613 e.Å ⁻³	0.693 and -1.307 e.Å ⁻³

References:

- (1) Kazmaier, U. *Angew. Chem. Int. Ed.* **2009**, *48*, 5790-5792.
- (2) Harder, S. *Chem. Rev.* **2010**, *110*, 3852-3876.
- (3) Kobayashi, S.; Yamashita, Y. *Acc. Chem. Res.* **2011**, *44*, 58-71.
- (4) Yanagisawa, A.; Yoshida, K. *Synlett.* **2011**, *20*, 2929-2938.
- (5) Yamashita, Y.; Tsubogo, T.; Kobayashi, S. *Chem. Sci.* **2012**, *3*, 967-975.
- (6) (a) Dechy-Cabaret, O.; Martin-Vaca, B.; Bourissou, D. *Chem. Rev.* **2004**, *104*, 6147-6176. (b) O'Keefe, B.; Hillmyer, J. M. A.; Tolman, W. B. *Dalton Trans.* **2001**, 2215-2225. (c) Wheaton, C. A.; Hayes, P. G.; Ireland, B. *Dalton Trans.* **2009**, 4832-4846. (d) Thomas, C. M. *Chem. Soc. Rev.* **2010**, *39*, 165-173.
- (7) (a) Li, S. M.; Rashkov, I.; Espartero, J. L.; Manolova, N.; Vert, M. *Macromolecules* **1996**, *29*, 57-62. (b) Dobrzyński, P.; Kasperczyk, J.; Bero, M. *Macromolecules* **1999**, *32*, 4735-4737. (c) Zhong, Z.; Dijkstra, P. J.; Birg, C.; Westerhausen, M.; Feijen, J. *Macromolecules* **2001**, *34*, 3863-3868. (d) Westerhausen, M.; Schneiderbauer, S.; Kneifel, A. N.; Sörtl, Y.; Mayer, P.; Nöth, H.; Zhong, Z.; Dijkstra, P. J.; Feijen, J. *Eur. J. Inorg. Chem.* **2003**, 3432-3439. (e) Chisholm, M. H.; Gallucci, J.; Phomphrai, K. *Chem. Commun.* **2003**, 48-49. (f) Hill, M. S.; Hitchcock, P. B. *Chem. Commun.* **2003**, 1758-1759. (g) Chisholm, M. H.; Gallucci, J. C.; Phomphrai, K. *Inorg. Chem.* **2004**, *43*, 6717-6725. (h) Sarazin, Y.; Howard, R. H.; Hughes, D. L.; Humphrey, S. M.; Bochmann, M. *Dalton Trans.* **2006**, 340-350. (i) Darensbourg, D. J.; Choi, W.; Ganguly, P.; Richers, C. P. *Macromolecules* **2006**, *39*, 4374-4379. (j) Davidson, M. G.; O'Hara, C. T.; Jones, M. D.; Keir, C. G.; Mahon, M. F.; Kociok-Köhn, G. *Inorg. Chem.* **2007**, *46*, 7686-7888. (k) Darensbourg, D. J.; Choi, W.; Richers, C. P. *Macromolecules* **2007**, *40*, 3521-3523. (l) Darensbourg, D. J.; Choi, W.; Karroonnirun, O.; Bhuvanesh, N. *Macromolecules* **2008**, *41*, 3493-3502. (m) Poirier, V.; Roisnel, T.; Carpentier, J.-F.; Sarazin, Y. *Dalton Trans.* **2009**, 9820-9827. (n) Xu, X.; Chen, Y.; Zou, G.; Ma, Z.; Li, G. *J. Organomet. Chem.* **2010**, *695*, 1155-1162. (o) Sarazin, Y.; Rosca, D.; Poirier, V.; Roisnel, T.; Silvestru, A.; Maron, L.; Carpentier, J.-F. *Organometallics* **2010**, *29*, 6569-6577. (p) Sarazin, Y.; Liu, B.; Roisnel, T.; Maron, L.; Carpentier, J.-F. *J. Am. Chem. Soc.* **2011**, *133*, 9069-9087.

- (8) (a) Harder, S.; Feil, F.; Knoll, K. *Angew. Chem., Int. Ed.* **2001**, *40*, 4261-4264. (b) Harder, S.; Feil, F. *Organometallics* **2002**, *21*, 2268-2274. (c) Jochmann, P.; Dols, T. S.; Spaniol, T. P.; Perrin, L.; Maron, L.; Okuda, J. *Angew. Chem., Int. Ed.* **2009**, *48*, 5715-5719.
- (9) (a) Barrett, A. G. M.; Crimmin, M. R.; Hill, M. S.; Procopiou, P. A. *Proc. R. Soc. London, Ser. A* **2010**, *466*, 927-963. (b) Harder, S. *Chem. Rev.* **2010**, *110*, 3852-3876.
- (10) Yamada, Y.M.; Shibasaki, M. *Tetrahedron Lett.* **1998**, *39*, 5561-5564.
- (11) Suzuki, T.; Yamagiwa, N.; Matsuo, Y.; Sakamoto, S.; Yamaguchi, K.; Shibasaki, M.; Noyori, R. *Tetrahedron Lett.* **2001**, *42*, 4669-4671.
- (12) Saito, S.; Kobayashi, S. *J. Am. Chem. Soc.* **2006**, *128*, 8704-8705.
- (13) Yamada, Y.M.A.; Ikegami, S. *Tetrahedron Lett.* **2000**, *41*, 2165-2169.
- (14) Yamaguchi, A.; Matsunaga, S.; Shibasaki, M. *J. Am. Chem. Soc.* **2009**, *131*, 10842-10843.
- (15) Jacobsen, E.N.; Pfaltz, A.; Yamamoto, H. (eds) **1999** *Comprehensive asymmetric catalysis*, 1st edn. Springer, Berlin.
- (16) Almasi, D.; Alonso, D.A.; Na'jera, C. *Tetrahed. Asym.* **2007**, *18*, 299-365.
- (17) Tsogoeva, S.B. *Eur. J. Org. Chem.* **2007**, *11*, 1701-1716.
- (18) Hayashi, T.; Yamasaki, K. *Chem. Rev.* **2003**, *103*, 2829-2844.
- (19) Christoffers, J.; Baro, A. *Angew. Chem. Int. Ed.* **2003**, *42*, 1688-1690.
- (20) Berner, O. M.; Tedeschi, L.; Enders, D. *Eur. J. Org. Chem.* **2002**, *12*, 1877-1894.
- (21) (a) Brunner, H.; Gastinger, R. G. *J. Organomet. Chem.* **1978**, *145*, 365-373. (b) Brunner, H.; G. O. Nelson *J. Organomet. Chem.* **1979**, *173*, 389-395. (c) Frauendorfer, E.; Brunner, H. *J. Organomet. Chem.* **1982**, *240*, 371-379.
- (22) Wiecko, M.; Girnt, D.; Rastatter, M.; Panda, T. K.; Roesky, P. W. *Dalton Trans.* **2005**, 2147-2150.
- (23) Panda, T. K.; Gamer, M. T.; Roesky, P. W. *Inorg. Chem.* **2006**, *45*, 910-916.
- (24) The bonding situation in the drawing of the ligand system is simplified for clarity.
- (25) Naktode, K.; Kottalanka, R. K.; Panda, T. K. *New J. Chem.* **2012**, *36*, 2280-2285.
- (26) Bhattacharjee, J.; Kottalanka, R. K.; Harinath, A.; Panda, T. K. *J. Chem. Sci.* **2014**, Accepted.

- (27) Greenwood, N. N.; Earnshaw, A. *Chemistry of the Elements*, Pergamon Press, Oxford, U.K., **1984**.
- (28) Panda, T. K.; Kaneko, H.; Michel, O.; Tsurugi, H.; Pal, K.; Törnroos, K. W.; Anwander, R.; Mashima, K. *Organometallics* **2012**, *31*, 3178–3184.
- (29) Kling, C.; Ott, H.; Schwab, G.; Stalke, D. *Organometallics* **2008**, *27*, 5038–5042.
- (30) English, U.; Ruhland-Senge, K. *Z. Anorg. Allg. Chem.* **2001**, *627*, 851–856.
- (31) Hao, H.; Bhandari, S.; Ding, Y.; Roesky, H. W.; Magull, J.; Schmidt, H. G.; Noltemeyer, M.; Cui, C. *Eur. J. Inorg. Chem.* **2002**, 1060-1065.
- (32) (a) Ruhlandt-Senge, K.; Davis, K.; Dalal, S.; English, U.; Senge, M. O. *Inorg. Chem.* **1995**, *34*, 2587-2592. (b) Al-Shboul, T. M. A.; Volland, G.; Görls, H.; Krieck, S.; Westerhausen, M. *Inorg. Chem.* **2012**, *51*, 7903-7912.
- (33) Balanta-Díaz, J. A.; Moya-Cabrera, M.; Jancik, V.; Morales-Juárez, T. J.; Cea-Olivares, R. *Polyhedron* **2013**, *63* 167-172.
- (34) Ruhlandt-Senge, K.; English, U. *Chem. Eur. J.* **2000**, *6*, 4063-4070.
- (35) (a) Anderson, B. J.; Glueck, D. S.; DiPasquale, A. G.; Rheingold, A. L. *Organometallics* **2008**, *27*, 4992–5001. (b) Hubert, S.; Stützer, A.; Bissinger, P.; Schier, A. *Z. Anorg. Allg. Chem.* **1993**, *619*, 1519-1525.
- (36) Kuzdrowska M.; Annunziata L.; Marks S.; Schmid M.; Jaffredo C. G.; Roesky P. W.; Guillaume S. M.; Maron L. *Dalton Trans.*, **2013**, *42*, 9352–9360.
- (37) Liu B.; Roisnel T.; Guegan J.-P.; Carpentier J.-F.; Sarazin Y. *Chem.–Eur. J.*, **2012**, *18*, 6289–6301.
- (38) Sarazin Y.; Liu B.; Maron L.; Carpentier J.-F. *J. Am. Chem. Soc.*, **2011**, *133*, 9069–9087.
- (39) Davidson M. G.; O'Hara C. T.; Jones M. D.; Keir C. G.; Mahon M. F.; Kociok-Köhne G.; *Inorg. Chem.*, **2007**, *46*, 7686–7688.
- (40) (a) Palard I.; Soum A.; Guillaume S. M.; *Chem.–Eur. J.*, **2004**, *10*, 4054–4062. (b) Jenter J.; Roesky P. W.; Ajellal N.; Guillaume S. M.; Susperregui N.; Maron L. *Chem.–Eur. J.*, **2010**, *16*, 4629–4638.
- (41) M. Sheldrick, SHELXS-97. *Program of Crystal Structure Solution, University of Göttingen, Germany*, **1997**.

- (42) G. M. Sheldrick, SHELXL-97. *Program of Crystal Structure Refinement, University of Göttingen, Germany, 1997.*

Chapter 6

Alkali and alkaline-earth metal complexes having rigid bulky-iminopyrrolyl ligand in the coordination sphere: syntheses, structures and ϵ -caprolactone polymerization

6.1 Introduction

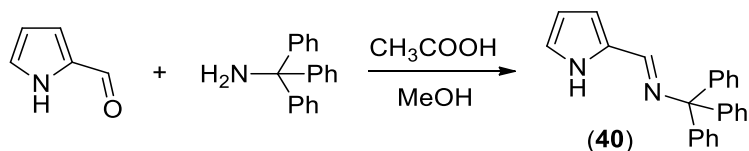
In recent years, monoanionic bidentate or tridentate nitrogen ligands are of particular interest because they can able to stabilize vast number of metal complexes. Among such type of ligands, 2-iminopyrrolyl bidentate chelating ligands have attracted in the recent times. 2-iminopyrrolyls contains an anionic pyrrolyl ring substituted in position 2 by a neutral imine donor moiety, and these are structurally similar to salicylaldiminate, anilidoimine or 2-(2-pyridyl)indolyl ligands. The 2-iminopyrrolyls are appealing ligands because they are readily accessible and easy to modify, either sterically or electronically, via straightforward Schiff-base condensation procedures.¹ The first examples of homoleptic 2-iminopyrrolyl metal complexes of Co(II), Ni(II), Pd(II), Cu(II) and Zn(II) have been described in the 1960s.² However, recently this class of ligands has been commonly employed in the synthesis of several transition-metals and rare-earth metal compounds.³ The metal complexes including main group metals, transition metals as well as rare-earth metals having 2-iminopyrrolyl in their coordination sphere are act as efficient polymerization catalysts.⁴ Very recently, *Roesky et al.* reported the heavier alkaline earth metal complexes of tridentate 2,5 bis{N-2,6-(diisopropylphenyl)iminomethyl}-pyrrolyl ligands as hydroamination catalysts.⁵ Recently, *Mashima* group also reported the synthesis and characterization of the group 2 metal complexes supported by bidentate iminopyrrolyl ligands and their application for catalytic ring-opening polymerization of ϵ -caprolactone with respect to the effects of the ionic radii of the group 2 metal centers.⁶ Inspired by these results and as a part of my thesis work to develop highly efficient and well-characterized homogenous single-site ROP catalysts by using alkaline-earth metals, we were interested to synthesize a very rigid bulky iminopyrrolyl system by using pyrrole-2-carboxyaldehyde

and tritylamine involving simple Schiff-base condensation procedure.¹ In this chapter, we have described the detailed synthesis and structural characterization of bidentate rigid bulky-iminopyrrolyl ligand (2-(Ph₃CN=CH)-C₄H₃NH) (**40**) and their corresponding alkali metal complexes of molecular composition {Li(2-(Ph₃CN=CH)-C₄H₃N)(THF)₂} (**41**) and {Na(2-(Ph₃CN=CH)-C₄H₃N)(THF)₂}₂ (**42**) and [(2-(Ph₃CN=CH)-C₄H₃N)K(THF)_{0.5}]₄ (**43**). The detailed syntheses and solid state structures of two magnesium complexes of composition {Mg(CH₂Ph)(2-(Ph₃CN=CH)-C₄H₃N)(THF)₂} (**44**) and {Mg(2-(Ph₃CN=CH)-C₄H₃N)₂(THF)₂} (**45**) were also described. The heavier alkaline-earth metal complexes of composition {M(2-(Ph₃CN=CH)-C₄H₃N)₂(THF)_n} (M = Ca (**46**), Sr (**47**) and n = 2; M = Ba (**48**), n = 3) were synthesized by using two synthetic routes and solid state structures were discussed in detailed. In this chapter, Ring-Opening Polymerization study of ε-caprolactone by using alkaline-earth metal complexes (**44-48**) with different monomer/catalyst ratios were discussed in detailed.

6.2 Results and Discussion

6.2.1. Ligand synthesis:

(*E*)-*N*-((1*H*-pyrrol-2-yl)methylene)-1,1,1-triphenylmethanamine ligand {2-(Ph₃CN=CH)-C₄H₃NH} (**40**) was prepared by the condensation reaction of pyrrol-2-carboxyaldehyde with 1 equiv. of tritylamine in the presence of a catalytic amount of glacial acetic acid in methanol solvent (Scheme 6.1). The bidentate ligand **40** was fully characterized by using standard spectroscopic/analytical techniques and solid state structure was established by using single crystal X-ray diffraction analysis.



Scheme 6.1. Synthesis of bulky iminopyrrolyl ligand **40**.

A strong absorption band observed at 1629 cm⁻¹ in FT-IR spectra indicates a C=N bond in the ligand **40**. This value is within the range of the literature reports.^{7,8} ¹H NMR spectrum of ligand **40** shows broad signal at δ 9.50 ppm for the N-H proton of the pyrrole moiety

and singlet peak assignable to imine N=C-H proton was observed at δ 7.67 ppm. In addition to these, the singlet resonance signal at 6.87 ppm, doublet at 6.39 ppm and multiplets at 6.22 ppm in the ^1H NMR spectra clearly represents the pyrrole ring protons. $^{13}\text{C}\{^1\text{H}\}$ NMR spectra also very informative in this case, we have observed strong resonance signal at δ 150.3 ppm for the imine carbon atom which is in good agreement with reported value δ 153.2 ppm for the compound [2-(2,6- i Pr $_2$ C $_6$ H $_3$ N=CH)-C $_4$ H $_3$ NH] and δ 148.7 ppm for the compound [2-(2-Ph $_2$ PC $_6$ H $_4$ N=CH)-C $_4$ H $_3$ NH].⁸ Another strong peak at δ 77.8 ppm corresponds to the tertiary carbon atom of the CPh $_3$ group. The bulky iminopyrrolyl ligand **40** was readily crystalizes in CH $_2$ Cl $_2$ at room temperature and therefore, the solid state structure of the iminopyrrolyl ligand **40** was also established by using single crystal X-ray diffraction analysis. The solid state structure of ligand **40** was shown in the Figure 6.1 and details of the structural parameter are given in the Table 6.2.

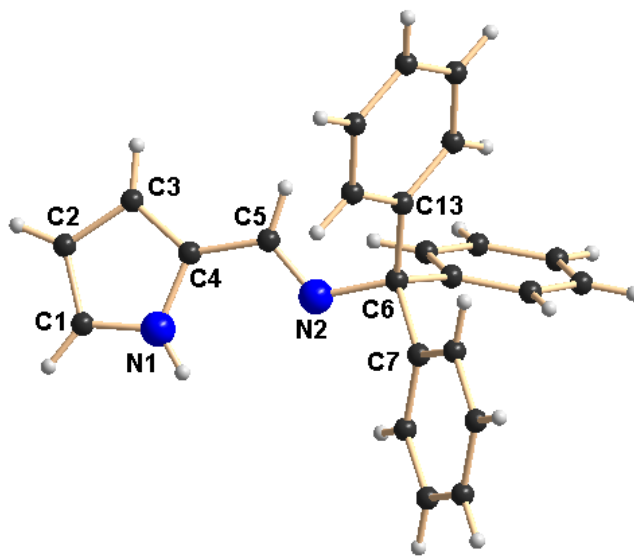


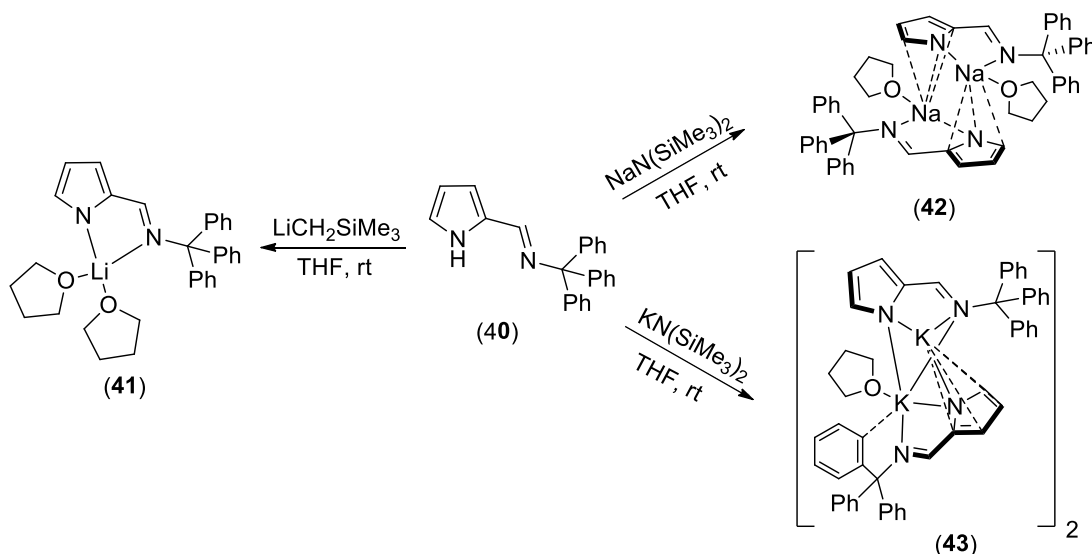
Figure 6.1. Solid-state structure of ligand **40**. Selected bond lengths (\AA) and bond angles ($^\circ$): C1-N1 1.357(6), C1-C2 1.364(8), C2-C3 1.410(7), C3-C4 1.372(7), C4-C5 1.433(6), N2-C5 1.260(6), N2-C6 1.485(6), C6-C7 1.544(7), C6-C13 1.552(6), C6-C19 1.530(6); C1-N1-C4 109.3(4), C4-C5-N2 122.6(5), C5-N2-C6 120.6(4), N2-C6-C7 104.2(4).

The bidentate iminopyrrolyl ligand **40** was crystalizes in monoclinic space group $P 2_1/c$ having 2 independent molecules in the asymmetric unit. The pyrrole ring showed bond

distances within 1.35-1.38 Å and a longer value of 1.410(7) Å for C2-C3 bond was observed. The C1-N1 bond distance 1.357(6) Å was observed which is in good agreement with the value 1.354(4) Å reported for the compound [2-(2,6-*i*Pr₂C₆H₃N=CH)-C₄H₃NH]⁹ and 1.3604(17) Å for the [2-(2,6-*i*Pr₂C₆H₃N=CMe)-C₄H₃NH].¹⁰ The C5-N2 bond distance was 1.260(6) Å which is slightly shorter value compared to the C2-N5 distance 1.2835(19) Å for the compound [2-(2,6-*i*Pr₂C₆H₃N=CMe)-C₄H₃NH].¹⁰ The coplanarity of the pyrrole ring with the acetimine group with torsion angle N1-C4-C5-N2 of 8.667(10)° was observed. The C4-C5 bond distance 1.433(6) Å, a value shorter than the typical C-C single bond distance, indicates the fact that extension of the pyrrole ring π -electron delocalization towards the its acetimine substituent.

6.2.2. Synthesis and characterization of alkali metal complexes:

Treatment of LiCH₂SiMe₃ with 1 equiv. of bulky iminopyrrolyl ligand **40** in THF solvent resulted the corresponding lithium complex of molecular formula {Li(2-(Ph₃CN=CH)-C₄H₃N)(THF)₂} (**41**) and treatment of ligand **40** with 1 equiv. of either sodium or potassium bis(trimethylsilyl)amide in THF solvent resulted the corresponding dimeric sodium complex of composition [(2-(Ph₃CN=CH)C₄H₃N)Na(THF)]₂ (**42**) and tetra-nuclear potassium complex of molecular composition [(2-(Ph₃CN=CH)C₄H₃N)K(THF)_{0.5}]₄ (**43**) in very good yield (Scheme 6.2).¹¹



Scheme 6.2. Synthesis of alkali-metal complexes of bulky iminopyrrolyl ligand **40**.

The alkali-metal complexes **41-43** were fully characterized by using standard spectroscopic/analytical techniques and solid state structures of **41-43** were established by using single crystal X-ray diffraction analysis. ^1H NMR spectra of compounds **41-43** showed a singlet resonance signal at δ 8.17 (for **41**), 8.03 (for **42**) and 7.99 (for **43**) indicate the presence of imine proton in each complex. $^{13}\text{C}\{^1\text{H}\}$ NMR spectra also further supported the presence of imine carbon atom in the each complex by showing the resonance signals at δ 149.3 (for **41**), 147.8 (for **42**) and 149.1 (for **43**). The other pyrrole protons and aromatic protons were showed a resonance signals in each complex at expected regions. Alkali-metal complexes **42-43** showed only one set of signals in each case, which indicates that dynamic behavior of the complex **42-43** in the solution state. The details of the structural parameters were given in the Table 6.2-6.3. In the solid state, lithium complex of composition $\{\text{Li}(2\text{-(Ph}_3\text{CN=CH)-C}_4\text{H}_3\text{N})(\text{THF})_2\}$ (**41**) was crystalizes in orthorhombic space group *P bca* having 16 molecules in the unit cell. The solid state structure and selected bond lengths and bond angles are shown in Figure 6.2.

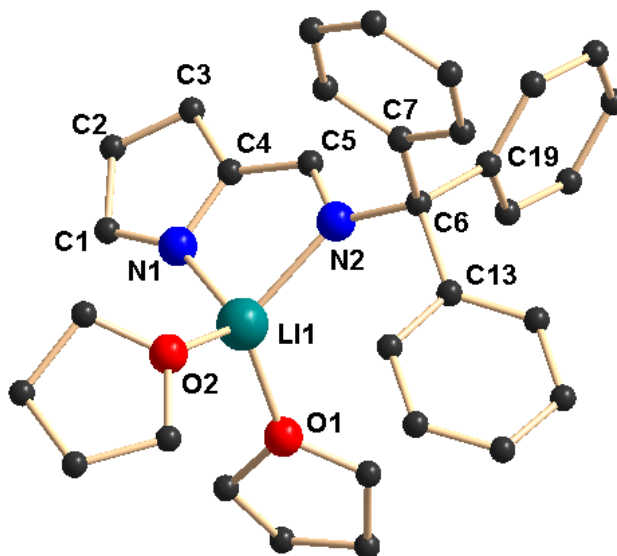


Figure 6.2. Solid state structure of lithium complex **41**. Hydrogen atoms are omitted for clarity. Selected bond lengths (Å) and bond angles (°): Li1-N1 1.993(8), Li1-N2 2.097(7), Li1-O1 1.944(7), Li-O2 1.946(9), N1-C1 1.345(4), C1-C2 1.397(6), C2-C3 1.401(5), C3-C4 1.408(5), N1-C4 1.366(4), C4-C5 1.431(4), N2-C5 1.289(5), N2-C6 1.492(4), C6-C13 1.550(5); N1-Li-N2 87.7(3), N1-Li-O1 114.0(4), N1-Li-O2 110.9(3), N2-Li-O1 115.5(4), N2-Li-O2 120.5(4), O1-Li-O2 107.2(3), C4-C5-N2 122.4(3), N1-C4-C5

121.3(3), N1-C4-C3 111.4(3), N1-C1-C2 112.3(3), Li1-N1-C4 104.6(3), Li1-N2-C5 103.6(3), Li1-N2-C6 138.4(3), N2-C6-C13 107.3(2).

In the lithium complex **41**, the central lithium ion is surrounded by one ligand moiety and two THF molecules. The iminopyrrolyl ligand (**40**) act as a bidentate chelating ligand and coordinates to the metal center through the pyrrolide nitrogen and imine nitrogen atoms. Therefore, the geometry of the lithium ion in the complex **41** was best described as distorted tetrahedral geometry with bond angles of N1-Li1-N2 87.7(3)°, O1-Li1-N1 114.0(4)°, O2-Li1-N1 110.9(3)°, N2-Li1-O1 115.5(4)°, N2-Li1-O2 120.5(4)°, and O1-Li1-O2 107.20(18)°. The Li-N bond lengths of 1.993(8) and 2.097(7) Å were observed in the compound **41** are in good agreement with the Li-N bond lengths found in the reported molecules. For example, Li-N bond length of 2.068(3) and 2.085(3) Å were observed in the complex $\{[\eta^2:\eta^1\text{-}2\text{-}(2,6\text{-Me}_2\text{C}_6\text{H}_3\text{N}=\text{CH})\text{-C}_4\text{H}_3\text{N}]\text{Li}(\text{THF})\}_2$ and 2.105(4) and 2.088(4) Å were observed in the lithium complex $\{[\eta^2:\eta^1\text{-}2\text{-}(2,6\text{-}^i\text{Pr}_2\text{C}_6\text{H}_3\text{N}=\text{CH})\text{-C}_4\text{H}_3\text{N}]\text{Li}(\text{THF})\}_2$.¹² The C1-N1 bond distance 1.345(4) Å and C5-N2 bond distance of 1.289(5) Å of anionic ligand moiety are slightly changed when compared to the free ligand **40** (C1-N1 1.357(6) Å and C5-N2 1.260(6) Å) upon coordination to the lithium ion. The C4-C5 bond distance 1.431(4) Å, a shorter value compared to the value observed in free ligand **40** (1.433(6) Å) demonstrate the extensive delocalization of pyrrole π -electron density was occurring in anionic ligand moiety in the lithium complex **41**. The Li-O bond distances of 1.944(7) and 1.946(9) Å are in within the range to the Li-O bond distances reported in the literature. Therefore, in the lithium complex **41** due to presence of bidentate chelating ligand, a five membered mettallacycle Li1-N1-C4-C5-N2 was formed with bite angle of 87.7(3)°.

The dimeric sodium complex **42**, crystallizes in monoclinic space group $P 2_1/n$ having 2 molecules in the unit cell. The details of the structural parameters are given in the Table 6.2. The solid state structure and selected bond lengths and bond angles were shown in the Figure 6.3. In the dimeric sodium complex **42**, each sodium ion is surrounded by one anionic ligand moiety in a bidentate fashion and one THF molecule. Each sodium ion, further has interactions with pyrrole ring π -electron density of another ligand to form dimeric structure through the bridging Na-pyrrole π -bonding. Therefore, each ligand in the

dimeric sodium complex **42** having ($\sigma + \pi$) bonding mode to the sodium ions and η^3 -coordination was observed for pyrrolyl ring of the each ligand moiety. Therefore, the geometry of the each Na-ion was best described as distorted tetrahedral geometry which is formed due to coordination from two nitrogen atoms of the iminopyrrolyl ligand moiety, one oxygen atom of the THF molecule and η^3 -coordination from pyrrolyl ring of the other iminopyrrolyl ligand. The bite angles of N1-Na1-N2 95.46(5) $^\circ$ and N1ⁱ-Na1-N2 75.44(5) $^\circ$ and N1-Na1-N1ⁱ 85.56(6) $^\circ$ were observed for each of the iminopyrrolyls chelated to sodium atoms. The Na-N bond distances of 2.3586(17) Å and 2.4641(16) Å were in the similar range of the reported Na-N distances observed for the compound [μ^2 : κ^2 -2-(2,6-Me₂C₆H₃N=CH)-C₄H₃N]Na(OEt₂)₂ (2.405(3) and 2.4285(3) Å).⁹ The distance between Na-ion with pyrrole ring atoms (C1, N1 and C4 or C1ⁱ, N1ⁱ and C4ⁱ) were found to be 2.790(2), 2.6998(17) and 2.8670(19) Å respectively.

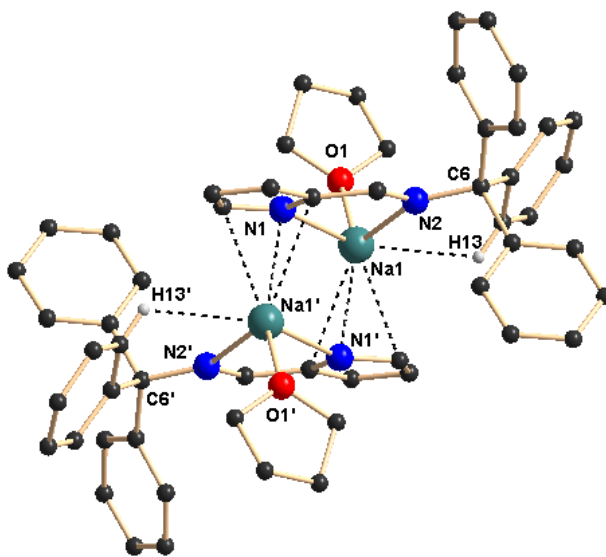
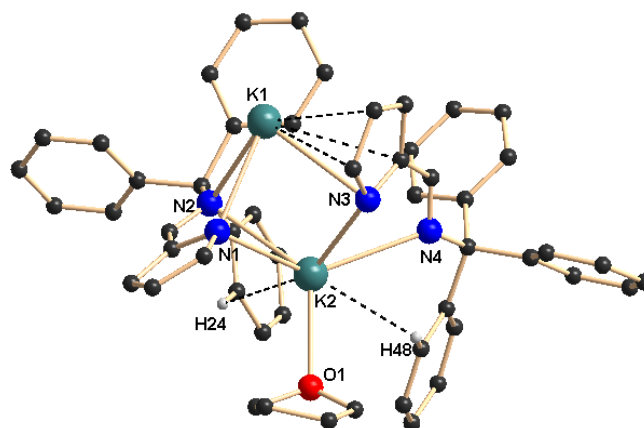


Figure 6.3. Solid state structure of sodium complex **42**. Hydrogen atoms are omitted except H13 for clarity. Selected bond lengths (Å) and bond angles ($^\circ$): Na1-N1ⁱ 2.3586(17), Na1-N2 2.4641(16), Na1-O1 2.3315(17), Na1-N1 2.6998(17), Na1-C1 2.8670(19), Na1-C2 3.080(2), Na1-C3 3.034(2), Na1-C4 2.790(2), Na1-C5 3.0870(19), C4-C5ⁱ 1.436(3), C5-N2 1.289(2), N2-C6 1.493(2), C1-N1 1.382(2), C1-C2 1.403(3), C2-C3 1.396(3), C3-C4 1.396(3); N2-Na1-N1ⁱ 75.44(5), N1-Na1-N2 95.46(5), N1-Na1-O1 147.46(6), N2-Na1-O1 117.06(6), N1ⁱ-Na1-O1 102.83(6), N1-Na1-N1ⁱ 85.56(6), C1-Na1-O1 144.32(7), C2-Na1-O1 117.02(6), C3-Na1-O1 105.33(6), C4-Na1-O1 118.92(6).

These distances are somewhat larger when compared to Na-Pyrrolyl_{centroid} distances 2.447(3) Å and 2.494(3) Å found in the polymeric sodium compounds of the type $[\{\text{Na}(\mu^2:\kappa^2\text{-}N,N^\text{z}\text{-iminopyrrolyl})\}_{2n}(\text{OEt}_2)_{2x}]$ ($n \geq 1$; $x = 0$ or 1), (aryl = C₆H₅ or 2,6-Me₂C₆H₃)⁹ indicating that a moderate π -interactions were exists between the Na-ions and pyrrolyl rings in the dimeric sodium complex **42**. The bond distance of C1-N1 1.349(2) and C4-C5 1.436(3) and C5-N2 1.289(2) Å were almost unchanged compared to free ligand (C1-N1 1.357(6) and C4-C5 1.433(6) and C5-N2 1.260(6) Å) upon coordination to sodium atom. Therefore, each bidentate iminopyrrolyl ligand forms a five membered mettallacycle Na1-N1-C4-C5-N2 or Na1ⁱ-N1ⁱ-C4ⁱ-C5ⁱ-N2ⁱ with sodium atom, where the Na-atoms were slightly deviated from the planarity. Each Na-ion in the dimeric complex **42** is further stabilized by the coordination from one THF molecule. The Na-O bond distance 2.3315(17) Å was well fitted with literature reports. A short contact Na \cdots H between sodium and one of the phenyl proton (Na1 \cdots H13 2.707 Å) is observed which can be attributed as remote or secondary M \cdots H interaction.¹³ However, in solution all phenyl protons were appeared equivalent as observed in ¹H NMR study presumably due to dynamic behavior of the complex.

In contrast to sodium complex **42**, the potassium complex **43**, crystallizes in monoclinic space group *P* 2₁/c having 2 molecules in the unit cell. The details of the structural parameters are given in the Table 6.3. The solid state structure and selected bond lengths and bond angles were shown in the Figure 6.4. The asymmetric unit of potassium complex **43**, having two iminopyrrolyls and two potassium ions and one coordinated THF molecule. In the asymmetric unit, one potassium atom (K2) chelated by two iminopyrrolyl ligands in a bidentate fashion and one THF molecule, whereas the second potassium ion (K1) was surrounded by one iminopyrrolyl ligand in a bidentate fashion and one pyrrolyl group (η^5 -mode) of another iminopyrrolyl ligand present in the asymmetric unit. Therefore, in the grown structure the two potassium atoms (K1 and K1ⁱ) were sandwiched between two pyrrolyl ring π -electron densities in η^5 -fashion and further chelated by imine-nitrogen atoms of the iminopyrrolyls. The other two potassium atoms (K2 and K2ⁱ) were surrounded by iminopyrrolyl moieties in a bidentate fashion and one THF molecule. The potassium

ion K2 further having weak interactions with aromatic ring hydrogen atoms (K2...H24 and K2 ...H48).



Asymmetric unit

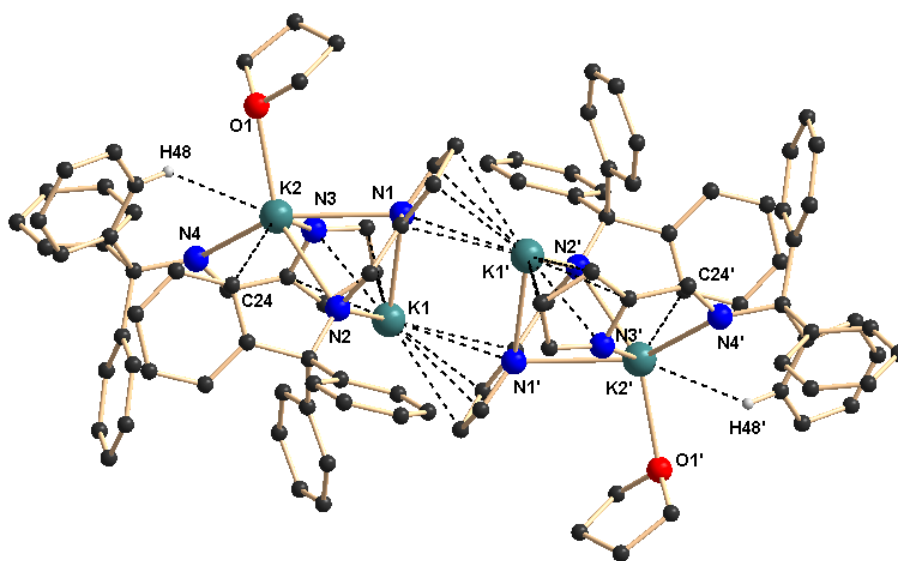


Figure 6.4. Solid state structure of potassium complex **43**. Hydrogen atoms are omitted except H24 for clarity. Selected bond lengths (Å) and bond angles (°): K1-N1 3.155(3), K1-N2 2.946(3), K1-N3 3.041(3), K1-C1 3.082(4), K1-C2 3.063(4), K1-C3 3.095(4), K1-C4 3.128(4), K2-N1 2.971(3), K2-N2 3.005(3), K2-N3 2.667(3), K2-N4 3.013(3), K2-O1 2.668(3), K2-C5 3.419(4), C1-N1 1.355(5), C4-N1 1.396(4), C5-N2 1.292(4), C6-N2 1.488(5), C25-N3 1.364(5), C28-N3 1.384(4), C29-N4 1.282(4), C30-N4 1.487(5); N1ⁱ-

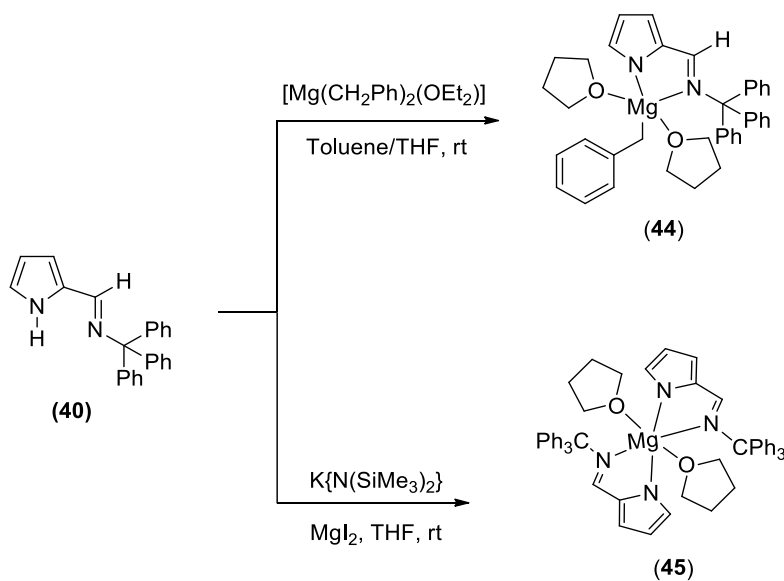
K1-N2 60.09(8), N1ⁱ-K1-N3 74.12(8), N2-K1-N3 97.26(8), N1ⁱ-K1-N1 92.85(8), N2-K1-N1 102.47(8), N3-K1-N1 146.71(9), N3-K2-O1 114.95(9), N3-K2-N1ⁱ 77.85(9), O1-K2-N1ⁱ 97.13(9), N3-K2-N2 104.62(8), O1-K2-N2 127.32(8), N1ⁱ-K2-N2 58.07(8), N3-K2-N4 60.28(9), O1-K2-N4 112.87(8), N1ⁱ-K2-N4 135.55(8), N2-K2-N4 116.53(8), N2-K2-C48 133.36(9), N4-K2-C48 50.33(9).

Therefore, in complex **43** each iminopyrrolyl ligand having ($\sigma+\pi$) coordination from each ligand moiety and further η^5 - coordination was observed for pyrrolyl group of each iminopyrrolyls. Therefore, the geometry of the each potassium atom was best described as distorted trigonal-bipyramidal geometry for K2 and distorted tetrahedral geometry for K1 respectively. The K1-N1_{pyrrolyl}, K1-N3_{pyrrolyl} bond distances 3.155(3) and 3.041(3) Å respectively are well fitted with K-N distances observed in [K(THF)₂{Ph₂P(Se)N(CMe₃)}]_n (3.047(3) Å).¹⁴ The K2-N1_{pyrrolyl}, and K2-N3_{pyrrolyl} bond distances 2.971(3) and 2.667(3) Å respectively, which are in good agreement with K-N distances were observed in [{Ph₂P(Se)NCHPh₂}K(THF)₂]₂ (2.725(3) Å) and [{Ph₂P(BH₃)NCHPh₂}K(THF)₂]₂ (2.691(2) Å) (see Chapter 2 and 3). The K1-N2_{imine} and K2-N4_{imine} bond distances of 2.946(3) and 3.013(3) Å were observed respectively. The average potassium-pyrrolyl ring centroid distance of 2.913 Å was observed in potassium complex **43** which indicates that highly electropositive and larger potassium atoms are having considerable interactions with pyrrolyl π -electron density. In addition, the potassium ion (K2) is having very weak interactions with aromatic ring hydrogen atoms (K2...H24 3.047 Å and K2...H48 2.891 Å) to reduce their coordination unsaturation. The K2-O1 bond distance of 2.668(3) Å is observed which is in similar range of K-O bond distance reported in the literature. The best of our knowledge this is the only example of μ^2 -(η^1 - η^5)-mode observed by a pyrrole ring towards potassium atoms when considering different binding modes such as μ^2 -(η^1 - η^n)-reported many times in the literature.¹⁵

6.2.3. Synthesis and characterization of alkaline-earth metal complexes:

We have synthesized the various alkaline-earth metal complexes of bulky iminopyrrolyl ligand by using alkane elimination, silylamine elimination methods and salt metathesis routes. The magnesium complex of composition [(THF)₂Mg{CH₂Ph}{2-(Ph₃CN=CH)-

C_4H_3N }] (**44**) was synthesized via alkane elimination process, in which the $[Mg(CH_2Ph)_2(OEt_2)_2]$ was treated with bulky iminopyrrole ligand **40** in 1:1 molar ratio in toluene at ambient temperature (Scheme 6.2). Recrystallization from THF/*n*-pentane combination afforded the magnesium complex **44** in very good yield. The bis(iminopyrrolyl)magnesium complex of composition $[(THF)_2Mg\{2-(Ph_3CN=CH)-C_4H_3N\}_2]$ (**45**) was synthesized by using salt metathesis route, in this process, potassium salt (**43**) of ligand **40** was treated with MgI_2 in 2:1 molar ratio in THF solvent afforded the complex **45** in 90% yield (Scheme 6.2). The two magnesium complexes **44** and **45** were fully characterized by using both spectroscopic/analytical techniques and single crystal X-ray diffraction analysis. In the 1H NMR spectrum, one singlet resonance assignable to imine moiety was observed at δ 7.91 ppm (for **44**) and 7.99 ppm (for **45**), additionally one singlet resonance at δ 1.73 ppm observed for complex **44** can be assigned to methylene protons of the benzyl group. In the $^{13}C\{^1H\}$ NMR spectra, strong resonance at δ 162.7 ppm (for **44**) and 157.8 ppm (for **45**) relates to the imine moiety and strong resonance at δ 38.4 ppm (for **44**) tells the presence of benzylic carbon atom in the complex **44**.



Scheme 6.3. Synthesis of magnesium complexes **44** and **45**.

In the solid state the mono(iminopyrrolyl)Mg-complex **44** was crystalizes in triclinic space group *P*-1 having four molecules in the unit cell. The details of the structural parameters were given in the Table 6.3. The solid state structure of complex **44** and selected bond

lengths and bond angles were shown in the Figure 6.5. In the magnesium complex **44**, the central magnesium atom was surrounded by one iminopyrrolyl moiety, one benzyl group and two solvated THF molecules. Therefore, the geometry of magnesium ion in the complex **44** can be best described as distorted trigonal bipyramidal, which is formed due to chelation of two nitrogen atoms of the iminopyrrolyl group, one carbon atom of the benzyl group and two oxygen atoms of the THF molecules.

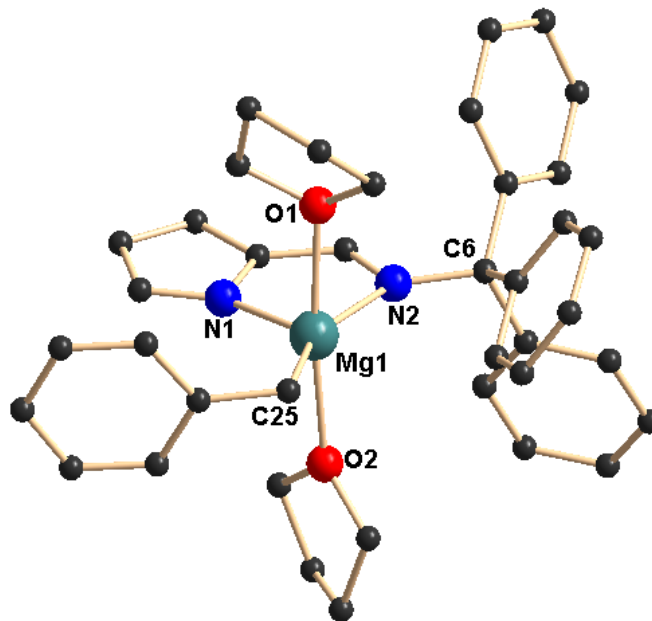


Figure 6.5. Solid state structure of magnesium complex **44**. Hydrogen atoms are omitted for clarity. Selected bond lengths (Å) and bond angles (°): Mg1-N1 2.070(2), Mg1-N2 2.200(2), Mg1-C25 2.185(3), Mg1-O1 2.2040(19), Mg1-O2 2.225(2), C1-N1 1.353(3), C1-C2 1.392(4), C2-C3 1.399(3), C3-C4 1.399(3), C4-C5 1.426(3), C4-N1 1.385(3), C5-N2 1.303(3), N2-C6 1.494(3), C6-C7 1.541(3), C25-C26 1.464(4); N1-Mg1-N2 80.98(8), O1-Mg1-O2 173.46(7), N1-Mg1-O1 89.79(8), N1-Mg1-O2 92.71(8), N2-Mg1-O1 84.74(7), N2-Mg1-O2 89.68(7), N1-Mg1-C25 123.72(10), O1-Mg1-C25 92.51(10), O2-Mg1-C25 91.13(10), N2-Mg1-C25 155.19(10), C1-N1-C4 105.8(2), N1-C4-C5 119.0(2), C4-C5-N2 121.2(2), C5-N2-C6 120.02(19), C4-N1-Mg1 110.34(15), C5-N2-Mg1 108.06(15).

The magnesium-nitrogen bond distances Mg1-N1 2.070(2) and Mg1-N2 2.200(2) Å were observed for the compound **44**; these are well fitted with the Mg-N bond distances reported

in the literature. For example, Mg-N bond distance reported as 1.970(3) Å for $[\{(L^{iPr})_2Mg(THF)_2\} \cdot (THF)]$, 2.094(3) Å for $[\{(L^{iPr})_2Mg\} \cdot (THF)]$ (where $L^{iPr} = [(2,6-iPr_2C_6H_3)NC(Me)]_2$) and 2.051(2) Å for $[(L^{Mes})_2Mg(THF)_3]$ and 2.070(2) Å for $[(L^{Mes})_2Mg]$, (where $L^{Mes} = [(2,4,6-Me_3C_6H_2)-NC(Me)]_2$).¹⁶ The Mg-N bond distances were also well agreement with the Mg-N bond distances [1.987-2.194 Å for $\{Mg(C_4H_3N(2-CH_2NMe_2))(N(SiMe_3)_2)\}_2$; 1.992-2.223 Å $\{Mg(C_4H_3N(2-CH_2NEt_2))(N(SiMe_3)_2)\}_2$; 1.996-2.064 Å $\{Mg(C_4H_3N(2-CH_2NHtBu))(N(SiMe_3)_2)\}_2$] reported by Ting-Yu Lee et al.¹⁷ Recently, our group also synthesized magnesium complexes of the type $[Mg\{C_2H_4(NPh_2P(Se))_2\}(THF)_3]$ in which we have observed Mg-N distance 2.066(3) and 2.083(3) Å which were in good agreement with the observed values 2.070(2) and 2.200(2) Å for the complex **44**.¹⁴ The nitrogen atom of the pyrrolyl ring (N1) and imine nitrogen atom (N2) have made bite angle of N1-Mg1-N2 80.98(8)° with the magnesium atom was observed. The Mg1-C25 bond distance of 2.185(3) Å is in good agreement with the Mg-C bond distance observed in the complexes $[(tmeda)Mg(CH_2Ph)_2]$ (2.1697(17) Å) and $[\eta^2-HC\{C(CH_3)NAr'\}_2Mg(CH_2Ph)(thf)]$ (2.1325(18) Å) reported by P. J. Bailey et al.¹⁸

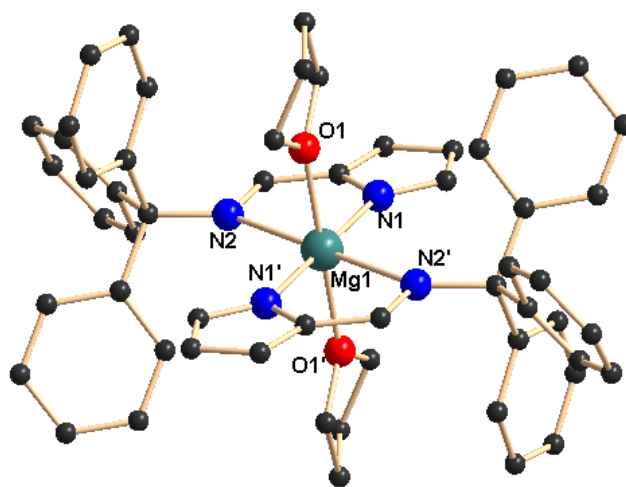
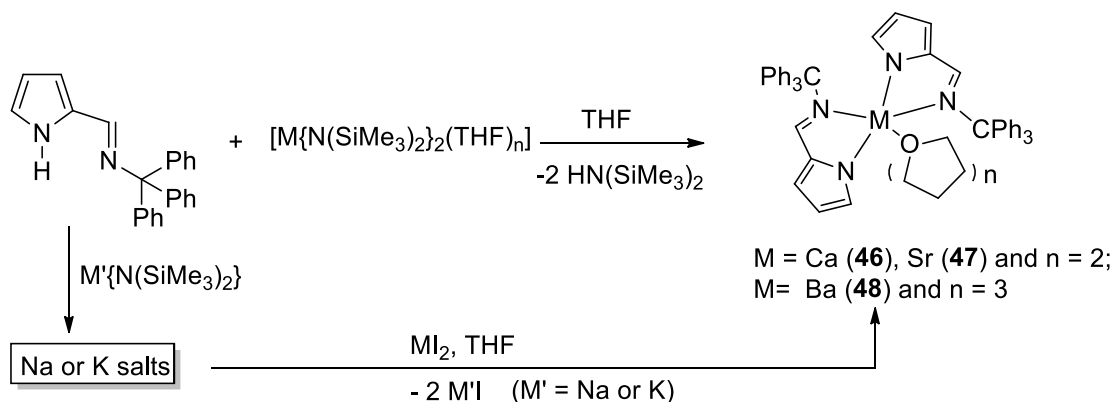


Figure 6.6. Solid state structure of magnesium complex **45**. Hydrogen atoms are omitted for clarity. Selected bond lengths (Å) and bond angles (°): Mg1-N1 2.0813(14), Mg1-N2 2.5422(14), Mg1-O1 2.1517(12), C1-N1 1.343(2), N1-C4 1.383(2), C4-C5 1.428(2), C5-N2 1.295(2), N2-C6 1.5030(19); N1-Mg1-N1ⁱ 180.0, N2-Mg1-N2ⁱ 180.0, O1-Mg1-O1ⁱ 180.0, N1-Mg1-O1 89.87(5), N2-Mg1-O1 90.80(4), N1-Mg1-N2 75.72(5), N1-Mg1-N2ⁱ

104.28(5), C1-N1-C4 104.92(13), N1-C4-C5 121.60(14), C4-C5-N2 122.89(15), C5-N2-Mg1 103.64(10).

The bis(iminopyrrolyl)Mg-complex **45** was crystalizes in triclinic space group *P*-1 having one molecule in the unit cell. The solid state structure of complex **45** and selected bond lengths and bond angles were shown in the Figure 6.6. In complex **45**, the central magnesium atom was surrounded by two iminopyrrolyl moieties, and two THF molecules. Therefore, the geometry of the central magnesium atom in the complex **45** was best described as distorted octahedral, which is formed due to the chelation from four nitrogen atoms of two iminopyrrolyl moieties and two oxygen atoms of the THF molecules. The Mg1-N1_{pyrrolyl} bond length of 2.0813(14) Å is well fitted with Mg-N_{pyrrolyl} bond distance observed in complex **44** (2.070(2) Å) and to the literature reports.^{14,16,17} Whereas the Mg1-N2_{imine} bond length 2.5422(14) Å is quite larger than the Mg-N_{imine} bond distance (2.200(2) Å) observed in the complex **44** and also to the literature reports.^{16,17} This is due to presence of bulky triphenyl group attached to the imine nitrogen atom of the bulky iminopyrrolyl moiety. In complex **45**, the Mg-O bond distance (2.1517(12) Å) is well fitted with the literature reports. Due to chelation of N_{pyrrolyl} and N_{imine} atoms of the bulky iminopyrrolyl moiety to the magnesium atom, there exists a five membered mettallacycle N1-C4-C5-N2-Mg1 or N1ⁱ-C4ⁱ-C5ⁱ-N2ⁱ-Mg1 with bite angle of N1-Mg1-N2 or N1ⁱ-Mg1-N2ⁱ 75.72(5)°.

The heavier alkaline-earth metal complexes of composition {M(2-(Ph₃CN=CH)-C₄H₃N)₂(THF)_n} (M = Ca (**46**), Sr (**47**) and n = 2; M = Ba (**48**), n = 3) were synthesized by using two synthetic methods; In the first method, the bulky iminopyrrolyl ligand **40** was directly treated with alkaline-earth metal bis(trimethylsilyl)amides [M{N(SiMe₃)₂}₂(THF)_n] (where M = Ca, Sr and Ba) in 2:1 molar ratio in THF solvent at ambient temperature. The same alkaline-earth metal complexes of composition {M(2-(Ph₃CN=CH)-C₄H₃N)₂(THF)_n} (M = Ca (**46**), Sr (**47**) and n = 2; M = Ba (**48**), n = 3) were also obtained by using salt metathesis reaction involves the treatment of potassium salt (**43**) of bulky iminopyrrolyl ligand with alkaline-earth metal diiodides MI₂ (M = Ca, Sr and Ba) in 2:1 molar ratio in THF solvent (Scheme 6.4).¹¹



Scheme 6.4. Synthesis of heavier alkaline-earth metal complexes of bulky iminopyrrolyl ligand **40**.

In the ^1H NMR spectra, each of compounds **46-48** shows sharp singlet resonance at δ 7.99 (for **46**), 8.04 (for **47**) and 7.89 (for **48**) ppm indicating the presence of imine -C-H proton in the metal complexes which is slightly downfield shifted compared to free ligand (7.67 ppm). The coordinated THF molecules can be easily recognized by ^1H NMR spectra as two multiplet signals centered at 3.61 and 1.76 ppm (for **46**), 3.38 and 1.18 ppm (for **47**) and 3.56 and 1.40 ppm (for **48**) were observed in each metal complex. One set of resonance signals were observed for aromatic ring protons in each metal complex indicating the dynamic behavior in solution state. The solid state structure of each alkaline-earth metal complex was established by single crystal X-ray diffraction analysis.

The centrosymmetric bis(iminopyrrolyl) Ca-complex was crystalizes in monoclinic space group $P 2_1/n$ having two molecules in the unit cell. The details of the structural parameters are given the Table 6.4. The solid state structure and selected bond lengths and bond angles were shown in the Figure 6.7. From the crystallographic data it is evident that the structure of calcium complex **46** is iso-structural to bis(iminopyrrolyl)Mg-complex **45**, in which the central calcium atom was surrounded by two anionic iminopyrrolyl ligands and two *trans*-THF molecules. Each ligand moiety coordinating to the metal center through the N_{pyrrolyl} and N_{imine} atoms and therefore there exists five membered metallacycle $N1-C4-C5-N2-Ca1$ or $N1^i-C4^i-C5^i-N2^i-Ca1$ with bite angle of $71.76(13)^\circ$. In the calcium complex **46**, the bond distance of $\text{Ca}-N_{\text{pyrrolyl}}$ 2.423(4) Å and bond distance of $\text{Ca}-N_{\text{imine}}$ 2.567(4) Å were

observed, these values are in well agreement with the Ca-N bond distances reported for the complexes of composition $[(\text{Imp}^{\text{Dipp}})_2\text{Ca}(\text{THF})_2]$ (Ca-N1 2.422(2) Å; Ca-N3 2.393(2) Å and (Ca-N2 2.526(2) Å; Ca-N4 2.534(2) Å) and $[(\text{Imp}^{\text{Dipp}})\text{Ca}(\text{N}(\text{SiMe}_3)_2)(\text{THF})_2]$ (Ca-N1 2.388(2) Å; Ca-N3 2.312(2) Å and Ca-N2 2.467(2) Å) and $[(\text{Imp}^{\text{Me}})_2\text{Ca}(\text{THF})_2]$ (Ca-N1 2.398(4) Å; Ca-N2 2.448(3) Å) (where $\text{Imp}^{\text{Dipp}} = 2-(2,6\text{-C}_6\text{H}_3^i\text{Pr}_2\text{-CN=CH})\text{-C}_4\text{H}_3\text{N}$) and $\text{Imp}^{\text{Me}} = 2-(2,6\text{-C}_6\text{H}_3\text{Me}_2\text{-CN=CH})\text{-C}_4\text{H}_3\text{N}$).¹⁹ The Ca-N bond distances were also comparable with our previous results discussed in Chapters 2-5. The Ca-O bond distance of Ca1-O1 2.361(4) Å is in the range of normal Ca-O bonds.²⁰ Therefore, the geometry of the central calcium atom can be best described as distorted octahedral in which the four nitrogen atoms of the two iminopyrrolys occupies the equatorial positions and two oxygen atoms of the THF molecules occupies the axial positions and *trans* to each other.

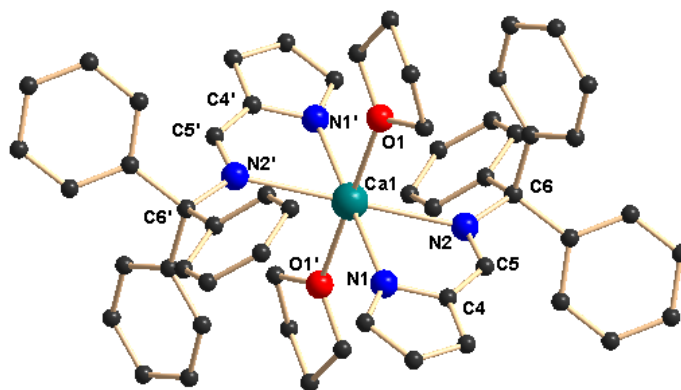


Figure 6.7. Solid state structure of bis(iminopyrrolyl)Ca-complex **46**. Hydrogen atoms are omitted for clarity. Selected bond lengths (Å) and selected bond angles (°): Ca1-N1 2.423(4), Ca1-N2 2.567(4), Ca1-O1 2.361(4), C4-N1 1.400(5), C4-C5 1.413(6), C6-N2 1.504(5); N1-Ca1-N2 71.76(13), N1-Ca1-O1 86.72(14), N2-Ca1-O1 89.32(15), C5-N2-Ca1 108.3(3), C4-N1-Ca1 111.4(3), C4-C5-N2 125.6(4), O1-Ca1-O1ⁱ 180.00(12), N1-Ca1-N1ⁱ 180.0, N2-Ca2-N2ⁱ 180.0.

Unlike magnesium (**45**) and calcium (**46**) complexes, the bis(iminopyrrolyl)Sr-complex (**47**) is non-centrosymmetric and crystalizes in triclinic space group *P*-1 having 2 molecules in the unit cell. The details of the structural parameters were given in the Table

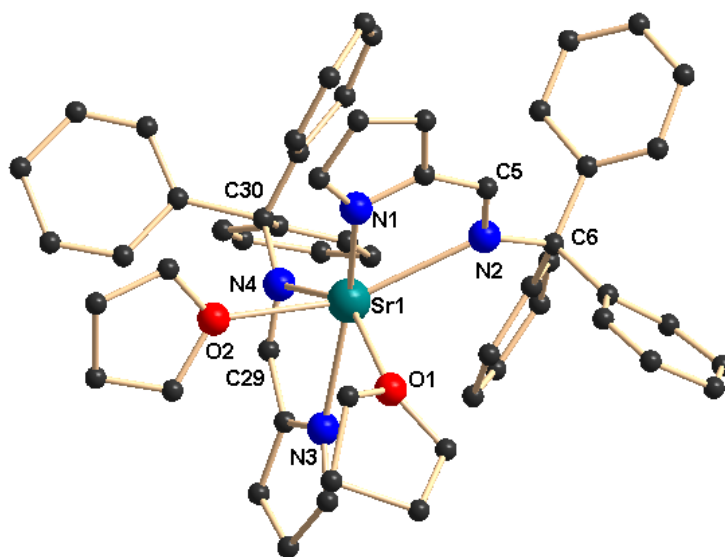


Figure 6.8. Solid state structure of bis(iminopyrrolyl)Sr-complex **47**. Hydrogen atoms are omitted for clarity. Selected bond lengths (Å) and selected bond angles (°): Sr1-N1 2.570(5), Sr1-N2 2.677(5), Sr1-N3 2.546(6), Sr1-N4 2.679(5), Sr1-O1 2.621(5), Sr1-O2 2.593(5), C4-N1 1.382(8), C4-C5 1.442(8), C5-N2 1.291(8), N2-C6 1.494(7), N4-C30 1.505(8); N1-Sr1-N2 68.35(15), N3-Sr1-N4 68.32(16), N1-Sr1-N3 154.21(18), N1-Sr1-N4 129.28(16), N2-Sr1-N3 124.93(16), N2-Sr1-N4 116.33(15), O1-Sr1-O2 89.05(17), N1-Sr1-O1 84.62(17), N1-Sr1-O2 79.56(17), N3-Sr1-O1 80.22(17), N3-Sr1-O2 79.45(17), N4-Sr1-O2 80.08(16).

6.4. The solid state structure and selected bond lengths and selected bond angles were shown in Figure 6.8. In the complex **47**, the strontium metal center was surrounded by two chelating bulky iminopyrrolyls and two THF molecules. Therefore, the geometry of the central strontium atom can be best described as distorted octahedral geometry in which two coordinated THF molecules are *cis* to each other. The Sr-N_{imine} bond distances of Sr1-N2 2.677(5) Å and Sr1-N4 2.679(5) Å are slightly longer than Sr-N_{pyrrolyl} bond distances of Sr1-N1 2.570(5) Å and Sr1-N3 2.546(6) Å were observed in the complex **47**. These values are in good agreement with the strontium-nitrogen bond distances (2.6512(2) and 2.669(2) Å) reported previously for the strontium complex [(Imp^{Dipp})₂Sr(THF)₃] (Imp^{Dipp} = 2,6-ⁱPr₂C₆H₃N=CH)-C₄H₃N).¹⁹ In the strontium complex **47**, each monoanionic bidentate chelate ligand forming five membered metallacycle with strontium atom N1-C4-C5-N2-

Sr1 with bite angle of $68.35(15)^\circ$ and N3-C28-C29-N4-Sr1 with bite angle of $68.32(16)^\circ$. The two planes containing the N1, N2, Sr1 and N3, N4, Sr1 atoms are almost orthogonal to each other with dihedral angle of 85.02° . The Sr-O bond distances Sr1-O1 $2.621(5)$ Å and Sr1-O2 $2.593(5)$ Å are in the range of normal Sr-O bonds.²⁰

Like strontium complex **47**, the bis(iminopyrrolyl)Ba-complex **48** also non-centrosymmetric and crystalizes in monoclinic space group *P*-1 having two molecules in the unit cell. The details of the structural parameters are given the Table 6.4. The solid state structure and selected bond lengths and bond angles were shown in the Figure 6.9. In the barium complex, Each ligand moiety coordinating to the metal center through the N_{pyrrolyl} and N_{imine} atoms and therefore there exists five membered mettallacycle N1-C1-C5-N2-Ba1 with bite angle of $63.78(14)^\circ$ and N3-C28-C29-N4-Ba1 with bite angle of $63.14(15)^\circ$. The plane containing N1, N2 and Ba1 is having dihedral angle of 87.08° with plane containing N3, N4 and Ba1 indicates that two five membered mettallacycles are almost orthogonal to each other. In the barium complex **48**, the Ba-N_{pyrrolyl} bond distance of Ba1-N1 $2.731(5)$ Å; Ba1-N3 $2.762(5)$ Å were observed well fitted to the Ba-N bond distances reported for the complexes of composition $[\text{Ba}((\text{Dipp})_2\text{DAD})(\mu\text{-I})(\text{THF})_2)_2$ ($2.720(4)$ and $2.706(4)$ Å)²¹ and Ba-N_{imine} bond distance of Ba1-N2 $2.946(5)$ Å; Ba1-N4 $2.933(5)$ Å are slightly larger than the Ba-N distances reported for the complexes of composition $[(\text{Imp}^{\text{Dipp}})_2\text{Ba}(\text{THF})_2]$ (Ba-N1 $2.821(5)$ Å and (Ba-N2 $2.823(4)$ Å) and $[\text{Ba}((\text{Dipp})_2\text{DAD})(\mu\text{-I})(\text{THF})_2)_2$ ($2.720(4)$ and $2.706(4)$ Å) (where $\text{Imp}^{\text{Dipp}} = 2\text{-}(2,6\text{-C}_6\text{H}_3\text{Pr}_2\text{-CN=CH)-C}_4\text{H}_3\text{N}$).^{19,21} The Ba-N bond distances were also comparable with our previous results discussed in Chapters 2-5. The Ba-O bond distance of Ba1-O1 $2.812(5)$, Ba1-O2 $2.842(4)$ and Ba1-O3 $2.830(4)$ Å are in the range of normal Ba-O bonds reported in the literature.²⁰ Therefore, the geometry of the central barium atom can be best described as distorted pentagonal bipyramidal which is formed due to chelation four nitrogen atoms of the two iminopyrrolyl moieties and three oxygen atoms of the three coordinated THF molecules.

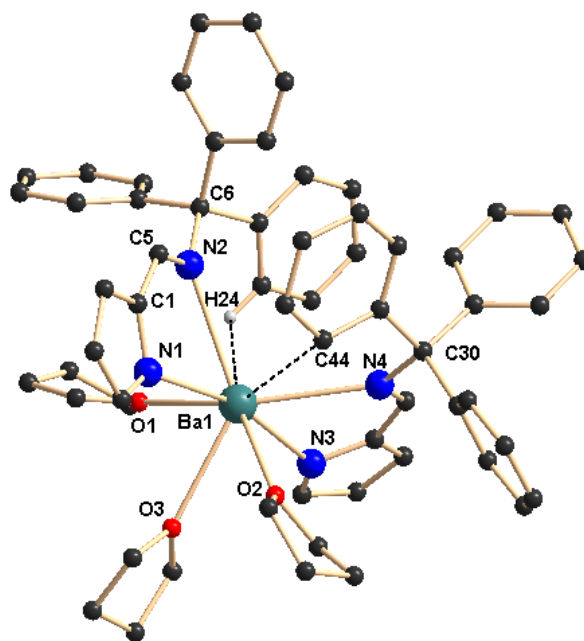
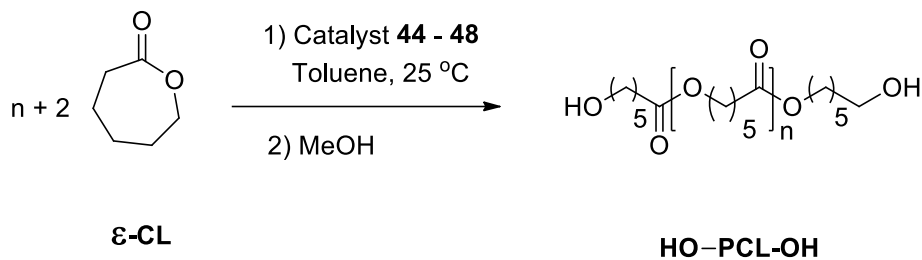


Figure 6.9. Solid state structure of bis(iminopyrrolyl)Ba-complex **48**. Hydrogen atoms are omitted except H24 for clarity. Selected bond lengths (Å) and selected bond angles (°): Ba1-N1 2.731(5), Ba1-N2 2.946(5), Ba1-N3 2.762(5), Ba1-N4 2.933(5), Ba1-O1 2.812(5), Ba1-O2 2.842(4), Ba1-O3 2.830(4), C4-N1 1.348(8), C4-C5 1.424(8), C5-N2 1.304(7), N2-C6 1.481(7), N4-C30 1.499(8), Ba1-C44 3.389(6); N1-Ba1-N2 63.78(14), N3-Ba1-N4 63.14(15), N1-Ba1-N3 166.32(15), N1-Ba1-N4 127.40(15), N2-Ba1-N3 125.77(14), N2-Ba1-N4 102.26(13), O1-Ba1-O2 134.20(14), O2-Ba1-O3 65.90(14), O1-Ba1-O3 68.76(15), N1-Ba1-O1 89.67(16), N1-Ba1-O2 80.25(14), N3-Ba1-O1 84.29(16), N3-Ba1-O2 95.20(14), N3-Ba1-O3 81.61(15).

6.3 Ring-Opening Polymerization of ϵ -caprolactone study

A series of alkaline-earth metal complexes supported by bulky iminopyrrolyl ligand were studied as initiators for living ROP of ϵ -CL. The typical ring-opening polymerization process was depicted in the Scheme 6.5. We were mostly concentrated on living ROP and not on immortal ROP of ϵ -CL in order to understand the influence of steric bulk on rate of polymerization and influence of nature of the metal centre. In the living ROP of cyclic esters, the metal complex acts an initiator, that is, each metal center produces only one polymer chain. On the other hand, an immortal ROP is performed upon addition of a large excess of a protic agent (typically an alcohol) acting as an exogenous initiator and a chain

transfer agent, and the complex acts as a catalyst: if the transfer between growing and dormant macromolecules is fast and reversible, the number of polymer chains generated per metal center is equal to the $[\text{transfer agent}]_0$ -to- $[\text{metal}]_0$. The selected data obtained with alkaline-earth metal complexes (**44-48**) as initiators for living ROP of ϵ -CL are collected in table 6.1. The catalytic efficiency of newly synthesized heteroleptic and homoleptic magnesium complexes **44** and **45** to promote ROP of ϵ -CL were first evaluated (table 6.1, entries 1-4). Indeed, although some previously reported studies with similar magnesium complexes having less-bulky iminopyrrolyls in their coordination sphere gave poor results under similar polymerization conditions,²¹ our preliminary investigations with magnesium complexes **44** and **45** showed that they are active in the ROP of ϵ -CL at 25 °C in toluene with conversion over 90% within 15 minutes (table 6.1, entries 1-6).



Scheme 6.5. ROP of ϵ -CL initiated by alkaline earth metal complexes **44 – 48**.

The molar mass distribution PDI values obtained from GPC analysis are narrow (PDI < 1.8, for entries 1-6) and controlled molecular weight distribution was observed. We noticed that the heteroleptic Mg complex (**44**) is more active compared to homoleptic Mg complex (**45**). The difference in reactivity could be understood by the initiation steps in both the cases. In case of complex **44** polymerization follows a nucleophilic route and is initiated by the transfer of an alkyl ligand to the monomer, with cleavage of the acyl-oxygen bond and formation of a metal alkoxide-propagating species.²² Similar mechanism was also suggested by the *A. M. Rodriguez group* for the magnesium complex of composition $[\text{Mg}(\text{CH}_2\text{SiMe}_3)(\text{K}^2\text{-}\eta^5\text{-bpzcp})]$ (where bpzcp = 2,2-bis(3,5-dimethylpyrazol-1-yl)-1,1-diphenylethyl cyclopentadienyl) as an initiator for the living ROP of ϵ -CL.²³ The results obtained therein (PDI < 1.5 with controlled molecular weights) are comparable with our observations (See Table 6.1) suggesting that the ligand steric bulk and nature of the metal centre play crucial role in ROP of ϵ -CL. The calcium complex **46** also showed the

comparable activity towards the ROP of ϵ -CL with magnesium analogues (**44** and **45**) with narrow PDI values and controlled molecular weight distributions (Table 6.1, entries 5–9). Indeed, the sluggish reactivity of the calcium complexes is very similar to that observed in some previously reported studies using other calcium complexes for ROP of ϵ -CL,^{24, 25} we have noticed that living polymerization characteristics at room temperature without using any initiating agent like alcohol (entry 9, PDI = 1.5 and $M_w = 52483$) indicating that triphenylmethyl group on ligand backbone strongly influencing the activity of calcium complexes towards the ROP of ϵ -CL. We anticipated that strontium (**47**) and barium (**48**) complexes could be more active than those of magnesium and calcium complexes having bulky iminopyrrolyls due to the larger ionic radii of Sr^{2+} and Ba^{2+} ions.^{26,27} Both strontium and barium analogues showed higher reactivity towards the conversion of ϵ -caprolactone to poly-caprolactone and up to 600 ϵ -CL units were successfully converted in high yields (90 to 98%) within 5-10 minutes at 25 °C. The control over the ROP process was rather good, affording PCLs, with controlled molar mass values, as well as very narrow dispersity data (PDI < 1.4, entries 10-19). Therefore, overall catalytic efficiency of ring-opening polymerization by heavier alkaline-earth metal complexes (Sr^{2+} and Ba^{2+}) supported by sterically hindered iminopyrrolyl ligands were much better and affording poly-caprolactone with controlled molecular weights and narrow PDI values.

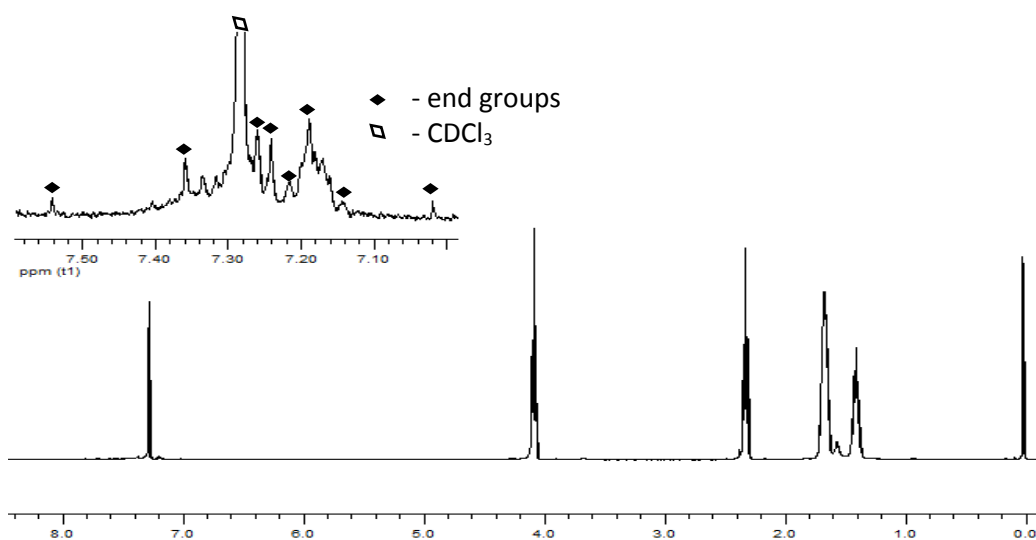


Figure 6.10. ^1H NMR spectrum (400 MHz, 25°C, CDCl_3) of Poly(ϵ -Caprolactone) initiated by complex (**48**)

From the ^1H NMR spectrum of low- molecular weight PCL by **48** (run 15), we found resonance signals assignable to a terminal iminopyrrolyl group (Figure 6.10), indicating that in case of amido complexes of alkaline-earth metal complexes (**45-48**) initial step of the polymerization was a nucleophilic attack of the pyrrolyl nitrogen atom towards the carbonyl carbon of the monomer followed by acyl-oxygen cleavage.

Table 6.1. Ring-Opening Polymerization of ϵ -caprolactone initiated by alkaline earth metal complexes (**44-48**)

Entry	Cat. [M]	$[\epsilon\text{CL}]_0/$ [M] ₀	Reac. time [min]	Conv. [%]	$Mn_{(\text{theo})}$ [g mol ⁻¹]	$Mn_{(\text{GPC})}$ [g mol ⁻¹]	$Mw_{(\text{GPC})}$ [g mol ⁻¹]	Mw/Mn
1	44	200/1	10	90	19826	21141	31440	1.48
2	44	400/1	10	87	34847	21147	31875	1.50
3	$[\text{Mg}(\text{CH}_2\text{SiMe}_3)(\text{K}^2\text{-}\eta^5\text{-bpzcp})]^{\text{g}}$	5000/1	10	65	2233	-	151000	1.45
4	$[\text{Mg}(\text{CH}_2\text{SiMe}_3)(\text{tbpamd})]^{\text{g}}$	500/1	1	97	3320	-	52000	1.41
5	45	200/1	15	89	17824	13781	21994	1.59
6	45	400/1	15	91	36449	39622	72653	1.83
7	46	150/1	5	96	14419	17263	26204	1.51
8	46	200/1	5	92	18425	22538	37073	1.64
9	46	300/1	10	94	28238	32219	50483	1.56
10	46	400/1	10	92	39613	60613	97678	1.61
11	46	500/1	15	95	48065	85808	138365	1.61
12	47	100/1	5	99	11896	11664	12173	1.04
13	47	200/1	5	97	20397	25190	34481	1.36
14	47	300/1	5	94	32944	36973	55396	1.49
15	47	400/1	10	91	35087	76030	93067	1.22
16	47	500/1	10	93	50288	86307	137623	1.59
17	48	100/1	5	99	12887	12480	13076	1.04
18	48	200/1	5	98	20608	36990	46567	1.25
19	48	300/1	5	95	32343	41739	55528	1.33
20	48	400/1	10	96	40374	73272	105361	1.43
21	48	600/1	10	98	61824	107891	139168	1.28

6.4 Conclusion

We have successfully prepared alkali metal complexes of the bulky iminopyrrolyl ligand and their solid-state structures reveal the flexibility and multidentate behavior of the iminopyrrolyl ligand **40**. In case of the sodium complex, we observed a dimeric structure whereas, due to lower charge density of the potassium ion, a tetranuclear structure was found in the solid state. The heteroleptic and homoleptic magnesium complexes **44** and **45** respectively were successfully synthesized and characterized using X-ray crystallography. In the solid state, complex **44** is five-fold coordinated and shows trigonal bipyramidal geometry around the magnesium ion, whereas the magnesium ion in complex **45** adopts a octahedral arrangement due to the six-fold coordination from ligand **40** and THF molecules. The heavier alkaline earth metal complexes **46–48** were synthesized either by silylamine elimination or salt metathesis routes using $[M\{N(SiMe_3)_2\}_2(THF)_n]$ or MI_2 ($M = Ca, Sr, \text{ and } Ba$) as starting materials. In the solid state, the effect of the ion radii of the central metal ions as well as the steric bulk of the ligand backbone determined the metal coordination sphere. The calcium complex **46** is centro-symmetric and adopts an octahedral geometry, whereas the strontium and barium complexes (**47** and **48**), due to their larger size, are non-centro-symmetric and adopt distorted octahedral and distorted pentagonal-bipyramidal geometries respectively. In addition, the $M-N_{pyr}$ and $M-N_{imin}$ bonds are relatively longer than those of the other amido-metal complexes of barium and strontium. The bis(iminopyrrolyl)complexes of strontium (**47**) and barium (**48**) were highly active for the of ϵ -CL, affording high molecular weight PCLs compared to the polymers produced by the calcium and magnesium complexes.

6.5 Experimental Procedure:

6.5.1. General

All manipulations of air-sensitive materials were performed with the rigorous exclusion of oxygen and moisture in flame-dried Schlenk-type glassware either on a dual manifold Schlenk line, interfaced to a high vacuum (10^{-4} torr) line, or in an argon-filled M. Braun glove box. THF was pre-dried over Na wire and distilled under nitrogen from sodium and

benzophenone ketyl prior to use. Hydrocarbon solvents (toluene and *n*-pentane) were distilled under nitrogen from LiAlH₄ and stored in the glove box. ¹H NMR (400 MHz), ¹³C{¹H} and spectra were recorded on a BRUKER AVANCE III-400 spectrometer. BRUKER ALPHA FT-IR was used for FT-IR measurement. Elemental analyses were performed on a BRUKER EURO EA at the Indian Institute of Technology Hyderabad. Metal diiodides (MgI₂, CaI₂, SrI₂ and BaI₂), [NaN(SiMe₃)₂], [KN(SiMe₃)₂], pyrrole-2-carboxyaldehyde, tritylamine and ε-caprolactone were purchased from Sigma Aldrich and used as such. The alkaline-earth metal bis(trimethylsilyl)amides [M{N(SiMe₃)₂}₂(THF)_n], [Mg(CH₂Ph)₂(OEt₂)₂] and LiCH₂SiMe₃ were prepared according to procedure prescribed in the literature.^{18,28,29} The NMR solvent C₆D₆ and CDCl₃ were purchased from Sigma Aldrich and dried under Na/K alloy prior to use.

6.5.2. Synthesis of [2-(Ph₃CN=CH)-C₄H₃NH] (40)

To a dried MeOH solution (10 ml) of pyrrole-2-carboxyaldehyde (2.0 g, 21.0 mmol), tritylamine in 10 ml of MeOH (5.45 g, 21.0 mmol) and a catalytic amount of glacial acetic acid (0.25 ml) were added under stirring. The reaction mixture was stirred for 12 h at room temperature. Filtration followed by the washing with cold methanol and then with *n*-hexane and removal of solvent afforded the final product as off-white powder. Recrystallization from hot toluene afforded the crystalline product in 79% yield (5.62 g). ¹H NMR (400 MHz, CDCl₃): δ 9.50 (br, 1H, N-H), 7.67 (s, 1H, N=C-H), 7.29-7.22 (m, 15H, CPh₃), 6.87 (s, 1H, 5-pyr), 6.39 (d, 1H, 3-pyr), 6.22 (m, 1H, 4-pyr) ppm. ¹³C NMR (100 MHz, CDCl₃): δ 150.3 (N=CH), 145.9 (ArC), 130.9 (2-pyr), 129.8 (*o*-ArC), 127.7 (*m*-ArC), 126.8 (*p*-ArC), 121.6 (5-pyr), 114.6 (3-pyr), 110.0 (4-pyr), 77.8 (CPh₃) ppm. FT-IR (Selected Frequencies, ν): 3445 (br, N-H), 3025 (w, ArC-H), 1629 (s, C=N) cm⁻¹. Elemental Analysis: C₂₄H₂₀N₂ (336.42): Calcd. C 85.68, H 5.99, N 8.33. Found C 84.57, H 5.32, N 7.83.

6.5.3. Synthesis of [{2-(Ph₃CN=CH)-C₄H₃N}Li(THF)₂] (41)

To a THF solution of LiCH₂SiMe₃ (50 mg, 0.53 mmol), 1 equivalent of ligand **40** (178.6 mg, 0.53 mmol) in THF was added dropwise at room temperature. The mixture was then stirred for 3 h. Removal of volatile product SiMe₄ gave a light yellow product, which was

washed by *n*-pentane and dried under vacuum to afford Li-complex in 85% yield (220.0 mg). Single crystals suitable for X-ray analysis were grown from THF/*n*-pentane mixture (1:2) solvent at -30 °C after 1 d. ¹H NMR (400 MHz, C₆D₆): δ 8.17 (s, 1H, N=C-*H*), 7.13-7.18 (m, 6H, CPh₃), 7.11 (s, 1H, 5-pyr), 7.03-7.05 (m, 9H, CPh₃), 6.74 (d, 1H, 3-pyr), 6.56 (m, 1H, 4-pyr), 3.19-3.23 (m, THF), 1.19-1.22 (m, THF) ppm. ¹³C NMR (100 MHz, C₆D₆): δ 149.3 (N=CH), 145.7 (ArC), 130.8 (2-pyr), 129.8 (*o*-ArC), 127.6 (*m*-ArC), 126.5 (*p*-ArC), 120.3 (5-pyr), 113.6 (3-pyr), 110.7 (4-pyr), 78.5 (CPh₃), 67.8 (THF), 25.5 (THF) ppm. FT-IR (Selected Frequencies, ν): 3025 (w, ArC-H), 1629 (s, C=N) cm⁻¹. Elemental Analysis: C₃₂H₃₅LiN₂O₂ (486.29): Calcd. C 78.99, H 7.25, N 5.76. Found C 77.69, H 6.15, N 5.06

6.5.4. Synthesis of [{2-(Ph₃CN=CH)-C₄H₃N}Na(THF)]₂ (**42**)

To a THF solution of ligand **40** (300 mg, 0.89 mmol), 1 equivalent of sodium bis(trimethylsilyl)amide (163.5 mg, 0.89 mmol) in THF was added dropwise under stirring at room temperature. Stirring was continued for another 12 h and then volatile compounds were removed under vacuum. The title compounds were obtained as white solids, which were further purified by washing with *n*-pentane. Single crystals suitable for X-ray diffraction analysis were obtained from the THF/*n*-pentane mixture (1:2) solvent at -30 °C after 1 d. 91% Yield (350.0 mg): ¹H NMR (400 MHz, C₆D₆): δ 8.03 (s, 1H, N=C-*H*), 7.14-7.17 (m, 6H, CPh₃), 6.98 (s, 1H, 5-pyr), 6.90-6.97 (m, 9H, CPh₃), 6.49 (d, 1H, 3-pyr), 6.27 (m, 1H, 4-pyr), 3.24-3.27 (m, THF), 1.18-1.21 (m, THF) ppm. ¹³C NMR (100 MHz, C₆D₆): δ 147.8 (N=CH), 145.9 (ArC), 130.2 (2-pyr), 128.3 (*o*-ArC), 128.1 (*m*-ArC), 127.8 (*p*-ArC), 126.8 (5-pyr), 119.1 (3-pyr), 111.1 (1C, 4-pyr), 78.3 (CPh₃), 67.8 (THF), 25.6 (THF) ppm. FT-IR (Selected Frequencies, ν): 3025 (w, ArC-H), 1629 (s, C=N) cm⁻¹. Elemental Analysis: C₅₆H₅₄N₄Na₂O₂ (861.01): Calcd. C 78.12, H 6.32, N 6.51. Found C 77.32, H 5.39, N 5.31.

6.5.5. Synthesis of [{2-(Ph₃CN=CH)-C₄H₃N}K(THF)_{0.5}]₄ (**43**)

To a THF solution of ligand **40** (300 mg, 0.89 mmol), 1 equivalent of potassium bis(trimethylsilyl)amide (177.8 mg, 0.89 mmol) in THF was added drop wise under stirring at room temperature. Stirring was continued for another 12 h and then volatile compounds

were removed under vacuum. The title compounds were obtained as white solids, which were further purified by washing with *n*-pentane. Single crystals suitable for X-ray diffraction analysis were obtained from the THF/*n*-pentane mixture (1:2) solvent at -30 °C after 1 d. 95% Yield (380.5 mg): ¹H NMR (400 MHz, C₆D₆): δ 7.99 (s, 1H, N=C-H), 7.12-7.15 (m, 6H, CPh₃), 6.94 (s, 1H, 5-pyr), 6.92-6.95 (m, 9H, CPh₃), 6.53 (d, 1H, 3-pyr), 6.31 (m, 1H, 4-pyr), 3.21-3.24 (m, THF), 1.17-1.21 (m, THF) ppm. ¹³C NMR (100 MHz, C₆D₆): δ 149.1 (N=CH), 143.7 (ArC), 131.3 (2-pyr), 128.6 (o-ArC), 128.3 (m-ArC), 128.1 (p-ArC), 123.3 (1C, 5-pyr), 117.5 (3-pyr), 111.3 (4-pyr), 78.5 (CPh₃), 67.3 (THF), 25.8 (THF) ppm. FT-IR (Selected Frequencies, ν): 3026 (w, ArC-H), 1630 (s, C=N) cm⁻¹. Elemental Analysis: C₁₀₄H₉₂K₄N₈O₂ (1642.26): Calcd. C 76.06, H 5.65, N 6.82. Found C 75.42, H 5.32, N 6.31.

6.5.6. Synthesis of [{2-(Ph₃CN=CH)-C₄H₃N}{PhCH₂}Mg(THF)₂] (44)

In a 25 ml of Schlenk flask one equivalent of ligand **40** (100 mg, 0.297 mmol) was dissolved in 10 ml of toluene. To this solution, one equivalent of [Mg(CH₂Ph)₂(Et₂O)₂] (105.4 mg, 0.297 mmol) in toluene (5 ml) was added dropwise at room temperature. The reaction mixture was stirred for 6 h and then solvents were removed under vacuum. The resultant Mg-complex was washed with *n*-pentane twice and crystals suitable for X-ray analysis were grown from THF/*n*-pentane solvent mixture. Yield 160.5 mg (90%). ¹H NMR (400 MHz, C₆D₆): δ 7.91 (s, 1H, N=C-H), 7.07-7.18 (m, 15H, CPh₃), 6.96-7.02 (m, 5H, Ar-H), 6.74 (d, 1H, 5-pyr), 6.66 (m, 1H, 3-pyr), 6.56 (m, 1H, 4-pyr), 1.73 (s, 2H, CH₂Ph) ppm. ¹³C NMR (100 MHz, C₆D₆): δ 162.7 (N=CH), 145.5 (ArC), 136.9 (CH₂Ph), 135.3 (2-pyr), 129.1 (o-CH₂Ph), 128.7 (o-ArC), 128.1 (m-CH₂Ph), 127.2 (m-ArC), 126.1 (p-ArC), 125.4 (p-CH₂Ph), 124.4 (5-pyr), 121.0 (3-pyr), 113.3 (4-pyr), 76.8 (CPh₃), 38.4 (CH₂Ph) ppm. FT-IR (Selected Frequencies, ν): 3025 (w, ArC-H), 1631 (s, C=N) cm⁻¹. Elemental Analysis: C₃₉H₄₂MgN₂O₂ (595.06): Calcd. C 78.72, H 7.11, N 4.71. Found C 77.89, H 6.13, N 4.01.

6.5.7. Synthesis of [{2-(Ph₃CN=CH)-C₄H₃N}₂Mg(THF)₂] (45)

In a pre-dried Schlenk flask potassium salt (**43**) of ligand **40** (200 mg, 0.448 mmol) and MgI_2 (62.30 mg, 0.224 mmol) were mixed in THF (10 ml) solvent. The reaction mixture was stirred for 12 h at room temperature and then precipitate of KI was removed by filtration. Solvent was removed under reduced pressure from the filtrate and then dried in *vacuo*. The magnesium complex (**45**) was obtained as white solid, which was recrystallized from THF/*n*-pentane (1:2) mixture solvents. Yield: 175 mg (93%). ^1H NMR (400 MHz, C_6D_6): δ 7.99 (s, 1H, N=C-H), 7.14-7.25 (m, 15H, CPh₃), 6.37 (d, 1H, 5-pyr), 6.10 (s, 1H, 3-pyr), 5.99 (m, 1H, 4-pyr), 3.62-3.64 (m, THF), 1.27-1.29 (m, THF) ppm. ^{13}C NMR (100 MHz, C_6D_6): δ 157.8 (N=CH), 147.2 (ArC), 136.3 (2-pyr), 128.9 (o-ArC), 128.2 (m-ArC), 125.3 (p-ArC), 116.8 (5-pyr), 113.4 (3-pyr), 111.4 (4-pyr), 66.7 (CPh₃), 65.5 (THF), 24.6 (THF) ppm. FT-IR (Selected Frequencies, ν): 3025 (w, ArC-H), 1629 (s, C=N) cm^{-1} . Elemental Analysis: $\text{C}_{56}\text{H}_{54}\text{MgN}_4\text{O}_2$ (839.34): Calcd. C 80.13, H 6.48, N 6.67. Found C 79.33, H 5.92, N 6.07.

6.5.8. *Synthesis of* $[\{2-(\text{Ph}_3\text{CN}=\text{CH})-\text{C}_4\text{H}_3\text{N}\}_2\text{M}(\text{THF})_n]$ (M = Ca (**46**), Sr (**47**) and $n = 2$; M = Ba (**48**) and $n = 3$)

46: *Route 1:* Ligand **40** (200 mg, 0.594 mmol) and $[\text{Ca}\{\text{N}(\text{SiMe}_3)_2\}_2(\text{THF})_2]$ (150 mg, 0.297 mmol) were dissolved in THF (5 ml). The reaction mixture was stirred for 6 h at room temperature and all volatiles were removed under reduced pressure. The remaining white solid was washed with *n*-pentane and then dried in *vacuo* to give calcium complex (**46**) as white powder. Recrystallization from THF/*n*-pentane (1:2) gave colorless crystals suitable for X-ray diffraction measurement. Yield: 241 mg (95%).

Route 2: In a pre-dried Schlenk flask potassium salt (**43**) of ligand **40** (200 mg, 0.448 mmol) and CaI_2 (65.8 mg, 0.224 mmol) were mixed in THF (10 ml) solvent. The reaction mixture was stirred for 12 h at room temperature and then precipitate of KI was removed by filtration. Solvent was removed under reduced pressure from the filtrate and then dried in vacuum. The calcium complex (**46**) was obtained as white solid, which was recrystallized from THF/*n*-pentane (1:2) mixture solvents. Yield: 172 mg (90%). ^1H NMR (400 MHz, C_6D_6): δ 7.99 (s, 1H, N=C-H), 7.14-7.25 (m, 15H, CPh₃), 6.37 (d, 1H, 5-pyr), 6.18 (s, 1H, 3-pyr), 5.92 (m, 1H, 4-pyr), 3.61-3.63 (m, THF), 1.25-1.27 (m, THF) ppm. ^{13}C NMR (100 MHz, C_6D_6): δ 157.7 (N=CH), 147.1 (ArC), 136.3 (2-pyr), 128.9 (o-ArC), 128.2 (m-ArC),

125.3 (p-ArC), 116.8 (5-pyr), 113.4 (3-pyr), 111.5 (4-pyr), 66.8 (CPh₃), 65.4 (THF), 25.1 (THF) ppm. FT-IR (Selected Frequencies, ν): 3025 (w, ArC-H), 1632 (s, C=N) cm^{-1} . Elemental Analysis: C₆₆H₇₀CaN₄O₄ (999.32): Calcd. C 77.46, H, 6.89, N 5.47. Found C 76.89, H 6.23, N 4.93.

Other heavier alkaline-earth bis(iminopyrrolyl) complexes were prepared in similar manner to **46** by using two routes.

47: *Route 1*: Yield 248 mg (92%) and *Route 2* Yield 182 mg (90%): ¹H NMR (400 MHz, C₆D₆): δ 8.04 (s, 1H, N=C-H), 6.94-7.16 (m, 15H, CPh₃), 6.35 (m, 1H, 5-pyr), 6.17 (m, 1H, 3-pyr), 5.92 (m, 1H, 4-pyr), 3.35-3.39 (m, THF), 1.17-1.20 (m, THF) ppm. ¹³C NMR (100 MHz, C₆D₆): δ 163.9 (N=CH), 148.1 (ArC), 137.3 (2-pyr), 130.3 (o-ArC), 128.6 (m-ArC), 127.8 (p-ArC), 122.6 (5-pyr), 116.4 (3-pyr), 111.4 (4-pyr), 78.3 (CPh₃), 68.3 (THF), 25.5 (THF) ppm. FT-IR (Selected Frequencies, ν): 3026 (w, ArC-H), 1629 (s, C=N) cm^{-1} . Elemental Analysis: C₆₀H₆₂N₄O₃Sr (974.76): Calcd. C 73.93, H 6.41, N 5.75. Found C 72.65, H 6.29, N 5.05.

48: *Route 1*: Yield 283 mg (93%) and *Route 2*: Yield 200 mg (88%): ¹H NMR (400 MHz, C₆D₆): δ 7.89 (s, 1H, N=C-H), 7.37-7.39 (m, 6H, CPh₃), 7.03-7.16 (m, 9H, CPh₃), 6.43 (m, 1H, 5-pyr), 6.25 (s, 1H, 3-pyr), 6.15 (m, 1H, 4-pyr), 3.55-3.58 (m, THF), 1.39-1.42 (m, THF) ppm. ¹³C NMR (100 MHz, C₆D₆): δ 157.7 (N=CH), 147.1 (ArC), 136.3 (2-pyr), 128.9 (o-ArC), 128.2 (m-ArC), 125.3 (p-ArC), 116.8 (5-pyr), 113.4 (3-pyr), 111.5 (4-pyr), 66.8 (CPh₃), 65.4 (THF), 15.1 (THF) ppm. FT-IR (Selected Frequencies, ν): 3025 (w, ArC-H), 1629 (s, C=N) cm^{-1} . Elemental Analysis: C₆₈H₇₇BaN₄O₅ (1167.68): Calcd. C 69.94, H 6.65, N 4.80. Found C 68.65, H 6.36, N 3.58.

6.6 X-ray crystallographic studies

Single crystals of compounds **41–48** were grown from THF and *n*-pentane mixture at -40 °C under inert atmosphere. The single crystals of compound **40** suitable for X-ray measurement was grown from CH₂Cl₂ at room temperature. For compounds **40–48**, (except **44** and **46**) a crystal of suitable dimensions was mounted on a CryoLoop (Hampton Research Corp.) with a layer of light mineral oil and placed in a nitrogen stream at 150(2)

K and all measurements were made on an Agilent Supernova X-calibur Eos CCD detector with graphite-monochromatic Cu-K α (1.54184 Å) radiation. Whereas for compounds **44** and **46**, the data were collected at 113(2) K and measurements were made on a Rigaku RAXIS RAPID imaging plate area detector or a Rigaku Mercury CCD area detector with graphite-monochromated Mo-K α (0.71075 Å) radiation. Crystal data and structure refinement parameters are summarised in Table 6.2-64. The structures were solved by direct methods (SIR92)³⁰ and refined on F^2 by full-matrix least-squares methods; using SHELXL-97.³¹ Non-hydrogen atoms were anisotropically refined. H atoms were included in the refinement in calculated positions riding on their carrier atoms. The function minimized was $[\sum w(F_o^2 - F_c^2)^2]$ ($w = 1 / [\sigma^2(F_o^2) + (aP)^2 + bP]$), where $P = (\text{Max}(F_o^2, 0) + 2F_c^2) / 3$ with $\sigma^2(F_o^2)$ from counting statistics. The function $R1$ and $wR2$ were $(\sum ||F_o| - |F_c||) / \sum |F_o|$ and $[\sum w(F_o^2 - F_c^2)^2 / \sum (wF_o^4)]^{1/2}$, respectively. The Diamond-3 program was used to draw the molecules.

6.7 Tables

Table 6.2. Crystallographic data of compounds **40**, **41** and **42**.

Crystal	40	41	42
CCDC No.			
Empirical formula	C ₂₄ H ₂₀ N ₂	C ₃₂ H ₃₅ LiN ₂ O ₂	C ₅₆ H ₅₄ N ₄ Na ₂ O ₂
Formula weight	336.42	486.56	861.01
<i>T</i> (K)	293(2)	150(2)	150(2)
λ (Å)	1.54184	1.54184	1.54184
Crystal system	Monoclinic	Orthorhombic	Monoclinic
Space group	<i>P</i> 2 ₁ / <i>c</i>	<i>P</i> <i>b c a</i>	<i>P</i> 2 ₁ / <i>c</i>
<i>a</i> (Å)	11.7601(8)	16.6177(16)	9.3375(5)
<i>b</i> (Å)	10.7213(9)	16.4089(8)	17.8616(9)
<i>c</i> (Å)	29.0076(15)	39.7532(16)	15.0867(10)
α (°)	90	90	90
β (°)	98.480(7)	90	111.528(5)
γ (°)	90	90	90
<i>V</i> (Å ³)	3617.4(4)	10839.8(12)	2340.7(2)
<i>Z</i>	8	16	2
<i>D</i> _{calc} g cm ⁻³	1.235	1.193	1.222
μ (mm ⁻¹)	0.557	0.570	1.54184
<i>F</i> (000)	1424.0	4160	912
Theta range for data collection	6.16 to 143.63 deg.	3.47 to 71.08 deg.	4.01 to 70.95 deg.
Limiting indices	-14 ≤ <i>h</i> ≤ 13 -11 ≤ <i>k</i> ≤ 13 -35 ≤ <i>l</i> ≤ 19	-17 ≤ <i>h</i> ≤ 19 -18 ≤ <i>k</i> ≤ 19 -48 ≤ <i>l</i> ≤ 47	-11 ≤ <i>h</i> ≤ 11, -16 ≤ <i>k</i> ≤ 21, -15 ≤ <i>l</i> ≤ 18
Reflections collected / unique	13546 / 6866 [<i>R</i> (int) = 0.0667]	24230 / 8741 [<i>R</i> (int) = 0.0562]	10068 / 4424 [<i>R</i> (int) = 0.0266]
Completeness to theta = 71.25	96.6 % (70.94)	83.3 % (71.08)	97.7 %
Absorption correction	Multi-scan	Multi-scan	Multi-scan
Max. and min. transmission	1.00000 and 0.25106	0.91 and 0.86	0.75 and 0.64
Refinement method	Full-matrix least-squares on <i>F</i> ²	Full-matrix least-squares on <i>F</i> ²	Full-matrix least-squares on <i>F</i> ²
Data / restraints / parameters	6866/0/470	8741 / 0 / 679	4424 / 0 / 289
Goodness-of-fit on <i>F</i> ²	1.045	1.028	1.045
Final <i>R</i> indices [I > 2σ(I)]	<i>R</i> ₁ = 0.1059, <i>wR</i> ₂ = 0.2790	<i>R</i> ₁ = 0.0792, <i>wR</i> ₂ = 0.2056	<i>R</i> ₁ = 0.0524, <i>wR</i> ₂ = 0.1416
<i>R</i> indices (all data)	<i>R</i> ₁ = 0.1878, <i>wR</i> ₂ = 0.3599	<i>R</i> ₁ = 0.1315, <i>wR</i> ₂ = 0.2412	<i>R</i> ₁ = 0.0597, <i>wR</i> ₂ = 0.1492
Largest diff. peak and hole	0.42 and -0.38 e.Å ⁻³	0.339 and -0.267 e.Å ⁻³	0.456 and -0.548 e.Å ⁻³

Table 6.3. Crystallographic data of compounds **43**, **44** and **45**.

Crystal	43	44	45
CCDC No.			
Empirical formula	C ₁₀₄ H ₉₂ K ₄ N ₈ O ₂	C ₃₉ H ₄₂ MgN ₂ O ₂	C ₅₆ H ₅₄ MgN ₄ O ₂
Formula weight	1642.26	595.06	839.34
<i>T</i> (K)	150(2)	113(2)	150(2)
λ (Å)	1.54184	0.71075	1.54184
Crystal system	Monoclinic	Triclinic	Triclinic
Space group	<i>P</i> 2 ₁ / <i>c</i>	<i>P</i> -1	<i>P</i> -1
<i>a</i> (Å)	16.7937(12)	9.530(3)	9.9208(12)
<i>b</i> (Å)	10.7713(6)	17.850(6)	9.9609(15)
<i>c</i> (Å)	24.1946(17)	20.350(7)	12.4778(12)
α (°)	90	109.890(4)	108.752(11)
β (°)	90.543(8)	96.251(2)	92.798(9)
γ (°)	90	93.303(3)	106.729(12)
<i>V</i> (Å ³)	4376.4(5)	3219.3(18)	1104.5(3)
<i>Z</i>	2	4	1
<i>D</i> _{calc} g cm ⁻³	1.246	1.228	1.262
μ (mm ⁻¹)	2.239	0.092	0.722
<i>F</i> (000)	1728	1272	446
Theta range for data collection	3.65 to 70.78 deg.	3.02 to 27.00 deg.	3.787 to 70.588 deg.
Limiting indices	-16 ≤ <i>h</i> ≤ 20 -13 ≤ <i>k</i> ≤ 12 -29 ≤ <i>l</i> ≤ 29	-12 ≤ <i>h</i> ≤ 12 -21 ≤ <i>k</i> ≤ 22 -25 ≤ <i>l</i> ≤ 25	-12 ≤ <i>h</i> ≤ 11, -9 ≤ <i>k</i> ≤ 12, -15 ≤ <i>l</i> ≤ 15
Reflections collected / unique	21120 / 8234 [<i>R</i> (int) = 0.0891]	30518 / 13802 [<i>R</i> (int) = 0.0333]	7976 / 4126 [<i>R</i> (int) = 0.0321]
Completeness to theta = 71.25	97.7 % (70.78)	98.2 % (27.00)	99.7 % (67.68)
Absorption correction	Multi-scan	Multi-scan	Multi-scan
Max. and min. transmission	1.00000 and 0.62549	0.9746 and 0.9728	1.00000 and 0.82260
Refinement method	Full-matrix least-squares on <i>F</i> ²	Full-matrix least-squares on <i>F</i> ²	Full-matrix least-squares on <i>F</i> ²
Data / restraints / parameters	8234 / 0 / 532	13802 / 0 / 793	4126 / 0 / 290
Goodness-of-fit on <i>F</i> ²	1.029	1.051	1.039
Final <i>R</i> indices [I > 2σ(I)]	<i>R</i> ₁ = 0.0796, <i>wR</i> ₂ = 0.2067	<i>R</i> ₁ = 0.0651, <i>wR</i> ₂ = 0.1577	<i>R</i> ₁ = 0.0417, <i>wR</i> ₂ = 0.1019
<i>R</i> indices (all data)	<i>R</i> ₁ = 0.1102, <i>wR</i> ₂ = 0.2461	<i>R</i> ₁ = 0.0988, <i>wR</i> ₂ = 0.1893	<i>R</i> ₁ = 0.0539, <i>wR</i> ₂ = 0.1114
Largest diff. peak and hole	0.641 and -0.574 e.Å ⁻³	0.906 and -0.526 e.Å ⁻³	0.155 and -0.266 e.Å ⁻³

Table 6.4. Crystallographic data of compounds **46**, **47** and **48**.

Crystal	46	47	48
CCDC No.			
Empirical formula	C ₆₆ H ₇₀ CaN ₄ O ₄	C ₆₀ H ₆₂ N ₄ O ₃ Sr	C ₆₈ H ₇₇ BaN ₄ O ₅
Formula weight	999.32	974.76	1167.68
<i>T</i> (K)	113(2)	150(2)	150(2)
λ (Å)	0.71075	1.54184	1.54184
Crystal system	Monoclinic	Triclinic	Triclinic
Space group	<i>P</i> 2 ₁ /n	<i>P</i> -1	<i>P</i> -1
<i>a</i> (Å)	11.185(18)	11.5131(13)	10.7818(11)
<i>b</i> (Å)	13.42(2)	13.2509(13)	14.4888(15)
<i>c</i> (Å)	18.43(3)	18.1457(15)	21.2076(19)
α (°)	90	75.334(8)	109.626(9)
β (°)	104.24(2)	78.968(9)	93.344(8)
γ (°)	90	71.140(10)	106.825(9)
<i>V</i> (Å ³)	2681(7)	2516.1(4)	2942.1(5)
<i>Z</i>	2	2	2
<i>D</i> _{calc} g cm ⁻³	1.238	1.287	1.318
μ (mm ⁻¹)	0.170	1.871	5.668
<i>F</i> (000)	1068	1024	1218
Theta range for data collection	3.04 to 26.00 deg.	3.60 to 71.27deg.	3.33 to 71.43 deg.
Limiting indices	-13<= <i>h</i> <=12 -15<= <i>k</i> <=16 -22<= <i>l</i> <=18	-14<= <i>h</i> <=14 -11<= <i>k</i> <=16 -21<= <i>l</i> <=22	-12<= <i>h</i> <=13, -17<= <i>k</i> <=17, -17<= <i>l</i> <=25
Reflections collected / unique	11436 / 5075 [<i>R</i> (int) = 0.1009]	19225 / 9452 [<i>R</i> (int) = 0.0559]	21652 / 11049 [<i>R</i> (int) = 0.0796]
Completeness to theta	96.3 % (26.00)	96.7 % (71.27)	96.5 %
Absorption correction	Multi-scan	Multi-scan	Multi-scan
Max. and min. transmission	0.9668 and 0.9668	1.00000 and 0.92842	1.000 and 0.51963
Refinement method	Full-matrix least-squares on <i>F</i> ²	Full-matrix least-squares on <i>F</i> ²	Full-matrix least-squares on <i>F</i> ²
Data / restraints / parameters	5075 / 0 / 331	9452 / 0 / 613	11049 / 0 / 703
Goodness-of-fit on <i>F</i> ²	0.999	1.094	1.009
Final <i>R</i> indices [<i>I</i> >2σ(<i>I</i>)]	<i>R</i> ₁ = 0.0766, <i>wR</i> ₂ = 0.1573	<i>R</i> ₁ = 0.0925, <i>wR</i> ₂ = 0.2361	<i>R</i> ₁ = 0.0667, <i>wR</i> ₂ = 0.1670
<i>R</i> indices (all data)	<i>R</i> ₁ = 0.1713, <i>wR</i> ₂ = 0.2128	<i>R</i> ₁ = 0.0975, <i>wR</i> ₂ = 0.2480	<i>R</i> ₁ = 0.0874, <i>wR</i> ₂ = 0.2011
Largest diff. peak and hole	0.393 and -0.361 e.Å ⁻³	2.717 and -1.215 e.Å ⁻³	1.832 and -2.737 e.Å ⁻³

References:

- (1) Mu, J.-S.; Wang, Y.-X.; Lia, B.-X.; Li, Y.-S. *Dalton Trans.* **2011**, 40, 3490-3497.
- (2) Holm, R. H.; Chakravorty, A.; Theriot, L. J. *Inorg. Chem.* **1966**, 5, 625-635 and references cited therein.
- (3) Mashima, K.; Tsurugi, H. *J. Organomet. Chem.* **2005**, 690, 4414-4423 and references cited therein.
- (4) (a) Johnson, L. K.; Killian, C. M.; Brookhart, M. *J. Am. Chem. Soc.* **1995**, 117, 6414-6415. (b) Britovsek, G. J. P.; Gibson, V.C.; Kimberley, B. S.; Maddox, P. J.; McTavish, S. J.; Solan, G. A.; White, A. J. P.; Williams, D. J. *Chem. Commun.* **1998**, 849-850. (c) Matsui, S.; Mitani, M.; Saito, J.; Tohi, Y.; Makio, H.; Matsukawa, N.; Takagi, Y.; Tsuru, K.; Nitabaru, M.; Nakano, T.; Tanaka, H.; Kashiwa, N.; Fujita, T. *J. Am. Chem. Soc.* **2001**, 123, 6847-6856 and references cited therein. (d) Tian, J.; Hustand, P. D.; Coates, G. W. *J. Am. Chem. Soc.* **2001**, 123, 5134-5135 and references cited therein. (e) Hao, H.; Bhandari, S.; Ding, Y.; Roesky, H. W.; Magull, J.; Schmidt, H. G.; Noltemeyer, M.; Cui, C. *Eur. J. Inorg. Chem.* **2002**, 1060-1065. (f) Matsuo, Y.; Mashima, K.; Tani, K. *Organometallics* **2001**, 20, 3510-3518. (g) Cui, C.; Shafir, A.; Reeder, C.L.; Arnold, J. *Organometallics* **2003**, 22, 3357-3359.
- (5) Jenter, J.; Koeppe, R.; Roesky, P. W. *Organometallics* **2011**, 30, 1404-1413.
- (6) Panda, T. K.; Yamamoto, K.; Yamamoto, K.; Kaneko, H.; Yang, Y.; Tsurugi, H.; Mashima, K. *Organometallics* **2012**, 31, 2268-2274.
- (7) Yang, Yi.; Liu, Bo.; Lv, K.; Gao, W.; Cui, D.; Chen, X.; Jing, X. *Organometallics* **2007**, 26, 4575-4584.
- (8) Yang, Yi.; Li, S.; Cui, D.; Chen, X.; Jing, X. *Organometallics* **2007**, 26, 671-678.
- (9) Clara, S. B.; Gomes, D.; Suresh, P. T.; Gomes, L. F.; Veiros, M. T.; Teresa, G. N.; Oliveira, M. C. *Dalton Trans.* **2010**, 39, 736-748.
- (10) Carabineiro, S. A.; Silva, L. C.; Gomes, P. T.; Pereira, L. C. J.; Veiros, L. F.; Pasco, S. I.; Duarte, M. T.; Namorado, S.; Henriques, R. T. *Inorg. Chem.* **2007**, 46, 6880-6890.
- (11) The bonding situation in the drawing of the ligand system is simplified for clarity.
- (12) Li, Q.; Rong, J.; Wang, S.; Zhou, S.; Zhang, L.; Zhu, X.; Wang, F.; Yang, S.; Wei, Y. *Organometallics* **2011**, 30, 992-1001.
- (13) (a) Klooster, W. T.; Brammer, L.; Schaverien, C. J.; Budzelaar, P. H. M. *J. Am. Chem. Soc.* **1999**, 121, 1381-1382. (b) Scherer, W.; McGrady, G. S. *Angew. Chem., Int. Ed.* **2004**, 43, 1782-1806.

- (14) Jayeeta, B.; Kottalanka, R. K.; Harinath, A.; Panda, T. K. *J. Chem. Sci.* **2014**, Accepted.
- (15) (a) Jacoby, D.; Isoz, S.; Floriani, C.; Chiesi-Villa, A.; Rizzoli, C. *J. Am. Chem. Soc.* **1995**, *117*, 2805–2816. (b) Bonomo, L.; Solari, E.; Scopelliti, R.; Floriani, C.; Re, N. *J. Am. Chem. Soc.* **2000**, *122*, 5312–5326. (c) De Angelis, S.; Solan, E.; Flonani, C.; Chiesi-Villa, A.; Rizzoli, C. *J. Am. Chem. Soc.* **1994**, *116*, 5702–5713. (d) De Angelis, S.; Solari, E.; Floriani, C.; Chiesi-Villa, A.; Rizzoli, C. *J. Chem. Soc. Dalton Trans.* **1994**, 2467–2469. (e) Jubb, J.; Gambarotta, S.; Duchateau, R.; Teuben, J. H. *J. Chem. Soc. Chem. Commun.* **1994**, 2641–2642.
- (16) Gao, J.; Liu, Y.; Zhao, Y.; Yang, X-J.; Sui, Y. *Organometallics* **2011**, *30*, 6071–6077.
- (17) Hsueh, L. -F.; Chuang, N.-T.; Lee, C. -Y.; Datta, A.; Huang, J.-H.; Lee, T. -Y. *Eur. J. Inorg. Chem.* **2011**, 5530–5537.
- (18) Bailey, P. J.; Coxall, R. A.; Dick, C. M.; Fabre, S.; Henderson, L. C.; Herber, C.; Liddle, S. T.; Loroño-González, D.; Parkin, A.; Parsons, S. *Chem. Eur. J.* **2003**, *9*, 4820–4828.
- (19) Panda, T. K.; Yamamoto, K.; Yamamoto, K.; Kaneko, H.; Yang, Y.; Tsurugi, H.; Mashima, K. *Organometallics* **2012**, *31*, 2268–2274.
- (20) (a) Harder, S.; Müller, S.; Hübner, E. *Organometallics* **2004**, *23*, 178–183. (b) Michel, O.; Meermann, C.; Toörnroos, K. W.; Anwander, R. *Organometallics* **2009**, *28*, 4783–4790.
- (21) Panda, T. K.; Kaneko, H.; Michel, O.; Tsurugi, H.; Pal, K.; Toernroos, K. W.; Anwander, R.; Mashima, K. *Organometallics* **2012**, *31*, 3178–3184.
- (22) (a) Sánchez-Barba L. F.; Hughes D. L.; Humphrey S. M.; Bochmann M. *Organometallics*, **2006**, *25*, 1012–1020. (b) Sánchez-Barba L. F.; Hughes D. L.; Humphrey S. M.; Bochmann M. *Organometallics*, **2005**, *24*, 5329–5334. (c) Sánchez-Barba L. F.; Hughes D. L.; Humphrey S. M.; Bochmann M. *Organometallics*, **2005**, *24*, 3792–3799.
- (23) Garcés A.; Sánchez-Barba L. F.; Alonso-Moreno C.; Fajardo M.; Fernández-Baeza J.; Otero A.; Lara-Sánchez A.; López-Solera I.; Rodríguez A. M. *Inorg. Chem.*, **2010**, *49*, 2859–2871.
- (24) Kuzdrowska M.; Annunziata L.; Marks S.; Schmid M.; Jaffredo C. G.; Roesky P. W.; Guillaume S. M.; Maron L. *Dalton Trans.*, **2013**, *42*, 9352–9360.
- (25) Cushion M. G.; Mountford P. *Chem. Commun.*, **2011**, *47*, 2276–2278.
- (26) Liu B.; Roisnel T.; Guegan J.-P.; Carpentier J.-F.; Sarazin Y. *Chem. – Eur J.*, **2012**, *18*, 6289–6301.
- (27) Sarazin Y.; Liu B.; Maron L.; Carpentier J.-F. *J. Am. Chem. Soc.*, **2011**, *133*, 9069–9087.
- (28) Westerhausen, M. *Coord. Chem. Rev.* **1998**, *176*, 157–210.
- (29) George, D.; Vaughn, K.; Alex, K.; Gladysz, J. A. *Organometallics* **1986**, *5*, 936–942.

- (30) M. Sheldrick, SHELXS-97. *Program of Crystal Structure Solution, University of Göttingen, Germany, 1997.*
- (31) G. M. Sheldrick, SHELXL-97. *Program of Crystal Structure Refinement, University of Göttingen, Germany, 1997.*

List of publications based on the research work:

1. **Ravi K. Kottalanka**, A. Harinath, Jayeeta Bhattacharjee, H. Vignesh Babu and Tarun K. Panda* “Bis(phosphinoselenoicamides) as versatile chelating ligands for alkaline-earth metal (Mg, Ca, Sr and Ba) complexes: syntheses, structure and ϵ -caprolactone polymerization” *Dalton Trans*, **2014**, *43*, 8757-8766.
2. **Ravi K. Kottalanka**, Srinivas Anga, K. Naktode, P. Laskar, Hari Pada Nayek and Tarun K. Panda* “Amidophosphine-borane complexes of alkali metals and the heavier alkaline-earth metals: syntheses and structural Studies” *Organometallics*, **2013**, *32*, 4473–4482.
3. **Ravi K. Kottalanka**, K. Naktode, S. Anga, Hari Pada Nayek and T. K. Panda* “Heavier alkaline-earth metal complexes with phosphinoselenoicamides: Evidence of direct M-Se contact (M = Ca, Sr and Ba)” *Dalton Trans*, **2013**, *42*, 4947-4956.
4. **Ravi K. Kottalanka**, Srinivas Anga, Salil K. Jana, and Tarun K. Panda* “Synthesis and structure of heavier group 2 metal complexes with diselenoimidodiphosphinato ligand containing Sr-Se and Ba-Se direct bonds” *J. Organomet. Chem.*, **2013**, *740*, 104-109.
5. **Ravi K. Kottalanka**, P. Laskar, K. Naktode, Bhabani S. Mallik* and Tarun K. Panda* “N- versus P- coordination for N-B and P-B bonded BH₃ adducts for various phosphine-amine ligands – an experimental and computational study” *J. Mol. Str.*, **2013**, *1047*, 302-309.
6. **Ravi K. Kottalanka**, K. Naktode and T. K. Panda* “Synthesis and structural studies of dimeric sodium compounds having pentametallooctane and hexametallacyclo undecane structure using different phosphinamide derivatives” *J. Mol. Str.*, **2013**, *1036*, 189-195.
7. **Ravi K. Kottalanka**, K. Naktode, Srinivas A., and Tarun K. Panda* “Synthesis and structure of potassium and barium complexes with diphenylphosphine thioicamido ligand containing Ba-S direct bonds” *Phosphorus, Sulfur, and Silicon and the Related Elements*, **2013**, in press.
8. **Ravi K. Kottalanka**, K. Naktode, and Tarun K. Panda* “Zirconium complexes of two different iminopyrrolyl ligands – syntheses and structures” *Z. Anorg. Allg. Chem.*, **2013**, *640*, 114-117.
9. **Ravi K. Kottalanka**, and Tarun K. Panda* “Novel alkaline-earth metal complexes having chiral phosphinoselenoic amides and boranes in the coordination sphere: chiral alkaline earth metal complexes having M-Se direct bond (M = Mg, Ca, Sr, Ba)” *manuscript in preparation*.

10. **Ravi K. Kottalanka**, and Tarun K. Panda* “Alkali and alkaline-earth metal complexes having rigid bulky-iminopyrrolyl ligand in the coordination sphere: syntheses, structures and ϵ -caprolactone polymerization” *manuscript in preparation*.

Conferences Attended:

Oral Presentation:

1. Oral Presentation in the conference on Recent Developments in Chemistry (RDC-2013), October 2013, NIT Durgapur, West Bengal.

Poster Presentations:

2. Poster presentation in Modern Trends in Inorganic Chemistry (MTIC – XIV), 10-13 December, 2011, School of Chemistry, University of Hyderabad, Hyderabad.
3. Aligent Single Crystal X-ray Diffractometer users meet, March 19-20, 2012, Indian Institute of Technology Indore, Madhya Pradesh.
4. Poster presentation in the conference on New Directions in Chemical Sciences (NDCS-2012), December, 2012, IIT Delhi, New Delhi.
5. Poster presentation in Indo-French collaborative meeting, February 2014, NISER Bhubaneswar, Odisha.

Curriculum vitae

Name: Ravi Kumar Kottalanka
Date of Birth: 28th January, 1984.
Place of Birth: Gopalapuram, East Godavari District, Andhra Pradesh, India.
Nationality: Indian
Sex: Male
Marital Status: Single

Education:

Bachelor of Science (B.Sc.)

- ✓ Chemistry as major, Physics and Mathematics as pass subjects.
- ✓ Govt. Degree College (A), Rajahmundry, Andhra University, India, 2001-2004.

Master of Science (M.Sc.)

- ✓ Inorganic Chemistry, Andhra University, Visakhapatnam, India, 2005-2007.

Teaching experience

- ✓ Worked as full-time lecturer for P.G course at Smt.Jasti Bullemai P.G. College, Rajahmundry, Andhra Pradesh, India, 2007-2009.
- ✓ Worked as part-time lecturer for P.G. course at Aadikavi Nannaya University, Rajahmundry, Andhra Pradesh, India, 2009-2010.

Current position: Submitted thesis from the research group of Dr. Tarun Kanti Panda, Department of Chemistry, IIT Hyderabad.

Awards and honors:

- ✓ Received *JASSO Scholarship* for the short-term student exchange promotion program from the Graduate School of Engineering Science, Osaka University, Japan, in January 2012.
- ✓ Received *Annual Research Award* (2nd Runner up) from K.V. Rao Scientific Society for the year 2014.
- ✓ Received *Academic Excellence Award* in PhD program for the year 2013 from the IIT Hyderabad.
- ✓ Qualified *National Eligibility Test* (NET) for research work (JRF) in India conducted by joint UGC-CSIR, India in December 2009.
- ✓ Qualified *Lecturership* (LS) in July 2009 conducted by joint UGC-CSIR, India.